

RD-A133 667

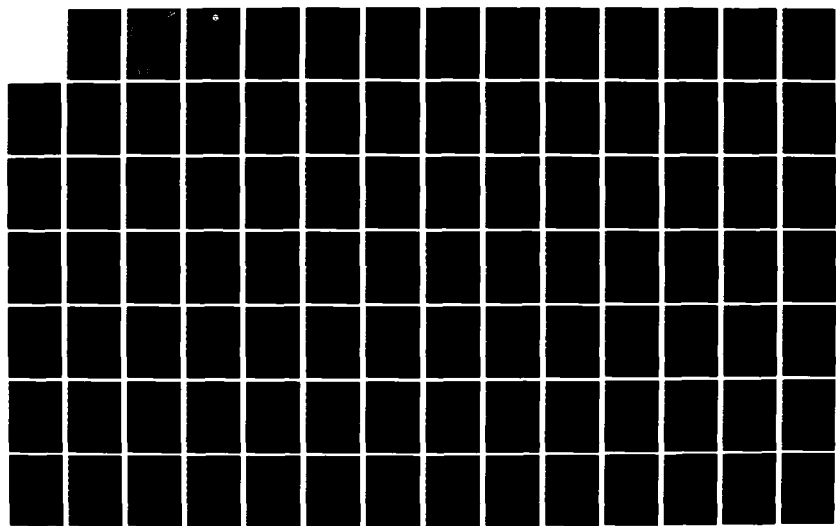
XWVG: A WAVEGUIDE PROGRAM FOR TRILINEAR TROPOSPHERIC
DUCTS COMPUTER PROGR. (U) NAVAL OCEAN SYSTEMS CENTER
SAN DIEGO CA G B BAUMGARTNER 30 JUN 83 NOSC/TD-610

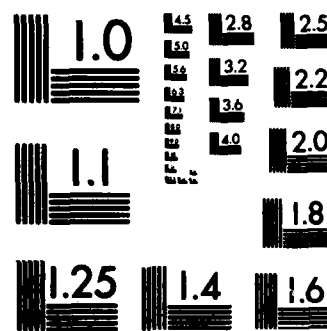
1/3

UNCLASSIFIED

F/G 20/14

NL





MICROCOPY RESOLUTION TEST CHART
NATIONAL BUREAU OF STANDARDS-1963-A

AD-A133 667

NOSC TD 610

Technical Document 610

**XWVG: A WAVEGUIDE PROGRAM FOR
TRILINEAR TROPOSPHERIC DUCTS**

Computer program for calculating the signal
levels of EM waves propagating over seawater

GB Baumgartner Jr

30 June 1983
Period of work: October 1982 – June 1983

Prepared for
Office of Naval Research

Approved for public release; distribution unlimited

Draft File Copy

DTIC
ELECTE
OCT 18 1983
S D
D

NOSC

NAVAL OCEAN SYSTEMS CENTER
San Diego, California 92152

83 10 18 037



NAVAL OCEAN SYSTEMS CENTER SAN DIEGO, CA 92152

AN ACTIVITY OF THE NAVAL MATERIAL COMMAND

JM PATTON, CAPT, USN

Commander

HL BLOOD

Technical Director

ADMINISTRATIVE INFORMATION

Work was performed under program element 61153N, project RR02101 (NOSC 532-MP02), by a member of the Modeling Branch (Code 5324) for the Office of Naval Research. This document covers work from October 1982 to June 1983 and was approved for publication 30 June 1983.

The many helpful remarks and suggestions of RA Pappert throughout the course of this work are gratefully acknowledged. The assistance of CH Shellman greatly facilitated my implementation of his root finding routine in XWVG.

Released by
JH Richter, Head
Ocean and Atmospheric
Sciences Division

Under authority of
JD Hightower, Head
Environmental Sciences Department

UNCLASSIFIED

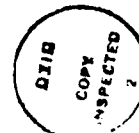
SECURITY CLASSIFICATION OF THIS PAGE (When Data Entered)

REPORT DOCUMENTATION PAGE		READ INSTRUCTIONS BEFORE COMPLETING FORM
1. REPORT NUMBER NOSC Technical Document 610 (TD 610)	2. GOVT ACCESSION NO. AD-A133 667	3. RECIPIENT'S CATALOG NUMBER
4. TITLE (and Subtitle) XWVG: A WAVEGUIDE PROGRAM FOR TRILINEAR TROPOSPHERIC DUCTS Computer program for calculating the signal levels of EM waves propagating over seawater		5. TYPE OF REPORT & PERIOD COVERED Computer program description October 1982–June 1983
7. AUTHOR(s) GB Baumgartner Jr		6. PERFORMING ORG. REPORT NUMBER
9. PERFORMING ORGANIZATION NAME AND ADDRESS Naval Ocean Systems Center San Diego CA 92152		10. PROGRAM ELEMENT, PROJECT, TASK AREA & WORK UNIT NUMBERS 61153N, RR02101 (NOSC 532-MP02)
11. CONTROLLING OFFICE NAME AND ADDRESS Office of Naval Research, Pasadena Branch Office 1030 E Green Street Pasadena CA 91106		12. REPORT DATE 30 June 1983
14. MONITORING AGENCY NAME & ADDRESS (if different from Controlling Office)		13. NUMBER OF PAGES 208
16. DISTRIBUTION STATEMENT (of this Report) Approved for public release; distribution unlimited		15. SECURITY CLASS. (of this report) Unclassified
17. DISTRIBUTION STATEMENT (of the abstract entered in Block 20, if different from Report)		
18. SUPPLEMENTARY NOTES		
19. KEY WORDS (Continue on reverse side if necessary and identify by block number) XWVG Computer program documentation Tropospheric duct propagation Electromagnetic field strength calculation		
20. ABSTRACT (Continue on reverse side if necessary and identify by block number) XWVG is a reliable waveguide program for calculating the coherent and incoherent mode sum values of the electromagnetic field strength in dB relative to the free space value, for signals propagating in a trilinear tropospheric duct over seawater. XWVG allows for the effects of surface roughness, absorption by atmospheric gases, and the variation of the complex index of refraction of seawater as a function of temperature, salinity, and frequency. XWVG has been successfully used in the frequency range 50 MHz to 94 GHz and should be usable at higher frequencies. XWVG uses the root-finding routine of Shellman and Morfitt to find the complex modes propagating in the duct. This guarantees that all modes with an attenuation rate below a prespecified level will be found. A description of XWVG is provided, along with a complete program listing and sample output.		

CONTENTS

- 1 INTRODUCTION . . . page 1
- 2 MATHEMATICAL FORMULATION OF THE MODEL . . . 3
 - Modified refractivity profile . . . 3
 - Horizontally polarized wave propagation . . . 6
 - Vertically polarized wave propagation . . . 20
 - Trilinear duct modal function . . . 22
 - Trilinear duct modal height-gain functions . . . 25
- 3 SURFACE ROUGHNESS . . . 35
- 4 COMPLEX INDEX OF REFRACTION OF SEAWATER . . . 46
- 5 SHELLMAN-MORFITT ROOT-FINDING ROUTINE . . . 51
- 6 SOLUTIONS OF STOKES' DIFFERENTIAL EQUATION . . . 60
- 7 EXTENDED COMPLEX ARITHMETIC . . . 86
- 8 DESCRIPTION OF XWVG PROGRAM ELEMENTS . . . 88
 - MAIN . . . 89
 - CADD . . . 94
 - ADDX . . . 96
 - HNKLX . . . 98
 - KHNKLX . . . 99
 - KHATX . . . 100
 - CTANH . . . 102
 - CSECH2 . . . 103
 - FCTVLX . . . 104
 - FDFDTX . . . 106
 - FZEROX . . . 108
 - QUAD . . . 111
 - NOMSHX . . . 112
 - FINDFX . . . 114
 - EXCFAC . . . 116
 - HTGAIN . . . 117
 - MODSUM . . . 118
 - SEAH20 . . . 119
 - DHORIZ . . . 121
 - CASIN . . . 122
- 9 SOURCE LISTING FOR XWVG . . . 123
- 10 SAMPLE OUTPUT FROM XWVG . . . 185
- 11 REMARKS . . . 201
- 12 REFERENCES . . . 203

Accession For	
NTIS GRA&I	
DTIC TAB	
Unannounced	
Justification	
By	
Distribution/	
Availability Codes	
Dist	Avail and/or Special
A	1 1974



1. INTRODUCTION

This document is a description of XWVG, a program for calculating the signal levels of electromagnetic waves propagating in a tropospheric ducting environment over seawater. This program is based on the waveguide formulation of the tropospheric ducting problem given by Marcus and Stuart [1, 2]. Like the program DUCT developed by Marcus, Stuart, and Ellis [2, 3], XWVG uses the root-finding program of Shellman and Morfitt [4] to find the complex modes that propagate in the tropospheric duct.

XWVG has been developed for the purpose of providing a program which guarantees that all waveguide modes with attenuation rates below a specified value will be found. XWVG is particularly useful for conducting case studies over a large dynamic range of frequencies, and its results can serve as a standard against which results of quicker but more approximate methods [5] may be measured.

XWVG assumes that the modified refractivity profile of the troposphere can be successfully modeled with three linear segments. For many naturally occurring tropospheric ducts this is a good assumption. The program DUCT of Marcus, Stuart, and Ellis allows the modified refractivity profile to be modeled with up to five linear segments and hence can describe a wider variety of refractivity profiles.

The waveguide modes that can propagate in a tropospheric ducting environment are the complex zeros of a transcendental function. In the Marcus and Stuart formulation of the tropospheric ducting problem this modal function is expressed as a determinant. In XWVG, where the modified refractivity profile is restricted to three linear segments, the modal function is evaluated by expanding the determinant and numerically evaluating the resulting expression. This allows the derivative of the modal function, which is needed by the Shellman and Morfitt root-finding program and for the evaluation of the modal excitation factors, to be evaluated easily. In DUCT, the modal function is evaluated by numerically evaluating the determinant. Because of the method used in DUCT to evaluate the derivative of the modal

function, DUCT is restricted to refractivity profiles with five or fewer linear segments.

XWVG includes an approximate allowance for surface roughness and atmospheric absorption, effects which are not included in DUCT. XWVG also includes a subroutine that evaluates the complex index of refraction of seawater as a function of frequency, temperature, and salinity.

The major advantage that DUCT and XWVG have over some other implementations of tropospheric ducting models is the use of the complex root-finding program of Shellman and Morfitt. Use of this routine guarantees that all modes with an attenuation rate below a prespecified level will be found. However, this advantage does not come without a price. The Shellman and Morfitt root-finding routine has an extremely long execution time compared with other less infallible methods of finding modes [6].

2. MATHEMATICAL FORMULATION OF THE MODEL

MODIFIED REFRACTIVITY PROFILE

The index of refraction of the atmosphere is given by

$$n(\bar{r}) = [\varepsilon_r(\bar{r})\mu_r(\bar{r})]^{\frac{1}{2}}, \quad (2.1)$$

where ε_r and μ_r are the relative permittivity and permeability of the atmosphere. Throughout this document the assumption is made that

$$\mu_r(\bar{r}) = 1, \quad (2.2)$$

and the only variation of the index of refraction is with height above the surface of the earth.

When modeling tropospheric propagation, it is mathematically convenient to utilize a rectangular coordinate system to describe atmospheric wave propagation over a curved earth. The curvature of the earth may be approximated by modifying the index of refraction of the atmosphere [7, 8]. This modification is accomplished by adding a term to $n(z)$, where z is the height above the surface of a flat earth, which would cause a ray to bend in such a way that its height above the flat earth at each point would be the same as if it were a straight ray over a curved earth. The modified index of refraction is then given by

$$m(z) = n(z) + \frac{z}{a}, \quad (2.3)$$

where a is the radius of the earth.

The accuracy of the flat-earth approximation depends upon the frequency of the electromagnetic wave and the height above the surface of the earth at which the signal level is measured [9, 10]. The approximation breaks down as the frequency and height above the earth's surface increase. For the standard atmosphere, Pekeris [9] finds that the fractional error in the height-gain functions is approximately

$$\Delta = \frac{2\pi\sqrt{6}}{5} \frac{h^{5/2}}{\lambda a^{3/2}} \quad (2.4)$$

$$= 1.911 \times 10^{-10} \frac{[h(m)]^{5/2}}{\lambda(m)} . \quad (2.5)$$

From this it can be seen that for signals with wavelength $\lambda = 3$ cm ($f = 10$ GHz) at a height of $h = 1000$ m the fractional error in the height-gain function is approximately 20%.

The modified index of refraction of the atmosphere, $m(z)$, is very nearly one, the difference being on the order of 10^{-3} . For this reason it is convenient to introduce the modified refractivity, $M(z)$, defined by

$$M(z) = [m(z) - 1] \times 10^6 . \quad (2.6)$$

Often, the modified refractivity can be approximated by three linear segments, as shown in figure 1. The model developed in this document assumes that the modified refractivity can be approximated with three straight line segments and that this one profile is valid for all range values, x . An additional assumption made is that the slope, $\frac{dM}{dz}$, of the modified refractivity profile is positive in the first and third layers. In the second layer, $\frac{dM}{dz}$ can be either positive or negative, but not zero.

Let $M_i(z)$ denote the value of the modified refractivity in the i -th layer. The modified refractivity profile shown in figure 1 can then be written

$$M_1(z) = M(z_{ref}) + \frac{dM_1}{dz}(z - z_{ref}) \quad (0 \leq z \leq z_2), \quad (2.7)$$

$$M_2(z) = M_1(z_2) + \frac{dM_2}{dz}(z - z_2) \quad (z_2 \leq z \leq z_3), \quad (2.8)$$

and

$$M_3(z) = M_2(z_3) + \frac{dM_3}{dz}(z - z_3) \quad (z_3 \leq z) . \quad (2.9)$$

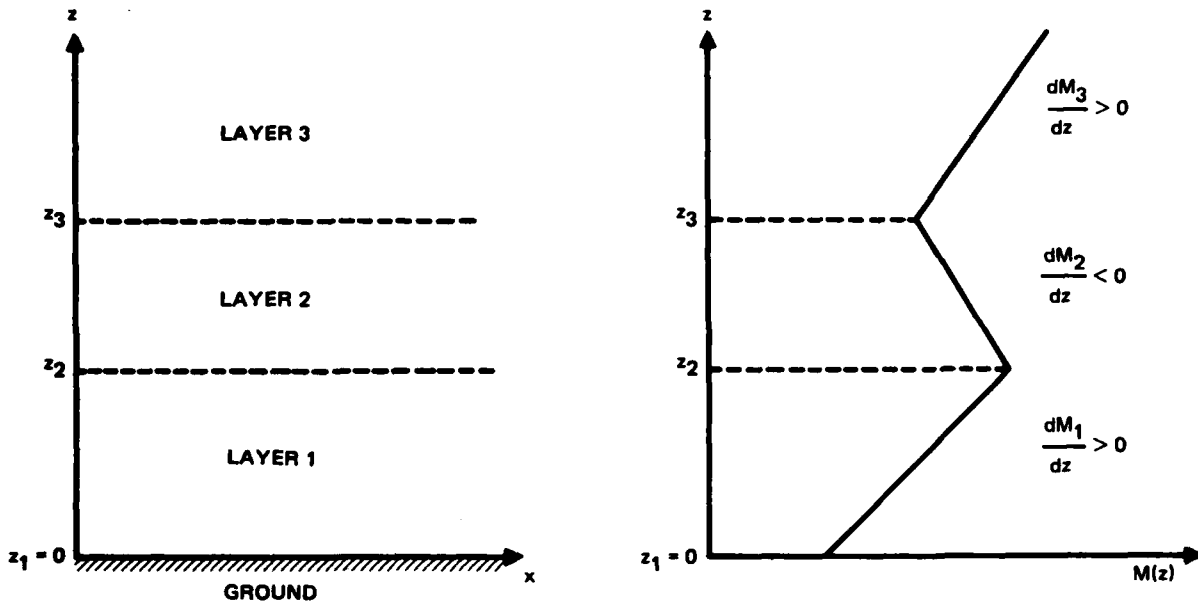


Figure 1. Trilinear modified refractivity profile. The slope of $M(z)$ is assumed to be positive in the first and third layers. In the second layer the slope can be positive or negative.

The square of the modified index of refraction is then

$$\begin{aligned} n_1^2(z) &\approx 1 + 2 \times 10^{-6} M_1(z) + i\eta \\ &\approx 1 + \alpha_1(z - H) + i\eta \quad (0 \leq z \leq z_2), \end{aligned} \quad (2.10)$$

$$\begin{aligned} n_2^2(z) &\approx 1 + 2 \times 10^{-6} M_2(z) + i\eta \\ &\approx 1 + \alpha_1(z_2 - H) + \alpha_2(z - z_2) + i\eta \quad (z_2 \leq z \leq z_3), \end{aligned} \quad (2.11)$$

and

$$\begin{aligned} n_3^2(z) &\approx 1 + 2 \times 10^{-6} M_3(z) + i\eta \\ &\approx 1 + \alpha_1(z_2 - H) + \alpha_2(z_3 - z_2) \\ &\quad + \alpha_3(z - z_3) + i\eta \quad (z_3 \leq z) . \end{aligned} \quad (2.12)$$

The slopes α_i are related to the slopes $\frac{dM_i}{dz}$ by

$$\alpha_i = 2 \times 10^{-6} \frac{dM_i}{dz} . \quad (2.13)$$

The term $i\eta$ introduced in equations (2.10-2.12) allows for attenuation of the signal due to absorption by atmospheric gases. The height H is chosen so that at some reference height, z_{ref} , in the first layer, $M(z_{ref})$ has a specified value. H is related to α_1 and $M(z_{ref})$ by

$$H = z_{ref} - \frac{2 \times 10^{-6} M(z_{ref})}{\alpha_1} . \quad (2.14)$$

The complex index of refraction of the ground is assumed to be independent of position and given by

$$n_g^2 = \epsilon_g - i \frac{\sigma_g}{\epsilon_0 w} , \quad (2.15)$$

where ϵ_g is the relative permittivity of the ground, σ_g is the ground conductivity, ϵ_0 is the permittivity of free space, and $w = \frac{\omega}{2\pi}$ is the frequency.

HORIZONTALLY POLARIZED WAVE PROPAGATION

Horizontally polarized waves may be considered as due to a radiating magnetic dipole \vec{p} oriented in the z -direction and located at $x = y = 0$, $z = z_p$. In a laterally homogeneous medium the fields due to such a dipole exhibit axial symmetry and may be obtained from the magnetic Hertz potential vector [11]

$$\vec{\Pi}(r, z) = \Pi(r, z) \vec{e}_z , \quad (2.16)$$

where \vec{e}_z is the unit vector in the z -direction and r is the lateral distance from the source location. A dependence of $e^{+i\omega t}$ is assumed. The

electric and magnetic fields are related to the magnetic Hertz potential vector by

$$\begin{aligned}\bar{D} &= -i\mu\epsilon\omega\bar{\nabla} \times \bar{\Pi} \\ &= -i\epsilon\mu_0\omega\bar{\nabla} \times \bar{\Pi}\end{aligned}\quad (2.17)$$

and

$$\bar{H} = \bar{\nabla} \times \bar{\nabla} \times \bar{\Pi} . \quad (2.18)$$

The Hertz potential may be expressed as [11]

$$\Pi(r, z) = \frac{1}{4\pi} \int_C \rho d\rho H_0^{(2)}(r\rho) \tilde{\Pi}(\rho, z) , \quad (2.19)$$

where $H_0^{(2)}(\xi)$ is the zeroth-order Hankel function of the second kind and the contour C is shown in figure 2. In the j -th atmospheric layer ($j = 1, 2, 3$) the function $\tilde{\Pi}(\rho, z)$ satisfies the differential equation

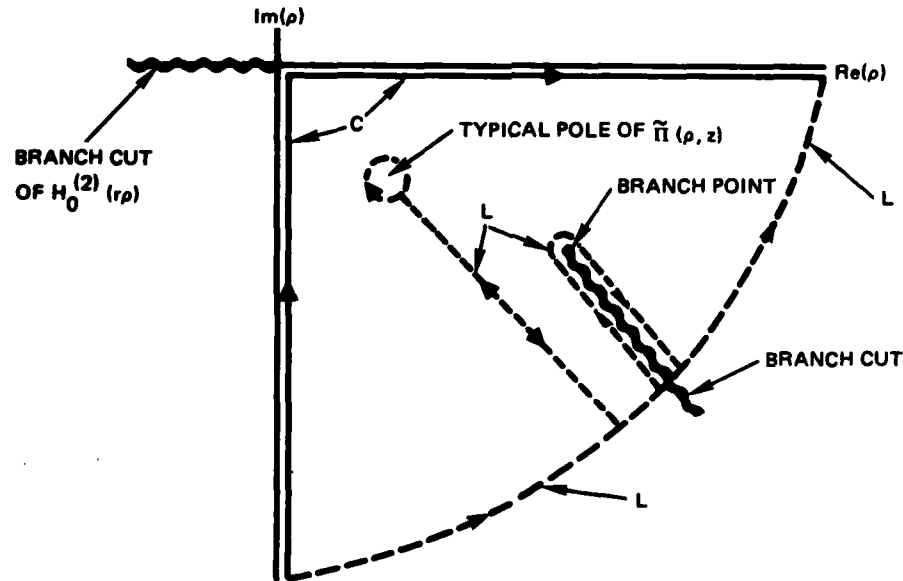


Figure 2. Contour of integration C for evaluation of equation (2.19). By Cauchy's Theorem the contour L is equivalent to the contour C . The branch cut in the fourth quadrant is due to the factor $\sqrt{n_g^2 - \rho^2/k^2}$ introduced into $\tilde{\Pi}$ because of the ground boundary condition.

$$\left\{ \frac{d^2}{dz^2} + k^2 \left[n_j^2(z) - \frac{\rho^2}{k^2} \right] \right\} \tilde{\Pi}_j(\rho, z) = -p\delta(z - z_T) , \quad (2.20)$$

where k is the free space wave number and $\delta(\xi)$ is the Dirac delta function. In the ground, $\tilde{\Pi}(\rho, z)$ satisfies the differential equation

$$\left\{ \frac{d^2}{dz^2} + k^2 \left[n_g^2 - \frac{\rho^2}{k^2} \right] \right\} \tilde{\Pi}_g(\rho, z) = 0 . \quad (2.21)$$

Continuity of the tangential components of the \bar{E} and \bar{H} fields yields the continuity conditions [12]

$$\tilde{\Pi}_g(\rho, 0) = \tilde{\Pi}_1(\rho, 0) , \quad (2.22)$$

$$\frac{d}{dz} \{ \tilde{\Pi}_g(\rho, 0) \} = \frac{d}{dz} \{ \tilde{\Pi}_1(\rho, 0) \} , \quad (2.23)$$

$$\tilde{\Pi}_j(\rho, z_{j+1}) = \tilde{\Pi}_{j+1}(\rho, z_{j+1}) \quad (j = 1, 2) , \quad (2.24)$$

and

$$\frac{d}{dz} \{ \tilde{\Pi}_j(\rho, z_{j+1}) \} = \frac{d}{dz} \{ \tilde{\Pi}_{j+1}(\rho, z_{j+1}) \} \quad (j = 1, 2) . \quad (2.25)$$

The boundary conditions that $\tilde{\Pi}(\rho, z)$ must satisfy are: as $z \rightarrow -\infty$, $\tilde{\Pi}_g(\rho, z)$ must represent an outgoing exponentially decaying wave; and as $z \rightarrow +\infty$, $\tilde{\Pi}_3(\rho, z)$ must represent an outgoing wave.

The solution to equation (2.21) is

$$\tilde{\Pi}_g(\rho, z) = A_g(\rho) e^{i\gamma z} , \quad (2.26)$$

where

$$\gamma = k[n_g^2 - \beta^2]^{1/2} \quad (2.27)$$

and

$$\beta = \frac{\rho}{k} . \quad (2.28)$$

With time dependence $e^{+i\omega t}$, equation (2.26) represents an outgoing wave as $z \rightarrow -\infty$. If the branch of the square root in equation (2.27) is chosen so that

$$\operatorname{Im}(\gamma) < 0 , \quad (2.29)$$

then as $z \rightarrow -\infty$, $|\tilde{\Pi}_g(\rho, z)|$ decays exponentially.

The complete solution of equation (2.20) will be the sum of the general solution of the homogeneous equation corresponding to (2.20) and a particular solution of the inhomogeneous equation. With the new independent variables

$$q_j(z) = \left(\frac{k}{|\alpha_j|} \right)^{2/3} [m_j^2(z) - \beta^2] \quad (j = 1, 2, 3) , \quad (2.30)$$

the homogeneous equation corresponding to (2.20) can be written as

$$\left\{ \frac{d^2}{dq_j^2} + q_j \right\} \tilde{\Pi}_j(\rho, q_j) = 0 \quad (j = 1, 2, 3) . \quad (2.31)$$

This is Stokes' differential equation and its solution can be written as

$$\tilde{\Pi}_j(\rho, q_j) = A_j(\rho) f_j(q_j) + B_j(\rho) g_j(q_j) \quad (j = 1, 2, 3) , \quad (2.32)$$

where $f_j(\xi)$ and $g_j(\xi)$ are any two linearly independent combinations of Airy functions. The functions $f_j(\xi)$ and $g_j(\xi)$ need not be the same combinations of Airy functions in each atmospheric layer. For numerical purposes it is convenient to choose [2]

$$f_j(\xi) = k_1(\xi) \quad (j = 1, 2) , \quad (2.33)$$

$$f_3(\xi) = h_1(\xi) - e^{-4\pi i/3} h_2(\xi) , \quad (2.34)$$

$$g_j(\xi) = k_2(\xi) \quad (j = 1, 2) , \quad (2.35)$$

and

$$g_3(\xi) = h_2(\xi) , \quad (2.36)$$

where the modified Hankel functions [13], $h_1(\xi)$ and $h_2(\xi)$, and the functions $k_1(z)$ and $k_2(z)$ are related to each other and the Airy functions through

$$\begin{aligned} k_1(z) &= h_1(z) \\ &= -2i(12)^{1/6} \text{Ai}(-ze^{2\pi i/3}) , \end{aligned} \quad (2.37)$$

$$\begin{aligned} k_2(z) &= h_2(z) - e^{4\pi i/3} h_1(z) \\ &= 2(12)^{1/6} e^{\pi i/6} \text{Ai}(-z) , \end{aligned} \quad (2.38)$$

and

$$h_2(z) = 2i(12)^{1/6} \text{Ai}(-ze^{-2\pi i/3}) . \quad (2.39)$$

Equation (2.32) represents the solution $\tilde{\Pi}(\rho, z)$ for every atmospheric layer except the one the transmitter is in. That is, only for the layer containing $z = z_T$ is equation (2.20) inhomogeneous. Assuming the transmitter to be located in the M -th layer ($M = 1, 2, 3$), two particular solutions to (2.20) are [1, 2]

$$\tilde{\Pi}_M^{(P)}(\rho, q_M) = \begin{cases} R_M k_1(q_{M<}) k_2(q_{M>}) & (M = 1, 2) \\ R_M [h_1(q_{M<}) - e^{-4\pi i/3} h_2(q_{M<})] h_2(q_{M>}) & (M = 3) \end{cases} \quad (2.40)$$

and

$$\tilde{\Pi}_M^{(P)}(\rho, q_M) = \begin{cases} -R_M k_1(q_{M>}) k_2(q_{M<}) & (M = 1, 2) \\ -R_M [h_1(q_{M>}) - e^{-4\pi i/3} h_2(q_{M>})] h_2(q_{M<}) & (M = 3) . \end{cases} \quad (2.41)$$

In these equations

$$q_{M<} = q_M(\min[z, z_T]) , \quad (2.42)$$

$$q_M >= q_M(\max[z, z_T]) , \quad (2.43)$$

and

$$R_M = \frac{p}{W q'_M} . \quad (2.44)$$

In equation (2.44)

$$q'_M = \frac{\partial q_M}{\partial z} = \left(\frac{k}{|\alpha_M|} \right)^{2/3} \alpha_M \quad (2.45)$$

and W is the Wronskian

$$W = f_j(\xi)g'_j(\xi) - f'_j(\xi)g_j(\xi) . \quad (2.46)$$

For the choice of solutions (2.33-2.36), the Wronskian has the constant value

$$W = - \frac{4i}{\pi} \left(\frac{3}{2} \right)^{1/3} \quad (2.47)$$

in all atmospheric layers.

Combining the general solution (2.32) of the homogeneous equation (2.31) with either one of the particular solutions (2.40, 2.41) of the inhomogeneous equation (2.20) yields

$$\tilde{\Pi}_j(\rho, z) = A_j(\rho)k_1(q_j) + B_j(\rho)k_2(q_j) + \tilde{\Pi}_M^{(P)}(\rho, q_M)\delta_{jM} \quad (j = 1, 2) \quad (2.48)$$

and

$$\begin{aligned} \tilde{\Pi}_3(\rho, z) = & A_3(\rho)[h_1(q_3) - e^{-4\pi i/3}h_2(q_3)] + B_3(\rho)h_2(q_3) \\ & + \tilde{\Pi}_M^{(P)}(\rho, q_M)\delta_{3M} , \end{aligned} \quad (2.49)$$

where δ_{jM} is the Kronecker delta

$$\delta_{jM} = \begin{cases} 1 & (j = M) \\ 0 & (j \neq M) . \end{cases} \quad (2.50)$$

For the assumed time dependence, $e^{i\omega t}$, the function (2.49) will represent an outgoing wave as $z \rightarrow +\infty$ if

$$A_3(\rho) = 0 . \quad (2.51)$$

The other coefficients A_j and B_j are determined from the continuity conditions (2.22-2.25). Thus, the coefficients A_j and B_j are solutions of the system of equations

$$\begin{aligned} A_1 k_1(q_{11}) + B_1 k_2(q_{11}) &= \frac{i\gamma}{\alpha_1} \left(\frac{|\alpha_1|}{k} \right)^{2/3} \tilde{\Pi}_1^{(P)}(\rho, q_{11}) \delta_{1M} \\ &- \frac{1}{\alpha_1} \left(\frac{|\alpha_1|}{k} \right)^{2/3} \frac{d}{dz} \left\{ \tilde{\Pi}_1^{(P)}(\rho, q_{11}) \right\} \delta_{1M} , \end{aligned} \quad (2.52)$$

$$\begin{aligned} A_1 k_1(q_{12}) + B_1 k_2(q_{12}) - A_2 k_1(q_{22}) - B_2 k_2(q_{22}) \\ = - \tilde{\Pi}_1^{(P)}(\rho, q_{12}) \delta_{1M} + \tilde{\Pi}_2^{(P)}(\rho, q_{22}) \delta_{2M} , \end{aligned} \quad (2.53)$$

$$\begin{aligned} A_1 k'_1(q_{12}) + B_1 k'_2(q_{12}) - A_2 \left(\left| \frac{\alpha_1}{\alpha_2} \right| \right)^{2/3} \frac{\alpha_2}{\alpha_1} k'_1(q_{22}) - B_2 \left(\left| \frac{\alpha_1}{\alpha_2} \right| \right)^{2/3} \frac{\alpha_2}{\alpha_1} k'_2(q_{22}) \\ = - \frac{1}{\alpha_1} \left(\frac{|\alpha_1|}{k} \right)^{2/3} \frac{d}{dz} \left\{ \tilde{\Pi}_1^{(P)}(\rho, q_{12}) \right\} \delta_{1M} \\ + \frac{1}{\alpha_1} \left(\frac{|\alpha_1|}{k} \right)^{2/3} \frac{d}{dz} \left\{ \tilde{\Pi}_2^{(P)}(\rho, q_{22}) \right\} \delta_{2M} , \end{aligned} \quad (2.54)$$

$$\begin{aligned} A_2 k_1(q_{23}) + B_2 k_2(q_{23}) - B_3 h_2(q_{33}) \\ = - \tilde{\Pi}_2^{(P)}(\rho, q_{23}) \delta_{2M} + \tilde{\Pi}_3^{(P)}(\rho, q_{33}) \delta_{3M} , \end{aligned} \quad (2.55)$$

and

$$\begin{aligned} A_2 k'_1(q_{23}) + B_2 k'_2(q_{23}) - B_3 \left(\left| \frac{\alpha_2}{\alpha_3} \right| \right)^{2/3} \frac{\alpha_3}{\alpha_2} h'_2(q_{33}) \\ = - \frac{1}{\alpha_2} \left(\frac{|\alpha_2|}{k} \right)^{2/3} \frac{d}{dz} \left\{ \tilde{\Pi}_2^{(P)}(\rho, q_{23}) \right\} \delta_{2M} \end{aligned}$$

$$+ \frac{1}{\alpha_2} \left(\frac{|\alpha_2|}{k} \right)^{2/3} \frac{d}{dz} \left\{ \tilde{\Pi}_3^{(P)}(\rho, q_{33}) \right\} \delta_{3M} , \quad (2.56)$$

where

$$k_1(q_{11}) = k'_1(q_{11}) - G_{SH} k_1(q_{11}) \quad (2.57)$$

and

$$k_2(q_{11}) = k'_2(q_{11}) - G_{SH} k_2(q_{11}) \quad (2.58)$$

with

$$G_{SH} = \frac{i\gamma}{\alpha_1} \left(\frac{|\alpha_1|}{k} \right)^{2/3}$$

$$= i \left(\frac{k}{\alpha_1} \right)^{1/3} \sqrt{n_g^2 - \beta^2} \quad (\alpha_1 > 0) . \quad (2.59)$$

The notation $q_{j\ell}$ means

$$q_{j\ell} = q_j(z_\ell) \quad (2.60)$$

and

$$q_{jT} = q_j(z_T) . \quad (2.61)$$

in equations (2.52-2.56) the prime denotes the derivative with respect to the argument.

The derivatives $\frac{d}{dz} \left\{ \tilde{\Pi}_j^{(P)}(\rho, q_{jj}) \right\}$ in equations (2.52-2.56) are equal to

$$\frac{d}{dz} \left\{ \tilde{\Pi}_j^{(P)}(\rho, q_{jj}) \right\} = \left(\frac{k}{|\alpha_j|} \right)^{2/3} \alpha_j R_j k'_1(q_{jj}) k_2(q_{jT}) \quad (j = 1, 2) , \quad (2.62)$$

$$\frac{d}{dz} \left\{ \tilde{\Pi}_3^{(P)}(\rho, q_{33}) \right\} = \left(\frac{k}{|\alpha_3|} \right)^{2/3} \alpha_3 R_3 \left[h'_1(q_{33}) - e^{-4\pi i/3} h'_2(q_{33}) \right] h_2(q_{3T}) , \quad (2.63)$$

$$\frac{d}{dz} \left\{ \tilde{n}_j^{(P)}(\rho, q_{j,j+1}) \right\} = \left(\frac{k}{|\alpha_j|} \right)^{2/3} \alpha_j R_j k_1(q_{jT}) k_2(q_{j,j+1}) \quad (j = 1, 2) , \quad (2.64)$$

or

$$\frac{d}{dz} \left\{ \tilde{n}_j^{(P)}(\rho, q_{jj}) \right\} = - \left(\frac{k}{|\alpha_j|} \right)^{2/3} \alpha_j R_j k_1(q_{jT}) k_2'(q_{jj}) \quad (j = 1, 2) , \quad (2.65)$$

$$\frac{d}{dz} \left\{ \tilde{n}_3^{(P)}(\rho, q_{33}) \right\} = - \left(\frac{k}{|\alpha_3|} \right)^{2/3} \alpha_3 R_3 \left[h_1(q_{3T}) - e^{-4\pi i/3} h_2(q_{3T}) \right] h_2'(q_{33}) , \quad (2.66)$$

$$\frac{d}{dz} \left\{ \tilde{n}_j^{(P)}(\rho, q_{j,j+1}) \right\} = - \left(\frac{k}{|\alpha_j|} \right)^{2/3} \alpha_j R_j k_1'(q_{j,j+1}) k_2(q_{jT}) \quad (j = 1, 2) , \quad (2.67)$$

depending upon the choice of particular solution (2.40, 2.41).

In matrix notation, equations (2.52-2.56) may be written as

$$\underline{\Delta} \underline{\xi} = \bar{\underline{\beta}} , \quad (2.68)$$

where the coefficient matrix $\underline{\Delta}$ is given by

$$\underline{\Delta} = \begin{pmatrix} \Delta_{11} & \Delta_{12} & 0 & 0 & 0 \\ \Delta_{21} & \Delta_{22} & \Delta_{23} & \Delta_{24} & 0 \\ \Delta_{31} & \Delta_{32} & \Delta_{33} & \Delta_{34} & 0 \\ 0 & 0 & \Delta_{43} & \Delta_{44} & \Delta_{45} \\ 0 & 0 & \Delta_{53} & \Delta_{54} & \Delta_{55} \end{pmatrix} \quad (2.69)$$

and the vectors $\underline{\xi}$ and $\bar{\underline{\beta}}$ are equal to

$$\underline{\xi} = \begin{pmatrix} A_1 \\ B_1 \\ A_2 \\ B_2 \\ B_3 \end{pmatrix} \quad (2.70)$$

and

$$\bar{\beta} = \begin{pmatrix} \beta_1 \\ \beta_2 \\ \beta_3 \\ \beta_4 \\ \beta_5 \end{pmatrix} \quad (2.71)$$

The non-zero elements of the 5×5 coefficient matrix Δ are

$$\Delta_{11} = k_1(q_{11}) , \quad (2.72)$$

$$\Delta_{12} = k_2(q_{11}) , \quad (2.73)$$

$$\Delta_{21} = k_1(q_{12}) , \quad (2.74)$$

$$\Delta_{22} = k_2(q_{12}) , \quad (2.75)$$

$$\Delta_{23} = -k_1(q_{22}) , \quad (2.76)$$

$$\Delta_{24} = -k_2(q_{22}) , \quad (2.77)$$

$$\Delta_{31} = k_1'(q_{12}) , \quad (2.78)$$

$$\Delta_{32} = k_2'(q_{12}) , \quad (2.79)$$

$$\Delta_{33} = - \left(\frac{|\alpha_1|}{|\alpha_2|} \right)^{2/3} \frac{\alpha_2}{\alpha_1} k_1'(q_{22}) , \quad (2.80)$$

$$\Delta_{34} = - \left(\frac{|\alpha_1|}{|\alpha_2|} \right)^{2/3} \frac{\alpha_2}{\alpha_1} k_2'(q_{22}) , \quad (2.81)$$

$$\Delta_{43} = k_1(q_{23}) , \quad (2.82)$$

$$\Delta_{44} = k_2(q_{23}) , \quad (2.83)$$

$$\Delta_{45} = -h_2(q_{33}) , \quad (2.84)$$

$$\Delta_{53} = k_1'(q_{23}) , \quad (2.85)$$

$$\Delta_{54} = k_2'(q_{23}) , \quad (2.86)$$

and

$$\Delta_{55} = - \left(\frac{|\alpha_2|}{|\alpha_3|} \right)^{2/3} \frac{\alpha_3 h_2'(q_{33})}{\alpha_2} . \quad (2.87)$$

The elements of the vector $\bar{\beta}$ are

$$\begin{aligned} \beta_1 &= \frac{i\gamma}{\alpha_1} \left(\frac{|\alpha_1|}{k} \right)^{2/3} \tilde{\Pi}_1^{(P)}(\rho, q_{11}) \delta_{1M} \\ &\quad - \frac{1}{\alpha_1} \left(\frac{|\alpha_1|}{k} \right)^{2/3} \frac{d}{dz} \left\{ \tilde{\Pi}_1^{(P)}(\rho, q_{11}) \right\} \delta_{1M} , \end{aligned} \quad (2.88)$$

$$\beta_2 = - \tilde{\Pi}_1^{(P)}(\rho, q_{12}) \delta_{1M} + \tilde{\Pi}_2^{(P)}(\rho, q_{22}) \delta_{2M} , \quad (2.89)$$

$$\begin{aligned} \beta_3 &= - \frac{1}{\alpha_1} \left(\frac{|\alpha_1|}{k} \right)^{2/3} \frac{d}{dz} \left\{ \tilde{\Pi}_1^{(P)}(\rho, q_{12}) \right\} \delta_{1M} \\ &\quad + \frac{1}{\alpha_1} \left(\frac{|\alpha_1|}{k} \right)^{2/3} \frac{d}{dz} \left\{ \tilde{\Pi}_2^{(P)}(\rho, q_{22}) \right\} \delta_{2M} , \end{aligned} \quad (2.90)$$

$$\beta_4 = - \tilde{\Pi}_2^{(P)}(\rho, q_{23}) \delta_{2M} + \tilde{\Pi}_3^{(P)}(\rho, q_{23}) \delta_{3M} , \quad (2.91)$$

and

$$\begin{aligned} \beta_5 &= - \frac{1}{\alpha_2} \left(\frac{|\alpha_2|}{k} \right)^{2/3} \frac{d}{dz} \left\{ \tilde{\Pi}_2^{(P)}(\rho, q_{23}) \right\} \delta_{2M} \\ &\quad + \frac{1}{\alpha_2} \left(\frac{|\alpha_2|}{k} \right)^{2/3} \frac{d}{dz} \left\{ \tilde{\Pi}_3^{(P)}(\rho, q_{33}) \right\} \delta_{3M} . \end{aligned} \quad (2.92)$$

The solution for the unknown coefficients A_j and B_j may be obtained from equation (2.68) by using Cramer's rule [14]. Thus

$$A_j = \frac{||\tilde{\alpha}_j||}{||\tilde{\alpha}||} \quad (2.93)$$

and

$$B_j = \frac{||\tilde{\beta}_j||}{||\tilde{\alpha}||} , \quad (2.94)$$

where for $j = 1, 2$, the matrix $\tilde{\mathcal{L}}_{Aj}$ is obtained by replacing the column of $\tilde{\Delta}$ in equation (2.69) containing the coefficients of A_j with the vector $\tilde{\beta}$; and for $j = 3$, $||\tilde{\mathcal{L}}_{A3}|| = 0$. The matrix $\tilde{\mathcal{L}}_{Bj}$ is obtained by replacing the column of $\tilde{\Delta}$ containing the coefficients of B_j with the vector $\tilde{\beta}$. The notation $||\tilde{\Delta}||$ indicates the determinant of the matrix $\tilde{\Delta}$.

Substituting equations (2.93, 2.94) into equations (2.48, 2.49) yields

$$\begin{aligned}\tilde{\Pi}_j(\rho, z) &= \frac{1}{||\tilde{\Delta}||} \{ ||\tilde{\mathcal{L}}_{Aj}|| k_1(q_j) + ||\tilde{\mathcal{L}}_{Bj}|| k_2(q_j) \} \\ &\quad + \tilde{\Pi}_M^{(P)}(\rho, q_M) \delta_{jM} \quad (j = 1, 2)\end{aligned}\quad (2.95)$$

and

$$\tilde{\Pi}_3(\rho, z) = \frac{1}{||\tilde{\Delta}||} \{ ||\tilde{\mathcal{L}}_{B3}|| h_2(q_3) \} + \tilde{\Pi}_M^{(P)}(\rho, q_M) \delta_{3M} . \quad (2.96)$$

From equation (2.19), the Hertz magnetic potential $\Pi_j(r, z)$ can be expressed as the contour integral

$$\Pi_j(r, z) = \frac{1}{4\pi} \int_C \rho d\rho H_0^{(2)}(\rho r) \tilde{\Pi}_j(\rho, z) , \quad (2.97)$$

where the contour C is shown in figure 2. By closing the contour C and using the theory of residues, equation (2.97) becomes

$$\begin{aligned}\Pi_j(r, z) &= -\frac{2\pi i}{4\pi} \sum_n b_j(n) + \frac{1}{4\pi} \int_{C_1} \rho d\rho H_0^{(2)}(\rho r) \tilde{\Pi}_j(\rho, z) \\ &\quad + \frac{1}{4\pi} \int_B \rho d\rho H_0^{(2)}(\rho r) \tilde{\Pi}_j(\rho, z) ,\end{aligned}\quad (2.98)$$

where the $b_j(n)$ are the residues of $\rho H_0^{(2)}(\rho r) \tilde{\Pi}_j(\rho, z)$ at the poles of $\tilde{\Pi}_j(\rho, z)$ in the fourth quadrant; the contour C_1 is the quarter-circle of infinite radius lying in the fourth quadrant; and the contour B encloses the branch cut which is present as a result of the square root in the expression for γ in equation (2.27). Through use of the asymptotic approximations for the Hankel and Airy functions it can be shown that

$$\frac{1}{4\pi} \int_{C_1} \rho d\rho H_0^{(2)}(\rho r) \tilde{\Pi}_j(\rho, z) = 0 . \quad (2.99)$$

The integral over the contour B represents the surface wave contribution to the total field and is assumed to be small relative to the other field contributions. Therefore,

$$\Pi_j(r, z) \approx -\frac{i}{2} \sum_n b_j(n) . \quad (2.100)$$

The residues $b_j(n)$ are given by [2]

$$b_j(n) = \rho_n H_o^{(2)}(\rho_n r) \frac{\left\{ ||\xi_{Aj}|| k_1(q_j) + ||\xi_{Bj}|| k_2(q_j) \right\}_{\rho=\rho_n}}{\left\{ \frac{\partial}{\partial \rho} ||\Delta|| \right\}_{\rho=\rho_n}} \quad (j = 1, 2) \quad (2.101)$$

and

$$b_3(n) = \rho_n H_o^{(2)}(\rho_n r) \frac{\left\{ ||\xi_{B3}|| h_2(q_3) \right\}_{\rho=\rho_n}}{\left\{ \frac{\partial}{\partial \rho} ||\Delta|| \right\}_{\rho=\rho_n}} , \quad (2.102)$$

where ρ_n is the n-th value of ρ for which $||\Delta|| = 0$.

Substituting equations (2.101, 2.102) into (2.100) yields

$$\Pi_j(r, z) = -\frac{i}{2} \sum_n \lambda_n E(n, z, z_T) \sqrt{\rho_n} H_o^{(2)}(\rho_n r) , \quad (2.103)$$

where

$$\begin{aligned} \lambda_n &= \frac{\sqrt{\rho_n}}{\left\{ \frac{\partial}{\partial \rho} ||\Delta|| \right\}_{\rho=\rho_n}} \\ &= \frac{k^2}{2\sqrt{\rho_n} \left(\frac{k}{|\alpha_1|} \right)^{2/3} \left\{ \frac{\partial}{\partial q} ||\Delta|| \right\}_{q_{11}=q_{11}(\rho_n)}} \end{aligned} \quad (2.104)$$

is the modal excitation factor and

$$E(n, z, z_T) = \begin{cases} \{ ||\zeta_{Aj}||k_1(q_j) + ||\zeta_{Bj}||k_2(q_j) \}_{\rho=\rho_n} & (j = 1, 2) \\ \{ ||\zeta_{B3}||h_2(q_3) \}_{\rho=\rho_n} & (j = 3) \end{cases} \quad (2.105)$$

is the modal height-gain function.

For the cases of interest $|\rho_n r| \gg 1$, so that the asymptotic approximation [15]

$$H_o^{(2)}(\rho_n r) \sim \left(\frac{2}{\pi \rho_n r} \right)^{1/2} \exp(-i\rho_n r + i\frac{\pi}{4}) \quad (2.106)$$

can be used in equation (2.103). This yields

$$\Pi_j(r, z) = - \frac{i}{\sqrt{2\pi r}} e^{i\pi/4} \sum_n \lambda_n E(n, z, z_T) e^{-i\rho_n r} . \quad (2.107)$$

Rather than evaluate the fields by using equation (2.107) together with equations (2.17, 2.18), it is more convenient to evaluate the magnitude of the electric field relative to its free space value. This is given by [2]

$$A_{coh} = \frac{|\bar{E}|}{|\bar{E}_{fs}|} = \frac{2\sqrt{2\pi r}}{p} \left| \sum_n \lambda_n E(n, z, z_T) e^{-i\rho_n r} \right| , \quad (2.108)$$

where p is the magnetic dipole strength. This expression takes into account the phase of each term in the sum and is known as the coherent mode sum. It is also useful to define the relative field strength that results when the phase of each term in (2.107) is ignored. This is the incoherent mode sum [2]

$$A_{incoh} = \frac{2\sqrt{2\pi r}}{p} \left[\sum_n |\lambda_n E(n, z, z_T) e^{-i\rho_n r}|^2 \right]^{1/2} . \quad (2.109)$$

Because $E(n, z, z_T)$ is proportional to $R_M = \frac{p}{Wq_M}$ through the coefficients A_j and B_j , the factor of p in $E(n, z, z_T)$ will cancel the factor of p^{-1} in the expressions (2.108, 2.109) for A_{coh} and A_{incoh} .

VERTICALLY POLARIZED WAVE PROPAGATION

Vertically polarized waves may be considered to be due to a radiating electric dipole \bar{p}_e oriented in the z -direction and located at $x = y = 0$, $z = z_T$. A time dependence of $e^{+i\omega t}$ again will be assumed. The medium again is assumed to be laterally homogeneous so that the fields due to the dipole exhibit axial symmetry. Because of the variation of the permittivity ϵ with height above the surface of the earth, the equations

$$\bar{H}(r, z) = i\epsilon\omega\bar{\nabla} \times \bar{\Pi}^*(r, z) \quad (2.110)$$

and

$$\bar{E}(r, z) = \bar{\nabla} \times \bar{\nabla} \times \bar{\Pi}^*(r, z) , \quad (2.111)$$

relating the electric and magnetic fields to the electric Hertz potential vector

$$\bar{\Pi}^*(r, z) = \Pi^*(r, z)\bar{e}_z , \quad (2.112)$$

are only approximately consistent with Maxwell's equations. However, because the variation of ϵ_r with height z in the atmosphere is so small, equations (2.110, 2.111) constitute a good approximation [11].

The calculation of the electric Hertz potential $\Pi^*(r, z)$ proceeds exactly as the calculation of the magnetic Hertz potential $\Pi(r, z)$, with some minor modifications. The magnetic dipole strength p in the differential equation (2.20) should be replaced by

$$p^* = \frac{p_e}{\epsilon} . \quad (2.113)$$

This yields the differential equation

$$\left\{ \frac{d^2}{dz^2} + k^2 \left[m_j^2(z) - \frac{\rho^2}{k^2} \right] \right\} \tilde{\Pi}_j^*(\rho, z) = -p^* \delta(z - z_T) . \quad (2.114)$$

The continuity conditions (2.22-2.25) become

$$\frac{n^2}{g} \tilde{n}_1^*(\rho, o) = n_1^2(o) \tilde{n}_1^*(\rho, o) , \quad (2.115)$$

$$\frac{d}{dz} \{ \tilde{n}_1^*(\rho, o) \} = \frac{d}{dz} \{ \tilde{n}_1^*(\rho, o) \} , \quad (2.116)$$

$$\tilde{n}_j^*(\rho, z_{j+1}) = \tilde{n}_{j+1}^*(\rho, z_{j+1}) \quad (j = 1, 2) , \quad (2.117)$$

and

$$\frac{d}{dz} \{ \tilde{n}_j^*(\rho, z_{j+1}) \} = \frac{d}{dz} \{ \tilde{n}_{j+1}^*(\rho, z_{j+1}) \} \quad (j = 1, 2) . \quad (2.118)$$

The particular solutions $\tilde{n}_M^{*(P)}(\rho, z)$ of (2.114) are the same as the particular solutions $\tilde{n}_M^{(P)}(\rho, z)$ given by equations (2.40, 2.41) except that R_M is replaced by

$$R_M^* = \frac{p^*}{Wq'_M} . \quad (2.119)$$

The system of equations (2.68) becomes

$$\tilde{\Delta}^* \tilde{\zeta}^* = \tilde{\beta}^* . \quad (2.120)$$

The elements of the coefficient matrix $\tilde{\Delta}^*$ are identical to the elements of $\tilde{\Delta}$ in equations (2.72-2.87) except that $\hat{k}_1(q_{11})$ and $\hat{k}_2(q_{11})$, as given by equations (2.57, 2.58), are now equal to

$$\hat{k}_1(q_{11}) = k'_1(q_{11}) - G_{SV} k_1(q_{11}) \quad (2.121)$$

and

$$\hat{k}_2(q_{11}) = k'_2(q_{11}) - G_{SV} k_2(q_{11}) , \quad (2.122)$$

where

$$G_{SV} = \frac{i\gamma}{\alpha_1} \left(\frac{|\alpha_1|}{k} \right)^{2/3} \frac{n_1^2(0)}{n^2 g} . \quad (2.123)$$

This change is due to the continuity condition (2.115). When considering the field strength relative to its free space value, the dipole strength p^* cancels out in the final results for A_{coh}^* and A_{incoh}^* , just as p does in A_{coh} and A_{incoh} . Therefore, the only significant change for vertical polarization

is the replacement of G_{SH} by G_{SV} in the expressions for $\hat{k}_1(q_{11})$ and $\hat{k}_2(q_{11})$, due to the changed continuity condition (2.115).

TRILINEAR DUCT MODAL FUNCTION

When evaluating the field strength relative to its free space value, equations (2.108, 2.109), the values $\rho = \rho_n$ for which $||\tilde{\Delta}|| = 0$ are needed. The determinant $||\tilde{\Delta}||$ is known as the modal function. The values $\rho = \rho_n$ for which $||\tilde{\Delta}|| = 0$ are the eigenvalues of the problem, each eigenvalue representing a different electromagnetic mode that propagates in the atmospheric waveguide formed by the trilinear refractivity profile. In XWVG the zeros of $||\tilde{\Delta}||$ are found by using the complex root-finding routine of Shellman and Morfitt, which will be discussed in a later section of this report. First, explicit formulas will be given for the modal function, its derivative, and the modal height-gain functions for the case of a trilinear refractivity profile.

The determinant of the coefficient matrix $\tilde{\Delta}$, equation (2.69), can be expanded to obtain

$$||\tilde{\Delta}|| = \mp \left(\frac{\alpha_3}{|\alpha_2|} \right)^{1/3} \left\{ \mp \left(\frac{|\alpha_2|}{\alpha_1} \right)^{1/3} [\zeta(q_{11})\chi(q_{11}) + \psi(q_{11})\phi(q_{11})] \right\}, \quad (2.124)$$

where both α_1 and α_3 are positive and the top sign is to be taken if $\alpha_2 > 0$ and the bottom sign if $\alpha_2 < 0$. The auxiliary functions $\zeta(q_{11})$, $\chi(q_{11})$, $\psi(q_{11})$, and $\phi(q_{11})$ are given by

$$\zeta(q_{11}) = k_2(q_{12})\hat{k}_1(q_{11}) - k_1(q_{12})\hat{k}_2(q_{11}), \quad (2.125)$$

$$\begin{aligned} \chi(q_{11}) = h_2'(q_{33})[k_1'(q_{22})k_2(q_{23}) - k_2'(q_{22})k_1(q_{23})] \\ \mp \left(\frac{|\alpha_2|}{\alpha_3} \right)^{1/3} h_2(q_{33})[k_1'(q_{22})k_2'(q_{23}) - k_2'(q_{22})k_1'(q_{23})], \end{aligned} \quad (2.126)$$

$$\psi(q_{11}) = k_2'(q_{12})\hat{k}_1(q_{11}) - k_1'(q_{12})\hat{k}_2(q_{11}), \quad (2.127)$$

and

$$\begin{aligned} \phi(q_{11}) = h_2'(q_{33})[k_1(q_{22})k_2(q_{23}) - k_2(q_{22})k_1(q_{23})] \\ \mp \left(\frac{|\alpha_2|}{\alpha_3} \right)^{1/3} h_2(q_{33})[k_1(q_{22})k_2'(q_{23}) - k_2(q_{22})k_1'(q_{23})]. \end{aligned} \quad (2.128)$$

The arguments q_{ij} appearing in equations (2.125-2.128) are equal to

$$q_{11} = \left(\frac{k}{\alpha_1}\right)^{2/3} [1 + i\eta - \alpha_1 H - \beta^2], \quad (2.129)$$

$$q_{12} = q_{11} + \left(\frac{k}{\alpha_1}\right)^{2/3} \alpha_1 z_2, \quad (2.130)$$

$$q_{22} = \left(\frac{\alpha_1}{|\alpha_2|}\right)^{2/3} q_{11} + \left(\frac{k}{|\alpha_2|}\right)^{2/3} \alpha_1 z_2, \quad (2.131)$$

$$q_{23} = \left(\frac{\alpha_1}{|\alpha_2|}\right)^{2/3} q_{11} + \left(\frac{k}{|\alpha_2|}\right)^{2/3} [\alpha_1 z_2 + \alpha_2 (z_3 - z_2)], \quad (2.132)$$

and

$$q_{33} = \left(\frac{\alpha_1}{\alpha_3}\right)^{2/3} q_{11} + \left(\frac{k}{\alpha_3}\right)^{2/3} [\alpha_1 z_2 + \alpha_2 (z_3 - z_2)], \quad (2.133)$$

with

$$\beta^2 = \frac{\rho^2}{k^2}. \quad (2.134)$$

The functions $k_1(q_{11})$ and $k_2(q_{11})$ are given by

$$k_1(q_{11}) = k'_1(q_{11}) - G_S k_1(q_{11}) \quad (2.135)$$

and

$$k_2(q_{11}) = k'_2(q_{11}) - G_S k_2(q_{11}), \quad (2.136)$$

where

$$G_S = G_{SH} = \frac{ik}{\alpha_1} \left(\frac{|\alpha_1|}{k}\right)^{2/3} \sqrt{n_g^2 - \beta^2} \quad (2.137)$$

for horizontal polarization and

$$G_S = G_{SV} = \frac{n_1^2(0)}{n_g^2} G_{SH} \quad (2.138)$$

for vertical polarization.

The derivative of the modal function $||\Delta||$ with respect to q_{11} is needed by the Shellman and Morfitt root-finding routine. The derivative is also needed for the evaluation of the modal excitation factors λ_n . Taking the derivative of equation (2.124) and making use of Stokes' differential equation to eliminate the second derivatives that occur yields

$$\frac{\partial}{\partial q_{11}} \{ ||\Delta|| \} = \mp \left(\frac{\alpha_3}{|\alpha_2|} \right)^{1/3} \left\{ \mp \left(\frac{|\alpha_2|}{\alpha_1} \right)^{1/3} \left[\zeta'(q_{11}) \chi(q_{11}) + \zeta(q_{11}) \chi'(q_{11}) \right] \right. \\ \left. + [\psi'(q_{11}) \phi(q_{11}) + \psi(q_{11}) \phi'(q_{11})] \right\}, \quad (2.139)$$

where again the upper sign is to be taken when $\alpha_2 > 0$ and the lower sign when $\alpha_2 < 0$. The derivatives with respect to q_{11} of the auxiliary functions are

$$\zeta'(q_{11}) = k_2'(q_{12}) k_1(q_{11}) - k_1'(q_{12}) k_2(q_{11}) + k_1(q_{12}) \left\{ \left[q_{11} + \frac{\partial G_S}{\partial q_{11}} \right] k_2(q_{11}) \right. \\ \left. + G_S k_2'(q_{11}) \right\} - k_2(q_{12}) \left\{ \left[q_{11} + \frac{\partial G_S}{\partial q_{11}} \right] k_1(q_{11}) + G_S k_1'(q_{11}) \right\}, \quad (2.140)$$

$$\chi'(q_{11}) = - q_{33} \left(\frac{\alpha_1}{\alpha_3} \right)^{2/3} h_2(q_{33}) [k_1'(q_{22}) k_2(q_{23}) - k_2'(q_{22}) k_1(q_{23})] \\ + \left(\frac{\alpha_1}{|\alpha_2|} \right)^{2/3} h_2'(q_{33}) \{ q_{22} [k_2(q_{22}) k_1(q_{23}) - k_1(q_{22}) k_2(q_{23})] \\ + [k_1'(q_{22}) k_2'(q_{23}) - k_2'(q_{22}) k_1'(q_{23})] \} \\ \mp \left(\frac{|\alpha_2|}{\alpha_3} \right)^{1/3} \left(\frac{\alpha_1}{\alpha_3} \right)^{2/3} h_2'(q_{33}) [k_1'(q_{22}) k_2'(q_{23}) - k_2'(q_{22}) k_1'(q_{23})] \\ \mp \left(\frac{|\alpha_2|}{\alpha_3} \right)^{1/3} \left(\frac{\alpha_1}{|\alpha_2|} \right)^{2/3} h_2(q_{33}) \{ q_{22} [k_2(q_{22}) k_1'(q_{23}) \\ - k_1(q_{22}) k_2'(q_{23})] + q_{23} [k_2'(q_{22}) k_1(q_{23}) - k_1'(q_{22}) k_2(q_{23})] \}, \quad (2.141)$$

$$\begin{aligned}\Psi'(q_{11}) = & -q_{12}k_2(q_{12})k_1(q_{11}) - k_2'(q_{12}) \left\{ \left[q_{11} + \frac{\partial G_S}{\partial q_{11}} \right] k_1(q_{11}) + G_S k_1'(q_{11}) \right\} \\ & + q_{12}k_1(q_{12})k_2(q_{11}) + k_1'(q_{12}) \left\{ \left[q_{11} + \frac{\partial G_S}{\partial q_{11}} \right] k_2(q_{11}) + G_S k_2'(q_{11}) \right\}, \quad (2.142)\end{aligned}$$

and

$$\begin{aligned}\Phi'(q_{11}) = & -q_{33} \left(\frac{\alpha_1}{\alpha_3} \right)^{2/3} h_2(q_{33}) [k_1(q_{22})k_2(q_{23}) - k_2(q_{22})k_1(q_{23})] \\ & + \left(\frac{\alpha_1}{|\alpha_2|} \right)^{2/3} h_2'(q_{33}) \{ [k_1'(q_{22})k_2(q_{23}) - k_2'(q_{22})k_1(q_{23})] \\ & + [k_1(q_{22})k_2'(q_{23}) - k_2(q_{22})k_1'(q_{23})] \} \\ & \mp \left(\frac{|\alpha_2|}{\alpha_3} \right)^{1/3} \left(\frac{\alpha_1}{\alpha_3} \right)^{2/3} h_2'(q_{33}) [k_1(q_{22})k_2'(q_{23}) - k_2(q_{22})k_1'(q_{23})] \\ & \mp \left(\frac{|\alpha_2|}{\alpha_3} \right)^{1/3} \left(\frac{\alpha_1}{|\alpha_2|} \right)^{2/3} h_2(q_{33}) \{ [k_1'(q_{22})k_2'(q_{23}) - k_2'(q_{22})k_1'(q_{23})] \\ & - q_{23} [k_1(q_{22})k_2(q_{23}) - k_2(q_{22})k_1(q_{23})] \}. \quad (2.143)\end{aligned}$$

For horizontal polarization

$$\frac{\partial G_S}{\partial q_{11}} = \frac{\partial G_{SH}}{\partial q_{11}} = \frac{i}{2} \left(\frac{\alpha_1}{k} \right)^{1/3} \left[n_g^2 - \beta^2 \right]^{-1/2}, \quad (2.144)$$

while for vertical polarization

$$\frac{\partial G_S}{\partial q_{11}} = \frac{\partial G_{SV}}{\partial q_{11}} = \frac{n_g^2(0)}{n_g^2} \frac{\partial G_{SH}}{\partial q_{11}}. \quad (2.145)$$

TRILINEAR DUCT MODAL HEIGHT-GAIN FUNCTIONS

The height-gain function corresponding to the n-th mode is

$$E(n, z, z_T) = \begin{cases} \{ ||\tilde{\tau}_{Aj}|| k_1(q_j) + ||\tilde{\tau}_{Bj}|| k_2(q_j) \}_{\rho=\rho_n} & (j = 1, 2) \\ \{ ||\tilde{\tau}_{B3}|| h_2(q_3) \}_{\rho=\rho_n} & (j = 3) \end{cases} \quad (2.146)$$

When $j = 1, 2$, the matrix $\tilde{\tau}_{Aj}$ is the matrix obtained by replacing the column of the matrix $\tilde{\Delta}$, equation (2.69), containing the coefficients of A_j by the vector $\bar{\beta}$; and when $j = 3$, $||\tilde{\tau}_{A3}|| = 0$. The matrix $\tilde{\tau}_{Bj}$ is obtained by replacing the column of $\tilde{\Delta}$ containing the coefficients of B_j by the vector $\bar{\beta}$. For example, $\tilde{\tau}_{B2}$ is given by

$$\tilde{\tau}_{B2} = \begin{pmatrix} \Delta_{11} & \Delta_{12} & 0 & \beta_1 & 0 \\ \Delta_{21} & \Delta_{22} & \Delta_{23} & \beta_2 & 0 \\ \Delta_{31} & \Delta_{32} & \Delta_{33} & \beta_3 & 0 \\ 0 & 0 & \Delta_{43} & \beta_4 & \Delta_{45} \\ 0 & 0 & \Delta_{53} & \beta_5 & \Delta_{55} \end{pmatrix} \quad (2.147)$$

The elements of the matrix $\tilde{\Delta}$ are given by equations (2.72-2.87) and the elements of the vector $\bar{\beta}$ are given by equations (2.88-2.92).

The elements of the vector $\bar{\beta}$ depend upon the choice of particular solution. Theoretically, either of the particular solutions

$$\tilde{\pi}_M^{(P)}(\rho, q_M) = \begin{cases} R_M k_1(q_{M<}) k_2(q_{M>}) & (M = 1, 2) \\ R_M [h_1(q_{M<}) - e^{-4\pi i/3} h_1(q_{M>})] h_2(q_{M>}) & (M = 3) \end{cases} \quad (2.148)$$

or

$$\tilde{\pi}_M^{(P)}(\rho, q_M) = \begin{cases} -R_M k_1(q_{M>}) k_2(q_{M<}) & (M = 1, 2) \\ -R_M [h_1(q_{M>}) - e^{-4\pi i/3} h_1(q_{M>})] h_2(q_{M<}) & (M = 3) \end{cases} \quad (2.149)$$

can be used. Numerically, however, one solution may be preferable to the other. Numerical experience shows that for the trilinear refractivity profiles shown in figure 1, when the transmitter and receiver are both in the first layer or the transmitter is in the second layer and $\frac{dM_2}{dz}$ is negative, the best choice for the particular solution is (2.149). When the transmitter is in the first layer and the receiver is in the second or third layer, when the transmitter is in the second layer and $\frac{dM_2}{dz}$ is positive, or when the transmitter is in the third layer, the best choice for the particular solution is (2.148).

When the transmitter is in the first layer and the receiver is in the first layer, the modal height-gain function is given by

$$\begin{aligned}
 E(n, z_R, z_T) = R_1 \left\{ \left[\left\{ \mp \left(\frac{\alpha_3}{|\alpha_2|} \right)^{1/3} h'_2(q_{33}) k_2(q_{23}) \right. \right. \right. \right. \\
 \left. \left. \left. \left. + h_2(q_{33}) k'_2(q_{23}) \right\} \left\{ \mp \left(\frac{|\alpha_2|}{\alpha_1} \right)^{1/3} k'_1(q_{22}) k_2(q_{12}) + k_1(q_{22}) k'_2(q_{12}) \right\} \right. \right. \\
 \left. \left. \left. \left. + \left\{ \mp \left(\frac{\alpha_3}{|\alpha_2|} \right)^{1/3} h'_2(q_{33}) k_1(q_{23}) + h_2(q_{33}) k'_1(q_{23}) \right\} \left\{ \mp \left(\frac{|\alpha_2|}{\alpha_1} \right)^{1/3} k'_2(q_{22}) k_2(q_{12}) \right. \right. \right. \right. \\
 \left. \left. \left. \left. - k_2(q_{22}) k'_2(q_{12}) \right\} \right] k_2(q_{11}) k_1(q_{1T}) k_1(q_{1R}) + \left[\left\{ \mp \left(\frac{\alpha_3}{|\alpha_2|} \right)^{1/3} h'_2(q_{33}) k_2(q_{23}) \right. \right. \right. \\
 \left. \left. \left. + h_2(q_{33}) k'_2(q_{23}) \right\} \left\{ \mp \left(\frac{|\alpha_2|}{\alpha_1} \right)^{1/3} k'_1(q_{22}) k_1(q_{12}) - k_1(q_{22}) k'_1(q_{12}) \right\} \right. \right. \\
 \left. \left. \left. \left. + \left\{ \mp \left(\frac{\alpha_3}{|\alpha_2|} \right)^{1/3} h'_2(q_{33}) k_1(q_{23}) + h_2(q_{33}) k'_1(q_{23}) \right\} \left\{ \mp \left(\frac{|\alpha_2|}{\alpha_1} \right)^{1/3} k'_2(q_{22}) k_1(q_{12}) \right. \right. \right. \right. \\
 \left. \left. \left. \left. + k_2(q_{22}) k'_1(q_{12}) \right\} \right] k_2(q_{11}) \{ k_2(q_{1T}) k_1(q_{1R}) + k_1(q_{1T}) k_2(q_{1R}) \}
 \end{aligned}$$

$$\begin{aligned}
& + \left[\left\{ \mp \left(\frac{\alpha_3}{|\alpha_2|} \right)^{1/3} h_2'(q_{33}) k_2(q_{23}) + h_2(q_{33}) k_2'(q_{23}) \right\} \left\{ \mp \left(\frac{|\alpha_2|}{\alpha_1} \right)^{1/3} k_1'(q_{22}) k_1(q_{12}) \right. \right. \\
& \quad \left. \left. + k_1(q_{22}) k_1'(q_{12}) \right\} \right. \\
& \quad \left. + \left\{ \mp \left(\frac{\alpha_3}{|\alpha_2|} \right)^{1/3} h_2'(q_{33}) k_1(q_{23}) + h_2(q_{33}) k_1'(q_{23}) \right\} \left\{ \pm \left(\frac{|\alpha_2|}{\alpha_1} \right)^{1/3} k_2'(q_{22}) k_1(q_{12}) \right. \right. \\
& \quad \left. \left. - k_2(q_{22}) k_1'(q_{12}) \right\} \right] k_1(q_{11}) k_2(q_{1T}) k_2(q_{1R}) \right\} \\
& \quad (0 \leq z_R \leq z_2 ; 0 \leq z_T \leq z_2) . \tag{2.150}
\end{aligned}$$

When the transmitter is in the first layer and the receiver is in the second layer, the modal height-gain function is given by

$$\begin{aligned}
E(n, z_R, z_T) = R_1 W \left\{ \left[\mp \left(\frac{\alpha_3}{|\alpha_2|} \right)^{1/3} h_2'(q_{33}) k_2(q_{23}) + h_2(q_{33}) k_2'(q_{23}) \right] k_2(q_{11}) k_1(q_{1T}) k_1(q_{2R}) \right. \\
- \left[\mp \left(\frac{\alpha_3}{|\alpha_2|} \right)^{1/3} h_2'(q_{33}) k_2(q_{23}) + h_2(q_{33}) k_2'(q_{23}) \right] k_1(q_{11}) k_2(q_{1T}) k_1(q_{2R}) \\
- \left[\mp \left(\frac{\alpha_3}{|\alpha_2|} \right)^{1/3} h_2'(q_{33}) k_1(q_{23}) + h_2(q_{33}) k_1'(q_{23}) \right] k_2(q_{11}) k_1(q_{1T}) k_2(q_{2R}) \\
\left. + \left[\mp \left(\frac{\alpha_3}{|\alpha_2|} \right)^{1/3} h_2'(q_{33}) k_1(q_{23}) + h_2(q_{33}) k_1'(q_{23}) \right] k_1(q_{11}) k_2(q_{1T}) k_2(q_{2R}) \right\} \\
(z_2 \leq z_R \leq z_3 ; 0 \leq z_T \leq z_2) . \tag{2.151}
\end{aligned}$$

When the transmitter is in the first layer and the receiver is in the third layer, the modal height-gain function is

$$\begin{aligned}
E(n, z_R, z_T) = -R_1 W^2 [k_1(q_{11}) k_2(q_{1T}) - k_2(q_{11}) k_1(q_{1T})] k_2(q_{3R}) \\
(z_3 \leq z_R ; 0 \leq z_T \leq z_2) . \tag{2.152}
\end{aligned}$$

In the above equations

$$R_1 = \frac{p}{Wq'_1} , \quad (2.153)$$

where p is the magnetic dipole strength, W is the Wronskian of $k_1(\xi)$ and $k_2(\xi)$ and has the value

$$W = - \frac{4i}{\pi} \left(\frac{3}{2} \right)^{1/3} , \quad (2.154)$$

and q'_1 is equal to

$$q'_1 = \frac{\partial q_1}{\partial z} = \left(\frac{k}{\alpha_1} \right)^{2/3} \alpha_1 . \quad (2.155)$$

When the transmitter is in the second layer and the receiver is in the first layer, the modal height-gain function is given by

$$E(n, z_R, z_T) = \pm R_2 W \left(\frac{|\alpha_2|}{\alpha_1} \right)^{1/3} \left\{ \left[\mp \left(\frac{\alpha_3}{|\alpha_2|} \right)^{1/3} h'_2(q_{33}) k_2(q_{23}) \right. \right. \\ \left. \left. + h_2(q_{33}) k'_2(q_{23}) \right] k_2(q_{11}) k_1(q_{2T}) k_1(q_{1R}) \right. \\ \left. - \left[\mp \left(\frac{\alpha_3}{|\alpha_2|} \right)^{1/3} h'_2(q_{33}) k_1(q_{23}) + h_2(q_{33}) k'_1(q_{23}) \right] k_2(q_{11}) k_2(q_{2T}) k_1(q_{1R}) \right. \\ \left. - \left[\mp \left(\frac{\alpha_3}{|\alpha_2|} \right)^{1/3} h'_2(q_{33}) k_2(q_{23}) + h_2(q_{33}) k'_2(q_{23}) \right] k_1(q_{11}) k_1(q_{2T}) k_2(q_{1R}) \right. \\ \left. + \left[\mp \left(\frac{\alpha_3}{|\alpha_2|} \right)^{1/3} h'_2(q_{33}) k_1(q_{23}) + h_2(q_{33}) k'_1(q_{23}) \right] k_1(q_{11}) k_2(q_{2T}) k_2(q_{1R}) \right\} \\ (0 \leq z_R \leq z_2 ; z_2 \leq z_T \leq z_3) . \quad (2.156)$$

When the transmitter is in the second layer and the receiver is in the second layer, the modal height-gain function is

$$\begin{aligned}
 E(n, z_R, z_T) = & R_2 \left\{ \left[\left\{ -\left(\frac{\alpha_3}{|\alpha_2|} \right)^{1/3} h'_2(q_{33}) k_2(q_{23}) + h_2(q_{33}) k'_2(q_{23}) \right\} \left\{ -\left(\frac{|\alpha_2|}{\alpha_1} \right)^{1/3} k'_2(q_{22}) k_2(q_{12}) \right. \right. \right. \\
 & + k_2(q_{22}) k'_2(q_{12}) \left. \right] \hat{k}_1(q_{11}) \\
 & + \left. \left[\left(\frac{|\alpha_2|}{\alpha_1} \right)^{1/3} k'_2(q_{22}) k_1(q_{12}) - k_2(q_{22}) k'_1(q_{12}) \right] \hat{k}_2(q_{11}) \right\} k_1(q_{2T}) k_1(q_{2R}) \\
 & + \left[\left\{ -\left(\frac{\alpha_3}{|\alpha_2|} \right)^{1/3} h'_2(q_{33}) k_2(q_{23}) + h_2(q_{33}) k'_2(q_{23}) \right\} \left\{ \left(\frac{|\alpha_2|}{\alpha_1} \right)^{1/3} k'_1(q_{22}) k_2(q_{12}) \right. \right. \\
 & - k_1(q_{22}) k'_2(q_{12}) \left. \right] \hat{k}_1(q_{11}) \\
 & + \left. \left[-\left(\frac{|\alpha_2|}{\alpha_1} \right)^{1/3} k'_1(q_{22}) k_1(q_{12}) + k_1(q_{22}) k'_1(q_{12}) \right] \hat{k}_2(q_{11}) \right\} k_2(q_{2T}) k_1(q_{2R}) \\
 & + k_1(q_{2T}) k_2(q_{2R}) \Big\} \\
 & + \left[\left\{ -\left(\frac{\alpha_3}{|\alpha_2|} \right)^{1/3} h'_2(q_{33}) k_1(q_{23}) + h_2(q_{33}) k'_1(q_{23}) \right\} \left\{ -\left(\frac{|\alpha_2|}{\alpha_1} \right)^{1/3} k'_1(q_{22}) k_2(q_{12}) \right. \right. \\
 & + k_1(q_{22}) k'_2(q_{12}) \left. \right] \hat{k}_1(q_{11}) \\
 & + \left. \left[\left(\frac{|\alpha_2|}{\alpha_1} \right)^{1/3} k'_1(q_{22}) k_1(q_{12}) - k_1(q_{22}) k'_1(q_{12}) \right] \hat{k}_2(q_{11}) \right\} k_2(q_{2T}) k_2(q_{2R}) \Big\} \\
 (z_2 \leq z_R \leq z_3 ; z_2 \leq z_T \leq z_3 ; \alpha_2 > 0) \quad (2.157)
 \end{aligned}$$

or

$$\begin{aligned}
& E(n, z_R, z_T) = \\
& R_2 \left\{ \left[\left\{ \left(\frac{\alpha_3}{|\alpha_2|} \right)^{1/3} h'_2(q_{33}) k_2(q_{23}) + h_2(q_{33}) k'_2(q_{23}) \right\} \left\{ \left[\left(\frac{|\alpha_2|}{\alpha_1} \right)^{1/3} k'_2(q_{22}) k_2(q_{12}) \right. \right. \right. \right. \right. \\
& + k_2(q_{22}) k'_2(q_{12}) \left. \right] \hat{k}_1(q_{11}) + \left[- \left(\frac{|\alpha_2|}{\alpha_1} \right)^{1/3} k'_2(q_{22}) k_1(q_{12}) \right. \\
& - k_2(q_{22}) k'_1(q_{12}) \left. \right] \hat{k}_2(q_{11}) \left. \right\} k_1(q_{2T}) k_1(q_{2R}) \\
& + \left[\left\{ \left(\frac{\alpha_3}{|\alpha_2|} \right)^{1/3} h'_2(q_{33}) k_1(q_{23}) + h_2(q_{33}) k'_1(q_{23}) \right\} \left\{ \left[- \left(\frac{|\alpha_2|}{\alpha_1} \right)^{1/3} k'_2(q_{22}) k_2(q_{12}) \right. \right. \right. \\
& - k_2(q_{22}) k'_2(q_{12}) \left. \right] \hat{k}_1(q_{11}) + \left[\left(\frac{|\alpha_2|}{\alpha_1} \right)^{1/3} k'_2(q_{22}) k_1(q_{12}) \right. \\
& + k_2(q_{22}) k'_1(q_{12}) \left. \right] \hat{k}_2(q_{11}) \left. \right\} \left\{ k_2(q_{2T}) k_1(q_{2R}) + k_1(q_{2T}) k_2(q_{2R}) \right\} \\
& + \left[\left\{ \left(\frac{\alpha_3}{|\alpha_2|} \right)^{1/3} h'_2(q_{33}) k_1(q_{23}) + h_2(q_{33}) k'_1(q_{23}) \right\} \left\{ \left[\left(\frac{|\alpha_2|}{\alpha_1} \right)^{1/3} k'_1(q_{22}) k_2(q_{12}) \right. \right. \right. \\
& + k_1(q_{22}) k'_2(q_{12}) \left. \right] \hat{k}_1(q_{11}) + \left[- \left(\frac{|\alpha_2|}{\alpha_1} \right)^{1/3} k'_1(q_{22}) k_1(q_{12}) \right. \\
& - k_1(q_{22}) k'_1(q_{12}) \left. \right] \hat{k}_2(q_{11}) \left. \right\} k_2(q_{2T}) k_2(q_{2R})
\end{aligned}$$

When the transmitter is in the second layer and the receiver is in the third layer, the modal height-gain function is

$$E(n, z_R, z_T) = R_2 W \left\{ \left[\left\{ \mp \left(\frac{|\alpha_2|}{\alpha_1} \right)^{1/3} k_2'(q_{22}) k_2(q_{12}) + k_2(q_{22}) k_2'(q_{12}) \right\} k_1(q_{11}) - \left\{ \mp \left(\frac{|\alpha_2|}{\alpha_1} \right)^{1/3} k_2'(q_{22}) k_1(q_{12}) + k_2(q_{22}) k_1'(q_{12}) \right\} k_2(q_{11}) \right] k_1(q_{2T}) h_2(q_{3R}) + \left[- \left\{ \mp \left(\frac{|\alpha_2|}{\alpha_1} \right)^{1/3} k_1'(q_{22}) k_2(q_{12}) + k_1(q_{22}) k_2'(q_{12}) \right\} k_1(q_{11}) \right. \right. \right. \\ \left. \left. \left. - \left\{ \mp \left(\frac{|\alpha_2|}{\alpha_1} \right)^{1/3} k_1'(q_{22}) k_1(q_{12}) + k_1(q_{22}) k_1'(q_{12}) \right\} k_2(q_{11}) \right] k_1(q_{2T}) h_2(q_{3R}) \right\}$$

$$+ \left\{ \mp \left(\frac{|\alpha_2|}{\alpha_1} \right)^{1/3} k'_1(q_{22}) k_1(q_{12}) + k_1(q_{22}) k'_1(q_{12}) \right\} k_2(q_{11}) \left[k_2(q_{2T}) h_2(q_{3R}) \right] \right\}$$

$$(z_3 \leq z_R ; z_2 \leq z_T \leq z_3) . \quad (2.159)$$

In the above equations

$$R_2 = \frac{p}{Wq'_2} , \quad (2.160)$$

where

$$q'_2 = \frac{\partial q_2}{\partial z} = \left(\frac{k}{|\alpha_2|} \right)^{2/3} \alpha_2 . \quad (2.161)$$

When the transmitter is in the third layer and the receiver is in the first layer, the modal height-gain function is given by

$$E(n, z_R, z_T) = - R_1 W^2 \{ k_1(q_{11}) k_2(q_{1R}) - k_2(q_{11}) k_1(q_{1R}) \} h_2(q_{3T})$$

$$(0 \leq z_R \leq z_2 ; z_3 \leq z_T) . \quad (2.162)$$

When the transmitter is in the third layer and the receiver is in the second layer, the modal height-gain function is

$$E(n, z_R, z_T) = \pm R_3 W \left(\frac{\alpha_3}{|\alpha_2|} \right)^{1/3} \left\{ \left[\left\{ \mp \left(\frac{|\alpha_2|}{\alpha_1} \right)^{1/3} k'_2(q_{22}) k_2(q_{12}) \right. \right. \right. \right. \\ \left. \left. \left. \left. + k_2(q_{22}) k'_2(q_{12}) \right\} k_1(q_{11}) \right. \right. \\ \left. \left. - \left\{ \mp \left(\frac{|\alpha_2|}{\alpha_1} \right)^{1/3} k''_2(q_{22}) k_1(q_{12}) + k_2(q_{22}) k'_1(q_{12}) \right\} k_2(q_{11}) \right] h_2(q_{3T}) k_1(q_{2R}) \right. \\ \left. + \left[- \left\{ \mp \left(\frac{|\alpha_2|}{\alpha_1} \right)^{1/3} k'_1(q_{22}) k_2(q_{12}) + k_1(q_{22}) k'_2(q_{12}) \right\} k_1(q_{11}) \right. \right]$$

$$+ \left\{ \mp \left(\frac{|\alpha_2|}{\alpha_1} \right)^{1/3} k_1'(q_{22}) k_1(q_{12}) + k_1(q_{22}) k_1'(q_{12}) \right\} k_2(q_{11}) \right] h_2(q_{3T}) k_2(q_{2R}) \} \\ (z_2 \leq z_R \leq z_3 ; z_3 \leq z_T) . \quad (2.163)$$

When the transmitter is in the third layer and the receiver is in the third layer, the modal height-gain function is given by

$$E(n, z_R, z_T) = R_3 \left\{ \left[\mp \left(\frac{|\alpha_2|}{\alpha_1} \right)^{1/3} k_1'(q_{22}) k_2(q_{12}) + k_1(q_{22}) k_2'(q_{12}) \right] \left[-k_2'(q_{23}) \left\{ h_1(q_{33}) - e^{-4\pi i/3} h_2'(q_{33}) \right\} \right. \right. \\ \left. \left. \pm \left(\frac{\alpha_3}{|\alpha_2|} \right)^{1/3} k_2(q_{23}) \left\{ h_1'(q_{33}) - e^{-4\pi i/3} h_2(q_{33}) \right\} \right] k_1(q_{11}) \right. \\ \left. + \left[\mp \left(\frac{|\alpha_2|}{\alpha_1} \right)^{1/3} k_2'(q_{22}) k_2(q_{12}) + k_2(q_{22}) k_2'(q_{12}) \right] \left[k_1'(q_{23}) \left\{ h_1(q_{33}) - e^{-4\pi i/3} h_2(q_{33}) \right\} \right. \right. \\ \left. \left. \mp \left(\frac{\alpha_3}{|\alpha_2|} \right)^{1/3} k_1(q_{23}) \left\{ h_1'(q_{33}) - e^{-4\pi i/3} h_2'(q_{33}) \right\} \right] k_1(q_{11}) \right. \\ \left. + \left[\mp \left(\frac{|\alpha_2|}{\alpha_1} \right)^{1/3} k_1'(q_{22}) k_1(q_{12}) + k_1(q_{22}) k_1'(q_{12}) \right] \left[k_2'(q_{23}) \left\{ h_1(q_{33}) - e^{-4\pi i/3} h_2(q_{33}) \right\} \right. \right. \\ \left. \left. \mp \left(\frac{\alpha_3}{|\alpha_2|} \right)^{1/3} k_2(q_{23}) \left\{ h_1'(q_{33}) - e^{-4\pi i/3} h_2'(q_{33}) \right\} \right] k_2(q_{11}) \right. \\ \left. + \left[\mp \left(\frac{|\alpha_2|}{\alpha_1} \right)^{1/3} k_2'(q_{22}) k_1(q_{12}) + k_2(q_{22}) k_1'(q_{12}) \right] \left[-k_1'(q_{23}) \left\{ h_1(q_{33}) - e^{-4\pi i/3} h_2(q_{33}) \right\} \right. \right. \\ \left. \left. \pm \left(\frac{\alpha_3}{|\alpha_2|} \right)^{1/3} k_1(q_{23}) \left\{ h_1'(q_{33}) - e^{-4\pi i/3} h_2'(q_{33}) \right\} \right] k_2(q_{11}) \right\} h_2(q_{3T}) h_2(q_{3R}) \\ (z_3 \leq z_R ; z_3 \leq z_T) . \quad (2.164)$$

In the above equations

$$R_3 = \frac{p}{wq'_3}, \quad (2.165)$$

where

$$q'_3 = \frac{\partial q_3}{\partial z} = \left(\frac{k}{\alpha_3} \right)^{2/3} \alpha_3. \quad (2.166)$$

In all of the above equations for the modal height-gain function, the upper sign is to be taken when $\alpha_2 > 0$ and the lower sign when $\alpha_2 < 0$.

3. SURFACE ROUGHNESS

The preceding results have assumed that the earth's surface is perfectly smooth. Because surface roughness could have a significant effect upon the signal levels at large ranges, especially for frequencies above several gigahertz, the modifications necessary to incorporate surface roughness into the previous results will now be made.

One way to introduce surface roughness, or any loss mechanism that can be modeled as a lossy boundary, is the following [16]. Instead of the trilinear layer shown in figure 1, consider the layer shown in figure 3, where the infinitesimally thin bottom layer, $z_1 = 0 \leq z \leq z_p$, has a constant modified refractivity. In the limit $z_p \rightarrow z_1 = 0$ this profile is exactly the same as the one considered before. In the bottom layer $0 \leq z \leq z_p$, the function $\tilde{M}(\rho, z)$ can be written as

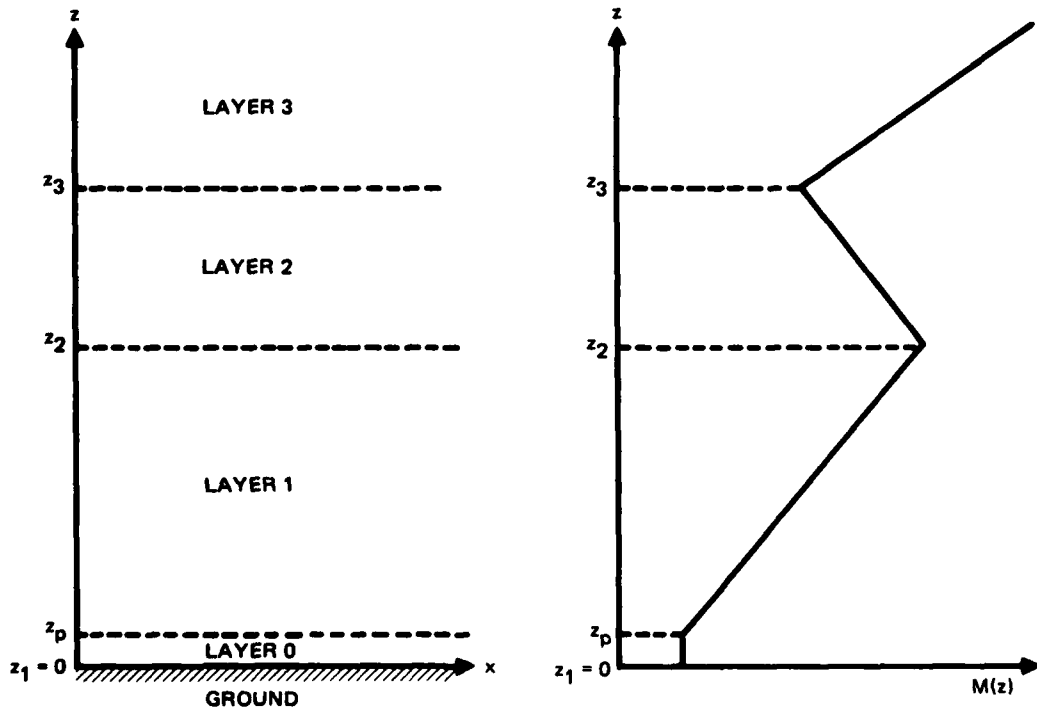


Figure 3. Modified refractivity profile used to introduce surface roughness loss into calculation of field strength. In layer 0, $\frac{dM}{dz} = 0$. The height z_p is infinitesimally small, and eventually $z_p \rightarrow 0$.

$$\tilde{\Pi}_0(\rho, z) = A_0(\rho) \{ e^{i\mu z} + R e^{-i\mu z} \} , \quad (3.1)$$

where

$$\mu = \sqrt{n_1^2(0) - \beta^2} \quad (3.2)$$

and

$$\beta^2 = \frac{\rho^2}{k^2} . \quad (3.3)$$

For a time dependence of $e^{+i\omega t}$ and with

$$\operatorname{Re}\{\sqrt{n_1^2(0) - \beta^2}\} = \operatorname{Re}\left\{\left(\frac{\alpha_1}{k}\right)^{1/3} \sqrt{q_{11}}\right\} > 0 , \quad (3.4)$$

the first term in (3.1) represents a down-going plane wave and the second term represents an up-going plane wave. The effect of surface roughness is introduced through the plane wave reflection coefficient R in equation (3.1). With the introduction of (3.1), the function $\tilde{\Pi}(\rho, z)$ is no longer required to satisfy the boundary condition that $\tilde{\Pi}(\rho, z)$ represent an outgoing decaying wave as $z \rightarrow -\infty$. In the other layers the solution $\tilde{\Pi}(\rho, z)$ is exactly as before:

$$\tilde{\Pi}_j(\rho, z) = \begin{cases} A_j(\rho) k_1(q_j) + B_j(\rho) k_2(q_j) + \tilde{\Pi}_j^{(P)}(\rho, q_j) \delta_{jM} & (j = 1, 2) \\ B_3(\rho) h_2(q_3) + \tilde{\Pi}_3^{(P)}(\rho, q_3) \delta_{3M} & (j = 3) , \end{cases} \quad (3.5)$$

where the particular solutions $\tilde{\Pi}_j^{(P)}$ are given by equations (2.40, 2.41).

The continuity conditions that $\tilde{\Pi}(\rho, z)$ now has to satisfy are

$$\tilde{\Pi}_0(\rho, z_p) = \tilde{\Pi}_1(\rho, z_p) , \quad (3.6)$$

$$\frac{d}{dz}\{\tilde{\Pi}_0(\rho, z_p)\} = \frac{d}{dz}\{\tilde{\Pi}_1(\rho, z_p)\} , \quad (3.7)$$

$$\tilde{\Pi}_j(\rho, z_{j+1}) = \tilde{\Pi}_{j+1}(\rho, z_{j+1}) \quad (j = 1, 2) , \quad (3.8)$$

and

$$\frac{d}{dz}\{\tilde{\Pi}_j(\rho, z_{j+1})\} = \frac{d}{dz}\{\tilde{\Pi}_{j+1}(\rho, z_{j+1})\} \quad (j = 1, 2), \quad (3.9)$$

for both vertical and horizontal polarization. Substituting equations (3.1) and (3.5) into equations (3.6, 3.7) yields

$$A_0 \left\{ e^{i\mu z_p} + R e^{-i\mu z_p} \right\} = A_1 k_1(q_{1p}) + B_1 k_2(q_{1p}) + \tilde{\Pi}_1^{(P)}(\rho, q_{1p}) \delta_{1M} \quad (3.10)$$

and

$$i\mu A_0 \left\{ e^{i\mu z_p} - R e^{-i\mu z_p} \right\} = \alpha_1 \left(\frac{k}{|\alpha_1|} \right)^{2/3} A_1 k'_1(q_{1p}) + \alpha_1 \left(\frac{k}{|\alpha_1|} \right)^{2/3} B_1 k'_2(q_{1p}) + \frac{d}{dz}\{\tilde{\Pi}_1^{(P)}(\rho, q_{1p})\} \delta_{1M}, \quad (3.11)$$

where

$$q_{1p} = q_1(z_p) = \left(\frac{k}{|\alpha_1|} \right)^{2/3} [1 + i\eta + \alpha_1(z_p - H) - \beta^2]. \quad (3.12)$$

In the limit $z_p \rightarrow 0$, equations (3.10, 3.11) become

$$A_0(1 + R) = A_1 k_1(q_{11}) + B_1 k_2(q_{11}) + \tilde{\Pi}_1^{(P)}(\rho, q_{11}) \delta_{1M} \quad (3.13)$$

and

$$i\mu A_0(1 - R) = \alpha_1 \left(\frac{k}{|\alpha_1|} \right)^{2/3} A_1 k'_1(q_{11}) + \alpha_1 \left(\frac{k}{|\alpha_1|} \right)^{2/3} B_1 k'_2(q_{11}) + \frac{d}{dz}\{\tilde{\Pi}_1^{(P)}(\rho, q_{11})\} \delta_{1M}. \quad (3.14)$$

Eliminating A_0 from equations (3.13, 3.14) finally yields

$$A_1 \left\{ k'_1(q_{11}) - \frac{i\mu}{\alpha_1} \left(\frac{|\alpha_1|}{k} \right)^{2/3} \left(\frac{1-R}{1+R} \right) k_1(q_{11}) \right\} + B_1 \left\{ k'_2(q_{11}) - \frac{i\mu}{\alpha_1} \left(\frac{|\alpha_1|}{k} \right)^{2/3} \left(\frac{1-R}{1+R} \right) k_2(q_{11}) \right\}$$

$$= - \frac{1}{\alpha_1} \left(\frac{|\alpha_1|}{k} \right)^{2/3} \frac{d}{dz} \left\{ \tilde{n}_1^{(P)}(\rho, q_{11}) \right\} \delta_{1M} + \frac{i\mu}{\alpha_1} \left(\frac{|\alpha_1|}{k} \right)^{2/3} \left(\frac{1-R}{1+R} \right) \tilde{n}_1^{(P)}(\rho, q_{11}) \delta_{1M} . \quad (3.15)$$

The continuity conditions (3.8, 3.9) yield equations (2.53-2.56) as before. In comparison of equations (2.52) and (3.15) it can be seen that the net effect of the modification to include surface roughness is the replacement

$$\gamma \rightarrow \mu \frac{1-R}{1+R} . \quad (3.16)$$

Therefore, all of the previous results hold if the functions $\tilde{k}_1(q_{11})$ and $\tilde{k}_2(q_{11})$ are defined to be

$$\tilde{k}_1(q_{11}) = k'_1(q_{11}) - G_R k_1(q_{11}) \quad (3.17)$$

and

$$\tilde{k}_2(q_{11}) = k'_2(q_{11}) - G_R k_1(q_{11}) , \quad (3.18)$$

where

$$G_R = \frac{i\mu}{\alpha_1} \left(\frac{|\alpha_1|}{k} \right)^{2/3} \left(\frac{1-R}{1+R} \right)$$

$$= i \left(\frac{k}{\alpha_1} \right)^{1/3} \sqrt{n_1^2(0) - \beta^2} \left(\frac{1-R}{1+R} \right) \quad (\alpha_1 > 0) . \quad (3.19)$$

When reflection occurs from a surface with a Gaussian distribution of bump heights, the reflection coefficient R can be represented as the product of the smooth surface plane wave reflection coefficient and a surface roughness factor [17]. For horizontal polarization, the reflection coefficient R is given by

$$R = \begin{cases} R_H \exp \left[-2k^2 \delta^2 \left(\frac{\alpha_1}{k} \right)^{2/3} q_{11} \right] & \operatorname{Re}(q_{11}) \geq 0 \\ R_H & \operatorname{Re}(q_{11}) < 0 , \end{cases} \quad (3.20)$$

where δ is the root mean square surface bump height and R_H is the Fresnel plane wave reflection coefficient for horizontal polarization

$$R_H = \frac{[n_f^2(0) - \beta^2]^{1/2} - [n_g^2 - \beta^2]^{1/2}}{[n_f^2(0) - \beta^2]^{1/2} + [n_g^2 - \beta^2]^{1/2}} \quad (3.21)$$

When $\text{Re}(q_{11}) < 0$, the magnitude of the exponential factor $\exp \left[-2k^2\delta^2 \left(\frac{\alpha_1}{k} \right)^{2/3} q_{11} \right]$ is greater than one. Since modes with $\text{Re}(q_{11}) < 0$ correspond to well-trapped modes and should be unaffected by the surface, the exponential factor is not included in R when $\text{Re}(q_{11}) < 0$.

In the case of vertical polarization, R is given by

$$R = \begin{cases} R_V \exp \left[-2k^2\delta^2 \left(\frac{\alpha_1}{k} \right)^{2/3} q_{11} \right] & \text{Re}(q_{11}) \geq 0 \\ R_V & \text{Re}(q_{11}) < 0, \end{cases} \quad (3.22)$$

where R_V is the Fresnel plane wave reflection coefficient for vertical polarization

$$R_V = \frac{n_g^2 [n_f^2(0) - \beta^2]^{1/2} - n_f^2(0) [n_g^2 - \beta^2]^{1/2}}{n_g^2 [n_f^2(0) - \beta^2]^{1/2} + n_f^2(0) [n_g^2 - \beta^2]^{1/2}} \quad (3.23)$$

The limits of G_R as the rms bump height δ approaches zero are

$$G_{RH} = \frac{i\mu}{\alpha_1} \left(\frac{\alpha_1}{k} \right)^{2/3} \left(\frac{1-R_H}{1+R_H} \right) = i[n_f^2(0) - \beta^2]^{1/2} \left(\frac{k}{\alpha_1} \right)^{1/3} \left(\frac{1-R_H}{1+R_H} \right)$$

$$\rightarrow \frac{i\gamma}{\alpha_1} \left(\frac{\alpha_1}{k} \right)^{2/3} = i[n_g^2 - \beta^2]^{1/2} \left(\frac{k}{\alpha_1} \right)^{1/3} = G_{SH} \quad (3.24)$$

for horizontal polarization and

$$G_{RV} = \frac{i\mu}{\alpha_1} \left(\frac{\alpha_1}{k} \right)^{2/3} \left(\frac{1-R_V}{1+R_V} \right) = i[n_f^2(0) - \beta^2]^{1/2} \left(\frac{k}{\alpha_1} \right)^{1/3} \left(\frac{1-R_V}{1+R_V} \right)$$

$$\rightarrow \frac{iY}{\alpha_1} \left(\frac{\alpha_1}{k}\right)^{2/3} \frac{n_g^2(0)}{n_g^2} = i[n_g^2 - \beta^2]^{1/2} \left(\frac{k}{\alpha_1}\right)^{1/3} \frac{n_g^2(0)}{n_g^2} = G_{SV} . \quad (3.25)$$

Thus, the above results for reflection from a rough surface contain the results for reflection from a smooth surface as a special case.

The coefficient G_R and its derivative $\frac{\partial G_R}{\partial q_{11}}$ are needed when evaluating the modal function and its derivative. For horizontal polarization, G_{RH} can be written as

$$G_{RH} = i \left(\frac{k}{\alpha_1}\right)^{1/3} \frac{a(q_{11})}{b(q_{11})} , \quad (3.26)$$

where

$$a(q_{11}) = \left(\frac{\alpha_1}{k}\right)^{1/3} (q_{11})^{1/2} \tanh\left(\frac{\phi}{2}\right) + \left[\tau + \left(\frac{\alpha_1}{k}\right)^{2/3} q_{11} \right]^{1/2} \quad (3.27)$$

and

$$b(q_{11}) = 1 + \left(\frac{k}{\alpha_1}\right)^{1/3} (q_{11})^{-1/2} \tanh\left(\frac{\phi}{2}\right) \left[\tau + \left(\frac{\alpha_1}{k}\right)^{2/3} q_{11} \right]^{1/2} \quad (3.28)$$

with

$$\tau = n_g^2 - 1 - i\eta - \alpha_1 H \quad (3.29)$$

and

$$\phi = 2k^2\delta^2 \left(\frac{\alpha_1}{k}\right)^{2/3} q_{11} . \quad (3.30)$$

For small values of $|q_{11}|$, $a(q_{11})$ and $b(q_{11})$ have the series expansions

$$\begin{aligned} a(q_{11}) &= \left(\frac{\alpha_1}{k}\right)^{1/3} (q_{11})^{1/2} \left\{ k^2\delta^2 \left(\frac{\alpha_1}{k}\right)^{2/3} q_{11} \right. \\ &\quad \left. - \frac{1}{3} k^6\delta^6 \left(\frac{\alpha_1}{k}\right)^2 q_{11}^3 + \frac{2}{15} k^{10}\delta^{10} \left(\frac{\alpha_1}{k}\right)^{10/3} q_{11}^5 - \dots \right\} \end{aligned}$$

$$\begin{aligned}
& + \tau^{1/2} \left\{ 1 + \frac{1}{2\tau} \left(\frac{\alpha_1}{k}\right)^{2/3} q_{11} - \frac{1}{8\tau^2} \left(\frac{\alpha_1}{k}\right)^{4/3} q_{11}^2 + \frac{1}{16\tau^3} \left(\frac{\alpha_1}{k}\right)^2 q_{11}^3 \right. \\
& \left. - \frac{5}{128\tau^4} \left(\frac{\alpha_1}{k}\right)^{8/3} q_{11}^4 + \frac{7}{256\tau^5} \left(\frac{\alpha_1}{k}\right)^{10/3} q_{11}^5 - \dots \right\} \quad (3.31)
\end{aligned}$$

and

$$\begin{aligned}
b(q_{11}) = & 1 + \tau^{1/2} (q_{11})^{1/2} \left\{ k^2 \delta^2 \left(\frac{\alpha_1}{k}\right)^{1/3} + \frac{1}{2\tau} k^2 \delta^2 \left(\frac{\alpha_1}{k}\right) q_{11} - \left[\frac{1}{3} k^6 \delta^6 + \right. \right. \\
& + \frac{1}{8\tau^2} k^2 \delta^2 \left] \left(\frac{\alpha_1}{k}\right)^{5/3} q_{11}^2 + \left[- \frac{1}{6\tau} k^6 \delta^6 + \frac{1}{16\tau^3} k^2 \delta^2 \right] \left(\frac{\alpha_1}{k}\right)^{7/3} q_{11}^3 \right. \\
& + \left[\frac{2}{15} k^{10} \delta^{10} + \frac{1}{24\tau^2} k^6 \delta^6 - \frac{5}{128\tau^4} k^2 \delta^2 \right] \left(\frac{\alpha_1}{k}\right)^3 q_{11}^4 + \left[\frac{1}{15\tau} k^{10} \delta^{10} \right. \\
& \left. \left. - \frac{1}{48\tau^3} k^6 \delta^6 + \frac{7}{256\tau^5} k^2 \delta^2 \right] \left(\frac{\alpha_1}{k}\right)^{11/3} q_{11}^5 + \dots \right\}. \quad (3.32)
\end{aligned}$$

The derivative of G_{RH} with respect to q_{11} is given by

$$\frac{\partial G_{RH}}{\partial q_{11}} = i \left(\frac{k}{\alpha_1}\right)^{1/3} \left\{ \frac{1}{b} \frac{\partial a}{\partial q_{11}} - \frac{a}{b^2} \frac{\partial b}{\partial q_{11}} \right\}, \quad (3.33)$$

where

$$\begin{aligned}
\frac{\partial a}{\partial q_{11}} = & \frac{1}{2} (q_{11})^{-1/2} \left(\frac{\alpha_1}{k}\right)^{1/3} \tanh\left(\frac{\Phi}{2}\right) + (q_{11})^{1/2} \left(\frac{\alpha_1}{k}\right) k^2 \delta^2 \operatorname{sech}^2\left(\frac{\Phi}{2}\right) \\
& + \frac{1}{2} \left(\frac{\alpha_1}{k}\right)^{2/3} \left[\tau + \left(\frac{\alpha_1}{k}\right)^{2/3} q_{11} \right]^{-1/2} \quad (3.34)
\end{aligned}$$

and

$$\begin{aligned}
\frac{\partial b}{\partial q_{11}} = & - \frac{1}{2} \left(\frac{k}{\alpha_1}\right)^{1/3} q_{11}^{-3/2} \tanh\left(\frac{\Phi}{2}\right) \left[\tau + \left(\frac{\alpha_1}{k}\right)^{2/3} q_{11} \right]^{1/2} \\
& + \frac{1}{2} q_{11}^{-1/2} \left(\frac{\alpha_1}{k}\right)^{1/3} \tanh\left(\frac{\Phi}{2}\right) \left[\tau + \left(\frac{\alpha_1}{k}\right)^{2/3} q_{11} \right]^{-1/2}
\end{aligned}$$

$$+ q_{11}^{-1/2} k^2 \delta^2 \left(\frac{\alpha_1}{k}\right)^{1/3} \operatorname{sech}^2\left(\frac{\phi}{2}\right) \left[\tau + \left(\frac{\alpha_1}{k}\right)^{2/3} q_{11} \right]^{1/2} . \quad (3.35)$$

For small values of $|q_{11}|$, $\frac{\partial a}{\partial q_{11}}$ and $\frac{\partial b}{\partial q_{11}}$ have the series expansions

$$\begin{aligned} \frac{\partial a}{\partial q_{11}} &= \left(\frac{\alpha_1}{k}\right)^{1/3} q_{11}^{1/2} \left\{ \frac{3}{2} k^2 \delta^2 \left(\frac{\alpha_1}{k}\right)^{2/3} - \frac{7}{6} k^6 \delta^6 \left(\frac{\alpha_1}{k}\right)^2 q_{11}^2 \right. \\ &\quad \left. + \frac{11}{15} k^{10} \delta^{10} \left(\frac{\alpha_1}{k}\right)^{10/3} q_{11}^4 - \dots \right\} + \tau^{1/2} \left\{ \frac{1}{2\tau} \left(\frac{\alpha_1}{k}\right)^{2/3} \right. \\ &\quad \left. - \frac{1}{4\tau^2} \left(\frac{\alpha_1}{k}\right)^{4/3} q_{11} + \frac{3}{16\tau^3} \left(\frac{\alpha_1}{k}\right)^2 q_{11}^2 - \frac{5}{32\tau^4} \left(\frac{\alpha_1}{k}\right)^{8/3} q_{11}^3 \right. \\ &\quad \left. + \frac{35}{256\tau^5} \left(\frac{\alpha_1}{k}\right)^{10/3} q_{11}^4 - \dots \right\} \end{aligned} \quad (3.36)$$

and

$$\begin{aligned} \frac{\partial b}{\partial q_{11}} &= \tau^{1/2} q_{11}^{-1/2} \left\{ \frac{1}{2} k^2 \delta^2 \left(\frac{\alpha_1}{k}\right)^{1/3} + \frac{3}{4\tau} k^2 \delta^2 \left(\frac{\alpha_1}{k}\right) q_{11} \right. \\ &\quad \left. - \frac{5}{2} \left[\frac{1}{3} k^6 \delta^6 + \frac{1}{8\tau^2} k^2 \delta^2 \right] \left(\frac{\alpha_1}{k}\right)^{5/3} q_{11}^2 \right. \\ &\quad \left. + \frac{7}{2} \left[-\frac{1}{6\tau} k^6 \delta^6 + \frac{1}{16\tau^3} k^2 \delta^2 \right] \left(\frac{\alpha_1}{k}\right)^{7/3} q_{11}^3 + \frac{9}{2} \left[\frac{2}{15} k^{10} \delta^{10} + \frac{1}{24\tau^2} k^6 \delta^6 \right. \right. \\ &\quad \left. \left. - \frac{5}{128\tau^4} k^2 \delta^2 \right] \left(\frac{\alpha_1}{k}\right)^3 q_{11}^4 + \frac{11}{2} \left[\frac{1}{15\tau} k^{10} \delta^{10} \right. \right. \\ &\quad \left. \left. - \frac{1}{48\tau^3} k^6 \delta^6 + \frac{7}{256\tau^5} k^2 \delta^2 \right] \left(\frac{\alpha_1}{k}\right)^{11/3} q_{11}^5 + \dots \right\} . \end{aligned} \quad (3.37)$$

The corresponding results for G_{RV} are

$$G_{RV} = i \left(\frac{k}{\alpha_1} \right)^{1/3} \frac{\tilde{a}(q_{11})}{\tilde{b}(q_{11})}, \quad (3.38)$$

where

$$\tilde{a}(q_{11}) = \left(\frac{\alpha_1}{k} \right)^{1/3} q_{11}^{1/2} \tanh \left(\frac{\phi}{2} \right) + \frac{n_1^2(0)}{n^2 g} \left[\tau + \left(\frac{\alpha_1}{k} \right)^{2/3} q_{11} \right]^{1/2} \quad (3.39)$$

and

$$\tilde{b}(q_{11}) = 1 + \frac{n_1^2(0)}{n^2 g} q_{11}^{-1/2} \left(\frac{k}{\alpha_1} \right)^{1/3} \tanh \left(\frac{\phi}{2} \right) \left[\tau + \left(\frac{\alpha_1}{k} \right)^{2/3} q_{11} \right]^{1/2}. \quad (3.40)$$

For small values of $|q_{11}|$, $\tilde{a}(q_{11})$ and $\tilde{b}(q_{11})$ have the expansions

$$\begin{aligned} \tilde{a}(q_{11}) = & \left(\frac{\alpha_1}{k} \right)^{1/3} q_{11}^{1/2} \left\{ k^2 \delta^2 \left(\frac{\alpha_1}{k} \right)^{2/3} q_{11} - \frac{1}{3} k^6 \delta^6 \left(\frac{\alpha_1}{k} \right)^2 q_{11}^3 \right. \\ & \left. + \frac{2}{15} k^{10} \delta^{10} \left(\frac{\alpha_1}{k} \right)^{10/3} q_{11}^5 - \dots \right\} \\ & + \frac{n_1^2(0)}{n^2 g} \tau^{1/2} \left\{ 1 + \frac{1}{2\tau} \left(\frac{\alpha_1}{k} \right)^{2/3} q_{11} - \frac{1}{8\tau^2} \left(\frac{\alpha_1}{k} \right)^{4/3} q_{11}^2 + \frac{1}{16\tau^3} \left(\frac{\alpha_1}{k} \right)^2 q_{11}^3 \right. \\ & \left. - \frac{5}{128\tau^4} \left(\frac{\alpha_1}{k} \right)^{8/3} q_{11}^4 + \frac{7}{256\tau^5} \left(\frac{\alpha_1}{k} \right)^{10/3} q_{11}^5 - \dots \right\} \end{aligned} \quad (3.41)$$

and

$$\begin{aligned} \tilde{b}(q_{11}) = & 1 + \frac{n_1^2(0)}{n^2 g} \tau^{1/2} q_{11}^{1/2} \left\{ k^2 \delta^2 \left(\frac{\alpha_1}{k} \right)^{1/3} + \frac{1}{2\tau} k^2 \delta^2 \left(\frac{\alpha_1}{k} \right) q_{11} - \left[\frac{1}{3} k^6 \delta^6 \right. \right. \\ & \left. \left. + \frac{1}{8\tau^2} k^2 \delta^2 \right] \left(\frac{\alpha_1}{k} \right)^{5/3} q_{11}^2 + \left[- \frac{1}{6\tau} k^6 \delta^6 + \frac{1}{16\tau^3} k^2 \delta^2 \right] \left(\frac{\alpha_1}{k} \right)^{7/3} q_{11}^3 \right. \\ & \left. + \left[\frac{2}{15} k^{10} \delta^{10} + \frac{1}{24\tau^2} k^6 \delta^6 - \frac{5}{128\tau^4} k^2 \delta^2 \right] \left(\frac{\alpha_1}{k} \right)^3 q_{11}^4 + \left[\frac{1}{15\tau} k^{10} \delta^{10} \right. \right. \right. \end{aligned}$$

$$- \frac{1}{48\tau^3} k^6 \delta^6 + \frac{7}{256\tau^5} k^2 \delta^2 \left[\left(\frac{\alpha_1}{k} \right)^{11/3} q_{11}^5 + \dots \right]. \quad (3.42)$$

The derivative of G_{RV} with respect to q_{11} is equal to

$$\frac{\partial G_{RV}}{\partial q_{11}} = i \left(\frac{k}{\alpha_1} \right)^{1/3} \left\{ \frac{1}{\tilde{b}} \frac{\partial \tilde{a}}{\partial q_{11}} - \frac{\tilde{a}}{\tilde{b}^2} \frac{\partial \tilde{b}}{\partial q_{11}} \right\}, \quad (3.43)$$

where

$$\begin{aligned} \frac{\partial \tilde{a}}{\partial q_{11}} &= \frac{1}{2} q_{11}^{-1/2} \left(\frac{\alpha_1}{k} \right)^{1/3} \tanh\left(\frac{\phi}{2}\right) + k^2 \delta^2 \frac{\alpha_1}{k} q_{11}^{1/2} \operatorname{sech}^2\left(\frac{\phi}{2}\right) \\ &+ \frac{1}{2} \frac{n_g^2(0)}{n_g^2} \left(\frac{\alpha_1}{k} \right)^{2/3} \left[\tau + \left(\frac{\alpha_1}{k} \right)^{2/3} q_{11} \right]^{-1/2} \end{aligned} \quad (3.44)$$

and

$$\begin{aligned} \frac{\partial \tilde{b}}{\partial q_{11}} &= \frac{n_g^2(0)}{n_g^2} \left\{ - \frac{1}{2} q_{11}^{-3/2} \left(\frac{\alpha_1}{k} \right)^{1/3} \tanh\left(\frac{\phi}{2}\right) \left[\tau + \left(\frac{\alpha_1}{k} \right)^{2/3} q_{11} \right]^{1/2} \right. \\ &+ \frac{1}{2} q_{11}^{-1/2} \left(\frac{\alpha_1}{k} \right)^{1/3} \tanh\left(\frac{\phi}{2}\right) \left[\tau + \left(\frac{\alpha_1}{k} \right)^{2/3} q_{11} \right]^{-1/2} \\ &\left. + k^2 \delta^2 q_{11}^{-1/2} \left(\frac{\alpha_1}{k} \right)^{1/3} \operatorname{sech}^2\left(\frac{\phi}{2}\right) \left[\tau + \left(\frac{\alpha_1}{k} \right)^{2/3} q_{11} \right]^{1/2} \right\}. \end{aligned} \quad (3.45)$$

For small values of $|q_{11}|$, $\frac{\partial \tilde{a}}{\partial q_{11}}$ and $\frac{\partial \tilde{b}}{\partial q_{11}}$ have the series expansions

$$\begin{aligned} \frac{\partial \tilde{a}}{\partial q_{11}} &= \left(\frac{\alpha_1}{k} \right)^{1/3} q_{11}^{1/2} \left\{ \frac{3}{2} k^2 \delta^2 \left(\frac{\alpha_1}{k} \right)^{2/3} - \frac{7}{6} k^6 \delta^6 \left(\frac{\alpha_1}{k} \right)^2 q_{11}^2 \right. \\ &\left. + \frac{11}{15} k^{10} \delta^{10} \left(\frac{\alpha_1}{k} \right)^{10/3} q_{11}^4 - \dots \right\} + \frac{n_g^2(0)}{n_g^2} \tau^{1/2} \left\{ \frac{1}{2\tau} \left(\frac{\alpha_1}{k} \right)^{2/3} \right. \\ &\left. + \dots \right\} \end{aligned}$$

$$\begin{aligned}
& - \frac{1}{4\tau^2} \left(\frac{\alpha_1}{k} \right)^{4/3} q_{11} + \frac{3}{16\tau^3} \left(\frac{\alpha_1}{k} \right)^2 q_{11}^2 - \frac{5}{32\tau^4} \left(\frac{\alpha_1}{k} \right)^{8/3} q_{11}^3 \\
& + \frac{35}{256\tau^5} \left(\frac{\alpha_1}{k} \right)^{10/3} q_{11}^4 - \dots \}
\end{aligned} \tag{3.46}$$

and

$$\begin{aligned}
\frac{\partial \tilde{b}}{\partial q_{11}} = & \frac{n_1^2(0)}{n_g^2} \tau^{1/2} q_{11}^{-1/2} \left\{ \frac{1}{2} k^2 \delta^2 \left(\frac{\alpha_1}{k} \right)^{1/3} + \frac{3}{4\tau} k^2 \delta^2 \left(\frac{\alpha_1}{k} \right) q_{11} \right. \\
& - \frac{5}{2} \left[\frac{1}{3} k^6 \delta^6 + \frac{1}{8\tau^2} k^2 \delta^2 \right] \left(\frac{\alpha_1}{k} \right)^{5/3} q_{11}^2 + \frac{7}{2} \left[- \frac{1}{6\tau} k^6 \delta^6 \right. \\
& + \frac{1}{16\tau^3} k^2 \delta^2 \left. \right] \left(\frac{\alpha_1}{k} \right)^{7/3} q_{11}^3 + \frac{9}{2} \left[\frac{2}{15} k^{10} \delta^{10} + \frac{1}{24\tau^2} k^6 \delta^6 \right. \\
& - \frac{5}{128\tau^4} k^2 \delta^2 \left. \right] \left(\frac{\alpha_1}{k} \right)^3 q_{11}^4 + \frac{11}{2} \left[\frac{1}{15\tau} k^{10} \delta^{10} \right. \\
& - \frac{1}{48\tau^3} k^6 \delta^6 + \frac{7}{256\tau^5} k^2 \delta^2 \left. \right] \left(\frac{\alpha_1}{k} \right)^{11/3} q_{11}^5 + \dots \left. \right\} .
\end{aligned} \tag{3.47}$$

4. COMPLEX INDEX OF REFRACTION OF SEAWATER

In the waveguide formulation for tropospheric ducting of electromagnetic waves, one of the physical parameters needed for evaluating the modal function and height-gain functions is the complex index of refraction of seawater. The complex index of refraction of seawater is a function of frequency, temperature, and salinity. The temperature of the ocean's surface lies between -2°C and 32°C , with about half of the ocean's surface being warmer than 20°C . Although the salinity of the ocean near the mouth of large rivers may approach zero, the salinity of most water in the open ocean lies between 33 and 37 grams of salt per kilogram of seawater, and 35 g salt/kg seawater is often chosen as standard [18].

The complex index of refraction of seawater, n_g , can be related to an effective relative dielectric function, ϵ_{eff} , and an effective conductivity, σ_{eff} , through

$$n_g^2 = \epsilon_{\text{eff}} - i \frac{\sigma_{\text{eff}}}{\omega \epsilon_0} , \quad (4.1)$$

where ϵ_0 is the permittivity of free space and has the value

$$\epsilon_0 = 8.85434 \times 10^{-12} \text{ F/m} , \quad (4.2)$$

while $f = \frac{\omega}{2\pi}$ is the frequency at which n_g is to be evaluated. The effective dielectric function and the effective conductivity are related to the complex dielectric function

$$\epsilon = \epsilon' - i\epsilon'' \quad (4.3)$$

and the ionic conductivity, σ , through

$$\epsilon_{\text{eff}} = \epsilon' \quad (4.4)$$

and

$$\sigma_{\text{eff}} = \sigma + \omega \epsilon_0 \epsilon'' . \quad (4.5)$$

The above equations assume the ionic conductivity to have an imaginary part of zero. For frequencies much less than 10^4 GHz this is a good approximation.

The theory of an ideal polar dielectric in an alternating electromagnetic field was given by Debye [19] in terms of a single relaxation time. While Debye's derivation assumes a spherical molecule whose free rotations are resisted by a viscous force, all that is needed is the assumption of exponential relaxation of the polarization [20]. In the Debye theory the complex dielectric function is given by

$$\epsilon = \epsilon' - i\epsilon'', \quad (4.6)$$

where

$$\begin{aligned} \epsilon' &= \epsilon_\infty + \frac{\epsilon_s - \epsilon_\infty}{1 + (\lambda_s/\lambda)^2} \\ &= \epsilon_\infty + \frac{\epsilon_s - \epsilon_\infty}{1 + \omega^2\tau^2} \end{aligned} \quad (4.7)$$

and

$$\epsilon'' = \frac{(\epsilon_s - \epsilon_\infty)(\lambda_s/\lambda)}{1 + (\lambda_s/\lambda)^2} \quad (4.8)$$

$$= \frac{(\epsilon_s - \epsilon_\infty)\omega\tau}{1 + \omega^2\tau^2}. \quad (4.9)$$

In equations (4.7, 4.8), ϵ_∞ is that part of the dielectric function which is due to the atomic and electronic polarization and is assumed to be real and independent of frequency, and ϵ_s is the static ($\omega \rightarrow 0$) value of the dielectric function. The wavelength of the alternating electromagnetic field is λ , while λ_s , the characteristic wavelength, is the wavelength corresponding to the frequency $\frac{1}{\tau}$, where τ is the dielectric relaxation time. Equations (4.6-4.8) represent the fall in the value of the dielectric function from ϵ_s ($\omega \rightarrow 0$) to ϵ_∞ ($\omega \rightarrow \infty$), the fall being accompanied by a single broad absorption band in the neighborhood of the characteristic wavelength, λ_s . The representation of the variation with frequency of the dielectric function in terms of a single dielectric relaxation time τ should be valid for frequencies up to 300 GHz [21]. For higher frequencies more than one relaxation time will be needed.

Some of the earliest experimental work on the dielectric properties of pure water and aqueous ionic solutions was performed by JB Hasted,

CH Collie, and DM Ritson [22, 23]. For pure water they measured the value of the complex dielectric function at the wavelengths, λ , of 10.00, 3.213, and 1.274 cm ($f = 2.998$, 9.331, and 23.53 GHz) for temperatures between 0°C and 75°C. For temperatures in the range 0°C to 40°C, the least-square fit to their values for the characteristic wavelength and static dielectric constant is

$$\epsilon_{\infty}^{(P)} = 5.5 , \quad (4.9)$$

$$\lambda_s^{(P)}(T) = 3.338 - 0.11417T + 0.0022T^2 - 1.833 \times 10^{-6}T^3 , \quad (4.10)$$

and

$$\epsilon_s^{(P)}(T) = 88.192 - 0.405T + 0.0007T^2 , \quad (4.11)$$

where T is in degrees Celsius and λ_s is in centimeters. Equations (4.9-4.11) give the parameters in the Debye equation for the complex dielectric function of pure water as a function of temperature. For seawater there is a lowering of the value of the dielectric function from its pure water value due to saturation of the dielectric in the neighborhood of the salt ions. Hasted, Ritson, and Collie [23] also measured the complex dielectric function of ionic solutions. For NaCl solutions less than 1.5 molar, their experimental values could be fit by the Debye formula with λ_s and ϵ_s , as functions of temperature and salinity, given by

$$\lambda_s(T,S) = \lambda_s^{(P)}(T) - 0.08 c \quad (4.12)$$

and

$$\epsilon_s(T,S) = \epsilon_s^{(P)}(T) - 11.0 c , \quad (4.13)$$

where λ_s is again in centimeters and c is the salt concentration in moles per liter. They assumed that the value of ϵ_{∞} for NaCl solutions was 5.5, the same as for pure water.

A more recent fit of the Debye model parameters has been obtained by Klein and Swift [24]. Assuming that

$$\epsilon_{\infty} = 4.9 \quad (4.14)$$

for both pure water and seawater, they found that the static dielectric constant of pure water is given by

$$\varepsilon_s^{(P)}(T) = 88.045 - 0.4147T + 6.295 \times 10^{-4}T^2 + 1.075 \times 10^{-5}T^3, \quad (4.15)$$

while the static dielectric constant of seawater is given by

$$\varepsilon_s(T, S) = \varepsilon_s(T)a(S, T), \quad (4.16)$$

where

$$\begin{aligned} \varepsilon_s(T) = & 87.134 - 1.949 \times 10^{-1}T - 1.276 \times 10^{-2}T^2 \\ & + 2.491 \times 10^{-4}T^3 \end{aligned} \quad (4.17)$$

and

$$\begin{aligned} a(S, T) = & 1.000 + 1.613 \times 10^{-5}ST - 3.656 \times 10^{-3}S \\ & + 3.210 \times 10^{-5}S^2 - 4.232 \times 10^{-7}S^3. \end{aligned} \quad (4.18)$$

The temperature T is in degrees Celsius and the salinity S is in grams of salt per kilogram of seawater. When $S = 0$ the expressions (4.16-4.18) for the static dielectric constant of seawater do not reduce to the expression (4.15) for the static dielectric constant of pure water. This may be due to the presence of sulphates and nitrates in the seawater samples measured [24]. The dielectric relaxation time of seawater in the Klein and Swift model is given by

$$\tau(T, S) = \tau(T, 0)b(S, T), \quad (4.19)$$

where $\tau(T, 0)$ is the pure water value of the relaxation time and is equal to

$$\begin{aligned} \tau(T, 0) = & 1.768 \times 10^{-11} - 6.086 \times 10^{-13}T + 1.104 \times 10^{-14}T^2 \\ & - 8.111 \times 10^{-17}T^3, \end{aligned} \quad (4.20)$$

and

$$\begin{aligned} b(S, T) = & 1.000 + 2.282 \times 10^{-5}ST - 7.638 \times 10^{-4}S \\ & - 7.760 \times 10^{-6}S^2 + 1.105 \times 10^{-8}S^3. \end{aligned} \quad (4.21)$$

The dielectric relaxation time is in seconds. The ionic conductivity of seawater is given by

$$\sigma(T, S) = \sigma(25, S)\exp(-\Delta\beta), \quad (4.22)$$

where

$$\Delta = 25 - T, \quad (4.23)$$

$$\begin{aligned} \beta = & 2.033 \times 10^{-2} + 1.266 \times 10^{-4}\Delta + 2.464 \times 10^{-6}\Delta^2 \\ & - S[1.849 \times 10^{-5} - 2.551 \times 10^{-7}\Delta + 2.551 \times 10^{-8}\Delta^2], \end{aligned} \quad (4.24)$$

and

$$\sigma(25, S) = S[0.182521 - 1.46192 \times 10^{-3}S + 2.09324 \times 10^{-5}S^2 - 1.28205 \times 10^{-7}S^3] . \quad (4.25)$$

The conductivity σ is in siemens per meter.

5. SHELLMAN-MORFITT ROOT-FINDING ROUTINE

When the mode sum formulation of the tropospheric ducting problem is used, the most difficult part of the field strength calculations is determining the zeros of the modal function. For the trilinear model of the tropospheric index of refraction considered in this document, the modal function is given by equation (2.124):

$$|\Delta| = \tilde{\tau} \left(\frac{\alpha_3}{|\alpha_2|} \right)^{1/3} \left\{ \tilde{\tau} \left(\frac{|\alpha_2|}{\alpha_1} \right)^{1/3} \zeta(q_{11}) \chi(q_{11}) + \psi(q_{11}) \phi(q_{11}) \right\} , \quad (5.1)$$

where $\zeta(q_{11})$, $\chi(q_{11})$, $\psi(q_{11})$, and $\phi(q_{11})$ are given by equations (2.125-2.128) and involve sums and products of Airy functions. It is not possible to solve equation (5.1) analytically for the complex zeros, q_{11} . Therefore, numerical methods must be used. Several algorithms exist for finding the complex roots of transcendental equations [4, 25-27]. In XWVG, the complex root-finding routine of Shellman and Morfitt is used to find the zeros of the modal function (5.1). This routine was also used by Goodhart and Pappert [28] and Marcus [1, 2] for finding the zeros of modal functions for linear segmented models of tropospheric refractivity.

The root-finding routine of Shellman and Morfitt locates all the simple zeros of an analytic function in a prescribed rectangular region of the complex plane. Initial guesses for the location of the zeros within the prescribed rectangular region of the complex plane are not required. The root-finding method of Shellman and Morfitt is based on the theorem [29]:

Theorem: Let $f(z)$ be a meromorphic function, i.e., analytic everywhere in the complex z -plane except at isolated poles. Let Γ be a closed contour in the z -plane such that there are no zeros or poles of $f(z)$ on Γ . Then, the accumulated phase change, $\Delta\phi$, of $f(z)$ around Γ traversed in a counterclockwise direction is equal to

$$(\Delta\phi)_\Gamma = 2\pi(N_z - N_p) . \quad (5.2)$$

N_z is the number of zeros enclosed by Γ and N_p is the number of poles enclosed by Γ . When determining N_z and N_p , n -th order zeros and poles are counted n times.

For a function that has only zeros in the region enclosed by Γ so that $N_p = 0$, this theorem implies that every phase contour associated with each zero crosses Γ .

Consider the analytic function $f(z)$. In terms of its modulus and phase, $f(z)$ can be written as

$$f(z) = \{\{\operatorname{Re}(f)\}^2 + \{\operatorname{Im}(f)\}^2\}^{\frac{1}{2}} e^{i\theta}, \quad (5.3)$$

where θ is the phase of f and is given by

$$\theta = \tan^{-1} \left\{ \frac{\operatorname{Im}(f)}{\operatorname{Re}(f)} \right\}. \quad (5.4)$$

If $f(z)$ has no poles or branch points, the curve for the constant phase value $\theta = \theta_c$ radiating from a zero of $f(z)$ must cross a closed contour Γ enclosing that zero at least once. Furthermore, no other zero of $f(z)$ may be on this phase curve. See figure 4. A curve of constant phase, e.g., $\theta_c = 0$, which crosses the closed contour Γ may be followed until it leads to a zero of $f(z)$ or until the phase curve again crosses the contour Γ . A zero of $f(z)$ may be determined by the crossing of the curves

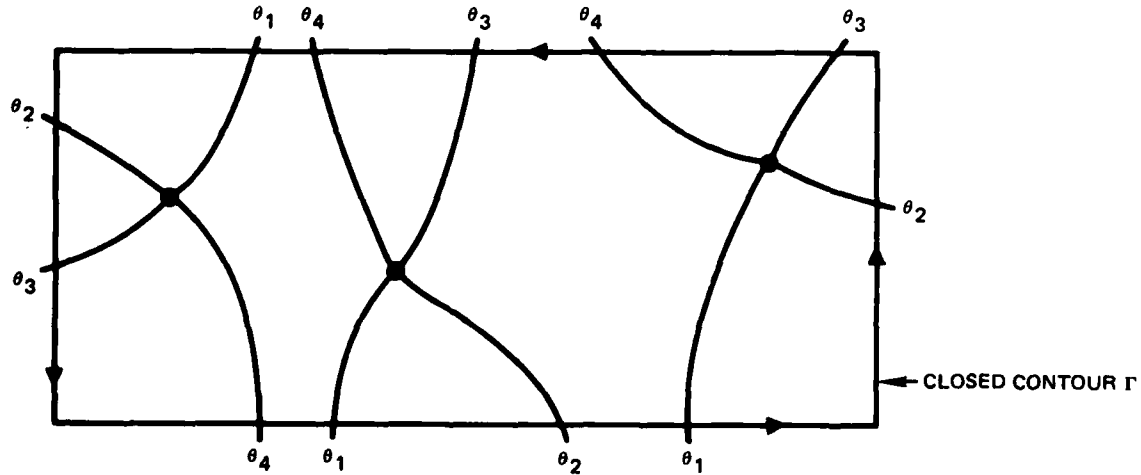


Figure 4. Constant phase curves for an analytic function with three simple zeros in the region enclosed by the rectangular contour Γ .

$$\operatorname{Im}(f) = 0 \quad (\theta_c = 0 \text{ or } \pi) \quad (5.5)$$

and

$$\operatorname{Re}(f) = 0 \quad \left(\theta_c = \frac{\pi}{2} \text{ or } \frac{3\pi}{2} \right) . \quad (5.6)$$

The routine of Shellman and Morfitt will search a specified rectangular region of the complex z -plane for the simple zeros of the analytic function $f(z)$. Let the edges of the specified search rectangle be denoted by t_L , t_R , t_T , and t_B , where t_L and t_R denote the value of the real part of z at the left and right edges of the search rectangle and t_T and t_B denote the value of the imaginary part of z at the top and bottom edges of the search rectangle. This search rectangle is divided into small mesh squares in which each mesh square side has length δ . Restrictions upon the size of δ will be discussed later. A new search rectangle is generated from the specified search rectangle. The left edge of this new search rectangle is given by

$$J_L = \operatorname{Int}\left(\frac{t_L}{\delta}\right) , \quad (5.7)$$

where $\operatorname{Int}(x)$ denotes the integer part of x . The other edges, J_R , J_T , and J_B , of this new search rectangle are similarly obtained. Thus, the new search rectangle is given in terms of mesh units, where one mesh unit is of length δ . Since truncation may occur in evaluating J_L , J_R , J_T , and J_B , this new search rectangle is made one mesh size larger on all sides in order to ensure that the original specified search rectangle falls completely within the new search rectangle. If the original specified search rectangle is near a branch cut or other discontinuity of $f(z)$, this expansion of the search region could cause problems.

Consider an individual mesh square in the new expanded search rectangle as shown in figure 5. A local mesh coordinate system, where each unit is of length δ , may be set up as shown in figure 6. The value of $f(z)$ evaluated in the local mesh coordinates of mesh square k is denoted by $f^{(k)}(x_k, w_k)$. Thus, as shown in figure 6, the value of $f(z)$ at the origin of mesh square k is denoted by $f^{(k)}(0,0)$. Note that for each mesh square the lower left-hand corner is taken as the origin in that mesh square's local coordinate system. The values of $f(z)$ at the corners of mesh square 1 are

$$f^{(1)}(0,1) = f(J_L \delta + i J_T \delta) , \quad (5.8)$$

$$f^{(1)}(0,0) = f(J_L \delta + i [J_T - 1] \delta) , \quad (5.9)$$

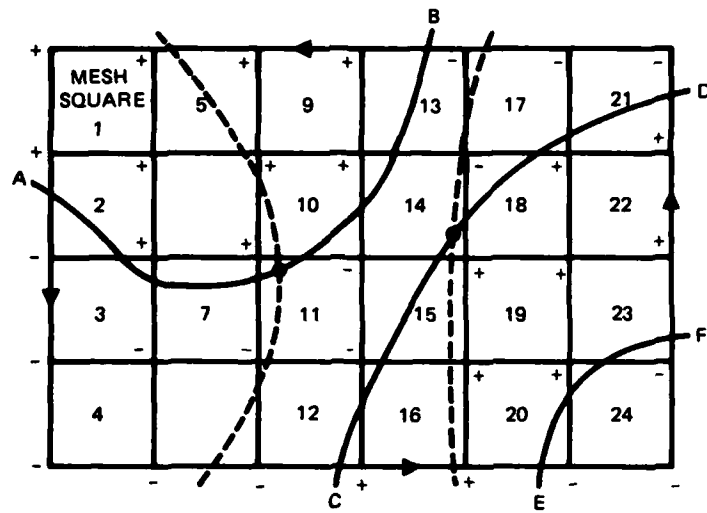


Figure 5. Illustration of search rectangle and mesh grid set up in the complex z -plane by the Shellman-Morritt root-finding routine. The plus and minus signs at the corners of the mesh squares indicate the sign of $\text{Im}(f)$. Along the solid curves $\text{Im}(f) = 0$; while along the dashed curves, $\text{Re}(f) = 0$. The zeros of $f(z)$ are located at the intersection of the $\text{Im}(f) = 0$ and $\text{Re}(f) = 0$ curves.

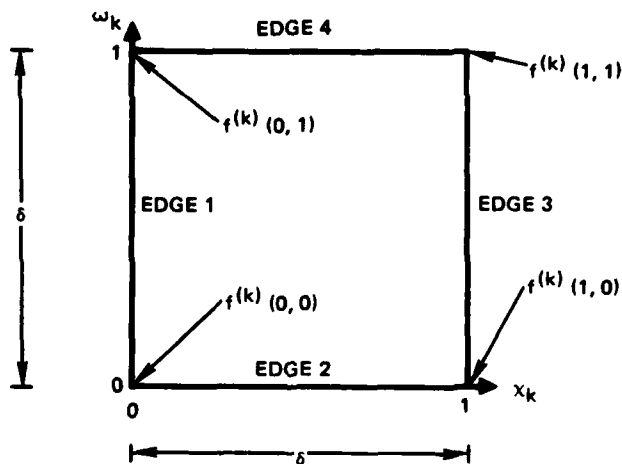


Figure 6. Local mesh coordinate system and numbering of the edges of mesh square k . The value of $f(z)$ evaluated at the corners of mesh square k are denoted by $f^{(k)}(x_k, \omega_k)$, where x_k and ω_k equal 0 or 1 at the corners.

$$f^{(1)}(1,0) = f([J_L + 1]\delta + i[J_T - 1]\delta) , \quad (5.10)$$

and $f^{(1)}(1,1) = f([J_L + 1]\delta + iJ_T\delta) . \quad (5.11)$

The values of $f(z)$ at the corners of all other mesh squares are obtained similarly.

A basic assumption concerning $f(z)$ made in the algorithm of Shellman and Morfitt is that along the edges of every mesh square k , $\text{Re}(f)$ and $\text{Im}(f)$ are linear functions of the local mesh coordinates χ_k and ω_k . This implies that in mesh square k , $f(z)$ can be written as

$$f^{(k)}(\chi_k, \omega_k) = a_k + b_k \omega_k + c_k \chi_k + d_k \omega_k \chi_k , \quad (5.12)$$

where a_k , b_k , c_k , and d_k are complex constants. This assumption puts an upper limit on the size of δ that can be used. If δ is too large, the assumption that $f(z)$ has a linear variation along the edges of the mesh squares breaks down. Thus, δ should be chosen small enough so that equation (5.12) is a good approximation to $f(z)$. In order to reduce computer run times, however, δ should not be excessively small. Note that equation (5.12) implies that in the mesh square, the curves $\text{Im}(f) = 0$ and $\text{Re}(f) = 0$ are hyperbolic curves with vertical and horizontal asymptotes.

In order to further describe the workings of the root-finding routine of Shellman and Morfitt, use will be made of the example shown in figure 5. The zeros of $f(z)$ in the new expanded search rectangle are looked for by examining the imaginary part of $f(z)$ counterclockwise around the rectangular contour. Intermediate steps of investigating mesh squares are also carried out counterclockwise. For the example shown in figure 5, the edges of the search rectangle are examined for crossings of phase curves along which $\text{Im}(f) = 0$, starting with mesh square 1 edge 1. The values $\text{Im}[f^{(1)}(0,1)]$ and $\text{Im}[f^{(1)}(0,0)]$ are computed. If, as shown in figure 5, the signs of these two values are the same, then there can be no $\text{Im}(f) = 0$ curve passing through edge 1 of mesh square 1. This is a consequence of assuming that $\text{Im}(f)$ varies linearly along the edges of the mesh squares.

Next, mesh square 2 is investigated. To obtain the values $\text{Im}[f^{(2)}(0,1)]$ and $\text{Im}[f^{(2)}(0,0)]$, use is made of the relationship

$$\text{Im}[f^{(2)}(0,1)] = \text{Im}[f^{(1)}(0,0)]. \quad (5.13)$$

The value of $\text{Im}[f^{(2)}(0,0)]$ will be a new computed value. If the signs of $\text{Im}[f^{(2)}(0,1)]$ and $\text{Im}[f^{(2)}(0,0)]$ are opposite, as shown in figure 5, then an $\text{Im}(f) = 0$ curve enters mesh square 2 somewhere along edge 1. Because of the assumed linearity of $\text{Im}(f)$ along the mesh edge, the $\text{Im}(f) = 0$ curve AB crosses edge 1 at

$$x_2 = 0 \quad (5.14)$$

and

$$w_2 = - \frac{\text{Im}[f^{(2)}(0,0)]}{\text{Im}[f^{(2)}(0,1)] - \text{Im}[f^{(2)}(0,0)]}. \quad (5.15)$$

The problem is now to find whether a zero of $f(z)$ lies within this mesh square and where the curve AB exits from the mesh square. First, the values $\text{Im}[f^{(2)}(1,0)]$ and $\text{Im}[f^{(2)}(1,1)]$ are obtained. The values of $\text{Im}(f)$ at all four corners of the mesh square are now known. Next, a test is made to determine whether there are one or two $\text{Im}(f) = 0$ curves entering and leaving the mesh square. If the values $\text{Im}[f^{(k)}(0,0)]$ and $\text{Im}[f^{(k)}(1,1)]$ have the same sign, e.g., minus, and the values $\text{Im}[f^{(k)}(0,1)]$ and $\text{Im}[f^{(k)}(1,0)]$ both have the opposite sign, e.g., plus, then there are two $\text{Im}(f) = 0$ curves entering and leaving the mesh square. This situation will arise in mesh square 14 of figure 5. Otherwise, there is only one $\text{Im}(f) = 0$ curve entering and leaving the mesh square, as in mesh square 2. Next, a test is performed to determine whether there is at least one $\text{Re}(f) = 0$ curve entering and leaving the mesh square. If the values $\text{Re}[f^{(k)}(0,0)]$, $\text{Re}[f^{(k)}(1,0)]$, $\text{Re}[f^{(k)}(1,1)]$, and $\text{Re}[f^{(k)}(0,1)]$ all have the same sign, then there are no $\text{Re}(f) = 0$ curves passing through the mesh square. If these values of $\text{Re}(f)$ do not all have the

same sign, then there is at least one $\text{Re}(f) = 0$ curve entering and leaving the mesh square. Mesh square 2 does not have a $\text{Re}(f) = 0$ curve passing through it and therefore does not contain a zero of $f(z)$. The edge through which the $\text{Im}(f) = 0$ curve exits the mesh square can be determined by using the signs of $\text{Im}(f)$ at the corners of the mesh square. In figure 5, the $\text{Im}(f) = 0$ curve AB exits mesh square 2 across edge 2, which means it enters mesh square 3 across edge 4. The local mesh coordinates of mesh square 3 where the curve AB enters mesh square 3 can be determined by using the values

$$\text{Im}[f^{(3)}(0,1)] = \text{Im}[f^{(2)}(0,0)] \quad (5.16)$$

and

$$\text{Im}[f^{(3)}(1,1)] = \text{Im}[f^{(2)}(1,0)] \quad (5.17)$$

together with the assumed linearity of $\text{Im}(f)$ along the mesh square edge.

The $\text{Im}(f) = 0$ curve is traced through the search rectangle, and each mesh square through which it passes is checked for zeros of $f(z)$. In figure 5, the $\text{Im}(f) = 0$ curve AB is followed through mesh squares 2, 3, 7, 11, 10, 14, and 13. The tests for a zero of $f(z)$ are made in mesh squares 3 and 7, with the same results as in mesh square 2. In mesh square 11, however, $\text{Im}(f) = 0$ and $\text{Re}(f) = 0$ curves both pass through the mesh square. On the basis of the values of $f(z)$ at the corners of the mesh square and the assumed linearity of $f(z)$ along the mesh square edges, the value of $f(z)$ at any point within the mesh square can be determined from

$$f^{(k)}(x_k, w_k) = a_k + b_k w_k + c_k x_k + d_k w_k x_k, \quad (5.18)$$

where

$$a_k = f^{(k)}(0,0), \quad (5.19)$$

$$b_k = f^{(k)}(0,1) - f^{(k)}(0,0), \quad (5.20)$$

$$c_k = f^{(k)}(1,0) - f^{(k)}(0,0), \quad (5.21)$$

and

$$d_k = f^{(k)}(0,0) + f^{(k)}(1,1) - f^{(k)}(0,1) - f^{(k)}(1,0). \quad (5.22)$$

The point of intersection, if any, of the curves $\text{Im}(f) = 0$ and $\text{Re}(f) = 0$ can then be determined. The mathematical details are presented in the report by Morfitt and Shellman [4].

After determining and storing the approximate location of the zero of $f(z)$ in mesh square 11, the contour AB is followed out of mesh square 11 into mesh square 10, then into mesh square 14. Two $\text{Im}(f) = 0$ curves and one $\text{Re}(f) = 0$ curve pass through mesh square 14. A solution for a zero of $f(z)$ in a mesh square is accepted if it lies on the $\text{Im}(f) = 0$ curve currently being followed [4]. When the contour AB is followed, the zero in mesh square 14 will be ignored since it falls on the $\text{Im}(f) = 0$ curve CD. When curve CD is traced through the search rectangle, this zero will be found again and stored. From mesh square 14, the contour AB is traced to mesh square 13, where it exits the search rectangle. Information that gives the mesh square and edge where the contour AB exits the search rectangle is stored. Identifying these exit points makes it possible to avoid later following the same $\text{Im}(f) = 0$ curve through the search rectangle. For example, if the $\text{Im}(f) = 0$ trace was later allowed to reenter the search rectangle at B, the same zero of $f(z)$ in mesh square 11 would be found.

After the $\text{Im}(f) = 0$ curve trace exits at point B, the search for zeros of $f(z)$ is continued by looking for more crossings of $\text{Im}(f) = 0$ curves with the rectangular contour. Since mesh square 2 was the last mesh square examined for such crossings, the next mesh square to be examined will be mesh square 3. The next crossing of an $\text{Im}(f) = 0$ curve with the rectangular contour will occur in mesh square 12. Since this crossing point is different from the previously stored exit point B, the $\text{Im}(f) = 0$ curve CD will be followed through the search rectangle. The zero of $f(z)$ in mesh square 14 will again be located; and since it lies on the $\text{Im}(f) = 0$ curve currently being traced, its location is stored. The curve CD is followed the rest of the way through the search rectangle, and the exit point D is stored. The search along the rectangular contour then continues at mesh square 16. At mesh square 20, a new crossing of an $\text{Im}(f) = 0$ curve with the rectangular contour is detected. The curve EF is followed through the search rectangle, and the exit point F is stored. No zeros of $f(z)$ are found along this curve. The rectangular contour search continues at mesh 24 edge 2 and goes until mesh square 23, where another

crossing of an $\text{Im}(f) = 0$ curve with the rectangular contour is found. But since this crossing point is the exit point found when following the curve EF, it is ignored and the rectangular contour search continues. The rectangular contour search will continue as described above until the search finally gets to mesh square 1 edge 4, where it stops.

The zeros of $f(z)$ found by the above search must be considered as approximate, since the approximation

$$f^{(k)}(\chi_k, \omega_k) = a_k + b_k \omega_k + c_k \chi_k + d_k \omega_k \chi_k \quad (5.23)$$

was used in each mesh square containing a zero, to solve for the location of the zero. These approximate zero locations can be used, however, as starting values in a Newton-Raphson iteration

$$z_{i+1} = z_i - \frac{f(z_i)}{f'(z_i)}, \quad (5.24)$$

in order to locate the zeros to within a preassigned tolerance ϵ .

When the Shellman-Morfitt root-finding routine was used to find zeros of the modal function (5.1), problems were encountered in locating the zeros that lie along the real q_{11} -axis. These zeros correspond to well-trapped modes. The cause of this difficulty is the fact that, as originally implemented, a mesh line would always fall on the real q_{11} -axis. The Shellman-Morfitt algorithm assumes that the zeros do not lie on a mesh line. Since some of the zeros of the modal function fall on or very close to the real q_{11} -axis, this assumption was not always true and difficulties ensued. To overcome this, a small offset was used to move the mesh lines off the real axis. No further difficulties were encountered once this was done.

6. SOLUTIONS OF STOKES' DIFFERENTIAL EQUATION

When the modified refractivity profile is approximated by linear segments, in the waveguide formulation of propagation of electromagnetic waves in tropospheric ducts, the modal equation and height-gain functions are expressible in terms of the solutions of Stokes' differential equation

$$\frac{d^2w}{d\xi^2} + \xi w(\xi) = 0 . \quad (6.1)$$

Since this is a second-order linear differential equation, there exist two linearly independent solutions $w_1(\xi)$ and $w_2(\xi)$. Any other solution to (6.1) can be expressed as a linear combination of $w_1(\xi)$ and $w_2(\xi)$:

$$y(\xi) = c_1 w_1(\xi) + c_2 w_2(\xi) . \quad (6.2)$$

One commonly chosen set of two linearly independent solutions of (6.1) consists of the Airy functions [30]

$$w_1(\xi) = \text{Ai}(-\xi) \quad (6.3)$$

and

$$w_2(\xi) = \text{Bi}(-\xi) . \quad (6.4)$$

The Wronskian for this set of linearly independent solutions is

$$\begin{aligned} W\{\text{Ai}(-\xi), \text{Bi}(-\xi)\} &= \text{Ai}(-\xi) \frac{d}{d\xi} [\text{Bi}(-\xi)] - \frac{d}{d\xi} [\text{Ai}(-\xi)] \text{Bi}(-\xi) \\ &= - \frac{1}{\pi} . \end{aligned} \quad (6.5)$$

While $\text{Ai}(-\xi)$ and $\text{Bi}(-\xi)$ are analytically linearly independent everywhere in the complex ξ -plane, they are numerically linearly independent only along the real axis and in the sector $|\text{ph}\xi| < \frac{\pi}{3}$. The advantage of this choice of solutions of (6.1) is that when ξ is real, both $\text{Ai}(-\xi)$ and $\text{Bi}(-\xi)$ are real. As $-\xi \rightarrow +\infty$, $\text{Ai}(-\xi)$ decays exponentially while $\text{Bi}(-\xi)$ grows exponentially. As $-\xi \rightarrow -\infty$, both $\text{Ai}(-\xi)$ and $\text{Bi}(-\xi)$ are decaying oscillatory functions of the same amplitude and with interlacing zeros.

Another possible set of linearly independent solutions of (6.1) consists of [30]

$$w_1(\xi) = \text{Ai}(-\xi) \quad (6.6)$$

and

$$w_2(\xi) = \text{Ai}(-\xi e^{2\pi i/3}) . \quad (6.7)$$

The Wronskian corresponding to this choice of linearly independent solutions is

$$W\{\text{Ai}(-\xi), \text{Ai}(-\xi e^{2\pi i/3})\} = -\frac{1}{2\pi} e^{-\pi i/6} . \quad (6.8)$$

The functions $\text{Ai}(-\xi)$ and $\text{Ai}(-\xi e^{2\pi i/3})$ are numerically linearly independent in the upper half of the complex ξ -plane.

A third possible choice for the linearly independent solutions of (6.1) consists of

$$w_1(\xi) = \text{Ai}(-\xi) \quad (6.9)$$

and

$$w_2(\xi) = \text{Ai}(-\xi e^{-2\pi i/3}) . \quad (6.10)$$

The Wronskian of these functions is

$$W\{\text{Ai}(-\xi), \text{Ai}(-\xi e^{-2\pi i/3})\} = -\frac{1}{2\pi} e^{\pi i/6} . \quad (6.11)$$

The functions $\text{Ai}(-\xi)$ and $\text{Ai}(-\xi e^{-2\pi i/3})$ are numerically linearly independent in the lower half of the complex ξ -plane.

In radio propagation work other choices for the two linearly independent solutions of Stokes' differential equation are frequently used. One such set of functions is the modified Hankel functions of order one-third [13], $h_1(\xi)$ and $h_2(\xi)$. The modified Hankel functions and their derivatives are related to the Airy functions by

$$\begin{aligned} h_1(\xi) &= (12)^{1/6} e^{-\pi i/6} [\text{Ai}(-\xi) - i\text{Bi}(-\xi)] \\ &= -2i(12)^{1/6} \text{Ai}(-\xi e^{2\pi i/3}) , \end{aligned} \quad (6.12)$$

$$\begin{aligned}
h_2(\xi) &= (12)^{1/6} e^{\pi i/6} [\text{Ai}(-\xi) + i\text{Bi}(-\xi)] \\
&= 2i(12)^{1/6} \text{Ai}(-\xi e^{-2\pi i/3}), \tag{6.13}
\end{aligned}$$

$$\begin{aligned}
h_1'(\xi) &= -(12)^{1/6} e^{-\pi i/6} [\text{Ai}'(-\xi) - i\text{Bi}'(-\xi)] \\
&= 2i(12)^{1/6} e^{2\pi i/3} \text{Ai}'(-\xi e^{2\pi i/3}), \tag{6.14}
\end{aligned}$$

and

$$\begin{aligned}
h_2'(\xi) &= -(12)^{1/6} e^{\pi i/6} [\text{Ai}'(-\xi) + i\text{Bi}'(-\xi)] \\
&= -2i(12)^{1/6} e^{-2\pi i/3} \text{Ai}'(-\xi e^{-2\pi i/3}), \tag{6.15}
\end{aligned}$$

where the prime denotes the derivative with respect to the argument. The Wronskian of $h_1(\xi)$ and $h_2(\xi)$ is

$$W\{h_1(\xi), h_2(\xi)\} = -\frac{4i}{\pi} \left(\frac{3}{2}\right)^{1/3}. \tag{6.16}$$

Marcus [1, 2] uses the functions $k_1(\xi)$ and $k_2(\xi)$ as the two linearly independent solutions of (6.1). These functions and their derivatives are related to the modified Hankel functions and the Airy functions by

$$\begin{aligned}
k_1(\xi) &= h_1(\xi) \\
&= -2i(12)^{1/6} \text{Ai}(-\xi e^{2\pi i/3}), \tag{6.17}
\end{aligned}$$

$$\begin{aligned}
k_2(\xi) &= h_2(\xi) - e^{4\pi i/3} h_1(\xi) \\
&= 2(12)^{1/6} e^{\pi i/6} \text{Ai}(-\xi), \tag{6.18}
\end{aligned}$$

$$\begin{aligned}
k_1'(\xi) &= h_1'(\xi) \\
&= 2i(12)^{1/6} e^{2\pi i/3} \text{Ai}'(-\xi e^{2\pi i/3}), \tag{6.19}
\end{aligned}$$

and

$$\begin{aligned}
k_2'(\xi) &= h_2'(\xi) - e^{4\pi i/3} h_1'(\xi) \\
&= -2(12)^{1/6} e^{\pi i/6} \text{Ai}'(-\xi). \tag{6.20}
\end{aligned}$$

The Wronskian of $k_1(\xi)$ and $k_2(\xi)$ is

$$W\{k_1(\xi), k_2(\xi)\} = -\frac{4i}{\pi} \left(\frac{3}{2}\right)^{1/3}. \quad (6.21)$$

The choice of which set of linearly independent solutions of Stokes' differential equation to use is dictated by the boundary conditions and numerical considerations. The arguments of the Airy functions appearing in the solution (2.32) for $\tilde{N}(\rho, q_j)$ are $q_j(z)$. Since $\text{Im}(q_{11})$ is proportional to the attenuation rate of the electromagnetic signal, from physical considerations $\text{Im}(q_{11}) > 0$. This, together with equations (2.30) and (2.129) implies that $\text{Im}[q_j(z)] > 0$. Therefore, the Airy functions occurring in $\tilde{N}(\rho, q_j)$ are all evaluated in the upper half of the complex q -plane. In the upper half of the complex plane a numerically satisfactory pair of linearly independent solutions of Stokes' differential equation consists of the Airy functions $\text{Ai}(-\xi)$ and $\text{Ai}(-\xi e^{2\pi i/3})$, or equivalently, $k_1(\xi)$ and $k_2(\xi)$.

The solution $\tilde{N}(\rho, z)$ to the tropospheric ducting problem has to satisfy the boundary condition that as $z \rightarrow +\infty$, $\tilde{N}(\rho, z)$ must represent an outgoing wave with time dependence e^{iwt} . A solution of Stokes' differential equation that asymptotically satisfies this requirement is $\text{Ai}(-\xi e^{-2\pi i/3})$. Therefore, in order to satisfy the outgoing wave condition in the topmost layer of the modified refractivity profile, $\text{Ai}(-\xi e^{-2\pi i/3})$ and $\text{Ai}(-\xi)$, [or equivalently, $h_2(\xi)$ and $h_1(\xi) - e^{-4\pi i/3} h_2(\xi)$] are chosen as the linearly independent set of solutions of Stokes' differential equation. While this set of solutions does satisfy the outgoing wave boundary condition, it is not a numerically satisfactory set of solutions in the upper half of the complex q -plane. For this reason this set of solutions is used only in the topmost layer of the modified refractivity profile.

While asymptotic expansions of the Airy functions $Ai(z)$ are available in the literature [30-32], none of these papers gives a rigorous upper bound for the magnitude of the error associated with these expansions. These bounds are useful for the writing of subroutines to evaluate the Airy functions. Error bounds for the asymptotic expansions of the Airy functions are next obtained by using the asymptotic expansions of the Hankel functions and modified Bessel functions and their error bounds.

The Airy function $Ai(z)$ and its derivative are related to the Hankel functions by

$$Ai(-z) = \frac{1}{2} \left(\frac{z}{3} \right)^{1/2} \left[e^{\pi i/6} H_{1/3}^{(1)}(\xi) + e^{-\pi i/6} H_{1/3}^{(2)}(\xi) \right] \quad (6.22)$$

and

$$Ai'(-z) = \frac{1}{2} \left(\frac{z}{\sqrt{3}} \right) \left[e^{-\pi i/6} H_{2/3}^{(1)}(\xi) + e^{\pi i/6} H_{2/3}^{(2)}(\xi) \right], \quad (6.23)$$

where

$$\xi = \frac{2}{3} z^{3/2} \quad . \quad (6.24)$$

The Hankel functions have the asymptotic expansions [33]

$$H_v^{(1)}(\xi) = \left(\frac{2}{\pi \xi} \right)^{1/2} \exp \left(i\xi - \frac{1}{2} v\pi i - \frac{1}{4} \pi i \right) \left\{ \sum_{k=0}^{n-1} i^k A_k(v) \xi^{-k} + \eta_n^{(1)}(\xi, v) \right\} \quad (-\pi + \delta \leq ph\xi \leq 2\pi - \delta) \quad (6.25)$$

and

$$H_v^{(2)}(\xi) = \left(\frac{2}{\pi \xi} \right)^{1/2} \exp \left(-i\xi + \frac{1}{2} v\pi i + \frac{1}{4} \pi i \right) \left\{ \sum_{k=0}^{n-1} (-i)^k A_k(v) \xi^{-k} + \eta_n^{(2)}(\xi, v) \right\} \quad (-2\pi + \delta \leq ph\xi \leq \pi - \delta), \quad (6.26)$$

where $\delta > 0$. The coefficients $A_k(v)$ are given by

$$A_0(v) = 1 \quad (6.27)$$

and

$$A_k(v) = \frac{[4v^2 - 1^2][4v^2 - 3^2] \cdots [4v^2 - (2k-1)^2]}{8^k k!} \quad (k \geq 1) . \quad (6.28)$$

The error term $\eta_n^{(1)}(\xi, v)$ is bounded by

$$|\eta_n^{(1)}(\xi, v)| \leq 2|A_n(v)|\phi_n^{(1)}(\xi) \exp\left\{ |v^2 - \frac{1}{4}| \phi_1^{(1)}(\xi) \right\} , \quad (6.29)$$

where the error control function $\phi_n^{(1)}(\xi)$ has the bounds

$$\phi_n^{(1)}(\xi) \leq \begin{cases} |\xi|^{-n} & (0 \leq ph\xi \leq \pi) \\ \chi(n) |\xi|^{-n} & \left(-\frac{\pi}{2} \leq ph\xi \leq 0; \pi \leq ph\xi \leq \frac{3\pi}{2}\right) \\ 2\chi(n) |\text{Im}(\xi)|^{-n} & \left(-\pi + \delta \leq ph\xi \leq -\frac{\pi}{2}; \frac{3\pi}{2} \leq ph\xi \leq 2\pi - \delta\right) \end{cases} \quad (6.30)$$

and

$$\chi(n) = \pi^{1/2} \frac{\Gamma\left(\frac{1}{2}n + 1\right)}{\Gamma\left(\frac{1}{2}n + \frac{1}{2}\right)} . \quad (6.31)$$

The error term $\eta_n^{(2)}(\xi, v)$ is bounded by

$$|\eta_n^{(2)}(\xi, v)| \leq 2|A_n(v)|\phi_n^{(2)}(\xi) \exp\left\{ |v^2 - \frac{1}{4}| \phi_1^{(2)}(\xi) \right\} , \quad (6.32)$$

where the error control function $\phi_n^{(2)}(\xi)$ is bounded by

$$\phi_n^{(2)}(\xi) \leq \begin{cases} |\xi|^{-n} & (-\pi \leq ph\xi \leq 0) \\ \chi(n) |\xi|^{-n} & (0 \leq ph\xi \leq \frac{\pi}{2}; -\frac{3\pi}{2} \leq ph\xi \leq -\pi) \\ 2\chi(n) |\text{Im}(\xi)|^{-n} & \left(\frac{\pi}{2} \leq ph\xi \leq \pi - \delta; -2\pi + \delta \leq ph\xi \leq -\frac{3\pi}{2}\right) \end{cases} \quad (6.33)$$

When $v = \frac{1}{3}$, equations (6.25, 6.26) become

$$\begin{aligned}
H_{1/3}^{(1)}(\xi) &= \left(\frac{2}{\pi\xi}\right)^{1/2} \exp\left(i\xi - \frac{5\pi i}{12}\right) \left\{ \sum_{k=0}^{n-1} i^k A_k \left(\frac{1}{3}\right) \xi^{-k} + \eta_n^{(1)}\left(\xi, \frac{1}{3}\right) \right\} \\
&\quad (-\pi + \delta \leq ph\xi \leq 2\pi - \delta) \\
&= \left(\frac{3}{\pi}\right)^{1/2} z^{-3/4} \exp\left(i\frac{2}{3}z^{3/2} - \frac{5\pi i}{12}\right) \left\{ \sum_{k=0}^{n-1} (-i)^k C_k z^{-3k/2} + \eta_n^{(1)}\left(\frac{2}{3}z^{3/2}, \frac{1}{3}\right) \right\} \\
&\quad (-\frac{2\pi}{3} + \delta' \leq phz \leq \frac{4\pi}{3} - \delta') \quad (6.34)
\end{aligned}$$

and

$$\begin{aligned}
H_{1/3}^{(2)}(\xi) &= \left(\frac{2}{\pi\xi}\right)^{1/2} \exp\left(-i\xi + \frac{5\pi i}{12}\right) \left\{ \sum_{k=0}^{n-1} (-i)^k A_k \left(\frac{1}{3}\right) \xi^{-k} + \eta_n^{(2)}\left(\xi, \frac{1}{3}\right) \right\} \\
&\quad (-2\pi + \delta \leq ph\xi \leq \pi - \delta) \\
&= \left(\frac{3}{\pi}\right)^{1/2} z^{-3/4} \exp\left(-i\frac{2}{3}z^{3/2} + \frac{5\pi i}{12}\right) \left\{ \sum_{k=0}^{n-1} i^k C_k z^{-3k/2} + \eta_n^{(2)}\left(\frac{2}{3}z^{3/2}, \frac{1}{3}\right) \right\} \\
&\quad (-\frac{4\pi}{3} + \delta' \leq phz \leq \frac{2\pi}{3} - \delta') \quad (6.35)
\end{aligned}$$

The coefficients $A_k \left(\frac{1}{3}\right)$ and C_k are given by

$$A_0 \left(\frac{1}{3}\right) = C_0 = 1 \quad (6.36)$$

and

$$\begin{aligned}
A_k \left(\frac{1}{3}\right) &= (-1)^k \frac{2^k}{3^k} C_k \\
&= (-1)^k \frac{[9-4][81-4]\cdots[9(2k-1)^2-4]}{3^{2k} 2^{3k} k!} \quad (k \geq 1) \quad (6.37)
\end{aligned}$$

The error terms $\eta_n^{(1)}\left(\xi, \frac{1}{3}\right)$ and $\eta_n^{(2)}\left(\xi, \frac{1}{3}\right)$ are bounded by

$$|\eta_n^{(1)}\left(\xi, \frac{1}{3}\right)| \leq \frac{2^{n+1}}{3^n} C_n \phi_n^{(1)}(\xi) \exp\left\{\frac{5}{36} \phi_1^{(1)}(\xi)\right\} \quad (6.38)$$

and

$$|\eta_n^{(2)}\left(\xi, \frac{1}{3}\right)| \leq \frac{2^{n+1}}{3^n} c_n \phi_n^{(2)}(\xi) \exp\left\{\frac{5}{36} \phi_1^{(2)}(\xi)\right\}. \quad (6.39)$$

Using the above results in equation (6.22) yields the asymptotic expansion

$$\begin{aligned} \text{Ai}(-z) &= \frac{1}{2} \pi^{-1/2} z^{-1/4} \left\{ \exp\left(i\xi - \frac{1}{4}\pi i\right) \left[\sum_{k=0}^{n-1} (-i)^k c_k z^{-3k/2} + \eta_n^{(1)}\left(\xi, \frac{1}{3}\right) \right] \right. \\ &\quad \left. + \exp\left(-i\xi + \frac{1}{4}\pi i\right) \left[\sum_{k=0}^{n-1} i^k c_k z^{-3k/2} + \eta_n^{(2)}\left(\xi, \frac{1}{3}\right) \right] \right\} \\ &\quad \left(-\frac{2\pi}{3} + \delta' \leq phz \leq \frac{2\pi}{3} - \delta' \right). \quad (6.40) \end{aligned}$$

Putting $v = \frac{2}{3}$ in equations (6.25, 6.26) yields

$$\begin{aligned} H_{2/3}^{(1)}(\xi) &= \left(\frac{2}{\pi\xi}\right)^{1/2} \exp\left(i\xi - \frac{7\pi i}{12}\right) \left\{ \sum_{k=0}^{n-1} i^k A_k\left(\frac{2}{3}\right) \xi^{-k} + \eta_n^{(1)}\left(\xi, \frac{2}{3}\right) \right\} \\ &\quad \left(-\pi + \delta \leq ph\xi \leq 2\pi - \delta \right) \\ &= \left(\frac{3}{\pi}\right)^{1/2} z^{-3/4} \exp\left(i\frac{2}{3}z^{3/2} - \frac{7\pi i}{12}\right) \left\{ \sum_{k=0}^{n-1} i^k D_k z^{-3k/2} + \eta_n^{(1)}\left(\frac{2}{3}z^{3/2}, \frac{2}{3}\right) \right\} \\ &\quad \left(-\frac{2\pi}{3} + \delta' \leq phz \leq \frac{4\pi}{3} - \delta' \right) \quad (6.41) \end{aligned}$$

and

$$\begin{aligned} H_{2/3}^{(2)}(\xi) &= \left(\frac{2}{\pi\xi}\right)^{1/2} \exp\left(-i\xi + \frac{7\pi i}{12}\right) \left\{ \sum_{k=0}^{n-1} (-i)^k A_k\left(\frac{2}{3}\right) \xi^{-k} + \eta_n^{(2)}\left(\xi, \frac{2}{3}\right) \right\} \\ &\quad \left(-2\pi + \delta \leq ph\xi \leq \pi - \delta \right) \\ &= \left(\frac{3}{\pi}\right)^{1/2} z^{-3/4} \exp\left(-i\frac{2}{3}z^{3/2} + \frac{7\pi i}{12}\right) \left\{ \sum_{k=0}^{n-1} (-i)^k D_k z^{-3k/2} + \eta_n^{(2)}\left(\frac{2}{3}z^{3/2}, \frac{2}{3}\right) \right\} \\ &\quad \left(-\frac{4\pi}{3} + \delta' \leq phz \leq \frac{2\pi}{3} - \delta' \right). \quad (6.42) \end{aligned}$$

The coefficients $A_k\left(\frac{2}{3}\right)$ and D_k are given by

$$A_0\left(\frac{2}{3}\right) = D_0 = 1 \quad (6.43)$$

and

$$A_k\left(\frac{2}{3}\right) = \frac{2^k}{3^k} D_k$$

$$= (-1)^k \frac{[9 - 16][81 - 16] \cdots [9(2k - 1)^2 - 16]}{3^{2k} 2^{3k} k!} \quad (k \geq 1) \quad (6.44)$$

The error terms $\eta_n^{(1)}\left(\xi, \frac{2}{3}\right)$ and $\eta_n^{(2)}\left(\xi, \frac{2}{3}\right)$ are bounded by

$$|\eta_n^{(1)}\left(\xi, \frac{2}{3}\right)| \leq \frac{2^{n+1}}{3^n} |D_n| \phi_n^{(1)}(\xi) \exp\left\{\frac{7}{36} \phi_1^{(1)}(\xi)\right\} \quad (6.45)$$

and

$$|\eta_n^{(2)}\left(\xi, \frac{2}{3}\right)| \leq \frac{2^{n+1}}{3^n} |D_n| \phi_n^{(2)}(\xi) \exp\left\{\frac{7}{36} \phi_1^{(2)}(\xi)\right\} \quad (6.46)$$

Combining the above results with equation (6.23) yields the asymptotic expansion

$$Ai'(-z) = -\frac{1}{2}\pi^{-1/2} z^{1/4} \left\{ \exp\left(i\xi + \frac{\pi i}{4}\right) \left[\sum_{k=0}^{n-1} i^k D_k z^{-3k/2} + \eta_n^{(1)}\left(\xi, \frac{2}{3}\right) \right] \right. \\ \left. + \exp\left(-i\xi - \frac{\pi i}{4}\right) \left[\sum_{k=0}^{n-1} (-i)^k D_k z^{-3k/2} + \eta_n^{(2)}\left(\xi, \frac{2}{3}\right) \right] \right\} \\ \left(-\frac{2\pi}{3} + \delta' \leq phz \leq \frac{2\pi}{3} - \delta' \right). \quad (6.47)$$

In order for asymptotic expansions of $Ai(z)$ and $Ai'(z)$ valid for other values of phz to be obtained, the equations [30]

$$Ai(z) = \frac{1}{\pi} \left(\frac{z}{3}\right)^{1/2} K_{1/3}(\xi) \quad (6.48)$$

and

$$Ai'(z) = -\frac{1}{\pi} \left(\frac{z}{\sqrt{3}}\right) K_{2/3}(\xi), \quad (6.49)$$

relating the Airy functions to the modified Bessel functions, are used. In equations (6.48, 6.49), ξ is again related to z by

$$\xi = \frac{2}{3}z^{3/2} . \quad (6.50)$$

The modified Bessel functions have the asymptotic expansion [33-35]

$$K_v(\xi) = \left(\frac{\pi}{2\xi}\right)^{1/2} e^{-\xi} \left\{ \sum_{k=0}^{n-1} A_k(v) \xi^{-k} + \gamma_n(\xi, v) \right\} \\ \left(-\frac{3\pi}{2} + \delta \leq ph\xi \leq \frac{3\pi}{2} - \delta \right) , \quad (6.51)$$

where the coefficients $A_k(v)$ are again given by equations (6.27, 6.28). The error term $\gamma_n(\xi, v)$ is bounded by

$$|\gamma_n(\xi, v)| \leq 2|A_n(v)|\psi_n(\xi) \exp\left\{ |v^2 - \frac{1}{4}\psi_1(\xi)| \right\} , \quad (6.52)$$

where the error control function $\psi_n(\xi)$ has the bounds

$$\psi_n(\xi) \leq \begin{cases} |\xi|^{-n} & \left(|ph\xi| \leq \frac{\pi}{2} \right) \\ \chi(n)|\xi|^{-n} & \left(\frac{\pi}{2} \leq |ph\xi| \leq \pi \right) \\ 2\chi(n)|\text{Re}(\xi)|^{-n} & \left(\pi \leq |ph\xi| \leq \frac{3\pi}{2} - \delta \right) . \end{cases} \quad (6.53)$$

When $v = \frac{1}{3}$, equations (6.51, 6.52) become

$$K_{1/3}(\xi) = \left(\frac{\pi}{2\xi}\right)^{1/2} e^{-\xi} \left\{ \sum_{k=0}^{n-1} A_k\left(\frac{1}{3}\right) \xi^{-k} + \gamma_n\left(\xi, \frac{1}{3}\right) \right\} \\ \left(-\frac{3\pi}{2} + \delta \leq ph\xi \leq \frac{3\pi}{2} - \delta \right) \\ = \left(\frac{3\pi}{4}\right)^{1/2} z^{-3/4} \exp\left(-\frac{2}{3}z^{3/2}\right) \left\{ \sum_{k=0}^{n-1} (-1)^k C_k z^{-3k/2} + \gamma_n\left(\frac{2}{3}z^{3/2}, \frac{1}{3}\right) \right\} \\ \left(-\pi + \delta' \leq phz \leq \pi - \delta' \right) , \quad (6.54)$$

where the error term is bounded by

$$|\gamma_n(\xi, \frac{1}{3})| \leq \frac{2^{n+1}}{3^n} C_n \psi_n(\xi) \exp \left\{ \frac{5}{36} \psi_1(\xi) \right\}. \quad (6.55)$$

Substituting equation (6.54) into equation (6.48) yields the asymptotic expansion

$$\begin{aligned} \text{Ai}(z) &= \frac{1}{2} \pi^{-1/2} z^{-1/4} e^{-\xi} \left\{ \sum_{k=0}^{n-1} (-1)^k C_k z^{-3k/2} + \gamma_n(\xi, \frac{1}{3}) \right\} \\ &\quad (-\pi + \delta' \leq phz \leq \pi - \delta') . \end{aligned} \quad (6.56)$$

Putting $v = \frac{2}{3}$ in equations (6.51, 6.52) yields the asymptotic expansion

$$\begin{aligned} K_{2/3}(\xi) &= \left(\frac{\pi}{2\xi} \right)^{1/2} e^{-\xi} \left\{ \sum_{k=0}^{n-1} A_k \left(\frac{2}{3} \right) \xi^{-k} + \gamma_n \left(\xi, \frac{2}{3} \right) \right\} \\ &\quad \left(-\frac{3\pi}{2} + \delta \leq ph\xi \leq \frac{3\pi}{2} - \delta \right) \\ &= \left(\frac{3\pi}{4} \right)^{1/2} z^{-3/4} \exp \left(-\frac{2}{3} z^{3/2} \right) \left\{ \sum_{k=0}^{n-1} D_k z^{-3k/2} + \gamma_n \left(\frac{2}{3} z^{3/2}, \frac{2}{3} \right) \right\} \\ &\quad (-\pi + \delta' \leq phz \leq \pi - \delta') , \end{aligned} \quad (6.57)$$

where the error term is bounded by

$$|\gamma_n(\xi, \frac{2}{3})| \leq \frac{2^{n+1}}{3^n} |D_n| \psi_n(\xi) \exp \left\{ \frac{7}{36} \psi_1(\xi) \right\} . \quad (6.58)$$

Combining equations (6.57) and (6.49) yields

$$\begin{aligned} \text{Ai}'(z) &= -\frac{1}{2} \pi^{-1/2} z^{1/4} e^{-\xi} \left\{ \sum_{k=0}^{n-1} D_k z^{-3k/2} + \gamma_n \left(\xi, \frac{2}{3} \right) \right\} \\ &\quad (-\pi + \delta \leq phz \leq \pi - \delta) . \end{aligned} \quad (6.59)$$

Consider the asymptotic expansion (6.40)

$$\begin{aligned}
 \text{Ai}(-z) = & \frac{1}{2}\pi^{-1/2}z^{-1/4} \left\{ \exp\left(i\xi - \frac{\pi i}{4}\right) \left[\sum_{k=0}^{n-1} (-i)^k c_k z^{-3k/2} + \eta_n^{(1)}\left(\xi, \frac{1}{3}\right) \right] \right. \\
 & \left. + \exp\left(-i\xi + \frac{\pi i}{4}\right) \left[\sum_{k=0}^{n-1} i^k c_k z^{-3k/2} + \eta_n^{(2)}\left(\xi, \frac{1}{3}\right) \right] \right\} \\
 & \left(-\frac{2\pi}{3} + \delta \leq \text{ph}z \leq \frac{2\pi}{3} - \delta \right). \quad (6.60)
 \end{aligned}$$

Let R_1 be the ratio of the bound for the error term $\eta_n^{(1)}\left(\xi, \frac{1}{3}\right)$ to the modulus of the first neglected term in the series $S_1 = \sum (-i)^k c_k z^{-3k/2}$. When $0 \leq \text{ph}z \leq \frac{2\pi}{3} - \delta$, this ratio is approximately 2. When $-\frac{\pi}{3} \leq \text{ph}z \leq 0$, R_1 is approximately $2\chi(n)$. When $-\frac{2\pi}{3} + \delta \leq \text{ph}z \leq -\frac{\pi}{3}$, R_1 is approximately $4\chi(n)\csc^n\left(\frac{3}{2}\delta\right)$. As $\delta \rightarrow 0$, this last bound grows sharply, warning that if $\eta_n^{(1)}\left(\xi, \frac{1}{3}\right)$ is neglected, this asymptotic expansion for $\text{Ai}(-z)$ is inaccurate for numerical work near the boundary $\text{ph}z = -\frac{2\pi}{3}$. Let R_2 be the ratio of the bound for the error term $\eta_n^{(2)}\left(\xi, \frac{1}{3}\right)$ to the modulus of the first neglected term in the series $S_2 = \sum i^k c_k z^{-3k/2}$. When $-\frac{2\pi}{3} + \delta \leq \text{ph}z \leq 0$, the ratio R_2 is approximately 2. When $0 \leq \text{ph}z \leq \frac{\pi}{3}$, the ratio R_2 is approximately $2\chi(n)$. When $\frac{\pi}{3} \leq \text{ph}z \leq \frac{2\pi}{3} - \delta$, the ratio R_2 is approximately $4\chi(n)\csc^n\left(\frac{3}{2}\delta\right)$. Again, as $\delta \rightarrow 0$, this bound grows sharply, indicating that the asymptotic expansion (6.60) is inaccurate for numerical work near the boundary $\text{ph}z = \frac{2\pi}{3}$. Therefore, the asymptotic expansion (6.60) for $\text{Ai}(-z)$ is satisfactory for numerical computation in the phase range $-\frac{\pi}{3} \leq \text{ph}z \leq \frac{\pi}{3}$. An identical argument gives the same result for the asymptotic expansion (6.47) for $\text{Ai}'(-z)$.

Now consider the asymptotic expansion (6.56)

$$\begin{aligned}
 \text{Ai}(z) = & \frac{1}{2}\pi^{-1/2}z^{-1/4}e^{-\xi} \left\{ \sum_{k=0}^{n-1} (-1)^k c_k z^{-3k/2} + \gamma_n\left(\xi, \frac{1}{3}\right) \right\} \\
 & \left(-\pi + \delta \leq \text{ph}z \leq \pi - \delta \right) \quad (6.61)
 \end{aligned}$$

Let R be the ratio of the bound for the error term $\gamma_n(\xi, \frac{1}{3})$ to the modulus of the first neglected term in the series $\sum (-1)^k C_k z^{-3k/2}$. When $-\frac{\pi}{3} \leq \text{phz} \leq \frac{\pi}{3}$, the ratio R is approximately 2. When $-\frac{2\pi}{3} \leq \text{phz} \leq -\frac{\pi}{3}$ or $\frac{\pi}{3} \leq \text{phz} \leq \frac{2\pi}{3}$, this ratio is approximately $2\chi(n)$. Finally, when $-\pi + \delta \leq \text{phz} \leq -\frac{2\pi}{3}$ or $\frac{2\pi}{3} \leq \text{phz} \leq \pi - \delta$, this ratio is approximately $4\chi(n) \sec^n(\frac{3}{2} \text{phz})$. This last value grows sharply as $\text{phz} \rightarrow -\pi$ or $\text{phz} \rightarrow \pi$, indicating that the asymptotic expansion (6.61) for $\text{Ai}(z)$ is inaccurate for numerical work near the boundaries $\text{phz} = -\pi$ and π . Therefore, this asymptotic expansion is satisfactory for numerical work in the sector $-\frac{2\pi}{3} \leq \text{phz} \leq \frac{2\pi}{3}$. An identical argument yields the same result for the asymptotic expansion (6.59) for $\text{Ai}'(z)$.

In summary, the Airy function $\text{Ai}(z)$ and its derivative have the asymptotic expansions

$$\text{Ai}(z) = \frac{1}{2}\pi^{-1/2} z^{-1/4} e^{-\xi} \left\{ \sum_{k=0}^{n-1} (-1)^k C_k z^{-3k/2} + \gamma_n(\xi, \frac{1}{3}) \right\} \left(-\frac{2\pi}{3} \leq \text{phz} \leq \frac{2\pi}{3} \right), \quad (6.62)$$

$$\begin{aligned} \text{Ai}(-z) = & \frac{1}{2}\pi^{-1/2} z^{-1/4} \left\{ \exp\left(i\xi - \frac{\pi i}{4}\right) \left[\sum_{k=0}^{n-1} (-i)^k C_k z^{-3k/2} + \eta_n^{(1)}\left(\xi, \frac{1}{3}\right) \right] \right. \\ & \left. + \exp\left(-i\xi + \frac{\pi i}{4}\right) \left[\sum_{k=0}^{n-1} i^k C_k z^{-3k/2} + \eta_n^{(2)}\left(\xi, \frac{1}{3}\right) \right] \right\} \\ & \left(-\frac{\pi}{3} \leq \text{phz} \leq \frac{\pi}{3} \right), \end{aligned} \quad (6.63)$$

$$\begin{aligned} \text{Ai}'(z) = & -\frac{1}{2}\pi^{-1/2} z^{1/4} e^{-\xi} \left\{ \sum_{k=0}^{n-1} D_k z^{-3k/2} + \gamma_n(\xi, \frac{2}{3}) \right\} \\ & \left(-\frac{2\pi}{3} \leq \text{phz} \leq \frac{2\pi}{3} \right), \end{aligned} \quad (6.64)$$

and

$$\begin{aligned}
 A(-z) = & -\frac{1}{2}\pi^{-1/2}z^{1/4} \left\{ \exp\left(i\xi + \frac{\pi i}{4}\right) \left[\sum_{k=0}^{n-1} i^k D_k z^{-3k/2} + \eta_n^{(1)}\left(\xi, \frac{2}{3}\right) \right] \right. \\
 & \left. + \exp\left(-i\xi - \frac{\pi i}{4}\right) \left[\sum_{k=0}^{n-1} (-i)^k D_k z^{-3k/2} + \eta_n^{(2)}\left(\xi, \frac{2}{3}\right) \right] \right\} \\
 & \left(-\frac{\pi}{3} \leq phz \leq \frac{\pi}{3} \right), \tag{6.65}
 \end{aligned}$$

where

$$\xi = \frac{2}{3}z^{3/2}. \tag{6.66}$$

The coefficients C_k and D_k are given by equations (6.37) and (6.44). They can be calculated using the recursion relations

$$C_0 = 1, \tag{6.67}$$

$$C_k = \frac{9(2k-1)^2 - 4}{48k} C_{k-1} \quad (k \geq 1), \tag{6.68}$$

$$D_0 = 1, \tag{6.69}$$

and

$$D_k = -\frac{9(2k-1)^2 - 16}{48k} D_{k-1} \quad (k \geq 1). \tag{6.70}$$

The error terms $\eta_n^{(1)}\left(\xi, \frac{1}{3}\right)$, $\eta_n^{(2)}\left(\xi, \frac{1}{3}\right)$, $\eta_n^{(1)}\left(\xi, \frac{2}{3}\right)$, $\eta_n^{(2)}\left(\xi, \frac{2}{3}\right)$,

$\gamma_n\left(\xi, \frac{1}{3}\right)$, and $\gamma_n\left(\xi, \frac{2}{3}\right)$ are bounded by

$$|\eta_n^{(1)}\left(\xi, \frac{1}{3}\right)| \leq \frac{2^{n+1}}{3^n} C_n \phi_n^{(1)}(\xi) \exp\left\{\frac{5}{36}\phi_1^{(1)}(\xi)\right\}, \tag{6.71}$$

$$|\eta_n^{(2)}\left(\xi, \frac{1}{3}\right)| \leq \frac{2^{n+1}}{3^n} C_n \phi_n^{(2)}(\xi) \exp\left\{\frac{5}{36}\phi_1^{(2)}(\xi)\right\}, \tag{6.72}$$

$$|\eta_n^{(1)}\left(\xi, \frac{2}{3}\right)| \leq \frac{2^{n+1}}{3^n} |D_n| \phi_n^{(1)}(\xi) \exp\left\{\frac{7}{36}\phi_1^{(1)}(\xi)\right\}, \quad (6.73)$$

$$|\eta_n^{(2)}\left(\xi, \frac{2}{3}\right)| \leq \frac{2^{n+1}}{3^n} |D_n| \phi_n^{(2)}(\xi) \exp\left\{\frac{7}{36}\phi_1^{(2)}(\xi)\right\}, \quad (6.74)$$

$$|\gamma_n\left(\xi, \frac{1}{3}\right)| \leq \frac{2^{n+1}}{3^n} C_n \psi_n(\xi) \exp\left\{\frac{5}{36}\psi_1(\xi)\right\}, \quad (6.75)$$

and

$$|\gamma_n\left(\xi, \frac{2}{3}\right)| \leq \frac{2^{n+1}}{3^n} |D_n| \psi_n(\xi) \exp\left\{\frac{7}{36}\psi_1(\xi)\right\}. \quad (6.76)$$

The error control functions $\phi_n^{(1)}(\xi)$, $\phi_n^{(2)}(\xi)$, and $\psi_n(\xi)$ are bounded by

$$\phi_n^{(1)}(\xi) \leq \begin{cases} |\xi|^{-n} & (0 \leq ph\xi \leq \pi) \\ \chi(n)|\xi|^{-n} & \left(-\frac{\pi}{2} \leq ph\xi \leq 0 ; \pi \leq ph\xi \leq \frac{3\pi}{2}\right) \\ 2\chi(n)|\text{Im}(\xi)|^{-n} & \left(-\pi + \delta \leq ph\xi \leq -\frac{\pi}{2} ; \frac{3\pi}{2} \leq ph\xi \leq 2\pi - \delta\right), \end{cases} \quad (6.77)$$

$$\phi_n^{(2)}(\xi) \leq \begin{cases} |\xi|^{-n} & (-\pi \leq ph\xi \leq 0) \\ \chi(n)|\xi|^{-n} & \left(0 \leq ph\xi \leq \frac{\pi}{2} ; -\frac{3}{2} \leq ph\xi \leq -\pi\right) \\ 2\chi(n)|\text{Im}(\xi)|^{-n} & \left(\frac{\pi}{2} \leq ph\xi \leq \pi - \delta ; -2\pi + \delta \leq ph\xi \leq -\frac{3\pi}{2}\right), \end{cases} \quad (6.78)$$

and

$$\psi_n(\xi) \leq \begin{cases} |\xi|^{-n} & \left(-\frac{\pi}{2} \leq ph\xi \leq \frac{\pi}{2}\right) \\ \chi(n)|\xi|^{-n} & \left(-\pi \leq ph\xi \leq -\frac{\pi}{2} ; \frac{\pi}{2} \leq ph\xi \leq \pi\right) \\ 2\chi(n)|\text{Re}(\xi)|^{-n} & \left(-\frac{3\pi}{2} + \delta \leq ph\xi \leq -\pi ; \pi \leq ph\xi \leq \frac{3\pi}{2} - \delta\right), \end{cases} \quad (6.79)$$

where $\delta > 0$ and

$$\chi(n) = \pi^{1/2} \frac{\Gamma\left(\frac{1}{2}n + 1\right)}{\Gamma\left(\frac{1}{2}n + \frac{1}{2}\right)} \quad (6.80)$$

Substituting the results for the asymptotic expansions of the Airy function and its derivative into equations (6.12-6.15) yields the asymptotic expansions of the modified Hankel functions of order one-third and their derivatives. The results are

$$h_1(z) = (12)^{1/6} \pi^{-1/2} z^{-1/4} \exp\left(i\xi - \frac{5\pi i}{12}\right) \left[\sum_{k=0}^{n-1} (-i)^k C_k z^{-3k/2} + \eta_n^{(1)}\left(\xi, \frac{1}{3}\right) \right] \\ \left(-\frac{\pi}{3} \leq phz \leq \pi \right), \quad (6.81)$$

$$h_1(z) = (12)^{1/6} \pi^{-1/2} z^{-1/4} \exp\left(-i\xi - \frac{11\pi i}{12}\right) \left[\sum_{k=0}^{n-1} i^k C_k z^{-3k/2} + \eta_n^{(1)}\left(\xi e^{\pi i}, \frac{1}{3}\right) \right] \\ + (12)^{1/6} \pi^{-1/2} z^{-1/4} \exp\left(i\xi - \frac{5\pi i}{12}\right) \left[\sum_{k=0}^{n-1} (-i)^k C_k z^{-3k/2} + \eta_n^{(1)}\left(\xi e^{2\pi i}, \frac{1}{3}\right) \right] \\ \left(-\pi \leq phz \leq -\frac{\pi}{3} \right), \quad (6.82)$$

$$h'_1(z) = i(12)^{1/6} \pi^{-1/2} z^{1/4} \exp\left(i\xi - \frac{5\pi i}{12}\right) \left[\sum_{k=0}^{n-1} i^k D_k z^{-3k/2} + \eta_n^{(1)}\left(\xi, \frac{2}{3}\right) \right] \\ \left(-\frac{\pi}{3} \leq phz \leq \pi \right), \quad (6.83)$$

$$h'_1(z) = i(12)^{1/6} \pi^{-1/2} z^{1/4} \exp\left(i\xi - \frac{5\pi i}{12}\right) \left[\sum_{k=0}^{n-1} i^k D_k z^{-3k/2} + \eta_n^{(1)}\left(\xi e^{2\pi i}, \frac{2}{3}\right) \right] \\ - i(12)^{1/6} \pi^{-1/2} z^{1/4} \exp\left(-i\xi - \frac{11\pi i}{12}\right) \left[\sum_{k=0}^{n-1} (-i)^k D_k z^{-3k/2} + \eta_n^{(1)}\left(\xi e^{\pi i}, \frac{2}{3}\right) \right] \\ \left(-\pi \leq phz \leq -\frac{\pi}{3} \right), \quad (6.84)$$

$$h_2(z) = (12)^{1/6} \pi^{-1/2} z^{-1/4} \exp\left(-i\xi + \frac{5\pi i}{12}\right) \left[\sum_{k=0}^{n-1} i^k C_k z^{-3k/2} + \eta_n^{(2)}\left(\xi, \frac{1}{3}\right) \right] \\ \left(-\pi \leq \text{ph}z \leq \frac{\pi}{3} \right), \quad (6.85)$$

$$h_2(z) = (12)^{1/6} \pi^{-1/2} z^{-1/4} \exp\left(-i\xi + \frac{5\pi i}{12}\right) \left[\sum_{k=0}^{n-1} i^k C_k z^{-3k/2} + \eta_n^{(2)}\left(\xi e^{-2\pi i}, \frac{1}{3}\right) \right] \\ + (12)^{1/6} \pi^{-1/2} z^{-1/4} \exp\left(i\xi + \frac{11\pi i}{12}\right) \left[\sum_{k=0}^{n-1} (-i)^k D_k z^{-3k/2} + \eta_n^{(2)}\left(\xi e^{-\pi i}, \frac{1}{3}\right) \right] \\ \left(\frac{\pi}{3} \leq \text{ph}z \leq \pi \right), \quad (6.86)$$

$$h_2'(z) = -i(12)^{1/6} \pi^{-1/2} z^{1/4} \exp\left(-i\xi + \frac{5\pi i}{12}\right) \left[\sum_{k=0}^{n-1} (-i)^k D_k z^{-3k/2} + \eta_n^{(2)}\left(\xi, \frac{2}{3}\right) \right] \\ \left(-\pi \leq \text{ph}z \leq \frac{\pi}{3} \right), \quad (6.87)$$

and

$$h_2'(z) = i(12)^{1/6} \pi^{-1/2} z^{1/4} \exp\left(i\xi + \frac{11\pi i}{12}\right) \left[\sum_{k=0}^{n-1} i^k D_k z^{-3k/2} + \eta_n^{(2)}\left(\xi e^{-\pi i}, \frac{2}{3}\right) \right] \\ - i(12)^{1/6} \pi^{-1/2} z^{1/4} \exp\left(-i\xi + \frac{5\pi i}{12}\right) \left[\sum_{k=0}^{n-1} (-i)^k D_k z^{-3k/2} + \eta_n^{(2)}\left(\xi e^{-2\pi i}, \frac{2}{3}\right) \right] \\ \left(\frac{\pi}{3} \leq \text{ph}z \leq \pi \right) \quad (6.88)$$

Using equations (6.17-6.20), which relate the functions $k_1(z)$ and $k_2(z)$ to the Airy functions, together with the asymptotic expansions for the Airy functions yields

$$k_1(z) = (12)^{1/6} \pi^{-1/2} z^{-1/4} \exp\left(i\xi - \frac{5\pi i}{12}\right) \left[\sum_{k=0}^{n-1} (-i)^k c_k z^{-3k/2} + \eta_n^{(1)}\left(\xi, \frac{1}{3}\right) \right] \\ \left(-\frac{\pi}{3} \leq phz \leq \pi \right), \quad (6.89)$$

$$k_1(z) = (12)^{1/6} \pi^{-1/2} z^{-1/4} \exp\left(-i\xi - \frac{11\pi i}{12}\right) \left[\sum_{k=0}^{n-1} i^k c_k z^{-3k/2} + \eta_n^{(1)}\left(\xi e^{\pi i}, \frac{1}{3}\right) \right] \\ + (12)^{1/6} \pi^{-1/2} z^{-1/4} \exp\left(i\xi - \frac{5\pi i}{12}\right) \left[\sum_{k=0}^{n-1} (-i)^k c_k z^{-3k/2} + \eta_n^{(1)}\left(\xi e^{2\pi i}, \frac{1}{3}\right) \right] \\ \left(-\pi \leq phz \leq -\frac{\pi}{3} \right), \quad (6.90)$$

$$k_1'(z) = i(12)^{1/6} \pi^{-1/2} z^{1/4} \exp\left(i\xi - \frac{5\pi i}{12}\right) \left[\sum_{k=0}^{n-1} i^k d_k z^{-3k/2} + \eta_n^{(1)}\left(\xi, \frac{2}{3}\right) \right] \\ \left(-\frac{\pi}{3} \leq phz \leq \pi \right), \quad (6.91)$$

$$k_1'(z) = i(12)^{1/6} \pi^{-1/2} z^{1/4} \exp\left(i\xi - \frac{5\pi i}{12}\right) \left[\sum_{k=0}^{n-1} i^k d_k z^{-3k/2} + \eta_n^{(1)}\left(\xi e^{2\pi i}, \frac{2}{3}\right) \right] \\ - i(12)^{1/6} \pi^{-1/2} z^{1/4} \exp\left(-i\xi - \frac{11\pi i}{12}\right) \left[\sum_{k=0}^{n-1} (-i)^k d_k z^{-3k/2} + \eta_n^{(2)}\left(\xi e^{\pi i}, \frac{2}{3}\right) \right] \\ \left(-\pi \leq phz \leq -\frac{\pi}{3} \right), \quad (6.92)$$

$$k_2(z) = (12)^{1/6} \pi^{-1/2} z^{-1/4} \exp\left(-i\xi + \frac{5\pi i}{12}\right) \left[\sum_{k=0}^{n-1} i^k c_k z^{-3k/2} + \eta_n^{(2)}\left(\xi, \frac{1}{3}\right) \right] \\ - (12)^{1/6} \pi^{-1/2} z^{-1/4} \exp\left(i\xi + \frac{11\pi i}{12}\right) \left[\sum_{k=0}^{n-1} (-i)^k c_k z^{-3k/2} + \eta_n^{(1)}\left(\xi, \frac{1}{3}\right) \right] \\ \left(-\frac{\pi}{3} \leq phz \leq \frac{\pi}{3} \right), \quad (6.93)$$

$$k_2(z) = -(12)^{1/6} \pi^{-1/2} z^{-1/4} \exp\left(i\xi + \frac{11\pi i}{12}\right) \left[\sum_{k=0}^{n-1} (-i)^k C_k z^{-3k/2} + \gamma_n\left(\xi e^{3\pi i/2}, \frac{1}{3}\right) \right]$$

$$\left(-\frac{5\pi}{3} \leq phz \leq -\frac{\pi}{3} \right), \quad (6.94)$$

$$k_2(z) = (12)^{1/6} \pi^{-1/2} z^{-1/4} \exp\left(-i\xi + \frac{5\pi i}{12}\right) \left[\sum_{k=0}^{n-1} i^k C_k z^{-3k/2} + \gamma_n\left(\xi e^{-3\pi i/2}, \frac{1}{3}\right) \right]$$

$$\left(\frac{\pi}{3} \leq phz \leq \frac{5\pi}{3} \right), \quad (6.95)$$

$$k'_2(z) = -i(12)^{1/6} \pi^{-1/2} z^{1/4} \exp\left(i\xi + \frac{11\pi i}{12}\right) \left[\sum_{k=0}^{n-1} i^k D_k z^{-3k/2} + \eta_n^{(1)}\left(\xi, \frac{2}{3}\right) \right]$$

$$- i(12)^{1/6} \pi^{-1/2} z^{1/4} \exp\left(-i\xi + \frac{5\pi i}{12}\right) \left[\sum_{k=0}^{n-1} (-i)^k D_k z^{-3k/2} + \eta_n^{(2)}\left(\xi, \frac{2}{3}\right) \right]$$

$$\left(-\frac{\pi}{3} \leq phz \leq \frac{\pi}{3} \right), \quad (6.96)$$

$$k'_2(z) = -i(12)^{1/6} \pi^{-1/2} z^{1/4} \exp\left(i\xi + \frac{11\pi i}{12}\right) \left[\sum_{k=0}^{n-1} i^k D_k z^{-3k/2} + \gamma_n\left(\xi e^{3\pi i/2}, \frac{2}{3}\right) \right]$$

$$\left(-\frac{5\pi}{3} \leq phz \leq -\frac{\pi}{3} \right), \quad (6.97)$$

and

$$k'_2(z) = -i(12)^{1/6} \pi^{-1/2} z^{1/4} \exp\left(-i\xi + \frac{5\pi i}{12}\right) \left[\sum_{k=0}^{n-1} (-i)^k D_k z^{-3k/2} + \gamma_n\left(\xi e^{-3\pi i/2}, \frac{2}{3}\right) \right]$$

$$\left(\frac{\pi}{3} \leq phz \leq \frac{5\pi}{3} \right). \quad (6.98)$$

Equations (6.94) and (6.95) are equivalent, as are equations (6.97) and (6.98). This is to be expected since the Airy function and its derivative are entire.

The preceding asymptotic expansions can be used to calculate $Ai(z)$ and $Ai'(z)$ when $|z|$ is large. The given error bounds can be used to determine how large $|z|$ must be in order to guarantee a given accuracy. For small values of $|z|$ the Airy functions can be evaluated by using the series expansions [30]

$$Ai(z) = c_1 f(z) - c_2 g(z) \quad (6.99)$$

and

$$Ai'(z) = c_1 f'(z) - c_2 g'(z) , \quad (6.100)$$

where

$$f(z) = \sum_{k=0}^{\infty} 3^k \frac{\Gamma\left(k + \frac{1}{3}\right)}{\Gamma\left(\frac{1}{3}\right)} \frac{z^{3k}}{(3k)!} , \quad (6.101)$$

$$f'(z) = \sum_{k=1}^{\infty} 3^k \frac{\Gamma\left(k + \frac{1}{3}\right)}{\Gamma\left(\frac{1}{3}\right)} \frac{z^{3k-1}}{(3k-1)!} , \quad (6.102)$$

$$g(z) = \sum_{k=0}^{\infty} 3^k \frac{\Gamma\left(k + \frac{2}{3}\right)}{\Gamma\left(\frac{2}{3}\right)} \frac{z^{3k+1}}{(3k+1)!} , \quad (6.103)$$

and

$$g'(z) = \sum_{k=0}^{\infty} 3^k \frac{\Gamma\left(k + \frac{2}{3}\right)}{\Gamma\left(\frac{2}{3}\right)} \frac{z^{3k}}{(3k)!} \quad (6.104)$$

The constants c_1 and c_2 are

$$c_1 = \frac{1}{3^{2/3} \Gamma\left(\frac{2}{3}\right)} \quad (6.105)$$

and

$$c_2 = \frac{1}{3^{1/3} \Gamma\left(\frac{1}{3}\right)} \quad (6.106)$$

In this section an upper bound for the error introduced by truncating the above series for $f(z)$ and $g(z)$ and their derivatives at N terms will be obtained. The largest absolute error due to truncation will occur when all the terms in the series have the same sign, i.e., when $z = x$ is real and positive. Except in the neighborhood of the zeros of $Ai(z)$ and $Ai'(z)$, the largest relative error will also occur when $z = x$ is real and positive.

The truncated series approximations for the Airy function and its derivative are given by

$$Ai_N(z) = c_1 f_N(z) - c_2 g_N(z) \quad (6.107)$$

and

$$Ai'_N(z) = c_1 f'_N(z) - c_2 g'_N(z) , \quad (6.108)$$

where

$$f_N(z) = \sum_{k=0}^{N-1} 3^k \frac{\Gamma\left(k + \frac{1}{3}\right)}{\Gamma\left(\frac{1}{3}\right)} \frac{z^{3k}}{(3k)!} , \quad (6.109)$$

$$f'_N(z) = \sum_{k=1}^{N-1} 3^k \frac{\Gamma\left(k + \frac{1}{3}\right)}{\Gamma\left(\frac{1}{3}\right)} \frac{z^{3k-1}}{(3k-1)!} , \quad (6.110)$$

$$g_N(z) = \sum_{k=0}^{N-1} 3^k \frac{\Gamma\left(k + \frac{2}{3}\right)}{\Gamma\left(\frac{2}{3}\right)} \frac{z^{3k+1}}{(3k+1)!} , \quad (6.111)$$

and

$$g'_N(z) = \sum_{k=0}^{N-1} 3^k \frac{\Gamma\left(k + \frac{2}{3}\right)}{\Gamma\left(\frac{2}{3}\right)} \frac{z^{3k}}{(3k)!} \quad (6.112)$$

are N term approximations to the infinite series (6.101-6.104).

The absolute error in approximating $Ai(z)$ with $Ai_N(z)$ is $|Ai(z) - Ai_N(z)|$. This is bounded by

$$|Ai(z) - Ai_N(z)| \leq c_1 |\varepsilon_N(z)| + c_2 |\delta_N(z)| , \quad (6.113)$$

where

$$\varepsilon_N(z) = f(z) - f_N(z) \quad (6.114)$$

and

$$\delta_N(z) = g(z) - g_N(z) . \quad (6.115)$$

Similarly, for the derivative $Ai'(z)$

$$|Ai'(z) - Ai'_N(z)| \leq c_1 |\bar{\varepsilon}_N(z)| + c_2 |\bar{\delta}_N(z)| , \quad (6.116)$$

where

$$\bar{\varepsilon}_N(z) = f'(z) - f'_N(z) \quad (6.117)$$

and

$$\bar{\delta}_N(z) = g'(z) - g'_N(z) . \quad (6.118)$$

An upper bound for $|\varepsilon_N(z)|$ can be obtained in the following manner. The truncation error $\varepsilon_N(z)$ for $f(z)$ is

$$\begin{aligned} \varepsilon_N(z) &= \sum_{k=N}^{\infty} 3^k \frac{\Gamma(k + \frac{1}{3})}{\Gamma(\frac{1}{3})} \frac{z^{3k}}{(3k)!} \\ &= \frac{3^N z^{3N}}{\Gamma(\frac{1}{3})} \sum_{j=0}^{\infty} 3^k \frac{\Gamma(j + N + \frac{1}{3})}{\Gamma(3j + 3N + 1)} 3^j z^{3j} . \end{aligned} \quad (6.119)$$

The triplication formula for the gamma function [36] yields

$$\begin{aligned} \Gamma(3j + 3N + 1) &= \Gamma\left(3\left[j + N + \frac{1}{3}\right]\right) \\ &= \frac{1}{2\pi} 3^{3j+3N+\frac{1}{2}} \Gamma\left(j + N + \frac{1}{3}\right) \Gamma\left(j + N + \frac{2}{3}\right) \Gamma\left(j + N + 1\right) . \end{aligned} \quad (6.120)$$

Therefore

$$\varepsilon_N(z) = \frac{2\pi z^{3N}}{\Gamma(\frac{1}{3}) 3^{2N+\frac{1}{2}}} \sum_{j=0}^{\infty} \frac{1}{\Gamma(j + N + \frac{1}{3}) \Gamma(j + N + 1)} \left(\frac{z^3}{3^2}\right)^j . \quad (6.121)$$

Now,

$$\Gamma(j + N + \frac{2}{3}) > \Gamma(j + N) \quad (6.122)$$

for all $j \geq 0$ if $N \geq 2$. Hence

$$|\varepsilon_N(z)| < \frac{2\pi|z|^{3N}}{\Gamma(\frac{1}{3})^{3^{2N+\frac{1}{2}}}} \sum_{j=0}^{\infty} \frac{1}{\Gamma(j + N) \Gamma(j + N + 1)} \left(\frac{|z|^3}{9}\right)^j \quad (N \geq 2). \quad (6.123)$$

The gamma functions in the sum in (6.123) satisfy the inequalities

$$\Gamma(j + N) \geq \Gamma(N)\Gamma(j + 1) = (N - 1)!j! \quad (6.124)$$

and

$$\Gamma(j + N + 1) \geq \Gamma(N + 1)\Gamma(j + 1) = N!j!. \quad (6.125)$$

Therefore,

$$|\varepsilon_N(z)| < \frac{2\pi|z|^{3N}}{\Gamma(\frac{1}{3})^{3^{2N+\frac{1}{2}}}(N - 1)!N!} \sum_{j=0}^{\infty} \frac{1}{(j!)^2} \left(\frac{|z|^3}{9}\right)^j. \quad (6.126)$$

The modified Bessel function

$$I_0\left(\frac{2}{3}|z|^{3/2}\right) = \sum_{j=0}^{\infty} \frac{1}{(j!)^2} \left(\frac{|z|^3}{9}\right)^j \quad (6.127)$$

satisfies the inequality [15]

$$I_0\left(\frac{2}{3}|z|^{3/2}\right) \leq \exp\left(\frac{2}{3}|z|^{3/2}\right). \quad (6.128)$$

This yields

$$|\varepsilon_N(z)| < \frac{2\pi}{3^{1/2}\Gamma(\frac{1}{3})(N - 1)!N!} \left(\frac{|z|^3}{9}\right)^N \exp\left(\frac{2}{3}|z|^{3/2}\right) \quad (N \geq 2), \quad (6.129)$$

or

$$c_1 |\varepsilon_N(z)| < \frac{1}{3^{2/3}(N - 1)!N!} \left(\frac{|z|^3}{9}\right)^N \exp\left(\frac{2}{3}|z|^{3/2}\right) \quad (N \geq 2). \quad (6.130)$$

Similarly, the truncation errors $\delta_N(z)$, $\bar{\varepsilon}_N(z)$, and $\bar{\delta}_N(z)$ are bounded by

$$|\delta_N(z)| < \frac{2\pi\sqrt{3}}{\Gamma\left(\frac{2}{3}\right)(N!)^2} |z| \left(\frac{|z|^3}{9}\right)^N \exp\left(\frac{2}{3}|z|^{3/2}\right) \quad (N \geq 1) , \quad (6.131)$$

$$|\bar{\varepsilon}_N(z)| < \frac{2\pi\sqrt{3}}{\Gamma\left(\frac{1}{3}\right)[(N-1)!]^2} \frac{1}{|z|} \left(\frac{|z|^3}{9}\right)^N \exp\left(\frac{2}{3}|z|^{3/2}\right) \quad (N \geq 2) , \quad (6.132)$$

and

$$|\bar{\delta}_N(z)| < \frac{2\pi}{\sqrt{3} \Gamma\left(\frac{2}{3}\right)(N-1)!N!} \left(\frac{|z|^3}{9}\right)^N \exp\left(\frac{2}{3}|z|^{3/2}\right) \quad (N \geq 2) . \quad (6.133)$$

The absolute errors due to truncation of the infinite series (6.101-6.104) for $\text{Ai}(z)$ and $\text{Ai}'(z)$ are therefore bounded by

$$|\text{Ai}(z) - \text{Ai}_N(z)| < \frac{1}{3^{2/3}(N-1)!N!} \left(\frac{|z|^3}{9}\right)^N \exp\left(\frac{2}{3}|z|^{3/2}\right) \left[1 + 3^{-2/3} \frac{|z|}{N}\right] \quad (N \geq 2) , \quad (6.134)$$

and

$$|\text{Ai}'(z) - \text{Ai}'_N(z)| < \frac{3^{1/3}}{[(N-1)!]^2} \frac{1}{|z|} \left(\frac{|z|^3}{9}\right)^N \exp\left(\frac{2}{3}|z|^{3/2}\right) \left[1 + 3^{-2/3} \frac{|z|}{N}\right] \quad (N \geq 2) . \quad (6.135)$$

When $z = x$ is real and positive, the asymptotic approximations for $\text{Ai}(x)$ and $\text{Ai}'(x)$ can be used easily to obtain bounds for the relative error. The Airy function $\text{Ai}(x)$ and its derivative have the asymptotic approximations

$$\text{Ai}(x) = \frac{1}{2}\pi^{-1/2} x^{-1/4} \exp\left(-\frac{2}{3}x^{3/2}\right) \left[1 + \gamma_1\left(\frac{2}{3}x^{3/2}, \frac{1}{3}\right)\right] \quad (x > 0) \quad (6.136)$$

and

$$\text{Ai}'(x) = -\frac{1}{2}\pi^{-1/2} x^{1/4} \exp\left(-\frac{2}{3}x^{3/2}\right) \left[1 + \gamma_1\left(\frac{2}{3}x^{3/2}, \frac{2}{3}\right)\right] \quad (x > 0) , \quad (6.137)$$

where the error terms are bounded by

$$|\gamma_1\left(\frac{2}{3}x^{3/2}, \frac{1}{3}\right)| \leq \frac{5}{24}x^{-3/2} \exp\left(\frac{5}{24}x^{-3/2}\right) \quad (6.138)$$

and

$$|\gamma_1\left(\frac{2}{3}x^{3/2}, \frac{2}{3}\right)| \leq \frac{7}{24}x^{-3/2} \exp\left(\frac{7}{24}x^{-3/2}\right). \quad (6.139)$$

The relative error in the value of $\text{Ai}(x)$ due to truncation is therefore bounded by

$$\begin{aligned} \frac{|\text{Ai}(x) - \text{Ai}_N(x)|}{|\text{Ai}(x)|} &< \frac{2\sqrt{\pi}x^{1/4}}{3^{2/3}(N-1)!N!} \left(\frac{x^3}{9}\right)^N \exp\left(\frac{4}{3}x^{3/2}\right) \left[1\right. \\ &\quad \left. + 3^{-2/3} \frac{x}{N} \left[1 - \frac{5}{24}x^{-3/2} \exp\left(\frac{5}{24}x^{-3/2}\right)\right]^{-1}\right] \quad (x > 0.52, N \geq 2), \end{aligned} \quad (6.140)$$

while the relative error in $\text{Ai}'(x)$ due to truncation is bounded by

$$\begin{aligned} \frac{|\text{Ai}'(x) - \text{Ai}'_N(x)|}{|\text{Ai}'(x)|} &< \frac{2\sqrt{\pi} 3^{1/3} x^{-5/4}}{\{(N-1)!\}^2} \left(\frac{x^3}{9}\right)^N \exp\left(\frac{4}{3}x^{3/2}\right) \left[1\right. \\ &\quad \left. + 3^{-2/3} \frac{x}{N} \left[1 - \frac{7}{24}x^{-3/2} \exp\left(\frac{7}{24}x^{-3/2}\right)\right]^{-1}\right] \quad (x > 0.65, N \geq 2). \end{aligned} \quad (6.141)$$

These bounds for the absolute and relative errors in $\text{Ai}(x)$ and $\text{Ai}'(x)$ due to truncation are upper bounds. In most cases these bounds are unduly pessimistic.

Another major source of error in calculating the Airy function and its derivative from equations (6.99, 6.100) is cancellation error. The functions $f(z)$ and $g(z)$ can be expressed in terms of the Airy functions $\text{Ai}(z)$ and $\text{Bi}(z)$ by [30]

$$f(z) = \frac{1}{2c_1} \left[\frac{1}{\sqrt{3}} \text{Bi}(z) + \text{Ai}(z) \right] \quad (6.142)$$

and

$$g(z) = \frac{1}{2c_2} \left[\frac{1}{\sqrt{3}} \text{Bi}(z) - \text{Ai}(z) \right]. \quad (6.143)$$

The derivatives of $f(z)$ and $g(z)$ are given by

$$f'(z) = \frac{1}{2c_1} \left[\frac{1}{\sqrt{3}} Bi'(z) + Ai'(z) \right] \quad (6.144)$$

and

$$g'(z) = \frac{1}{2c_2} \left[\frac{1}{\sqrt{3}} Bi'(z) + Ai'(z) \right]. \quad (6.145)$$

When $z = x$ is real and positive, the Airy functions $Ai(x)$ and $Bi(x)$ and their derivatives have the asymptotic approximations [30]

$$Ai(x) \sim \frac{1}{2} \pi^{-1/2} x^{-1/4} e^{-\xi}, \quad (6.146)$$

$$Bi(x) \sim \pi^{-1/2} x^{-1/4} e^{\xi}, \quad (6.147)$$

$$Ai'(x) \sim -\frac{1}{2} \pi^{-1/2} x^{1/4} e^{-\xi}, \quad (6.148)$$

and

$$Bi'(x) \sim \pi^{-1/2} x^{1/4} e^{\xi}, \quad (6.149)$$

where

$$\xi = \frac{2}{3} x^{3/2}. \quad (6.150)$$

Thus, the functions $f(x)$ and $g(x)$ and their derivatives all increase exponentially with increasing x . Since $Ai(x)$ and $Ai'(x)$ decrease exponentially with increasing x , severe cancellation errors can arise when using equations (6.99, 6.100) to calculate $Ai(x)$ and $Ai'(x)$. For example, at $x = 4.0$ the value of $Ai(x)$ is $Ai(x) \approx 0.000952$, while the values of $c_1 f(x)$ and $c_2 g(x)$ are $c_1 f(x) \approx 24.204$ and $c_2 g(x) \approx 24.204$. In order to obtain three significant figures for $Ai(x)$ at $x = 4.0$, eight significant figures are needed in $c_1 f(x)$ and $c_2 g(x)$. For reasonably large values of N , cancellation error is much more significant than truncation error.

7. EXTENDED COMPLEX ARITHMETIC

Because of the exponential nature of the Airy functions, the numerical evaluation of the modal function (2.124) easily can yield complex numbers with magnitudes as large as 10^{+1000} or as small as 10^{-1000} . Numbers of this size are outside the range of most computers, so special methods to handle them had to be incorporated into the waveguide program. A complex amplitude, ξ , and a real exponent, ϕ , were associated with each complex number z , i.e.,

$$z = \xi e^\phi . \quad (7.1)$$

No attempt was made to normalize the complex amplitudes ξ in XWVG. The complex amplitudes ξ typically have a magnitude falling between 10^{+3} and 10^{-3} . By handling the complex amplitude and real exponent separately, the very large and very small numbers obtained when evaluating the modal function over the search region of the complex q_{11} -plane are easily handled.

If $z_1 = \xi_1 e^{\phi_1}$ and $z_2 = \xi_2 e^{\phi_2}$ are two extended complex numbers, their product is the extended complex number

$$z = z_1 z_2 = \xi e^\phi , \quad (7.2)$$

where

$$\xi = \xi_1 \xi_2 \quad (7.3)$$

and

$$\phi = \phi_1 + \phi_2 . \quad (7.3)$$

If $\phi_1 \geq \phi_2$, the sum of the two extended complex numbers z_1 and z_2 is the extended complex number

$$z = z_1 + z_2 = \xi e^\phi , \quad (7.4)$$

where

$$\xi = \xi_1 + \xi_2 \exp(\phi_2 - \phi_1) \quad (7.5)$$

and

$$\phi = \phi_1 . \quad (7.6)$$

If $\phi_2 > \phi_1$, the complex amplitude and the real exponent for the sum would equal

$$\xi = \xi_2 + \xi_1 \exp(\phi_1 - \phi_2) \quad (7.7)$$

and

$$\phi = \phi_2 . \quad (7.8)$$

8. DESCRIPTION OF XWVG PROGRAM ELEMENTS

This section describes the 20 program elements comprising XWVG and gives the relationship between the different program elements.

MAIN

Description: MAIN is the controlling program element for the trilinear modified refractivity profile tropospheric propagation program XWVG. Besides calling the appropriate subroutines to determine the modal eigenvalues and evaluate the coherent and incoherent mode sums for the field strength, MAIN also performs all data input and output, sets up the search rectangles for the Shellman-Morfitt root-finding routine, and calculates the "constants" needed by other program elements.

The data for MAIN is read in from logical file number 13, the read file. Logical file number 13 is assumed to have one data item per record, with the data items in the following order:

- MFILE - If MFILE = 0 calculate eigenvalues. If MFILE = 1 read eigenvalues from logical file number 12.
- MPOL - If MPOL = 0 horizontal polarization. If MPOL = 1 vertical polarization.
- FREQ - The frequency, in MHz, of the propagating electromagnetic wave.
- ALPHA1 - The slope, in units of 1/meter, of the first (lowest) layer in the trilinear model of the troposphere. The α_i 's are related to $\frac{dM_i}{dz}$ by equation (2.13). ALPHA1 must be positive.
- ALPHA2 - The slope of the second (middle) layer in the trilinear model of the troposphere. ALPHA2 may be positive or negative but may not be zero.
- ALPHA3 - The slope of the third (top) layer in the trilinear model of the troposphere. ALPHA3 must be positive. For the standard atmosphere $\alpha = 0.236 \times 10^{-6}/m$.
- Z2 - The height, in meters, of the interface between the first and second layers of the trilinear model of the troposphere. The ground is assumed to be located at $z = 0$.
- Z3 - The height, in meters, of the interface between the second and third layers of the trilinear model of the troposphere. Z3 must be greater than Z2.

ZREF - The height, in meters, at which the value of the modified refractivity, $M(z)$, is specified. ZREF is assumed to be in the first layer, i.e.,

$$0 \leq ZREF \leq 22.$$

REFM - The value of the modified refractivity, in M-units, at the reference height ZREF.

ETA - The absorptivity of the tropospheric gases.

TEMP - The temperature of the seawater, in degrees Celsius, over the propagation path.

SALT - The salinity of the seawater, in grams of salt per kilogram of seawater, over the propagation path.

DELTA - The root mean square bump height, in meters, of the ocean surface over the propagation path.

ALOSS - The maximum loss rate, in dB/km, of the modes which will be found.

RNGINT - The initial range separation, in kilometers, between the transmitter and receiver.

NRNG - The number of range values for which field strength values will be calculated.

RNGSTP - The increment, in kilometers, by which the range changes.

ZRINIT - The initial height, in meters, of the receiver.

NZRCVR - The number of receiver heights for which the field strength will be calculated.

ZRSTEP - The increment, in meters, by which the receiver height changes.

ZXINIT - The initial height, in meters, of the transmitter.

NZXMTR - The number of transmitter heights for which the field strength will be calculated.

ZXSTEP - The increment, in meters, by which the transmitter height changes.

If the modal eigenvalues for a particular model have already been calculated and are stored in logical file number 12, then MFILE can be set equal to one and the modal eigenvalues will not be calculated again. This can save considerable computer time and expense. If the modal eigenvalues are to be calculated then set MFILE = 0. After the modal eigenvalues are calculated, MAIN writes their value in logical file number 12 so they can be stored for future use. MAIN writes the output of the trilinear duct tropospheric program to logical file number 11, the write file.

MAIN evaluates many of the quantities depending only upon the frequency, polarization, and duct parameters which are used by other program elements. These quantities are passed to the appropriate subroutines via Common Block areas.

The search rectangles used by the Shellman-Morfitt root-finding routine are set up by MAIN. The bottom of the search rectangle is

$$[\text{Im}(q_{11})]_{\text{bottom}} = \text{TBOT} = 0.0 ,$$

while the top of the search rectangle is given by [2]

$$[\text{Im}(q_{11})]_{\text{top}} = \text{TTOP} = 2 \left[\frac{1 \times 10^{-3} A_{\text{loss}}}{20k \log_{10}(e)} + \frac{\eta}{2} \right] \left(\frac{k}{\alpha_1} \right)^{2/3} .$$

In this equation for determining the top of the search rectangle, A_{loss} is the maximum attenuation rate in dB/km for the modes to be found, $k = \frac{w}{c}$ is the free space wave number, η is the tropospheric absorptivity, and α_1 is the slope of

the duct in the bottom layer. The left and right edges of the initial search rectangle are located at

$$[\operatorname{Re}(q_{11})]_{\text{left}} = \text{TLEFT} = \text{TLOLD} = 0.0$$

and

$$[\operatorname{Re}(q_{11})]_{\text{right}} = \text{TRIGHT} = \text{TROLD} = 2.0 .$$

Because of the discontinuity in $\hat{k}_1(q_{11})$ and $\hat{k}_2(q_{11})$ along the imaginary q_{11} -axis introduced by our implementation of surface roughness, it is necessary for the initial search rectangle to have its left edge on the imaginary axis. For further details see the description of subroutine KHATX. The location of the right edge of the initial search rectangle can be changed by changing the value of TROLD.

The Shellman-Morfitt root-finding routine is used to find the zeros of the modal function in each search rectangle. In order to find the zeros along the real axis, an offset of 0.003 is introduced in subroutines FCTVLX and FDFDTX. This offset in the modal eigenvalues is corrected in MAIN by the statement

$$\text{EIGEN}(\text{LK}) = \text{EIGEN}(\text{LK}) - \text{I}^* 0.003.$$

See the description of subroutine FCTVLX for more details.

After using the Shellman-Morfitt root-finding routine to search the initial search rectangle for modal eigenvalues, MAIN forms a new search rectangle to the left of the original by the statements

$$\text{TLEFT} = \text{TLOLD} - \text{TLSTEP}$$

$$\text{TRIGHT} = \text{TLOLD}$$

$$\text{TLOLD} = \text{TLEFT}$$

The width of the search rectangles formed to the left of the original can be varied by changing TLSTEP. If no zeros are found in NLEFT consecutive search rectangles, the search for modal eigenvalues to the left of the initial search rectangle is stopped. Next, MAIN starts forming search rectangles to the right of the initial search rectangle by using the statements

AD-A133 667

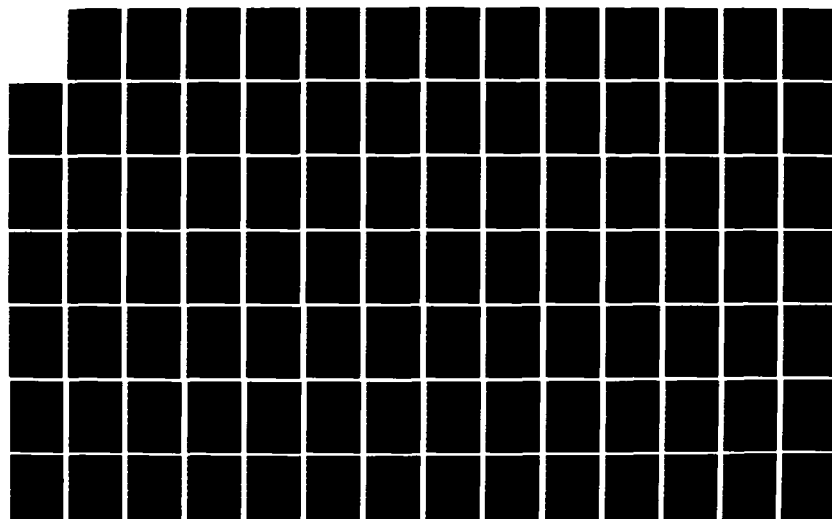
XWVG: A WAVEGUIDE PROGRAM FOR TRILINEAR TROPOSPHERIC
DUCTS COMPUTER PROGR. (U) NAVAL OCEAN SYSTEMS CENTER
SAN DIEGO CA G B BAUMGARTNER 30 JUN 83 NOSC/TD-610

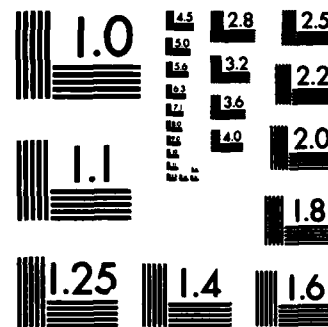
2/3

UNCLASSIFIED

F/G 20/14

NL





MICROCOPY RESOLUTION TEST CHART
NATIONAL BUREAU OF STANDARDS-1963-A

TLEFT = TROLD

TRIGHT = TROLD + TRSTEP

TROLD = TRIGHT.

The width of the search rectangles formed to the right of the original can be varied by changing TRSTEP. If no zeros are found in NRIGHT consecutive search rectangles, the search for modal eigenvalues to the right of the initial search rectangle is stopped.

The complete set of modes found by using the Shellman-Morfitt root-finding routine are stored in the array ZEROS. This array can hold up to NRZ elements. The value of NRZ can be changed by changing the PARAMETER statement in MAIN. If more than NRZ modes are found, MAIN will write a message indicating the search rectangles where the total number of modes exceeded NRZ. Only the first NRZ modes found are stored in ZEROS. After all the modes have been found, the modes stored in the array ZEROS are arranged by order of increasing real part, and any duplicate modes, i.e., modes within a distance $TOL = 0.0001$ of each other, are eliminated. These modes are then used by subroutine MODSUM to evaluate the field strength in dB relative to the free space value.

Calling Program Element: None.

Program Elements Called: CASIN, DHORIZ, FZEROX, MODSUM.

Common Block Areas: COMONE, COMTWO, COMTHR, COMFOR, COMFIV, COMSIX, COMSEV, COMEIG, COMNIN.

CADD

Description: Subroutine CADD adds two extended complex numbers of the form

$$z = \xi e^\phi ,$$

where ξ is a complex amplitude and ϕ a real exponent. If z_1 and z_2 are two extended complex numbers, their sum is

$$\begin{aligned} z &= z_1 + z_2 \\ &= \xi e^\phi , \end{aligned}$$

where, assuming $\phi_1 \geq \phi_2$,

$$\xi = \xi_1 + \xi_2 \exp(\phi_2 - \phi_1)$$

and

$$\phi = \phi_1 .$$

The complex amplitude ξ is not normalized in any way.

Call Statement: Subroutine CADD is called by the statement

CALL CADD (ZA, ZE, XA, XE, YA, YE).

The input variables of subroutine CADD are:

XA - The complex amplitude of the extended complex number x.

XE - The real exponent of the extended complex number x.

YA - The complex amplitude of the extended complex number y.

YE - The real exponent of the extended complex number y.

The output variables of subroutine CADD are:

ZA - The complex amplitude of the extended complex number
 $z = x + y$.

ZE - The real exponent of the extended complex number
 $z = x + y$.

Calling Program Elements: HTGAIN, FDFDTX, FCTVLX, KHATX, MODSUM.

Program Elements Called: None.

Common Block Areas: None.

ADDX

Description: Subroutine ADDX adds two extended real numbers of the form

$$z = \xi e^\phi ,$$

where ξ is a real amplitude and ϕ a real exponent. If z_1 and z_2 are two extended real numbers, their sum is

$$\begin{aligned} z &= z_1 + z_2 \\ &= \xi e^\phi , \end{aligned}$$

where, assuming $\phi_1 \geq \phi_2$,

$$\xi = \xi_1 + \xi_2 \exp(\phi_2 - \phi_1)$$

and

$$\phi = \phi_1 .$$

The real amplitude ξ is not normalized in any way.

Call Statement: Subroutine ADDX is called by the statement

```
CALL ADDX (ZA, ZE, XA, XE, YA, YE).
```

The input variables of subroutine ADDX are:

XA - The real amplitude of the extended real number x.

XE - The real exponent of the extended real number x.

YA - The real amplitude of the extended real number y.

YE - The real exponent of the extended real number y.

The output variables of subroutine ADDX are:

ZA - The real amplitude of the extended real number $z = x + y$.

ZE - The real exponent of the extended real number $z = x + y$.

Calling Program Element: MODSUM.

Program Elements Called: None.

Common Block Areas: None.

HNKLX

Description: Subroutine HNKLX evaluates the modified Hankel functions of order one-third, $h_1(z)$ and $h_2(z)$, and their derivatives in extended complex arithmetic.

Call Statement: Subroutine HNKLX is called by the statement

```
CALL HNKLX (Z, H1A, H1E, H2A, H2E, DH1A, DH1E, DH2A, DH2E).
```

The input variable of subroutine HNKLX is:

Z - The location in the complex plane where the modified Hankel functions of order one-third and their derivatives are to be evaluated.

The output variables of subroutine HNKLX are:

- H1A - The complex amplitude of $h_1(z)$ in extended complex arithmetic.
- H1E - The real exponent of $h_1(z)$ in extended complex arithmetic.
- H2A - The complex amplitude of $h_2(z)$.
- H2E - The real exponent of $h_2(z)$.
- DH1A - The complex amplitude of $h'_1(z)$.
- DH1E - The real exponent of $h'_1(z)$.
- DH2A - The complex amplitude of $h'_2(z)$.
- DH2E - The real exponent of $h'_2(z)$.

Calling Program Elements: HTGAIN, FDFDTX, FCTVLX.

Program Elements Called: None.

Common Block Areas: None.

KHNKLX

Description: Subroutine KHNKLX evaluates the modified Hankel functions $k_1(z)$ and $k_2(z)$ and their derivatives in extended complex arithmetic.

Call Statement: Subroutine KHNKLX is called by the statement

```
CALL KHNKLX (Z, K1A, K1E, K2A, K2E, DK1A, DK1E, DK2A, DK2E).
```

The input variable of subroutine KHNKLX is:

Z - The location in the complex plane where the modified Hankel functions and their derivatives are to be evaluated.

The output variables of subroutine KHNKLX are:

K1A - The complex amplitude of $k_1(z)$ in extended complex arithmetic.
K1E - The real exponent of $k_1(z)$ in extended complex arithmetic.
K2A - The complex amplitude of $k_2(z)$.
K2E - The real exponent of $k_2(z)$.
DK1A - The complex amplitude of $k'_1(z)$.
DK1E - The real exponent of $k'_1(z)$.
DK2A - The complex amplitude of $k'_2(z)$.
DK2E - The real exponent of $k'_2(z)$.

Calling Program Elements: HTGAIN, FDFDTX, FCTVLX.

Program Elements Called: None.

Common Block Areas: None.

KHATX

Description: Subroutine KHATX evaluates the modified Hankel function combinations $k_1(q_{11})$ and $k_2(q_{11})$ and their derivatives in extended complex arithmetic. For the surface roughness model used in this program, the rms surface bump height δ was always taken to be zero when $\text{Re}(q_{11}) < 0$ since modes with $\text{Re}(q_{11}) < 0$ correspond to well-trapped modes and should be unaffected by the surface. This creates a discontinuity in $k_1(q_{11})$ and $k_2(q_{11})$ and hence, in the modal function, at $\text{Re}(q_{11}) = 0$ when $\delta \neq 0$. In order to use the Shellman-Morfitt root-finding routine with this discontinuity, when $\text{Re}(q_{11}) = 0$, subroutine KHATX has to know whether the current search rectangle lies to the left or right of the imaginary q_{11} axis and to evaluate $k_1(q_{11})$ and $k_2(q_{11})$ so that they will be continuous over the entire search rectangle. The information needed to do this is passed to KHATX from MAIN in the form of the flag INTCHK. When the initial search rectangle is set up, it is located at $0 \leq \text{Re}(q_{11}) \leq \text{TROLD}$ and $\text{INTCHK} = 0$. For search rectangles to the left of the initial search rectangle, that is for $\text{Re}(q_{11}) \leq 0$, $\text{INTCHK} = 1$. When $\text{Re}(q_{11}) = 0$, KHATX tests INTCHK to determine whether the search rectangle is to the left or right of the imaginary q_{11} axis and evaluates the proper "branch" of $k_1(q_{11})$ and $k_2(q_{11})$.

Call Statement: Subroutine KHATX is called by the statement

```
CALL KHATX (Q11, KHA1, KHE1, KHA2, KHE2, DKHA1, DKHE1, DKHA2, DKHE2).
```

The input variable of subroutine KHATX is:

Q11 - The location in the complex q_{11} -plane where $k_1(q_{11})$ and $k_2(q_{11})$ and their derivatives are to be evaluated.

The output variables of subroutine KHATX are:

KHA1 - The complex amplitude of $k_1(q_{11})$ in extended complex arithmetic.

KHE1 - The real exponent of $k_1(q_{11})$ in extended complex arithmetic.

KHA2 - The complex amplitude of $k_2(q_{11})$.
KHE2 - The real exponent of $k_2(q_{11})$.
DKHA1 - The complex amplitude of $k_1'(q_{11})$.
DKHE1 - The real exponent of $k_1'(q_{11})$.
DKHA2 - The complex amplitude of $k_2'(q_{11})$.
DKHE2 - The real exponent of $k_2'(q_{11})$.

Calling Program Elements: HTGAIN, FDFDTX, FCTVLX.

Program Elements Called: KHNKLX, CADD, CTANH, CSECH2.

Common Block Areas: COMTWO, COMTHR, COMFOR, COMFIV, COMSIX, COMSEV, COMEIG, COMININ.

CTANH

Description: The complex function subroutine CTANH evaluates the complex hyperbolic tangent of the complex number z. If

$$|\operatorname{Re}(z)| > \frac{1}{10\sqrt{2}} \text{ or } |\operatorname{Im}(z)| > \frac{1}{10\sqrt{2}} ,$$

then $\tanh(z)$ is evaluated by using

$$\tanh(z) = \frac{e^z - e^{-z}}{e^z + e^{-z}} .$$

If

$$|\operatorname{Re}(z)| \leq \frac{1}{10\sqrt{2}} \text{ and } |\operatorname{Im}(z)| \leq \frac{1}{10\sqrt{2}} ,$$

then $\tanh(z)$ is evaluated by using the first five terms of the Taylor series expansion

$$\tanh(z) = z - \frac{1}{3}z^3 + \frac{2}{15}z^5 - \frac{17}{315}z^7 + \frac{62}{2835}z^9 - \dots .$$

Calling Statement: The complex function subroutine CTANH is called by
CTANH(Z).

The input variable of function subroutine CTANH is:

Z - A complex number.

The output variable of function subroutine CTANH is:

CTANH - The hyperbolic tangent of the complex number z.

Calling Program Element: KHATX.

Program Elements Called: None.

Common Block Areas: None.

CSECH2

Description: The complex function subroutine CSECH2 evaluates the square of the hyperbolic secant of the complex variable z by using

$$\operatorname{sech}^2(z) = \frac{4}{e^{2z} + 2 + e^{-2z}}.$$

Calling Statement: The complex function subroutine CSECH2 is called by

CSECH2(Z).

The input variable of function subroutine CSECH2 is:

Z - A complex number.

The output variable of function subroutine CSECH2 is:

CSECH2 - The square of the hyperbolic secant of the complex variable z.

Calling Program Element: KHATX.

Program Elements Called: None.

Common Block Areas: None.

FCTVLX

Description: Subroutine FCTVLX evaluates the modal function $||\tilde{\Delta}(q_{11})||$ in extended complex arithmetic. When using the Shellman-Morfitt root-finding routine to locate the zeros of a complex function, it is assumed that these zeros do not fall on a mesh line. Since the imaginary part of some of the zeros of $||\tilde{\Delta}(q_{11})||$ are numerically indistinguishable from zero, the real q_{11} axis should not be a mesh line. However, because of the way the Shellman-Morfitt root-finding routine sets up mesh squares, if the real axis passes through a search rectangle, the real axis will always be a mesh line. One way to avoid problems caused by this is to find the zeros of the functions $||\tilde{\Delta}(t_{11})||$ where

$$t_{11} = q_{11} - i\Delta q . \quad (8.1)$$

The shift Δq is chosen to satisfy

$$\delta_T < \Delta q < \frac{1}{2n_{\max}}\delta_m , \quad (8.2)$$

where δ_T is the tolerance to which zeros are located, δ_m is the initial mesh size, and n_{\max} is the maximum number of times that subroutine FZEROX will reduce the mesh size by a factor of two. In XWVG where $\delta_T = 0.0001$, $\delta_m = 0.04$, and $n_{\max} = 2$, a value $\Delta q = 0.003$ is chosen. With Δq chosen to satisfy (8.2), even if subroutine FZEROX reduces the mesh size by a factor of two n_{\max} times, the values of t_{11} corresponding to $\text{Im}(q_{11}) = 0$ will still not lie on a mesh line. From equation (8.1) it is seen that the zeros of $||\tilde{\Delta}(q_{11})||$ that were along the line $\text{Im}(q_{11}) = 0$ are now shifted to the line $\text{Im}(q_{11}) = +i\Delta q$. Thus, the zeros of $||\tilde{\Delta}(t_{11})||$ are related to the zeros of $||\tilde{\Delta}(q_{11})||$ by

$$q_{11} = t_{11} - i\Delta q . \quad (8.3)$$

The shift to the new variable t_{11} occurs inside subroutine FCTVLX as well as inside subroutine FDFDTX. The shift back to q_{11} , equation (8.3), occurs in MAIN. Subroutine EXCFAC, which uses subroutine FDFDTX, also has a statement that compensates for the shift, Δq .

Calling Statement: Subroutine FCTVLX is called by the statement

CALL FCTVLX (Q11, DETA, DETE).

The input variable of subroutine FCTVLX is:

Q11 - The location in the complex q_{11} -plane where the modal function is to be evaluated.

The output variables of subroutine FCTVLX are:

DETA - The complex amplitude of the modal function in extended complex arithmetic.

DETE - The real exponent of the modal function in extended complex arithmetic.

Calling Program Element: FINDFX.

Program Elements Called: HNKLX, KHNKLX, KHATX, CADD.

Common Block Areas: COMONE, COMTWO.

FDFDTX

Description: Subroutine FDFDTX evaluates the modal function $||\Delta(q_{11})||$ and its derivative

$$\frac{\partial}{\partial q_{11}} \{ ||\Delta(q_{11})|| \}$$

in extended complex arithmetic. As in subroutine FCTVLX, the value of q_{11} is shifted inside the subroutine to

$$t_{11} = q_{11} - i\Delta q ,$$

where $\Delta q = 0.003$. This shift by Δq is compensated for in MAIN when FDFDTX is used by the Shellman-Morfitt root-finding routine. When FDFDTX is used in the evaluation of the modal excitation factors, this shift by Δq is compensated for in subroutine EXCFAC.

Calling Statement: Subroutine FDFDTX is called by the statement

```
CALL FDFDTX (Q11, DETA, DETE, DETPA, DETPE).
```

The input variable of subroutine FDFDTX is:

Q11 - The location in the complex q_{11} -plane where the modal function and its derivative are to be evaluated.

The output variables of subroutine FDFDTX are:

DETA - The complex amplitude of the modal function in extended complex arithmetic.

DETE - The real exponent of the modal function in extended complex arithmetic.

DETPA - The complex amplitude of the derivative of the modal function.

DETPE - The real exponent of the derivative of the modal function.

Calling Program Elements: NOMSHX, EXCFAC.

Program Elements Called: HNKLX, KHNKLX, KHATX, CADD.

Common Block Areas: COMONE, COMTWO.

FZEROX

Description: Subroutine FZEROX is the main subroutine of the Shellman-Morfitt root-finding routine modified for extended complex arithmetic and the trilinear tropospheric duct model. The other subroutines comprising the Shellman-Morfitt root-finding routine are subroutines QUAD, NOMSHX, and FINDFX. Subroutine FZEROX divides a specified rectangular region of the complex plane into mesh squares and determines approximate values for the complex zeros of an analytic function $f(z)$. These approximate values for the zeros of $f(z)$ are improved by subroutine NOMSHX by using Newton-Raphson iteration. The function $f(z)$ is assumed to have no poles or branch cuts in the rectangular region of the complex plane being searched. The zeros of $f(z)$ in the search region are assumed to be simple zeros. Other assumptions made are that the zeros of $f(z)$ do not fall on the mesh lines and that the lines $\text{Im}[f(z)] = 0$ and $\text{Re}[f(z)] = 0$ do not coincide with mesh lines. The maximum number of crossings of $\text{Im}[f(z)] = 0$ with any one edge of the search rectangle that is currently allowed by FZEROX is 50. This value can be changed by changing the dimensions of KEDGE1, KEDGE2, KEDGE3, and KEDGE4.

Because of the discontinuity of the modal function along the imaginary axis that is introduced by the discontinuity in the surface roughness formula, special care has to be taken when finding the complex roots of the modal function in a search rectangle that has TLEFT = 0.0 or TRIGHT = 0.0. Since FZEROX will normally extend the search rectangle by one mesh square in all directions, this expansion to the left or right has to be suppressed when TLEFT = 0.0 or TRIGHT = 0.0. This is done with the statements

```
IF(TLEFT.EQ.0.0)    JLT = 0
```

and

```
IF(TRIGHT.EQ.0.0)    JRT = 0
```

in subroutine FZEROX. When the modal function $||\tilde{\Delta}(q_{11})||$ is evaluated along the imaginary axis, the value of q_{11} is offset by an amount SHIFT = $\pm 1.0 \times 10^{-9}$ in subroutine FINDFX. The plus sign is taken if the search rectangle

lies to the right of the imaginary axis and the minus sign is taken if the search rectangle lies to the left of the imaginary axis.

Calling Statement: Subroutine FZEROX is called by the statement

CALL FZEROX (TLEFT, TRIGHT, TBOT, TTOP, TMSH0, TOL, MPRINT, ZEROS, NRZ).

The input variables of subroutine FZEROX are:

TLEFT - The value of the real part of z at the left edge of the search rectangle.

TRIGHT - The value of the real part of z at the right edge of the search rectangle.

TBOT - The value of the imaginary part of z at the bottom edge of the search rectangle.

TTOP - The value of the imaginary part of z at the top edge of the search rectangle.

TMSH0 - The initial size of the mesh squares used to divide the search rectangle. TMSH0 should be small enough so that the variation of $\text{Im}[f(z)]$ and $\text{Re}[f(z)]$ along the mesh square edges is approximately linear. Subroutine FZEROX assumes that this is true. The smaller TMSH0 is, the longer the program running time. Under some circumstances FZEROX will automatically reduce the mesh size by a factor of 2 a total of $\text{MAXNT} = 2$ times. If FZEROX still experiences difficulties after these reductions in mesh size, an error message will be output and the program will stop. FZEROX allows a maximum number, MAXNSQ, of mesh squares to lie on any one phase curve $\text{Im}[f(z)] = 0$ in the search rectangle. If this number is exceeded, an error message is output and the program stops. MAXNSQ is currently set at four times the number of mesh squares along the longest side of the search rectangle.

TOL - The tolerance to which zeros are located. Zeros located closer together than TOL cannot be distinguished.

MPRINT - A flag for debugging output. If MPRINT = 0, no debugging printout is given; while if MPRINT = 1, debugging printout is given. A value of MPRINT = 0 is recommended except when absolutely necessary, because of the large amount of printout produced.

The output variables of subroutine FZEROX are:

ZEROS - An array containing the complex zeros of $f(z)$ in the specified rectangular region of the complex plane. The array ZEROS assumes the dimensions specified in MAIN.

NRZ - The number of complex zeros of $f(z)$ in the specified rectangular region of the complex plane.

Calling Program Element: MAIN.

Program Elements Called: QUAD, NOMSHX, FINDFX.

Common Block Areas: NEWMSH, TMCCOM.

QUAD

Description: Subroutine QUAD is an auxiliary subroutine in the Shellman-Morfitt root-finding routine. The other subroutines comprising the Shellman-Morfitt root-finding routine are FZEROX, NOMSHX, and FINDFX. Subroutine QUAD finds the real roots of a quadratic equation of the form

$$ax^2 + 2bx + c = 0.$$

Calling Statement: Subroutine QUAD is called by the statement

```
CALL QUAD (A, B, C, SOL, NRSOL).
```

The input variables of subroutine QUAD are:

A - The coefficient of x^2 in the quadratic equation.

B - The coefficient of $2x$ in the quadratic equation.

C - The constant term in the quadratic equation.

The output variables of subroutine QUAD are:

SOL - An array containing the real roots of the quadratic equation.

NRSOL - The number of real roots of the quadratic equation found. A value of NRSOL = 1 results when the quadratic equation approaches linearity.

Calling Program Element: FZEROX.

Program Elements Called: None.

Common Block Areas: None.

NOMSHX

Description: Subroutine NOMSHX is an auxiliary subroutine of the Shellman-Morfitt root-finding routine modified for extended complex arithmetic. The other subroutines that comprise the Shellman-Morfitt root-finding routine are FZEROX, FINDFX, and QUAD. Subroutine NOMSHX takes the approximate locations of the complex zeros of $f(z)$ provided by subroutine FZEROX and improves them by using Newton-Raphson iteration.

Calling Statement: Subroutine NOMSHX is called by the statement

```
CALL NOMSHX (TMESH, TOL, MPRINT, ZEROS, NRZ).
```

The input variables of subroutine NOMSHX are:

TMESH - The size of the mesh squares used to divide the search rectangle.

TOL - The tolerance to which zeros are to be located. Zeros located closer than TOL cannot be distinguished.

MPRINT - A flag for debugging output. If MPRINT = 0, no debugging printout is given; while if MPRINT = 1, debugging printout is given.

ZEROS - An array containing the approximate location of the complex zeros of $f(z)$.

NRZ - The number of complex zeros stored in array ZEROS.

The output variable of subroutine NOMSHX is:

ZEROS - An array containing the Newton-Raphson iterated values for the complex zeros of $f(z)$. ZEROS is used for both input and output.

Calling Program Element: FZEROX.

Program Elements Called: FDFDTX.

Common Block Areas: NEWMSH.

FINDFX

Description: Subroutine FINDFX is an auxiliary subroutine of the Shellman-Morfitt root-finding routine modified for extended complex arithmetic and the trilinear tropospheric duct propagation model. The other subroutines that comprise the Shellman-Morfitt root-finding routine are FZEROX, QUAD, and NOMSHX. Subroutine FINDFX takes the coordinates of the mesh square corners and evaluates the modal function $||\Delta(q_{11})||$ there. The modal function is evaluated in extended complex arithmetic. Because of the discontinuity of the modal function along the imaginary q_{11} axis introduced by the surface roughness formulation, special care has to be taken when finding the complex zeros of $||\Delta(q_{11})||$ in a search rectangle that has TLEFT = 0.0 or TRIGHT = 0.0. The Shellman-Morfitt root-finding routine requires that $||\Delta(q_{11})||$ have no poles, branch cuts, or other discontinuities in the search rectangle. In order to ensure that this condition is met when the search rectangle has TLEFT = 0.0 or TRIGHT = 0.0, a small offset value $OFFSET = 1.0 \times 10^{-9}$ is introduced. If TLEFT = 0.0, then instead of evaluating $||\Delta(q_{11})||$ along $Re(q_{11}) = 0$, $||\Delta(q_{11})||$ is evaluated along $Re(q_{11}) = + OFFSET$. If TRIGHT = 0.0, then instead of evaluating $||\Delta(q_{11})||$ along $Re(q_{11}) = 0$, $||\Delta(q_{11})||$ is evaluated at $Re(q_{11}) = - OFFSET$.

Calling Statement: Subroutine FINDFX is called by the statement

```
CALL FINDFX (JR, JI, F, FE, TLEFT, TRIGHT).
```

The input variables of subroutine FINDFX are:

JR - The real part of the mesh square corner coordinates in mesh units.

JI - The imaginary part of the mesh square corner coordinates in mesh units.

TLEFT - The value of the real part of q_{11} at the left edge of the search rectangle.

TRIGHT - The value of the real part of q_{11} at the right edge of the search rectangle.

The output variables of subroutine FINDFX are:

F - The complex amplitude of the modal function in extended complex arithmetic.

FE - The real exponent of the modal function in extended complex arithmetic.

Calling Program Element: FZEROX.

Program Elements Called: FCTVLX.

Common Block Areas: TMCCOM.

EXCFAC

Description: Subroutine EXCFAC calculates the modal excitation factor $\lambda_n(q_{11})$ given by equation (2.104) in extended complex arithmetic. Because of the shift in q_{11} by the amount $-i\Delta q = -0.003i$ built into subroutine FDFDTX, before EXCFAC calls FDFDTX it shifts q_{11} by the amount $+i\Delta q = +0.003i$. This exactly compensates for the shift inside FDFDTX.

Calling Statement: Subroutine EXCFAC is called by the statement

```
CALL EXCFAC (XFAC, XFACE, Q11).
```

The input variable of subroutine EXCFAC is:

Q11 - The modal eigenvalue for which the excitation factor is to be evaluated.

The output variables of subroutine EXCFAC are:

XFAC - The complex amplitude of the excitation factor in extended complex arithmetic.

XFACE - The real exponent of the excitation factor in extended complex arithmetic.

Calling Program Element: MODSUM.

Program Elements Called: FDFDTX.

Common Block Areas: COMTWO, COMTHR.

HTGAIN

Description: Subroutine HTGAIN calculates the modal height-gain functions $E(n, z_R, z_T)$ corresponding to the n -th modal eigenvalue q_{11} for the trilinear tropospheric duct propagation model. The height-gain functions are given by equations (2.150-2.166).

Calling Statement: Subroutine HTGAIN is called by the statement

```
CALL HTGAIN (ENZA, ENZE, Q11, ZRCVR, ZXMTTR).
```

The input variables of subroutine HTGAIN are:

Q11 - The modal eigenvalue for which the height-gain function is to be calculated.

ZRCVR - The height in meters of the receiver above ground level.

ZXMTTR - The height in meters of the transmitter above ground level.

The output variables of subroutine HTGAIN are:

ENZA - The complex amplitude of the height-gain function in extended complex arithmetic.

ENZE - The real exponent of the height-gain function in extended complex arithmetic.

Calling Program Element: MODSUM.

Program Elements Called: HNKLX, KHNKLX, KHATX, CADD.

Common Block Areas: COMONE, COMTWO, COMTHR.

MODSUM

Description: Subroutine MODSUM calculates the coherent and incoherent mode sum field strength values in dB relative to the free space value. These field strength values are calculated by using equations (2.108) and (2.109).

Calling Statement: Subroutine MODSUM is called by the statement

```
CALL MODSUM (ECMS, EIMS, RNG, ZRCVR, ZXMTTR, ZEROS, NRZ, NRMODE).
```

The input variables of subroutine MODSUM are:

- RNG - The range in kilometers at which the field strength is to be evaluated.
- ZRCVR - The height in meters of the receiver.
- ZXMTTR - The height in meters of the transmitter.
- ZEROS - An array containing the complex modal eigenvalues q_{11} .
- NRZ - The dimension of the complex array ZEROS.
- NRMODE - The number of modal eigenvalues contained in array ZEROS.

The output variables of subroutine MODSUM are:

- ECMS - The coherent mode sum field strength value in dB relative to the free space value.
- EIMS - The incoherent mode sum field strength value in dB relative to the free space value.

Calling Program Element: MAIN.

Program Elements Called: EXCFAC, HTGAIN, CADD, ADDX.

Common Block Areas: COMTWO, COMTHR.

SEAH20

Description: Subroutine SEAH20 evaluates the effective relative dielectric constant ϵ_r and the effective conductivity σ of seawater as a function of temperature, salinity, and frequency. The complex refractive index of seawater is then given by

$$n_g^2 = \epsilon_r - i \frac{\sigma}{2\pi f \epsilon_0},$$

where f is the frequency and ϵ_0 is the permittivity of free space. The model used to evaluate ϵ_r and σ is from the paper by Klein and Swift [24]. There is a discontinuity in the values of ϵ_r and σ calculated by this model as the salinity goes to zero.

Calling Statement: Subroutine SEAH20 is called by the statement

```
CALL SEAH20 (SIGEFF, EPSEFF, T, S, FREQ).
```

The input variables of subroutine SEAH20 are:

T - The temperature of the seawater in degrees Celsius. The temperature is assumed to be in the interval -2°C to +40°C.

S - The salinity of the seawater in grams of salt per kilogram of seawater. The salinity is assumed to be in the interval 0 to 40 g salt/kg seawater.

FREQ - The frequency in hertz. The frequency is assumed to be in the range 0 to 300 GHz.

The output variables of subroutine SEAH20 are:

SIGEFF - The effective conductivity of the seawater in siemens per meter.

EPSEFF - The effective relative dielectric constant.

Calling Program Element: MAIN.

Program Elements Called: None.

Common Block Areas: None.

DHORIZ

Description: Subroutine DHORIZ calculates the radio horizon distance for a receiver at height z_R and a transmitter at height z_T . The horizon distance is given by

$$d = \sqrt{2r_{\text{eff}}z_R} + \sqrt{2r_{\text{eff}}z_T}$$

The effective earth radius r_{eff} is related to the true earth radius r_t by

$$r_{\text{eff}} = \frac{4}{3}r_t .$$

Calling Statement: Subroutine DHORIZ is called by the statement

```
CALL DHORIZ (DHZ, ZRCVR, ZXMTTR).
```

The input variables of subroutine DHORIZ are:

ZRCVR - The receiver height in meters.

ZXMTTR - The transmitter height in meters.

The output variable of subroutine DHORIZ is:

DHZ - The radio horizon distance in kilometers for the given transmitter and receiver heights.

Calling Program Element: MAIN.

Program Elements Called: None.

Common Block Areas: None.

CASIN

Description: The complex function subroutine CASIN evaluates the complex arcsine of a complex number z by using the equation

$$\sin^{-1}(z) = -i \ln[(1 - z^2)^{1/2} + iz].$$

Calling Statement: The complex function subroutine CASIN is called by

CASIN(Z).

The input variable of function subroutine CASIN is:

Z - A complex number.

The output variable of function subroutine CASIN is:

CASIN - The complex arcsine of the complex number z .

Calling Program Element: MAIN.

Program Elements Called: None.

Common Block Areas: None.

9. SOURCE LISTING FOR XWVG

```

1 ****
2 C THIS PROGRAM FINDS THE COMPLEX MODES IN THE CII-PLANE FOR A
3 C TRILINEAR MODEL OF THE REFRACTIVITY PROFILE OF THE TROPOSPHERE.
4 C THESE MODES ARE FOUND USING THE COMPLEX ROOT FINDING ROUTINE OF
5 C MORFITT AND SHELLMAN.
6 C THE MODES IN THE COMPLEX CII-PLANE ARE CONVERTED TO
7 C VALUES IN THE COMPLEX THETA-PLANE.
8 C BOTH THE COHERENT AND INCOHERENT MODE SUM VALUES OF THE
9 C FIELD STRENGTH RELATIVE TO FREE SPACE ARE EVALUATED

10 C
11 C INPUTS...
12 C MFILE = IF MFILE=0 CALCULATE EIGENVALUES
13 C IF MFILE=1 READ EIGENVALUES FROM LOGICAL FILE 12
14 C
15 C MPOL = IF MPOL=0 HORIZONTAL POLARIZATION
16 C IF MPOL=1 VERTICAL POLARIZATION
17 C FREQ = FREQUENCY (IN MHZ) FOR WHICH MODES ARE TO BE FOUND
18 C ALPHA1 = SLOPE (IN UNITS OF 1/METER) OF FIRST(LOWEST) LAYER
19 C IN TRILINEAR MODEL. MUST BE POSITIVE.
20 C ALPHA2 = SLOPE OF SECOND(MIDDLE) LAYER IN TRILINEAR MODEL. MAY
21 C BE POSITIVE OR NEGATIVE.
22 C ALPHA3 = SLOPE OF THIRD(TOP) LAYER IN TRILINEAR MODEL. MUST BE
23 C POSITIVE
24 C Z2 = HEIGHT (IN METERS) OF INTERFACE BETWEEN FIRST AND SECOND
25 C LAYERS OF TRILINEAR MODEL. MUST BE POSITIVE.
26 C Z3 = HEIGHT (IN METERS) OF INTERFACE BETWEEN SECOND AND THIRD
27 C LAYERS OF TRILINEAR MODEL. MUST BE GREATER THAN Z2.
28 C TC FIELD STRENGTH LEVEL FOR WHICH MODES WILL BE FOUND.
29 C ZREF = HEIGHT (IN METERS) AT WHICH THE VALUE OF THE
30 C MODIFIED REFRACTIVITY, M(Z), IS SPECIFIED
31 C ZREF IS ASSUMED TO BE IN THE FIRST LAYER, I.E.
32 C (U.0).LE.(ZREF).LE.(Z2)
33 C RFFM = VALUE OF THE MODIFIED REFRACTIVITY (IN M-UNITS)
34 C AT THE REFERENCE HEIGHT ZREF
35 C
36 C FTA = ABSORPTIVITY OF TROPOSPHERE. ZERO OR NEGATIVE.
37 C TEMP = SEAWATER TEMPERATURE (IN DEGREES CELSIUS)
38 C SALT = SEAWATER SALINITY (IN GRAMS SALT / KG SEAWATER)
39 C DEFLA = P.M.S. BLIP HEIGHT (IN METERS) OF THE GROUND
40 C ALoss = MAXIMUM LOSS RATE (IN DB/KM) OF MODES WHICH WILL BE
41 C FOUND.
42 C
43 C RNGINT = INITIAL RANGE (IN KILOMETERS) AT WHICH FIELD STRENGTH
44 C IS TO BE CALCULATED.
45 C NRNG = NUMBER OF RANGE VALUES AT WHICH FIELD STRENGTH IS TO BE
46 C CALCULATED.
47 C RNGSTP = INCREMENT (IN KILOMETERS) BY WHICH THE RANGE CHANGES.
48 C
49 C ZINIT = HEIGHT (IN METERS) AT WHICH THE RECEIVER IS
50 C INITIALLY LOCATED.
51 C NRPCTR = NUMBER OF RECEIVER HEIGHTS AT WHICH THE
52 C FIELD STRENGTH IS TO BE CALCULATED.
53 C ZRSTP = INCREMENT (IN METERS) BY WHICH THE RECEIVER
54 C HEIGHT CHANGES.
55 C

```

```

56 C      ZXINIT - HEIGHT (IN METERS) AT WHICH THE TRANSMITTER
57 C      IS INITIALLY LOCATED.
58 C      N7XMT - NUMBER OF TRANSMITTER HEIGHTS AT WHICH THE
59 C      FIELD STRENGTH IS TO BE CALCULATED.
60 C      ZXSTEP - INCREMENT (IN METERS) BY WHICH THE TRANSMITTER
61 C      HEIGHT CHANGES
62 C
63 C      OUTPUTS...
64 C      ZFROS - ARRAY CONTAINING MODES IN THE COMPLEX RII-PLANE FOR
65 C      THE GIVEN TRILINEAR PROFILE.
66 C      THETA - ARRAY CONTAINING CORRESPONDING MODES IN THE COMPLEX
67 C      THETA-PLANE.
68 C      ATNU - ATTENUATION (IN DB/KM) OF THE GIVEN MODE
69 C      FCMS - COHERENT MODE SUM FIELD STRENGTH RELATIVE TO THE
70 C      FREE SPACE VALUE (IN DECIBELS).
71 C      FIMS - INCOHERENT MODE SUM FIELD STRENGTH RELATIVE TO THE
72 C      FREE SPACE VALUE (IN DECIBELS).
73 C
74 C      PARAMETER INPUTS...
75 C      NR7 - MAXIMUM NUMBER OF MODES EXPECTED TO BE FOUND
76 C
77 C      SUBROUTINES USED...
78 C      FZEROS,FINDFX,QUAD,NOMSHX,FKLX,KENKLX,CASIN,FCTVLX,
79 C      FRFITX,CADD,APTX,FKCFAC,HTGATN,MCESUM,KLATX,CTANH,CSECH2,
80 C      DHORIT
81 C*****
82 C      IMPLICIT DOUBLE PRECISION*6 (A-H,O-Z)
83 C      DOUBLE PRECISION*6 KDEL2,KDEL6,KDEL10
84 C      COMPLEX*16 ZFROS,THETA,SGNG,I,CASIN,EIGEN,CTEMP,RAT,CSQPT,RETASG,
85 C      * TAU,TAUSP,TAU2,TAU3,TAU4,A0,A2,A4,A6,A8,A10,R1,R3,R5,R7,
86 C      * R9,F11,D0,D2,D4,D6,D8,D0,D1,E3,E5,E7,R9,CNE,RNONG
87 C      EXTERNAL CASIN
88 C****
89 C      PARAMETERS USED IN PROGRAM
90 C
91 C      PARAMETER (NR7=600)
92 C****
93 C      DIMENSION ZFROS(NR7),THETA(NR7),EIGEN(NR7)
94 C      COMMON/COMONE/C1,C3,C4,C5,C6,C7,C8,C9,SGNA2
95 C      COMMON/COMTWO/ETAARS,ALPHA1,F,C11,SGNG
96 C      COMMON/COMTHR/72,73,ARMAG,ALPHA3,HAVENO,ALPHA2
97 C      COMMON/COMFCR/DELTA,KDEL2,RNONG
98 C      COMMON/COMFIV/A0,A2,A3,A4,A6,A7,A8,A10,A11
99 C      COMMON/COMSIX/P0,R1,R3,R5,R7,F9,R11
100 C      COMMON/COMSEV/D0,D1,D2,D4,D5,D6,D8,D9
101 C      COMMON/COMFIG/D0,D1,D3,D5,D7,D9
102 C      COMMON/COMININ/INTCHK
103 C      DATA EPS0,C/8.85434E-12*2.9979250E8/
104 C      DATA I,PI,C20LOG/(0.0+1.0)*3.14159265,8.68588964/
105 C      DATA CNF/(1.0+0.0)/
106 C*****
107 C      FUNCTION DEFINITION
108 C
109 C      CBRT(Y) = Y**(1.0/3.0)
110 C

```

```

111 ****
112 902 FORMAT(1/6X, *IN THE SEARCH RECTANGLE*, 10X, *TLEFT = *, F7.2, 2Y,
113   * *TRIGHT = *, F7.2/6X, *THE TOTAL NUMBER OF ZEROS NOW EXCEEDS *
114   * *NRZ BY *, I4/6Y, *EXCESS ZEROS IN CURRENT SEARCH RECTANGLE *
115   * *WILL BE DISCARDED*)
116 903 FORMAT(1//10X, *SOLUTIONS OF THE MODAL EQUATION*//)
117 904 FORMAT(2X, *011(*, I3, *) = *, 1P2E14.4, 5X, *THETA(*, I3, *) = *, 1P2E14.4, 3X, *ATNU = *, 1P2E12.4, * DB/KM*)
118
119 C
120 800 FORMAT(1//10X, *ZEROS FOUND IN EXPANDED SEARCH RECTANGLE DEFINED*, 5Y, *TLEFT = *, F7.2, 5X, *TRIGHT = *, F7.2, 5X, *TROT = *, F7.2
121   * *Y*//10X, *TLEFT = *, F7.2, 5X, *TRIGHT = *, F7.2, 5X, *TROT = *, F7.2
122   * *5Y, *TTOP = *, F7.2//)
123 801 FORMAT(20Y, *EIGEN(*, I3, *) = *, 1P2E14.4)
124 C
125 905 FORMAT(1H1//5X, *FIELD STRENGTH RELATIVE TO FREE SPACE VALUE*//)
126 907 FORMAT(5X, *RANGE*, 8X, *7XMTR*, 8Y, *7RCVR*, 6X, *COHERENT*, 4X,
127   * *INCOHERENT*, 8X, *HORIZONTAL*/5X, * (KM)*, 10X, * (M)*, 10X, * (M)*, 7X,
128   * *HFIELD SUM*, 5X, *MODE SUM*, 5X, *DISTANCE*/48Y, * (DB)*, 9X, * (DB)*,
129   * *9Y, * (KM)*//)
130 908 FORMAT(2X, F10.2, 3Y, F10.3, 3Y, F10.3, 3Y, F10.4, 3X, F10.4, 3X, F10.2)
131 930 FORMAT(1//5X, *FREQ = *, F11.4, 1Y, *MHZ*/5X, *ALPHA1 = *, 714.4, * /M*/,
132   * *5Y, *ALPHA2 = *, E14.4, * /M*/5X, *ALPHA3 = *, E14.4, * /M*/,
133   * *5Y, *72 = *, F12.4, * M*/5X, *73 = *, F12.4, * M*/
134   * *5Y, *ALOSS = *, F12.4, * DB/KM//)
135 931 FORMAT(5X, *DELTA = *, 1P2E14.4, * M*/5X, *EPSGND = *, 1P2E14.4,
136   * * FARADS/M*/5X, *SGMGND = *, 1P2E14.4, * MHOS/M*/5X, *ETA = *, 1P2E14.4//)
137
138 932 FORMAT(5X, *SEAWATER TEMPERATURE = *, 1P2E14.4, * DEGREES CELSIUS*/,
139   * *5Y, *SEAWATER SALINITY = *, 1P2E14.4, * GRAMS SALT/KG SEAWATER*)
140 970 FORMAT(1Y, *011(*, I4, *)=*, 2022.11)
141 971 FORMAT(8Y, I4)
142 972 FORMAT(1Y, *NRMODE=*, I4)
143 973 FORMAT(11Y, 2022.11)
144 976 FORMAT(5X, *HORIZONTAL POLARIZATION*)
145 977 FORMAT(5X, *VERTICAL POLARIZATION*)
146 979 FORMAT(5X, *M(*, F6.2, *) = *, F6.2//)
147 ****
148 C READ INPUT VALUES FROM LOGICAL FILE NUMBER 13
149 C
150 READ(13,1) MFILE
151 READ(13,1) MPOL
152 READ(13,1) FREQ
153 READ(13,1) ALPHA1
154 READ(13,1) ALPHA2
155 READ(13,1) ALPHA3
156 READ(13,1) Z2
157 READ(13,1) Z3
158 READ(13,1) ZREF
159 READ(13,1) PFFM
160 READ(13,1) FTA
161 READ(13,1) TEMP
162 READ(13,1) SALT
163 READ(13,1) DELTA
164 READ(13,1) ALOSS
165 READ(13,1) RNGINT

```

```

166      READ(13, ) NRNG
167      READ(13, ) RNGSTP
168      READ(13, ) 7RINIT
169      READ(13, ) N7RCVR
170      READ(13, ) 7RSTEP
171      READ(13, ) ZXINIT
172      READ(13, ) NZXMTR
173      READ(13, ) 7XSTEP
174 C*****
175 C      WRITE DATA TO LOGICAL FILE NUMBER 11
176 C
177      WRITE(11, 930) FREQ,ALPHA1,ALPHA2,ALPHA3,Z2,Z3,ALOSS
178      WRITE(11, 979) 7REF,REFM
179      IF(MPCL.EQ.0) THEN
180      WRITE(11, 976)
181      ELSE
182      WRITE(11, 977)
183      END IF
184      FREQ=FREQ*1.0E6
185      CALL SEAH20(SGMGND,EPSREL,TEMP,SALT,FREQ)
186      EPSGND=EPSREL*EPS0
187      WRITE(11, 932) TEMP,SALT
188      WRITE(11, 931) DELTA,EPSGND,SGMGND,ETA
189 C*****
190 C      CALCULATE "CONSTANTS" NEEDED FOR THE EVALUATION OF MODAL EQUATIONS
191 C
192      FTAABS=ETA
193      WAVENO = 2.0*PI*FREQ/C
194      A2MAG = ABS(ALPHA2)
195      SGNA2=-SIGN(1.0,ALPHA2)
196      C1 = CBRT(A2MAG/ALPHA1)
197      C3 = CBRT(A2MAG/ALPHA3)
198      C11 = CBRT(ALPHA1/WAVENO)
199      C4 = ALPHA1*Z2/(C11*C11)
200      C5 = CBRT(ALPHA1*ALPHA1/(A2MAG*A2MAG))
201      TEMP = CBRT(WAVENO*WAVENO/(A2MAG*A2MAG))
202      C6 = TEMP*ALPHA1*Z2
203      C7 = TEMP*(ALPHA1*Z2+ALPHA2*(Z3-Z2))
204      C8 = CBRT(ALPHA1*ALPHA1/(ALPHA3*ALPHA3))
205      C9=(ALPHA1*Z2+ALPHA2*(Z3-Z2))*CBRT(WAVENO*WAVENO/(ALPHA3*ALPHA3))
206      SONG=EPSGND/EPS0-I*SGMGND/(EPS0*2.0*PI*FREQ)
207      H=-2.0F-6*REFM/ALPHA1+7REF
208      C1180=C11*C11
209 C
210 C      THE FOLLOWING VALUES ARE NEEDED BY SUBROUTINE K4ATX
211 C      THESE VALUES DEPEND UPON THE POLARIZATION OF THE FIELD
212 C
213 C      FOR HORIZONTAL POLARIZATION WE HAVE
214 C
215      IF(MPCL.EQ.0) THEN
216      PNONG=CNE
217 C
218 C      FOR VERTICAL POLARIZATION WE HAVE
219 C
220      ELSE

```

```

221      RNONG=(1.0-I*ETAABS+ALPHA1*I)/SONG
222      END IF
223  C
224      TAU=SONG-1.0-I*ETAABS+ALPHA1*I
225      TAUSR=CSQRT(TAU)
226      TAU2=TAU*TAU
227      TAU3=TAU2*TAU
228      TAU4=TAU2*TAU2
229      KDEL2=HAVENO*HAVENO*DELTA*DELTA
230      KDFL6=KDEL2**3
231      KDEL10=KDEL2**5
232      A0=RNONG*TAUSR
233      A2=RNONG/(2.0*TAUSR)
234      A3=KDFL2
235      A4=RNONG/(8.0*TAU*TAUSR)
236      A6=RNONG/(16.0*TAU2*TAUSR)
237      A7=-KDEL6/3.0
238      A8=-5.0*RNONG/(128.0*TAU3*TAUSR)
239      A10=7.0*RNONG/(256.0*TAU4*TAUSR)
240      A11=2.0*KDEL10/15.0
241      B0=1.0
242      B1=RNONG*TAUSR*KDEL2
243      B3=RNONG*KDEL2/(2.0*TAUSR)
244      B5=RNONG*(-TAUSR*KDEL6/3.0-KDEL2/(8.0*TAU*TAUSR))
245      B7=RNONG*(-KDEL6/(6.0*TAUSR)+KDEL2/(16.0*TAU2*TAUSR))
246      B9=RNONG*(2.0*TAUSR*KDEL10/15.0+KDEL6/(24.0*TAL*TAUSR)
247      $ -5.0*KDEL2/(128.0*TAU3*TAUSR))
248      B11=RNONG*(KDEL10/(15.0*TAUSR)-KDEL6/(48.0*TAU2*TAUSR)
249      $ +7.0*KDEL2/(256.0*TAU4*TAUSR))
250      DA0=A2*C11SQ
251      DA1=1.5*A3*C11SQ
252      DA2=2.0*A4*C11SQ
253      DA4=3.0*A6*C11SQ
254      DA5=3.5*A7*C11SQ
255      DA6=4.0*A8*C11SQ
256      DA8=5.0*A10*C11SQ
257      DA9=5.5*A11*C11SQ
258      D0=0.5*P1*C11SQ
259      D1=1.5*P3*C11SQ
260      D3=2.5*B5*C11SQ
261      D5=3.5*B7*C11SQ
262      D7=4.5*B9*C11SQ
263      D9=5.5*B11*C11SQ
264  C*****
265  C      ARE MODE EIGENVALUES TO BE CALCULATED OR ARE THEY ALREADY
266  C      STORED ON FILE
267  C
268  C
269  C      MFILE - IF MFILE=0 CALCULATE EIGENVALUES
270  C              IF MFILE=1 READ EIGENVALUES FROM FILE 12
271  C
272  C      IF(MFILE.EQ.1) THEN
273      READ(12,971) NRMODE
274      DO 90  K0=1,NRMODE
275      READ(12,973) ZEROS(K0)

```

```

276 90    CONTINUE
277    GO TO 520
278    END IF
279 C*** SET UP SEARCH RECTANGLES FOR FINDING MODES AND SOLVE FOR MCES
280 C
281 C
282 C
283 C      NLEFT = NUMBER OF CONSECUTIVE SEARCH RECTANGLES WITH NO ZEROS TO
284 C      BE FOUND TO THE LEFT OF THE ORIGINAL SEARCH RECTANGLE BEFORE
285 C      STOPPING SEARCH TO THE LEFT.
286 C      NRIGHT = NUMBER OF CONSECUTIVE SEARCH RECTANGLES WITH NO ZEROS TO
287 C      BE FOUND TO THE RIGHT OF THE ORIGINAL SEARCH RECTANGLE BEFORE
288 C      STOPPING SEARCH TO THE RIGHT.
289 C
290      NLEFT=5
291      NRIGHT=5
292 C
293 C      IF INITIALIZE 'ILFLAG=NLEFT' PROGRAM WILL NOT SEARCH TO THE LEFT
294 C      OF THE ORIGINAL SEARCH RECTANGLE
295 C      IF INITIALIZE 'IRFLAG=NRIGHT' PROGRAM WILL NOT SEARCH TO THE RIGHT
296 C      OF THE ORIGINAL SEARCH RECTANGLE
297 C
298      ILFLAG=0
299      IRFLAG=0
300 C
301 C      TOL - TOLERANCE TO WHICH MODES ARE TO BE FOUND
302 C      TMESH - MESH SIZE USED BY ROOT FINDING SUBROUTINE 'FZEROX'
303 C      MPRINT - MPRINT=0 GIVES NO 'DEBUGGING' PRINTOUT FROM
304 C      SUBROUTINE 'FZEROX' WHILE MPRINT=1 DOES GIVE 'DEBUGGING'
305 C      PRINTOUT
306 C      TLOLD - LEFT COORDINATE OF INITIAL SEARCH RECTANGLE
307 C      TROLD - RIGHT COORDINATE OF INITIAL SEARCH RECTANGLE
308 C      TBOT - BOTTOM COORDINATE OF SEARCH RECTANGLES
309 C      TTOP - TOP COORDINATE OF SEARCH RECTANGLES
310 C      TLSTEP - SIZE OF SEARCH RECTANGLES TO THE LEFT OF THE
311 C      INITIAL SEARCH RECTANGLE
312 C      TRSTEP - SIZE OF SEARCH RECTANGLES TO THE RIGHT OF THE
313 C      INITIAL SEARCH RECTANGLE
314 C
315 C      ***
316 C      IN SUBROUTINE 'FZEROX' THE ERROR CONDITION 'X MODES FOUND
317 C      ON SAME PHASE LINE' WITH X.GT.1 CAN OFTEN BE CORRECTED BY
318 C      REDUCING BOTH TMESH AND THE SIZE OF THE SEARCH RECTANGLE.
319 C      SUBROUTINE 'FZEROX' WILL AUTOMATICALLY REDUCE TMESH BY
320 C      2.0 TWICE BUT IT DOES NOT REDUCE THE SIZE OF THE
321 C      SEARCH RECTANGLE.
322 C      ***
323 C
324      TOL =0.0001
325      TMESH=0.04
326      MPRINT=0
327      NRMODE=0
328      TLOLD=0.0
329      TROLD=2.0
330      TBOT=-TOL

```

```

331 TTOP=2.0*(ALOSS*1.0E-3/(WAVENO*C20LCG)+ETA/2.0)/(C11+C11)
332 TLEFT=TL0LD
333 TRIGHT=TR0LD
334 TLSTEP=2.0
335 TRSTEP=2.0
336 C
337 C THE FLAG 'INTCHK' IS USED TO KEEP TRACK OF WHERE THE CURRENT
338 C SEARCH RECTANGLE IS IN RELATION TO THE INITIAL SEARCH
339 C RECTANGLE
340 C
341 C     INTCHK=0 - INITIAL SEARCH RECTANGLE
342 C     INTCHK=1 - SEARCH RECTANGLE TO THE LEFT OF INITIAL SEARCH
343 C             RECTANGLE
344 C     INTCHK=2 - SEARCH RECTANGLE TO THE RIGHT OF INITIAL SEARCH
345 C             RECTANGLE
346 C
347 C ***
348 C     NOTE 1: BECAUSE INTCHK IS USED IN SUBROUTINE KHATX TO FORCE THE
349 C             EVALUATION OF KHAT(Q11) TO BE ON THE 'CORRECT BRANCH'
350 C             WHEN DELTA IS NOT EQUAL TO ZERO, THE VALUE OF TLCL1
351 C             MUST EQUAL 0.0
352 C
353 C     NOTE 2: AFTER THE MODE SEARCH IS COMPLETED INTCHK IS AGAIN SET
354 C             EQUAL TO ZERO. THIS IS AGAIN FOR USE IN SUBROUTINE
355 C             KHATX WHEN EVALUATING KHAT(Q11) IN THE HEIGHT-GAIN
356 C             CALCULATIONS.
357 C ***
358 C
359 C     INTCHK=0
360 C
361 C     CALL ROOT FINDING ROUTINE OF MORFITT AND SHELLMAN TO FIND ZEROS
362 C     IN CURRENT SEARCH RECTANGLE
363 C
364 C210 CALL FZEROX(TLEFT,TRIGHT,TROT,TTOP,TMESH,TOL,MPRINT,EIGEN,NRE)
365 C     WRITE(11,800) TLEFT,TRIGHT,TROT,TTOP
366 C     IF(NRE.GT.0) THEN
367 C     DO 300 LK=1,NRE
368 C
369 C     THE FOLLOWING STATEMENT COMPENSATES FOR THE SHIFT IN Q11
370 C     INTRODUCED IN SUBROUTINES 'FDFDTX' AND 'FCTVLX' IN ORDER TO AVOID
371 C     HAVING A MESH LINE ON THE REAL AXIS
372 C
373 C     EIGEN(LK)=EIGEN(LK)-T*0.003
374 C
375 C ***
376 C     IF THE VALUE OF TMESH IS CHANGED THE OFFSET IN THE
377 C     VALUE OF Q11 IN THIS STATEMENT AND IN THE CORRESPONDING
378 C     STATEMENTS IN SUBROUTINES 'FDFDTX' AND 'FCTVLX' MAY
379 C     ALSO HAVE TO BE CHANGED IN ORDER THAT A MESH LINE
380 C     DOES NOT FALL ON THE REAL AXIS
381 C     SUBROUTINE 'EXCFAC' ALSO HAS A STATEMENT THAT DEPENDS UPON THE
382 C     SIZE OF THIS OFFSET
383 C ***
384 C
385 C     WRITE(11,801) LK,EIGEN(LK)

```

```

386 300 CONTINUE
387 END IF
388 IF(NRF.EQ.0) GO TO 100
389 C
390 C SINCE SUBROUTINE *FZEROX* EXTENDS THE SEARCH RECTANGLE
391 C SLIGHTLY, CHECK FOR AND ELIMINATE ZEROS FOUND OUTSIDE CURRENT
392 C SEARCH RECTANGLE
393 C
394 JKFLAG=0
395 DO 150 JK=1,NRE
396 IF((REAL(EIGEN(JK-JKFLAG)).GE.TRIGHT).OR.(REAL(EIGEN(JK-JKFLAG)).LT.TLEFT).OR.(AIMAG(EIGEN(JK-JKFLAG)).LT.TBOT).OR.(AIMAG(EIGEN(JK-JKFLAG)).GT.TTOP)) THEN
397 JSTOP = NRE-1
398 JSTART= JK-JKFLAG
399 DO 160 J=JSTART,JSTOP
400 EIGEN(J) = EIGEN(J+1)
401 160 CONTINUE
402 NRE=NRE-1
403 JKFLAG=JKFLAG+1
404 END IF
405 150 CONTINUE
406 C
407 C STORE ZEROS FOUND IN CURRENT SEARCH RECTANGLE IN ARRAY
408 C CONTAINING ALL ZEROS.
409 C
410 C
411 C
412 IF(NRE.GT.0) KN=NRMODE+NRE
413 IF(KN.GT.NRZ) THEN
414 NROVER=KN-NRZ
415 KN=NRZ
416 NRMODE=NRZ-NRE
417 WRITE(11,902) TLEFT,TRIGHT,NROVER
418 END IF
419 IF(KN.LT.NRZ) THEN
420 JEND=NRE
421 ELSE
422 JEND=NRE-NROVER
423 END IF
424 DO 190 J=1,JEND
425 ZEROS(NRMODE+J)=EIGEN(J)
426 190 CONTINUE
427 NRMODE=NRMODE+NRE
428 C
429 C IF *ILFLAG.NE.NLEFT* FORM NEW SEARCH RECTANGLE TO THE LEFT OF
430 C TOTAL REGION SEARCHED.
431 C
432 100 IF(ILFLAG.EQ.NLEFT) GO TO 400
433 IF((NRE.EQ.0).AND.(INTCHK.EQ.1)) THEN
434 IFLAG=ILFLAG+1
435 ELSE
436 IFLAG=0
437 END IF
438 IF(ILFLAG.EQ.NLEFT) GO TO 400
439 INTCHK=1
440 TLEFT=TLOLD-TLSTEP

```

```

441      TRIGHT=TLOLD
442      TLOLD=TLLEFT
443      GO TO 210
444 C
445 C      IF 'IRFLAG.NE.NRIGHT' FORM NEW SEARCH RECTANGLE TO THE RIGHT OF
446 C      TOTAL REGION SEARCHED.
447 C
448 400 IF(IRFLAG.F0.NRIGHT) GO TO 200
449      IF((NPF.EQ.0).AND.(INTCHK.EQ.2)) THEN
450          IRFLAG=IRFLAG+1
451      ELSE
452          IRFLAG=0
453      END IF
454      IF(IRFLAG.EQ.NRIGHT) GO TO 200
455      INTCHK=2
456      TLLEFT=TLOLD
457      TRIGHT=TLOLD+TRSTEP
458      TLOLD=TRIGHT
459      GO TO 210
460 C*****
461 C      MODE SEARCH COMPLETED
462 C
463 C
464 C      ORDER ZEROS FOUND BY ORDER OF INCREASING REAL PART.
465 C
466 200 IF(NRMODE.GT.1) THEN
467      JKEND=NRMODE-1
468      DO 410 JK=1,JKEND
469      NEND=NRMODE-JK
470      DO 420 J=1,NEND
471      IF(REAL(ZEROS(NRMODE+1-J)).LT.REAL(ZEROS(NRMODE-J))) THEN
472          CTEMP=ZEROS(NRMODE+1-J)
473          ZEROS(NRMODE+1-J)=ZEROS(NRMODE-J)
474          ZEROS(NRMODE-J)=CTEMP
475      END IF
476      420 CONTINUE
477      410 CONTINUE
478      END IF
479 C
480 C      THE POSSIBILITY EXISTS THAT DUPLICATE (WITHIN THE TOLERANCE 'TOL')
481 C      ZEROS OF THE MODAL EQUATION WILL BE FOUND.  ELIMINATE THESE
482 C      DUPLICATE ZEROS.
483 C
484      JKFLAG=0
485      JKEND=NRMODE-1
486      DO 240 JK=1,JKEND
487          CHKR=ABS(REAL(ZEROS(JK-JKFLAG))-REAL(ZEROS(JK+1-JKFLAG)))
488          CHKI=ABS(AIMAG(ZEROS(JK-JKFLAG))-AIMAG(ZEROS(JK+1-JKFLAG)))
489          CHKSQ=SQRT(CHKR*CHKR+CHKI*CHKI)
490          IF(CHKSQ.LT.TOL) THEN,
491              JSTOP=NRMODE-1
492              JSTART=JK-JKFLAG
493              DO 250 J=JSTART,JSTOP
494                  ZEROS(J)=7FR0S(J+1)
495      250 CONTINUE

```

```

496      NRMODE=NRMODE-1
497      JKFLAG=JKFLAG+1
498      END IF
499      240 CONTINUE
500      C
501      C FOR VERY WELL TRAPPED MODES THE IMAGINARY PART OF THE ZEROS
502      C OF THE MODAL EQUATION MAY BE FOUND TO BE NEGATIVE (BUT LESS
503      C IN ABSOLUTE VALUE THAN 'TOL'). SET THESE IMAGINARY PARTS
504      C EQUAL TO ZERO
505      C
506      DO 405 J=1,NRMODE
507      IF(AIMAG(ZEROS(J)).LT.0.0) ZEROS(J)=ONE*REAL(ZEROS(J))
508      405 CONTINUE
509      C
510      C CONVERT MODES IN COMPLEX C11-PLANE TO MODES IN THE COMPLEX
511      C THETA PLANE. THIS OUTPUT IS FOR COMPARISON PURPOSES ONLY.
512      C
513      C ANGLES ARE REFERENCED TO THE HEIGHT ZREF WHERE M(Z)=1/(ZREF)
514      C IS SPECIFIED.
515      C
516      DO 220 J=1,NRMODE
517      RAD=CSQRT(ZEROS(J)*C11*C11+ALPHA1*H)
518      THETA(J)=CASIN(RAD)
519      220 CONTINUE
520      C
521      C CALCULATE ATTENUATION RATE FOR DIFFERENT MODES AND OUTPUT RESULTS
522      C
523      WRITE(11,903)
524      IF(NRMODE.GT. 0.0) THEN
525      WRITE(12,972) NRMODE
526      DO 230 J=1,NRMODE
527      BETASQ=1.0+I*ETAABS-ALPHA1*H-C11*C11*ZEROS(J)
528      BETAI=AIMAG(CSQRT(BETASQ))
529      ATNU=-C20LOG*WAVENO*BETAI*1.0E+3
530      WRITE(11,904) J,ZEROS(J),J,THETA(J),ATNU
531      WRITE(12,970) J,ZEROS(J)
532      230 CONTINUE
533      END IF
534      C*****
535      C CALCULATE FIELD STRENGTH RELATIVE TO FREE SPACE VALUE
536      C
537      520 WRITE(11,905)
538      WRITE(11,907)
539      INTCHK=0
540      DO 505 JRNG=1,NRNG
541      RNG=RNGINT+FLOAT(JRNG-1)*RNGSTP
542      DO 500 JXMTR=1,NZXMTR
543      ZXMTTR=ZXMTR+FLOAT(JXMTR-1)*ZXSTEP
544      DO 510 JRCVR=1,NZRCVR
545      ZRCVR=ZRCVR+FLOAT(JRCVR-1)*ZRSTEP
546      CALL MODSUM(ECMS,EIMS,RNG,ZRCVR,ZXMTR,ZEROS,NR2,NRMODE)
547      CALL DHDRIZ(DHZ,ZRCVR,ZXMTR)
548      WRITE(11,908) RNG,ZXMTR,ZRCVR,ECMS,EIMS,DHZ
549      510 CONTINUE
550      500 CONTINUE

```

```
551 505 CONTINUF
552 C*****
553      STOP
554      END
```

```
1      SUBROUTINE CADD(ZA,ZE,XA,XE,YA,YE)
2 C*****+
3 C      THIS SUBROUTINE TAKES THE EXTENDED COMPLEX NUMBERS 'XA' AND 'YE'
4 C      AND ADDS THEM TO FORM THE EXTENDED COMPLEX NUMBER 'ZA'
5 C
6 C      THE EXTENDED COMPLEX NUMBER 'ZA' IS MADE UP OF THE COMPLEX
7 C      AMPLITUDE 'ZA' AND THE REAL EXPONENT 'ZE'.  THUS, 'ZA' IS
8 C      EQUAL TO 'ZA=ZA*EXP(ZE)'
9 C*****+
10     IMPLICIT DOUBLE PRECISION*6 (A-H,O-Z)
11     COMPLEX ZA,XA,YA
12     IF((REAL(XA).EQ.0.0).AND.(AIMAG(XA).EQ.0.0)) THEN
13       IF((REAL(YA).EQ.0.0).AND.(AIMAG(YA).EQ.0.0)) THEN
14         ZA=(0.0,0.0)
15         ZE=0.0
16         RETURN
17       ELSE
18         ZA=YA
19         ZE=YE
20         RETURN
21       END IF
22     END IF
23     IF((REAL(YA).EQ.0.0).AND.(AIMAG(YA).EQ.0.0)) THEN
24       ZA=XA
25       ZE=XE
26       RETURN
27     END IF
28     E=YE-YE
29     IF(XF.GE.YE) THEN
30       IF(E.GT.-85.0) THEN
31         R=EXP(E)
32       ELSE
33         R=0.0
34       END IF
35       ZA=YA+R*YA
36       ZE=YF
37     ELSE
38       IF(-F.GT.-85.0) THEN
39         R=EXP(-E)
40       ELSE
41         R=0.0
42       END IF
43       ZA=YA+R*XA
44       ZE=YF
45     END IF
46     IF((REAL(ZA).EQ.0.0).AND.(AIMAG(ZA).EQ.0.0)) ZF=0.0
47     RETURN
48   END
```

```

1      SUBROUTINE ADDX(ZA,ZE,XA,XE,YA,YE)
2 C*****  

3 C      THIS PROGRAM TAKES THE EXTENDED REAL NUMBERS 'XA' AND 'XE'  

4 C      AND ADDS THEM TO FORM THE EXTENDED REAL NUMBER 'ZA'  

5 C
6 C      THE EXTENDED REAL NUMBER 'ZA' IS MADE UP OF THE  

7 C      AMPLITUDE 'ZA' AND THE EXPONENT 'ZE'. 'ZA' IS EQUAL TO  

8 C      'Z=ZA*EXP(ZE)'  

9 C*****  

10     IMPLICIT DOUBLE PRECISION*6 (A-H,O-Z)
11     IF(XA.EQ.0.0) THEN
12       IF(YA.EQ.0.0) THEN
13         ZA=0.0
14         ZE=0.0
15         RETURN
16       ELSE
17         ZA=YA
18         ZE=YE
19         RETURN
20       END IF
21     END IF
22     IF(YA.EQ.0.0) THEN
23       ZA=XA
24       ZE=XE
25       RETURN
26     END IF
27     E=YE-XE
28     IF(XE.GE.YE) THEN
29       IF(E.GT.-85.0) THEN
30         R=EXP(E)
31       ELSE
32         R=0.0
33       END IF
34       ZA=YA+R*YA
35       ZE=YE
36     ELSE
37       IF(-E.GT.-85.0) THEN
38         R=EXP(-E)
39       ELSE
40         R=0.0
41       END IF
42       ZA=YA+R*XA
43       ZE=YE
44     END IF
45     IF(ZA.EQ.0.0) ZE=0.0
46     RETURN
47   END

```

```

1      SUBROUTINE HNKLX17(H1A,H1E,H2A,H2E,DH1A,DH1E,DH2A,DH2E)
2 C*****
3 C      THIS PROGRAM EVALUATES THE MODIFIED HANKEL FUNCTIONS H1(Z) AND
4 C      H2(Z) AND THEIR DERIVATIVES H1'(Z) AND H2'(Z) WITH A *RELATIVE
5 C      ACCURACY* BETTER THAN 10**(-3)
6 C
7 C      THE VALUES ARE RETURNED AS A COMPLEX AMPLITUDE (F.G. H1A)
8 C      AND A REAL EXPONENT(F.G. H1E). THE MODIFIED HANKEL FUNCTION
9 C      H1(Z) WOULD THEN EQUAL H1(Z)=H1A*EXP(H1E)
10 C*****
11      IMPLICIT DOUBLE PRECISION*6 (A-H,D-7)
12      DOUBLE PRECISION*6 IMZ,IMXI
13      COMPLEX 1,CON1,CON2,CON2CJ,CE1,CE1CJ,CE2,CE2CJ,Z,ZSQ,ZCUEE,
14      * SUMF7,SUMGZ,SUMFP7,SUMGPZ,FZ,GZ,FP7,GP7,H1A,H2A,DH1A,DH2A,
15      * CONFPZ,ZSQR,CSGR,ZR,XI,CEXP,TH,ZMTH,EXT,SUMCKP,SUMCKM,
16      * SUMCKP,SUMDKM,CONFZ
17      DIMENSION A(9),B(9),C(9),D(9),CK(5),EK(5)
18 C**      ARRAY CONTAINING COEFFICIENTS FOR F(Z)
19      DATA (A(N),N=1,9)/ -1.66666667E-1, +5.55555556E-3, -7.71604938E-5,
20      * +5.84549196E-7, -2.78356760E-9, +9.09662614E-12,
21      * -2.16586337E-14, +3.92366552E-17, -5.58926712E-20/
22 C**      ARRAY CONTAINING COEFFICIENTS FOR G(Z)
23      DATA (B(N),N=1,9)/ -8.33333333E-2, +1.9841269E-3, -2.20458554E-5,
24      * +1.41319586E-7, -5.88831607E-10, +1.72172985E-12,
25      * -3.72668798E-15, +6.21114663E-18, -8.21580242E-21/
26 C**      ARRAY CONTAINING COEFFICIENTS FOR F'(Z)
27      DATA (C(N),N=1,9)/ -6.66666667E-2, +1.38888889E-3, -1.40291807E-5,
28      * +8.35070280E-8, -3.27478541E-10, +9.09662614E-13,
29      * -1.88335945E-15, +3.01820425E-18, -3.85466698E-21/
30 C**      ARRAY CONTAINING COEFFICIENTS FOR G'(Z)
31      DATA (D(N),N=1,9)/ -3.33333333E-1, +1.38888889E-2, -2.20458554E-4,
32      * +1.83715461E-6, -9.42130572E-9, +3.27128671E-11,
33      * -8.19871355E-14, +1.55278666E-16, -2.30042468E-19/
34 C**      ARRAY CONTAINING COEFFICIENTS IN ASYMPTOTIC EXPANSION OF H1(Z)
35 C      AND H2(Z)
36      DATA (CK(N),N=1,5)/ 1.04166667E-1, 8.35503472E-2, 1.28226575E-1,
37      * 2.91849026E-1, 8.81627267E-1/
38 C**      ARRAY CONTAINING COEFFICIENTS IN ASYMPTOTIC EXPANSION OF H1'(Z)
39 C      AND H2'(Z)
40      DATA (EK(N),N=1,5)/ +1.45833333E-1, -9.87413194E-2,
41      * +1.43312054E-1, -3.17227203E-1, +9.42429148E-1/
42 C
43      DATA X0,Y1,ALPHA,PI,PI3/ 9.30436717E-1, 6.78298725E-1,
44      * 8.53667219E-1, 3.14159265E0, 1.04719755E0/
45 C
46      DATA I,CON1,CON2,CON2CJ/ (0.0,1.0), (0.0,1.15470054),
47      * (1.0,0.577350269), (1.0,-0.577350269)/
48 C
49      DATA CE1,CE1CJ,CE2,CE2CJ/ (0.258819045,0.965925826),
50      * (0.258819045,-0.965925826), (-0.965925826,0.258819045),
51      * (-0.965925826,-0.258819045)/
52 C***      TEST WHETHER TO EVALUATE MODIFIED HANKEL FUNCTIONS BY SERIES
53 C      EXPANSION OR ASYMPTOTIC EXPANSION
54 C
55 C

```

```

56      AMP7=CABS(7)
57      IF(AMP7.LT.(3.5)) THEN
58 C*****  

59 C      EVALUATE MODIFIED HANKEL FUNCTIONS USING SERIES EXPANSIONS
60 C
61      ZSQ=7*7
62      ZCUBE=7*7*SQ
63      SUMF7=A(9)*ZCUBE
64      SUMG7=F(9)*ZCUBE
65      SUMFP7=C(9)*ZCUBE
66      SUMGP7=I(9)*ZCUBE
67      DO 100 K=8,1,-1
68      SUMF7=(SUMF7+A(K))*ZCUBE
69      SUMG7=(SUMG7+F(K))*ZCUBE
70      SUMFP7=(SUMFP7+C(K))*ZCUBE
71      SUMGP7=(SUMGP7+I(K))*ZCUBE
72      100 CONTINUE
73      F7=(SUMF7+1.0)*X0
74      GZ=(SUMG7+1.0)*X1*Z
75      FPZ=-(SUMFP7+1.0)*X0*ZSQ/2.0
76      GPZ=(SUMGP7+1.0)*X1
77      CONF7=CON1*F7
78      CONF7=CON1*FPZ
79 C
80      K1A=CON2*GZ-CONF7
81      K1E=0.0
82      K2A=CON2*(GZ+FZ)
83      K2E=0.0
84      DK1A=CON2*GPZ-CONF7
85      DK1E=0.0
86      DK2A=CON2*(GPZ+FPZ)
87      DK2E=0.0
88      RETURN
89 C*****  

90      FALSE
91 C*****  

92 C      EVALUATE MODIFIED HANKEL FUNCTIONS USING ASYMPTOTIC EXPANSIONS
93 C
94      ZSQR=CSQRT(7)
95      ZFR=CSQRT(7*SQR)
96      ZTH=7*7*SQR
97      ZMTH=1/ZTH
98      X1=2.0*ZTH/3.0
99      REXI=REAL(X1)
100     IMXI=AIMAG(X1)
101     FXI=CFXP(1*REXI)
102     SUMCKP=CK(5)*ZMTH
103     SUMCKM=-SUMCKP
104     SUMDKP=DK(5)*ZMTH
105     SUMDKM=-SUMDKP
106     DO 102 K=4,1,-1
107     SUMCKP=(SUMCKP+CK(K))*ZMTH
108     SUMCKM=(SUMCKM+CK(K))*ZMTH
109     SUMDKP=(SUMDKP+DK(K))*ZMTH
110     SUMDKM=(SUMDKM+DK(K))*ZMTH

```

```

111 102 CONTINUE
112  SUMCKP=1.0+SUMCKP
113  SUMCKM=1.0+SUMCKM
114  SUMDKP=1.0+SUMDKP
115  SUMDKM=1.0+SUMDKM
116 C
117 C      EVALUATE PH(Z)
118 C
119  REZ=RREAL(Z)
120  IMZ=AIMAG(Z)
121  IF(REZ.GT.(0.0)) THEN
122  PHZ=ATAN(IMZ/REZ)
123  ELSE IF(REZ.LT.(0.0)) THEN
124  IF(IMZ.GE.(0.0)) THEN
125  PHZ=PI+ATAN(IMZ/REZ)
126  ELSE
127  PHZ=-PI+ATAN(IMZ/REZ)
128  END IF
129  ELSE
130  IF(IMZ.GT.(0.0)) THEN
131  PHZ=PI/2.0
132  ELSE IF(IMZ.LT.(0.0)) THEN
133  PHZ=-PI/2.0
134  ELSE
135  PHZ=0.0
136  END IF
137  END IF
138 C
139 C      EVALUATE MODIFIED HANKEL FUNCTIONS
140 C
141  IF(PHZ.GE.-PI) THEN
142  H1A=ALPHA*EXI*CE1CJ*SUMCKM/ZFR
143  H1E=-IMXI
144  IF((REAL(H1A).EQ.0.0).AND.(AIMAG(H1A).EQ.0.0)) H1E=0.0
145  DH1A=ALPHA*I*ZFR*EXI*CE1CJ*SUMCKP
146  DH1E=-IMXI
147  IF((REAL(DH1A).EQ.0.0).AND.(AIMAG(DH1A).EQ.0.0)) DH1E=0.0
148  ELSE
149  IF(IMXI.GE.0.0) THEN
150  ESM=-2.0*IMXI
151  IF(ESM.GT.-85.0) THEN
152  REEXP=EXP(ESM)
153  ELSE
154  REEXP=0.0
155  END IF
156  H1A=ALPHA*(CE2CJ*SUMCKP/EXI+REEXP*EXI*CE1CJ*SUMCKM)/ZFR
157  H1E=IMXI
158  IF((REAL(H1A).EQ.0.0).AND.(AIMAG(H1A).EQ.0.0)) H1E=0.0
159  DH1A=ALPHA*I*ZFR*(REEXP*EXI*CE1CJ*SUMDKP-CE2CJ*SUMDKM/EXI)
160  DH1E=IMXI
161  IF((REAL(DH1A).EQ.0.0).AND.(AIMAG(DH1A).EQ.0.0)) DH1E=0.0
162  ELSE
163  FSH=2.0*IMXI
164  IF(ESM.GT.-85.0) THEN
165  REEXP=EXP(ESM)

```

```

166      FLSF
167      REEXP=0.0
168      END IF
169      H1A=ALPHA*(REEXP*CE2CJ*SUMCKP/EXI+EXI*CE1CJ*SUMCKM)/ZFR
170      H1F=-IMXI
171      IF((RFAL(H1A),EQ.0.0).AND.(AIMAG(H1A),EQ.0.0)) H1E=0.0
172      DH1A=ALPHA*I*ZFR*(EXI*CE1CJ*SUMCKP-REEXP*CE2CJ*SUMCKM/EXI)
173      DH1E=-IMXI
174      IF((REAL(DH1A),EQ.0.0).AND.(AIMAG(DH1A),EQ.0.0)) DH1E=0.0
175      END IF
176      END IF
177      IF(PH7,GT,PI3) THEN
178      IF(IMXI,GE,0.0) THEN
179      ESM=-2.0*IMXI
180      IF(ESM,GT,-85.0) THEN
181      REEXP=EXP(ESM)
182      ELSE
183      REEXP=0.0
184      END IF
185      H2A=ALPHA*(CE1*SUMCKP/EXI+REEXP*EXI*CE2*SUMCKM)/ZFR
186      H2F=IMXI
187      IF((REAL(H2A),EQ.0.0).AND.(AIMAG(H2A),EQ.0.0)) H2E=0.0
188      DH2A=ALPHA*I*ZFR*(REEXP*EXI*CE2*SUMCKP-CE1*SUMCKM/EXI)
189      DH2E=IMXI
190      IF((REAL(DH2A),EQ.0.0).AND.(AIMAG(DH2A),EQ.0.0)) DH2E=0.0
191      ELSE
192      ESM=2.0*IMXI
193      IF(ESM,GT,-85.0) THEN
194      REEXP=EXP(ESM)
195      ELSE
196      REEXP=0.0
197      END IF
198      H2A=ALPHA*(REEXP*CE1*SUMCKP/EXI+EXI*CE2*SUMCKM)/ZFR
199      H2E=-IMXI
200      IF((REAL(H2A),EQ.0.0).AND.(AIMAG(H2A),EQ.0.0)) H2E=0.0
201      DH2A=ALPHA*I*ZFR*(EXI*CE2*SUMCKP-REEXP*CE1*SUMCKM/EXI)
202      DH2E=-IMXI
203      IF((REAL(DH2A),EQ.0.0).AND.(AIMAG(DH2A),EQ.0.0)) DH2E=0.0
204      END IF
205      ELSE
206      H2A=ALPHA*CE1*SUMCKP/(ZFR*EXI)
207      H2F=IMXI
208      IF((REAL(H2A),EQ.0.0).AND.(AIMAG(H2A),EQ.0.0)) H2E=0.0
209      DH2A=-ALPHA*I*ZFR*CE1*SUMCKM/EXI
210      DH2E=IMXI
211      IF((REAL(DH2A),EQ.0.0).AND.(AIMAG(DH2A),EQ.0.0)) DH2E=0.0
212      END IF
213      END IF
214      RETURN
215 ****
216      END

```

```

1      SUBROUTINE KHNKLX1(Z,K1A,K1E,K2A,K2E,DK1A,DK1E,DK2A,DK2E)
2 C*****+
3 C      THIS PROGRAM EVALUATES THE MODIFIED HANKEL FUNCTIONS K1(Z) AND
4 C      K2(Z) AND THEIR DERIVATIVES K1'(Z) AND K2'(Z) WITH A *RELATIVE
5 C      ERROR* BETTER THAN 10**(-3)
6 C
7 C      THE VALUES ARE RETURNED AS A COMPLEX AMPLITUDE (E.G. K1A)
8 C      AND A REAL EXPONENT (E.G. K1E). THE MODIFIED HANKEL FUNCTION
9 C      K1(Z) WOULD THEN EQUAL K1(Z)=K1A*EXP(K1E)
10 C*****
11      IMPLICIT DOUBLE PRECISION*6 (A-H,O-Z)
12      DOUBLE PRECISION*6 IMZ,K1E,K2E,THX1
13      COMPLEX  I,CON1,CON2,CON2CJ,CE1,CE1CJ,CE2,CE2CJ,Z,ZS0,ZCLEE,
14      SUMFZ,SUMGZ,SUMFPZ,SUMGPZ,FZ,GZ,FPZ,GPZ,K1A,K2A,DK1A,DK2A,
15      CONFPZ,ZSQR,CSQRT,ZFR,Y1,CEXP,ZTH,ZMTH,EXI,SUMCKP,SUMCKM,
16      SUMDKP,SUMDKM,CONFZ
17      DIMENSION A(9),B(9),C(9),D(9),CK(5),EK(5)
18 C**  ARRAY CONTAINING COEFFICIENTS FOR F(Z)
19      DATA (A(N),N=1,9)/ -1.66666667E-1, +5.55555556E-34, -7.71604938E-5,
20      * +5.84549196E-7, -2.78356760E-9, +9.09662614E-12,
21      * -2.16586337E-14, +3.92366552E-17, -5.58926712E-20/
22 C**  ARRAY CONTAINING COEFFICIENTS FOR G(Z)
23      DATA (B(N),N=1,9)/ -8.33333333E-2, +1.98412698E-3, -2.20458554E-5,
24      * +1.41319586E-7, -5.88831607E-10, +1.72172985E-12,
25      * -3.72668798E-15, +6.21114663E-18, -8.21580242E-21/
26 C**  ARRAY CONTAINING COEFFICIENTS FOR F'(Z)
27      DATA (C(N),N=1,9)/ -6.66666667E-2, +1.38888889E-3, -1.40291807E-5,
28      * +8.35070280E-6, -3.27478541E-10, +9.09662614E-13,
29      * -1.88335945E-15, +3.01820425E-18, -3.85466698E-21/
30 C**  ARRAY CONTAINING COEFFICIENTS FOR G'(Z)
31      DATA (D(N),N=1,9)/ -3.33333333E-1, +1.38888889E-2, -2.20458554E-4,
32      * +1.83715461E-6, -9.42130572E-9, +3.27128671E-11,
33      * -8.19871355E-14, +1.55278666E-16, -2.30042468E-19/
34 C**  ARRAY CONTAINING COEFFICIENTS IN ASYMPTOTIC EXPANSION OF K1(Z)
35 C      AND K2(Z)
36      DATA (CK(N),N=1,5)/ 1.04166667E-1, 8.35503472E-2, 1.28226575E-1,
37      * 2.91849026E-1, 8.81627267E-1/
38 C**  ARRAY CONTAINING COEFFICIENTS IN ASYMPTOTIC EXPANSION OF K1'(Z)
39 C      AND K2'(Z)
40      DATA (EK(N),N=1,5)/ +1.45833333E-1, -9.87413194E-2,
41      * +1.43312054E-1, -3.17227203E-1, +9.42429148E-1/
42 C
43      DATA X0,X1,ALPHA,PI,PI3/ 9.30436717E-1, 6.78298725E-1,
44      * 8.53667219E-1, 3.14159265E0, 1.04719755E0/
45 C
46      DATA I,CON1,CON2,CON2CJ/ (0.0,1.0), (0.0,1.15470054),
47      * (1.0,0.577350269), (1.0,-0.577350269)/
48 C
49      DATA CE1,CE1CJ,CE2,CE2CJ/ (0.258819045,0.965925826),
50      * (0.258819045,-0.965925826), (-0.965925826,0.258819045),
51      * (-0.965925826,-0.258819045)/
52 C***+
53 C      TEST WHETHER TO EVALUATE MODIFIED HANKEL FUNCTIONS BY SERIES
54 C      EXPANSION OR ASYMPTOTIC EXPANSION
55 C

```

```

56      AMP7=CAPS(7)
57      IF(AMP7.LT.(3.5)) THEN
58 C*****+
59 C      EVALUATE MODIFIED HANKEL FUNCTIONS USING SERIES EXPANSIONS
60 C
61      ZSQ=7*7
62      ZCUBF=7*ZSQ
63      SUMF7=A(9)*ZCUBE
64      SUMG7=B(9)*ZCUBE
65      SUMFP7=C(9)*ZCUBE
66      SUMGP7=D(9)*ZCUBE
67      DO 100 K=A,1,-1
68      SUMF7=(SUMF7+A(K))*ZCUBE
69      SUMG7=(SUMG7+B(K))*ZCUBE
70      SUMFP7=(SUMFP7+C(K))*ZCUBE
71      SUMGP7=(SUMGP7+D(K))*ZCUBE
72 100  CONTINUE
73      F7=(SUMF7+1.0)*X0
74      G7=(SUMG7+1.0)*X1*Z
75      FPZ=-(SUMFP7+1.0)*X0*ZSQ/2.0
76      GPZ=(SUMGP7+1.0)*X1
77      CONF7=CON1*F7
78      CONF7=CON1*FPZ
79 C
80      H1A=CON2*GZ-CONF7
81      H1E=0.0
82      H2A=CON2CJ*G7+CONF7
83      H2E=0.0
84      DH1A=CON2*GP7-CONF7
85      DH1E=0.0
86      DH2A=CON2CJ*GPZ+CONF7
87      DH2E=0.0
88      RETURN
89 C*****+
90      ELSE
91 C*****+
92 C      EVALUATE MODIFIED HANKEL FUNCTIONS USING ASYMPTOTIC EXPANSIONS
93 C
94      ZSQR=CSQRT(7)
95      ZFR=CSQRT(ZSQR)
96      ZTH=7*ZSQR
97      ZMTH=1/ZTH
98      XI=2.0*ZTH/3.0
99      REXT=RFL(XI)
100     IMXI=AIMAG(XI)
101     FXI=CFXP(I*REXT)
102     SUMCKP=CK(5)*ZMTH
103     SUMCKM=-SUMCKP
104     SUMDKP=DK(5)*ZMTH
105     SUMDKM=-SUMDKP
106     DO 102 K=4,1,-1
107     SUMCKP=(SUMCKP+CK(K))*ZMTH
108     SUMCKM=-(SUMCKM+CK(K))*ZMTH
109     SUMDKP=(SUMDKP+DK(K))*ZMTH
110     SUMDKM=-(SUMDKM+DK(K))*ZMTH

```

```

111 102 CONTINUE
112  SUMCKP=1.0+SUMCKP
113  SUMCKM=1.0+SUMCKM
114  SUMDKP=1.0+SUMDKP
115  SUMDKM=1.0+SUMDKM
116 C
117 C      EVALUATE PH(Z)
118 C
119  REZ=REAL(Z)
120  IMZ=AIMAG(Z)
121  IF(REZ.GT.(0.0)) THEN
122  PHZ=ATAN(IMZ/REZ)
123  ELSE IF(REZ.LT.(0.0)) THEN
124  IF(IMZ.GE.(0.0)) THEN
125  PHZ=PI+ATAN(IMZ/REZ)
126  ELSE
127  PHZ=-PI+ATAN(IMZ/REZ)
128  END IF
129  ELSE
130  IF(IMZ.GT.(0.0)) THEN
131  PHZ=PI/2.0
132  ELSE IF(IMZ.LT.(0.0)) THEN
133  PHZ=-PI/2.0
134  ELSE
135  PHZ=0.0
136  END IF
137  END IF
138 C
139 C      EVALUATE MODIFIED HANKEL FUNCTIONS
140 C
141  IF(PHZ.GE.-PI3) THEN
142  K1A=ALPHA*EXI*CE1CJ*SUMCKM/ZFR
143  K1E=-IMXI
144  IF((REAL(K1A).EQ.0.0).AND.(AIMAG(K1A).EQ.0.0)) K1E=0.0
145  DK1A=ALPHA*I*ZFR*FXI*CE1CJ*SUMDKP
146  DK1E=-IMXI
147  IF((REAL(DK1A).EQ.0.0).AND.(AIMAG(DK1A).EQ.0.0)) DK1E=0.0
148  ELSE
149  IF(IMXI.GE.0.0) THEN
150  ESM=-2.0*IMXI
151  IF(ESM.GT.-85.0) THEN
152  REEXP=EXP(ESM)
153  ELSE
154  REEXP=0.0
155  END IF
156  K1A=ALPHA*(CE2CJ*SUMCKP/EXI+EXT*CE1CJ*SUMCKM*REEXP)/ZFR
157  K1E=IMXI
158  IF((REAL(K1A).EQ.0.0).AND.(AIMAG(K1A).EQ.0.0)) K1E=0.0
159  DK1A=ALPHA*I*ZFR*(EXT*CE1CJ*SUMDKP*REEXP-CE2CJ*SUMDKM/EXI)
160  DK1E=IMXI
161  IF((REAL(DK1A).EQ.0.0).AND.(AIMAG(DK1A).EQ.0.0)) DK1E=0.0
162  ELSE
163  ESM=2.0*IMXI
164  IF(ESM.GT.-85.0) THEN
165  REEXP=EXP(ESM)

```

```

166      ELSEF
167      REFP=0.0
168      END IF
169      K1A=ALPHA*(CE2CJ*SUMCKP*REEXP/EXI+EXI*CE1CJ*SUMCKM)/ZFR
170      K1E=-IMXI
171      IF((REAL(K1A).EQ.0.0).AND.(AIMAG(K1A).EQ.0.0)) K1E=0.0
172      DK1A=ALPHA*I*ZFR*(EXI*CE1CJ*SUMDKP+CE2CJ*SUMDKM*REEXP/EXI)
173      DK1E=-IMXI
174      IF((REAL(DK1A).EQ.0.0).AND.(AIMAG(DK1A).EQ.0.0)) DK1E=0.0
175      END IF
176      END IF
177      IF(PH7.GT.PI3) THEN
178      K2A=ALPHA*CE1*SUMCKP/(ZFR*EXI)
179      K2E=IMXI
180      IF((REAL(K2A).EQ.0.0).AND.(AIMAG(K2A).EQ.0.0)) K2E=0.0
181      DK2A=-ALPHA*I*ZFR*CE1*SUMCKM/EXI
182      DK2E=IMXI
183      IF((REAL(DK2A).EQ.0.0).AND.(AIMAG(DK2A).EQ.0.0)) DK2E=0.0
184      ELSE IF(PH7.LT.-PI3) THEN
185      K2A=-ALPHA*EXI*CE2*SUMCKM/ZFR
186      K2E=-IMXI
187      IF((REAL(K2A).EQ.0.0).AND.(AIMAG(K2A).EQ.0.0)) K2E=0.0
188      DK2A=-ALPHA*I*ZFR*EXI*CE2*SUMCKP
189      DK2E=-IMXI
190      IF((REAL(DK2A).EQ.0.0).AND.(AIMAG(DK2A).EQ.0.0)) DK2E=0.0
191      ELSE
192      IF(IMXI.GE.0.0) THEN
193      ESM=-2.0*IMXI
194      IF(ESM.GT.-85.0) THEN
195      REEXP=EXP(ESM)
196      ELSE
197      REEXP=0.0
198      END IF
199      K2A=ALPHA*(CE1*SUMCKP/EXI-REEXP*CE2*EXI*SUMCKM)/ZFR
200      K2E=IMXI
201      IF((REAL(K2A).EQ.0.0).AND.(AIMAG(K2A).EQ.0.0)) K2E=0.0
202      DK2A=-ALPHA*I*ZFR*(CE1*SUMDKM/EXI+REEXP*EXI*CE2*SUMDKP)
203      DK2E=IMXI
204      IF((REAL(DK2A).EQ.0.0).AND.(AIMAG(DK2A).EQ.0.0)) DK2E=0.0
205      ELSE
206      ESM=2.0*IMXI
207      IF(ESM.GT.-85.0) THEN
208      REEXP=EXP(ESM)
209      ELSE
210      REEXP=0.0
211      END IF
212      K2A=ALPHA*(CE1*REEXP*SUMCKP/EXI-EXI*CE2*SUMCKM)/ZFR
213      K2E=-IMXI
214      IF((REAL(K2A).EQ.0.0).AND.(AIMAG(K2A).EQ.0.0)) K2E=0.0
215      DK2A=-ALPHA*I*ZFR*(REEXP*CE1*SUMDKM/EXI+EXI*CE2*SUMDKP)
216      DK2E=-IMXI
217      IF((REAL(DK2A).EQ.0.0).AND.(AIMAG(DK2A).EQ.0.0)) DK2E=0.0
218      END IF
219      END IF
220      END IF
221      RETURN
222      ****
223      END

```

```

1      SUBROUTINE KHATX(Q11,KHA1,KHE1,KHA2,KHE2,DKHA1,TKHE1,DKHA2,TKHE2)
2 C*****
3 C      THIS SUBROUTINE CALCULATES THE MODIFIED HANKEL FUNCTION
4 C      COMBINATIONS KHAT1(Q11), KHAT2(Q11), AND THEIR DERIVATIVES
5 C
6 C      SUBROUTINES USED...
7 C          KHNKLX,CADD,CTANH,CSECH2
8 C*****
9      IMPLICIT DOUBLE PRECISION*6 (A-F,0-7)
10     DOUBLE PRECISION*6 KHE1,KHF2,KDEL2
11     COMPLEX  I,Q11,KHA1,KHA2,DKHA1,DKHA2,Q11A1,Q11A2,DQ11A1,DQ11A2,
12     S  CMU,DCMU,SCNG,BETASQ,FAC,XAA,XRA,XCA,CSPRT,CTANH,CSECH2,
13     *  GAM,HTAN,HSEC2,G11SR,Z,7SG,A,B,DA,DB,A0,A2,A4,A6,A8,A10,
14     *  B1,B3,B5,B7,B9,B11,DA0,DA2,DA4,DA6,DA8,D0,D1,D3,D5,D7,ES
15     EXTERNAL CTANH,CSECH2
16     COMMON/COMTWO/ETAARS,ALPHA1,H,C11,SCNG
17     COMMON/COMTHR/Z2,Z3,A2MAG,ALPHA3,HAENO,ALPHA2
18     COMMON/COMFOR/DELTA,KDEL2,RNONG
19     COMMON/COMFIV/A0,A2,A3,A4,A6,A7,A8,A10,A11
20     COMMON/COMSIX/B0,B1,B3,B5,P7,P9,R11
21     COMMON/COMSEV/DA0,DA1,DA2,DA4,DA5,DA6,DA8,DA9
22     COMMON/COMEIG/D0,D1,D3,D5,D7,P9
23     COMMON/COMNIN/INTCHK
24     DATA  I/1.0,0.1,0.1/
25     DATA  SMALL/0.70710687119D-1/
26 C****
27 C      CALCULATE MODIFIED HANKEL FUNCTIONS NEEDED
28 C
29     CALL KHNKLX(Q11,Q11A1,Q11E1,Q11A2,Q11E2,DQ11A1,ES11E1,
30     S  DQ11A2,DQ11E2)
31 C****
32 C      CALCULATE MU(Q11) AND ITS DERIVATIVES
33 C
34 C
35 C      ***
36 C      BECAUSE OF THE DISCONTINUITY IN KHAT(Q11) AT RE(Q11)=0 WHEN
37 C      DELTA IS NOT EQUAL TO ZERO, WHEN DOING THE MOVE SEARCH WE
38 C      HAVE TO FORCE KHAT(Q11) TO BE ON THE >CORRECT BRANCH< WHEN
39 C      SEARCHING THE RECTANGLE WITH LEFT HAND SIDE RE(Q11)=0 AND
40 C      WHEN SEARCHING THE RECTANGLE WITH RIGHT HAND SIDE RE(Q11)=0.
41 C      THE FLAG 'INTCHK' FROM THE MAIN PROGRAM IS USED FOR THIS
42 C      PURPOSE.
43 C      ***
44 C
45     IF(REAL(Q11).GT.0.0) MDEL=1
46     IF((REAL(Q11).EQ.0.0).AND.((INTCHK.EQ.0).OR.(INTCHK.EQ.2))) MDEL=1
47     IF(REAL(Q11).LT.0.0) MDEL=0
48     IF((REAL(Q11).EQ.0.0).AND.(INTCHK.EQ.1)) MDEL=0
49     IF(MDEL.EQ.0) THEN
50 C
51 C
52     BETASQ=1.0+I*ETAARS-ALPHA1*H-C11*C11*Q11
53     FAC=CSPRT(SCNG-BETASQ)
54     CMU=-I*FAC*RNONG/C11
55     DCMU=-I*C11*RNONG/(2.0*FAC)

```

```

56      END IF
57 C*** 
58 C
59      IF(MDEL.EQ.1) THEN
60 C
61 C
62      IF(DELTA.EQ.0.0) THEN
63      BETASQ=1.0+I*ETAABS-ALPHA1*H-C11*C11*Q11
64      FAC=CSQRT(SQNG-BETASQ)
65      CMU=-I*FAC*RNONG/C11
66      DCMU=-I*C11*RNONG/(2.0*FAC)
67 C
68 C
69      ELSE
70 C
71 C
72      Q11SR=CSQRT(Q11)
73      GAM=KDFL2*C11*C11*Q11
74 C
75 C
76      IF((REAL(Q11).LT.SMALL).AND.(AIMAG(Q11).LT.SMALL)) THEN
77 C
78 C
79      Z=C11*C11SR
80      ZSQ=C11*C11*Q11
81      A=A0+ZSQ*(A2+Z*(A3+Z*(A4+Z*(A6+Z*(A7+Z*(A8+Z*(A10+Z*A11)))))))
82      B=B0+Z*(B1+ZSQ*(B3+ZSQ*(B5+ZSQ*(B7+ZSQ*(B9+ZSQ*B11))))) )
83      DA=DA0+Z*(DA1+Z*(DA2+ZSQ*(DA4+Z*(DA5+Z*(DA6+ZSQ*(DA8+Z*DA9))))))
84      DB=(D0+ZSQ*(D1+ZSQ*(D3+ZSQ*(D5+ZSQ*(D7+ZSQ*D9)))))/7
85      CMU=-I*A/(B*C11)
86      DCMU=(-I/C11)*(DA/B-A*DB/(B*B))
87 C
88 C
89      ELSE
90 C
91 C
92      BETASQ=1.0+I*ETAABS-ALPHA1*H-C11*C11*Q11
93      FAC=CSQRT(SQNG-BETASQ)
94      HTAN=CTANH(GAM)
95      A=C11*C11SR*HTAN+FAC*RNONG
96      B=1.0+FAC*RNONG*HTAN/(Q11SR*C11)
97      HSEC2=CSECH2(GAM)
98      DA=HTAN*C11/(2.0*Q11SR)+KDFL2*ALPHA1*Q11SR*HSEC2/WAVENO
99      $ +C11*C11*RNONG/(2.0*FAC)
100     $ +DB=RNONG*(-FAC*HTAN/(2.0*C11*Q11*Q11SR)+C11*HTAN/(2.0*FAC*C11SR))
101     $ +C11*FAC*KDFL2*HSEC2/Q11SR)
102     CMU=-I*A/(B*C11)
103     DCMU=(-I/C11)*(DA/B-A*DB/(B*B))
104     END IF
105     END IF
106     END IF
107 C*** 
108 C      CALCULATE KHAT1(Q11), KHAT2(Q11), AND THEIR DERIVATIVES
109 C
110     XAA=CMU*Q11A1

```

```
111      XAF=C11E1
112      CALL CADD(KHA1,KHE1,DC11A1,DC11E1,XAA,XAE)
113      XAA=CML*G11A2
114      XAF=G11E2
115      CALL CADD(KHA2,KHE2,DC11A2,DC11E2,XAA,XAE)
116      XAA=CML*DC11A1
117      XAF=DC11E1
118      XBA=PCMU*G11A1
119      XBF=G11E1
120      CALL CADD(XCA,XCF,XAA,XAF,XBA,XRE)
121      XAA=-G11*G11A1
122      XAF=G11E1
123      CALL CADD(CKHA1,CKHE1,XAA,XAE,XCA,XCE)
124      XAA=CML*DC11A2
125      XAF=DC11E2
126      XBA=PCMU*G11A2
127      XBF=G11E2
128      CALL CADD(XCA,XCE,XAA,XAE,XBA,XRE)
129      XAA=-G11*G11A2
130      XAE=G11E2
131      CALL CADD(CKHA2,CKHE2,XAA,XAE,XCA,XCE)
132      RETURN
133  *****
```

```
134      END
```

```

1      FUNCTION CTANH(Z)
2 C*****C
3 C      THIS FUNCTION SUBROUTINE EVALUATES TANH(Z) FOR COMPLEX Z
4 C*****C
5      IMPLICIT DOUBLE PRECISION*6 (A-F,0-7)
6      COMPLEX CTANH,Z,ZSG,E,EINV,CEXP
7      DATA SMALL/0.70710687119E-1/
8      DATA D1,D3,D5,D7,D9/1.0,-0.3333333333,0.1333333333,
9      *-0.53968253968E-1,0.21869488536E-1/
10     IF((DABS(REAL(Z)).GT.SMALL).OR.(DABS(AIMAG(Z)).GT.SMALL)) THEN
11     E=CEXP(Z)
12     FINV=1.0/E
13     CTANH=(E-EINV)/(E+EINV)
14     ELSE
15     ZSG=Z*Z
16     CTANH=Z*(D1+ZSG*(D3+ZSG*(D5+ZSG*(D7+ZSG*D9))))
17     END IF
18     RETURN
19     END

```

```
1      FUNCTION CSECH2(Z)
2 C*****C
3 C      THIS FUNCTION SURROUTINE EVALUATES SECH(Z)*SECH(Z)
4 C      FOR COMPLEX Z
5 C*****C
6      COMPLEX CSECH2,Z,E,FINV,CEXP
7      E=CEXP(2.0D0*Z)
8      FINV=1.0D0/E
9      CSECH2=4.0D0/(E+2.0D0+FINV)
10     RETURN
11     END
```

```

1      SUBROUTINE FCTVLX(Q11S,DETA,DETE)
2 C*****+
3 C      THIS SUBROUTINE EVALUATES THE MODAL FUNCTION *DET(DETA(011))*
4 C
5 C      THE VALUES ARE RETURNED AS A COMPLEX AMPLITUDE *DETA* AND A
6 C      REAL EXPONENT *DETE*. THE VALUE OF THE MODAL FUNCTION IS THEN
7 C      *DET(DETA(011))=DETA*EXP(DETE)*
8 C
9 C      SUBROUTINES USED - HNKLY,KHNKLX,CADD,KHATX
10 C*****+
11      IMPLICIT DOUBLE PRECISION*6  (A-H,O-Z)
12      DOUBLE PRECISION*6 KHE1,KHE2
13      COMPLEX Q11,Q12,Q22,Q23,Q33,I,SGNG,C11S,
14      * KHA1,KHA2,DKHA1,DKHA2,Q12A1,Q12A2,DQ12A1,DQ12A2,
15      * Q22A1,Q22A2,DQ22A1,DQ22A2,Q23A1,Q23A2,DQ23A1,DQ23A2,
16      * Q33A1,Q33A2,DQ33A1,DQ33A2,TA,TR,ZETA,PSI,
17      * XKA,YKB,PKA,PKB,CHT,PHI,DETA
18      COMMON/COMONE/C1,C3,C4,C5,C6,C7,C8,C9,SGNA2
19      COMMON/COMTWO/ETAABS,ALPHA1,H,C11,SGNG
20      DATA I/(0.0,1.0)/
21 C*****
22 C      EVALUATE Q12,Q22,Q23,Q33
23 C
24 C
25 C      THE FOLLOWING STATEMENT SHIFTS Q11 IN ORDER TO AVOID HAVING A
26 C      MESH LINE ON THE REAL AXIS. THIS SHIFT IN Q11 IS COMPENSATED
27 C      FOR IN THE MAIN PROGRAM.
28 C
29      Q11=Q11S-I*0.003
30 C
31      Q12=Q11+C4
32      Q22=C5*C11+C6
33      Q23=C5*C11+C7
34      Q33=C8*C11+C9
35 C
36 C      EVALUATE MODIFIED HANKEL FUNCTIONS NEEDED
37 C
38      CALL KHNKLX(Q12,Q12A1,Q12E1,Q12A2,Q12E2,DQ12A1,DQ12E1,
39      * DQ12A2,DQ12E2)
40      CALL KHNKLX(Q22,Q22A1,Q22E1,Q22A2,Q22E2,DQ22A1,DQ22E1,DQ22A2,
41      * DQ22E2)
42      CALL KHNKLX(Q23,Q23A1,Q23E1,Q23A2,Q23E2,DQ23A1,DQ23E1,
43      * DQ23A2,DQ23E2)
44      CALL HNKLY(Q33,Q33A1,Q33E1,Q33A2,Q33E2,DQ33A1,DQ33E1,
45      * DQ33A2,DQ33E2)
46      CALL KHATX(Q11,KHA1,KHE1,KHA2,DKHA1,DKHE1,DKHA2,DKHE2)
47 C
48 C      EVALUATE ZETA(Q11)
49 C
50      TA=Q12A2*KHA1
51      TAE=Q12E2*KHE1
52      TR=-Q12A1*KHA2
53      TRE=Q12E1*KHE2
54      CALL CADD(ZETA,ZETA,E,TA,TAE,TR,TRE)
55 C

```

```

56 C      EVALUATE PSI(Q11)
57 C
58      TA=DQ12A2*KHA1
59      TAE=DQ12E2+KHE1
60      TB=-DQ12A1*KHA2
61      TBE=DQ12E1+KHE2
62      CALL CADD(PSI,PSIE,TA,TAE,TB,TBE)
63 C
64 C      EVALUATE MODIFIED HANKEL FUNCTION COMBINATIONS NEEDED FOR
65 C      CALCULATING CHI(Q11) AND PHI(Q11)
66 C
67      TA=DQ22A1*Q23A2
68      TAE=DQ22E1+Q23E2
69      TB=-DQ22A2*Q23A1
70      TBE=DQ22E2+Q23E1
71      CALL CADD(XKA,XKAE,TA,TAE,TB,TBE)
72      TA=DQ22A1*DQ23A2
73      TAE=DQ22E1+DQ23E2
74      TB=-DQ22A2*DQ23A1
75      TBE=DQ22E2+DQ23E1
76      CALL CADD(XKB,XKRE,TA,TAE,TB,TBE)
77      TA=Q22A1*Q23A2
78      TAE=Q22E1+Q23E2
79      TB=-Q22A2*Q23A1
80      TBE=Q22E2+Q23E1
81      CALL CADD(PKA,PKAE,TA,TAE,TB,TBE)
82      TA=Q22A1*DQ23A2
83      TAE=Q22E1+DQ23E2
84      TB=-Q22A2*DQ23A1
85      TBE=Q22E2+DQ23E1
86      CALL CADD(PKB,PKRE,TA,TAE,TB,TBE)
87 C
88 C      EVALUATE CHI(Q11)
89 C
90      TA=DQ33A2*XKA
91      TAE=DQ33E2+XKAE
92      TB=SGNA2*C3*Q33A2*XKA
93      TBE=Q33E2+XKBE
94      CALL CADD(CHI,CHIE,TA,TAE,TB,TBE)
95 C
96 C      EVALUATE PHI(Q11)
97 C
98      TA=DQ33A2*PKA
99      TAE=DQ33E2+PKAE
100     TB=SGNA2*C3*Q33A2*PKB
101     TBF=Q33E2+PKRF
102     CALL CADD(PHI,PHIE,TA,TAE,TB,TBE)
103 C
104 C      EVALUATE *DET(DELTA(Q11))*
105 C
106     TA=SGNA2*C1*ZETA*CHI
107     TAF=7ETAE+CHIE
108     TB=PSI*PHI
109     TBE=PSIE+PHIE
110     CALL CADD(DETA,DETE,TA,TAE,TB,TBE)
111     DETA=SGNA2*DETA/C3
112     RETURN
113 C*****
114     END

```

```

1      SUBROUTINE FDFDTX(Q11S,DETA,DETE,DETPA,DETPE)
2 C******
3 C      THIS SUBROUTINE EVALUATES 'DET(DELTA(Q11))'
4 C      AND ITS DERIVATIVE WITH RESPECT TO Q11
5 C
6 C      THESE VALUES ARE RETURNED AS A COMPLEX AMPLITUDE AND A
7 C      REAL EXPONENT. WE HAVE
8 C          DET(DELTA(Q11))=DETA*EXP(DETE)
9 C          (DET(DELTA(Q11)))'=DETPA*EXP(DETPE)
10 C
11 C      SUBROUTINES USED = HNKLX,KHNKLX,CADT,KHATX
12 C******
13 C      IMPLICIT DOUBLE PRECISION*6 (A-H,O-Z)
14 C      DOUBLE PRECISION*6 KHE1,KHE2
15 C      COMPLEX Q11,Q12,Q22,Q23,Q33,I,SGNG,Q11S,
16 C      * KHA1,KHA2,DKHA1,DKHA2,Q12A1,Q12A2,DQ12A1,FG12A2,
17 C      * Q22A1,Q22A2,DQ22A1,DQ22A2,C23A1,Q23A2,FG23A1,FG23A2,
18 C      * Q33A1,Q33A2,DQ33A1,DQ33A2,TA,TR,TC,TD,TE,TF,TG,
19 C      * ZETA,PSI,DZETA,DPsi,XKA,XKF,PKA,
20 C      * PKB,XKAP,XKBP,XKCP,XKEP,CHI,PHI,DCHI,DPHI,DETA,DETPA
21 C      COMMON/COMONE/C1,C3,C4,C5,C6,C7,C8,C9,SGNA2
22 C      COMMON/COMTWO/ETAABS,ALPHA1,H,C11,SGNG
23 C      DATA I/10.0,1.0/
24 C*****
25 C      EVALUATE Q12,Q22,Q23,Q33
26 C
27 C
28 C      THE FOLLOWING STATEMENT SHIFTS Q11 IN ORDER TO AVOID HAVING A
29 C      MESH LINE ON THE REAL AXIS. THIS SHIFT IN Q11 IS COMPENSATED
30 C      FOR IN THE MAIN PROGRAM.
31 C
32 C      Q11=Q11S-I*0.003
33 C
34 C      Q12=Q11+C4
35 C      Q22=C5+C11+C6
36 C      Q23=C5+C11+C7
37 C      Q33=C8+C11+C9
38 C
39 C      EVALUATE MODIFIED HANKEL FUNCTIONS NEEDED
40 C
41 C      CALL KHNKLX(Q12,Q12A1,Q12E1,Q12A2,Q12E2,DQ12A1,FG12E1,
42 C      *DQ12A2,FG12E2)
43 C      CALL KHNKLX(Q22,Q22A1,Q22E1,Q22A2,Q22E2,DQ22A1,FG22E1,
44 C      *DQ22A2,DQ22E2)
45 C      CALL KHNKLX(Q23,Q23A1,Q23E1,Q23A2,Q23E2,DQ23A1,FG23E1,
46 C      *DQ23A2,DQ23E2)
47 C      CALL HNKLX(Q33,Q33A1,Q33E1,Q33A2,Q33E2,DQ33A1,FG33E1,
48 C      *DQ33A2,DQ33E2)
49 C      CALL KHATX(Q11,KHA1,KHE1,KHA2,KHE2,DKHA1,DKHE1,FKHA2,DKHE2)
50 C
51 C      EVALUATE ZETA(Q11)
52 C
53 C      TA=Q12A2*KHA1
54 C      TAE=Q12E2*KHE1
55 C      TB=-Q12A1*KHA2

```

```

56      TBE=Q12E1+KHE2
57      CALL CADD(ZFTA,ZETA,E,TA,TAE,TP,TBE)
58 C
59 C      EVALUATE PSI(Q11)
60 C
61      TA=DQ12A2*KHA1
62      TAE=DQ12E2+KHE1
63      TB=-DQ12A1*KHA2
64      TBE=DQ12F1+KHE2
65      CALL CADD(PSI,PSIE,TA,TAE,TB,TBE)
66 C
67 C      EVALUATE ZETAP(Q11)
68 C
69      TA=DQ12A2*KHA1
70      TAE=DQ12E2+KHE1
71      TB=Q12A2*DKHA1
72      TBE=Q12E2+DKHE1
73      CALL CADD(TC,TCE,TA,TAE,TP,TBE)
74      TA=-DQ12A1*KHA2
75      TAE=DQ12E1+KHE2
76      TB=-Q12A1*DKHA2
77      TBE=Q12E1+DKHE2
78      CALL CADD(TD,TDE,TA,TAE,TP,TBE)
79      CALL CADD(DZETA,DZETA,E,TC,TCE,TD,TDE)
80 C
81 C      EVALUATE PSI*(Q11)
82 C
83      TA=-Q12*Q12A2*KHA1
84      TAE=Q12E2+KHE1
85      TB=DQ12A2*DKHA1
86      TBE=DQ12E2+DKHE1
87      CALL CADD(TC,TCE,TA,TAE,TP,TBE)
88      TA=Q12*Q12A1*KHA2
89      TAE=Q12E1+KHE2
90      TB=-DQ12A1*DKHA2
91      TBE=DQ12E1+DKHE2
92      CALL CADD(TD,TDE,TA,TAE,TP,TBE)
93      CALL CADD(DPSI,DPSIE,TC,TCE,TD,TDE)
94 C
95 C      EVALUATE MODIFIED HANKEL FUNCTION COMBINATIONS NEEDED FOR
96 C      CALCULATING CHI(Q11),CHI*(Q11),PHI(Q11) AND PHI*(Q11)
97 C
98      TA=DQ22A1+Q23A2
99      TAE=DQ22E1+Q23E2
100     TB=-DQ22A2+Q23A1
101     TBE=DQ22E2+Q23E1
102     CALL CADD(XKA,XKAE,TA,TAE,TB,TBE)
103     TA=DQ22A1*DQ23A2
104     TAE=DQ22E1+DQ23E2
105     TB=-DQ22A2*DQ23A1
106     TBE=TC22E2+DQ23E1
107     CALL CADD(XKB,XKBE,TA,TAE,TB,TBE)
108     TA=Q22A1+Q23A2
109     TAE=Q22E1+Q23E2
110     TB=-Q22A2+Q23A1

```

```

111      TBE=Q22E2+Q23E1
112      CALL CADD(PKA,PKAE,TA,TAE,TB,TBE)
113      TA=Q22A1+DQ23A2
114      TAE=Q22E1+DQ23E2
115      TB=-Q22A2+DQ23A1
116      TBE=Q22E2+DQ23E1
117      CALL CADD(PKB,PKBE,TA,TAE,TB,TBE)
118      TA=Q22A2+Q23A1
119      TAE=Q22E2+Q23E1
120      TB=-Q22A1+Q23A2
121      TBE=Q22E1+Q23E2
122      CALL CADD(XKAP,XKAPE,TA,TAE,TB,TBE)
123      TA=DQ22A1+DQ23A2
124      TAE=DQ22E1+DQ23E2
125      TB=-DQ22A2+DQ23A1
126      TBE=DQ22E2+DQ23E1
127      CALL CADD(XKBP,XKBPE,TA,TAE,TB,TBE)
128      TA=Q22A2+DQ23A1
129      TAE=Q22E2+DQ23E1
130      TB=-Q22A1+DQ23A2
131      TBE=Q22E1+DQ23E2
132      CALL CADD(XKCP,XKCPE,TA,TAE,TB,TBE)
133      TA=DQ22A2+Q23A1
134      TAE=DQ22E2+Q23E1
135      TB=-DQ22A1+Q23A2
136      TBE=DQ22E1+Q23E2
137      CALL CADD(XKDP,XKDPE,TA,TAE,TB,TBE)
138      C
139      C
140      C
141      TA=DQ33A2+XKA
142      TAE=DQ33E2+XKAE
143      TB=SGNA2+C3+Q33A2*XKB
144      TBE=Q33E2+XKBE
145      CALL CADD(CHI,CHIE,TA,TAE,TB,TBE)
146      C
147      C
148      C
149      TA=DQ33A2+PKA
150      TAE=DQ33E2+PKAE
151      TB=SGNA2+C3+Q33A2+PKB
152      TBE=Q33E2+PKBE
153      CALL CADD(PHI,PHIE,TA,TAE,TB,TBE)
154      C
155      C
156      C
157      TA=-Q33+C8+Q33A2+XKA
158      TAE=Q33E2+XKAE
159      TB=C5+DQ33A2+Q22*XKAP
160      TBE=DQ33E2+XKAPE
161      TC=C5+DQ33A2*XKBP
162      TCE=DQ33E2+XKBPE
163      TD=SGNA2+C3+C8+DQ33A2*XKB
164      TDE=DQ33E2+XKBE
165      TE=SGNA2+C3+C5+Q33A2+Q22*XKCP

```

```

166      TEE=Q33E2*XKCP
167      TF=SGNA2*C3*C5*Q33A2*Q23*XKDP
168      TFE=Q33E2*XKDP
169      CALL CADD(TG,TGE,TA,TAE,TB,TBE)
170      CALL CADD(TA,TAE,TG,TGE,TC,TCE)
171      CALL CADD(TB,TBE,TA,TAE,TD,TCE)
172      CALL CADD(TA,TAE,TB,TBE,TE,TEE)
173      CALL CADD(DCHI,DCHIE,TA,TAE,TF,TFE)
174 C
175 C      EVALUATE PHI'(Q11)
176 C
177      TA=-Q33*C8*Q33A2*PKA
178      TAE=Q33E2*PKAE
179      TB=C5*DQ33A2*XKA
180      TBE=DQ33E2*XKAE
181      CALL CADD(TC,TCE,TA,TAE,TR,TBE)
182      TA=C5*DQ33A2*PKR
183      TAF=DQ33E2*PKBE
184      CALL CADD(TB,TBE,TA,TAE,TC,TCE)
185      TA=SGNA2*C3*C8*DQ33A2*PKR
186      TAE=DQ33E2*PKBE
187      CALL CADD(TC,TCE,TB,TBE,TA,TAE)
188      TA=SGNA2*C3*C5*Q33A2*XKE
189      TAE=Q33E2*XKAE
190      CALL CADD(TB,TBE,TC,TCE,TA,TAE)
191      TA=-SGNA2*C3*C5*Q33A2*Q23*PKA
192      TAE=Q33E2*PKAE
193      CALL CADD(DPHI,DPHIE,TB,TBE,TA,TAE)
194 C
195 C      EVALUATE DET(DELTA(Q11))
196 C
197      TA=SGNA2*C1*ZETA*CHI
198      TAE=ZETAE+CHIE
199      TB=PSI*PHI
200      TBE=PSIE+PHIE
201      CALL CADD(DETA,DETE,TA,TAE,TR,TBE)
202      DETA=SGNA2*DETA/C3
203 C
204 C      EVALUATE (DET(DELTA(Q11)))'
205 C
206      TA=SGNA2*C1*DZETA*CHI
207      TAE=DZETAE+CHIE
208      TB=SGNA2*C1*ZETA*DCHI
209      TBE=ZETAE+DCHIE
210      CALL CADD(TC,TCE,TA,TAE,TB,TBE)
211      TA=DPSI*PHI
212      TAE=PSIE+PHIE
213      TB=PSI*DPHI
214      TBE=PSIE+DPHIE
215      CALL CADD(TD,TDE,TA,TAE,TB,TBE)
216      CALL CADD(DETPA,DETPB,TC,TCE,TD,TDE)
217      DETPA=SGNA2*DETPA/C3
218      RETURN
219 C*****
220      END

```

```

1      SUBROUTINE FZEROX(TLEFT,TRIGHT,TROT,TTOP,TMESH0,TOL,MPRINT,ZEROS,
2      &                           NRZ)
3 C  FOR ROOT-FINDER
4 C  THIS VERSION UPDATED TO MODIFY GMAX AND TMESH. JAN 6 1982.
5 C  FZEROS IS A ROUTINE FOR FINDING THE ZEROS OF A COMPLEX FUNCTION, F,
6 C  WHICH LIE WITHIN A SPECIFIED RECTANGULAR REGION OF THE
7 C  COMPLEX (THETA) PLANE, PROVIDED THE FUNCTION HAS NO
8 C  POLES IN THE VICINITY OF THE RECTANGLE.
9 C  EXPLANATION OF PARAMETERS--
10 C    TLEFT - VALUE OF REAL PART OF THETA AT LEFT EDGE OF RECTANGLE.
11 C    TRIGHT - VALUE OF REAL PART OF THETA AT RT EDGE OF RECTANGLE.
12 C    TROT - VALUE OF IMAG PART OF THETA AT BOTTOM EDGE OF RECTANGLE.
13 C    TTOP - VALUE OF IMAG PART OF THETA AT TOP EDGE OF RECTANGLE.
14 C    TMESH - SET EQUAL TO ABOUT HALF THE AVERAGE SPACING BETWEEN
15 C          ZEROS WITHIN THE RECTANGLE. A SMALLER VALUE MAY BE USED
16 C          AS A SAFETY MEASURE, BUT TOO SMALL A VALUE WILL RESULT
17 C          IN EXCESSIVE RUN TIME.
18 C    TOL - TOLERANCE TO WHICH ZEROS ARE TO BE FOUND. IF TWO
19 C          ZEROS ARE CLOSER THAN 'TOL', THE ROOT-FINDER WILL STOP
20 C          WITH AN ERROR MESSAGE.
21 C    MPRINT - NORMALLY SET TO ZERO. A NON-ZERO VALUE LEADS TO
22 C          PRINT-OUT FOR DEBUGGING.
23 C    ZEROS - OUTPUT LIST OF (COMPLEX) VALUES OF THETA AT WHICH
24 C          ZEROS ARE FOUND.
25 C    NRZ - THE NUMBER OF ZEROS FOUND.
26 C  SUBROUTINES TO BE PROVIDED--
27 C    FCTVLY(Z,F,FE) - TO RETURN THE VALUE OF THE FUNCTION, F*EXP(FE),
28 C                      AT THE POINT IN THE COMPLEX PLANE SPECIFIED BY Z.
29 C    FDFDTX(Z,F,FE,DFDT,DFDTE) - SAME AS 'FCTVLY' EXCEPT THAT THE
30 C          DERIVATIVE, DFDT*EXP(DFDTE), OF THE FUNCTION KRT Z MUST ALSO
31 C          BE RETURNED.
32 C
33 C  IMPLICIT DOUBLE PRECISION*6 (A-H,O-Z)
34 C  COMMON/NEWMSH/NEWMSH
35 C  COMMON/TMC/COM/TMESH
36 C
37 C  DIMENSION ZEROS(2,1)
38 C  COMPLEX F,PREV F,F00,F10,F01,F11,PARTS
39 C  DIMENSION PART(2),SOL(2),THETA(2)
40 C  DIMENSION K EDGE1(50),K EDGE2(50),K EDGE3(50),K EDGE4(50)
41 C  EQUIVALENCE (PART(1),PARTS)
42 C  MAXNSG=MAX0(INT(4.0*(TTOP-TROT)/TMESH0),INT(4.0*(TRIGHT-TLEFT)
43 C  /TMESH0))
44 C  MAXNT=2
45 C
46 C
47 C  IF (MPRINT.NE.0) WRITE(11,906)
48 C  906 FORMAT ('1')
49 C
50 C  TMESH = TMESH0
51 C  NTIME = 0
52 C  GO TO 7
53 C  5 TMESH = TMESH/2.0
54 C  NTIME = NTIME+1
55 C  IF (NTIME .GT. MAX NT) GO TO 97

```

```

56 7      NEWMSH = 0
57 C
58 C SIDES OF RECTANGLE IN TMESH UNITS
59     JLT=INT(TLEFT/TMESH)
60     IF(TLEFT.GT.0.0) JLT=JLT-1
61     IF (TLEFT .LT. 0.0) JLT = JLT-2
62     IF(TLEFT.EQ.0.0) JLT=0
63 C
64     JRT=INT(TRIGHT/TMESH)
65     IF (TRIGHT .GT. 0.0) JRT = JRT+2
66     IF(TRIGHT.LT.0.0) JRT=JRT+1
67     IF(TRIGHT.EQ.0.0) JRT=0
68 C
69     JBOT = INT(TBOT/TMESH)
70     IF (TBOT .GE. 0.0) JBOT = JBOT-1
71     IF (TBOT .LT. 0.0) JBOT = JBOT-2
72 C
73     JT0P = INT(TTOP/TMESH)
74     IF (TTOP .GT. 0.0) JT0P = JT0P+2
75     IF (TTOP .LE. 0.0) JT0P = JT0P+1
76 C
77 C INITIALIZATION OF PARAMETERS.
78     K1 = JT0P
79     KR = JLT
80     KEDGE = 1
81     CALL FINDFX(KR,K1,F,FE,TLEFT,TRIGHT)
82     E00=1.0
83     E01=1.0
84     E10=1.0
85     E11=1.0
86     NR E1 = 0
87     NR E2 = 0
88     NR E3 = 0
89     NR E4 = 0
90     NR Z = 0
91     GO TO 15
92 C
93     10 IF(NR ZL .LE. 1) GO TO 15
94     WRITE(11,2000) NRZL
95     2000 FORMAT ('>0>,I3,1X,>M0DES FOUND ON SAME PHASE LINE>')
96     GO TO 5
97     15 NR ZL = 0
98     NRSOU = 0
99 C
100    20 PREVF=F
101    PREVFF=FE
102    IF(MPRINT.NE.0) WRITE(11,2200) KR,K1,F,FE
103    2200 FORMAT(30X,2I4,5X,'F = ',1P2E12.3,5X,'FE = ',1P2E12.3)
104    GO TO (21,26,31,36),KEDGE
105 C
106 C SEARCH ALONG LEFT EDGE OF RECTANGLE FOR SIGN CHANGES IN IMAG(F).
107    21 IF (K1 .EQ. JBOT) KEDGE = 2
108    IF (KEDGE .EQ. 2) GO TO 26
109    K1 = K1-1
110    CALL FINDFX(KR,K1,F,FE,TLEFT,TRIGHT)

```

```

111      IF ((AIMAG(PREV F) .GT. 0.0 .AND. AIMAG(F) .GT. 0.0)
112      *          .OR. (AIMAG(PREV F) .LT. 0.0 .AND. AIMAG(F) .LT. 0.0))
113      *          GO TO 20
114      IF (NR F1 .EQ. 0) GO TO 23
115      DO 22 K=1, NR F1
116      IF (KI .EQ. K EDGE1(K)) GO TO 20
117      22 CONTINUE
118      23 F01 = PREV F
119      F01E=PREVFF
120      F00 = F
121      F00E=FE
122      LI = KI
123      LR = JLT
124      GO TO 43
125 C  SEARCH ALONG BOTTOM EDGE OF RECTANGLE FOR SIGN CHANGES IN IMAG(F).
126 26 IF (KR .EQ. JRT) KEDGE = 3
127      IF (KEDGE .EQ. 3) GO TO 31
128      KR = KR+1
129      CALL FINDFX(KR,KI,F,FE,TLEFT,TRIGHT)
130      IF ((AIMAG(PREV F) .GT. 0.0 .AND. AIMAG(F) .GT. 0.0)
131      *          .OR. (AIMAG(PREV F) .LT. 0.0 .AND. AIMAG(F) .LT. 0.0))
132      *          GO TO 20
133      *          IF (NR E2 .EQ. 0) GO TO 2A
134      *          DO 27 K=1, NR E2
135      *          IF (KR .EQ. K EDGE2(K)) GO TO 20
136      27 CONTINUE
137      28 F00 = PREV F
138      F00E=PREVFE
139      F10 = F
140      F10E=FE
141      LI = JBOT
142      LR = KR-1
143      GO TO 48
144
145 C  SEARCH ALONG RIGHT EDGE OF RECTANGLE FOR SIGN CHANGES IN IMAG(F).
146 31 IF (KI .EQ. JTOP) KEDGE = 4
147      IF (KEDGE .EQ. 4) GO TO 36
148      KI = KI+1
149      CALL FINDFX(KR,KI,F,FE,TLEFT,TRIGHT)
150      IF ((AIMAG(PREV F) .GT. 0.0 .AND. AIMAG(F) .GT. 0.0)
151      *          .OR. (AIMAG(PREV F) .LT. 0.0 .AND. AIMAG(F) .LT. 0.0))
152      *          GO TO 20
153      *          IF (NR E3 .EQ. 0) GO TO 33
154      *          DO 32 K=1, NR E3
155      *          IF (KI .EQ. K EDGE3(K)) GO TO 20
156      32 CONTINUE
157      33 F10 = PREV F
158      F10E=PREVFE
159      F11 = F
160      F11E=FE
161      LI = KI-1
162      LR = JRT-1
163      GO TO 53
164
165 C

```

```

166 C SEARCH ALONG TOP EDGE OF RECTANGLE FOR SIGN CHANGES IN AIMAG(F).
167 36 IF (KR .EQ. JLT) GO TO 80
168     KR = KR-1
169     CALL FINDFX(KR,KI,F,FE,TLEFT,TRIGHT)
170     IF ((AIMAG(PREV F) .GT. 0.0 .AND. AIMAG(F) .GT. 0.0)
171     S           .OR. (AIMAG(PREV F) .LT. 0.0 .AND. AIMAG(F) .LT. 0.0))
172     S           GO TO 20
173     IF (NR E4 .EQ. 0) GO TO 38
174     DO 37 K=1, NR E4
175     IF (KR .EQ. K EDGE4(K)) GO TO 20
176     37 CONTINUE
177     38 F11 = PREV F
178     F11F=PREVFE
179     F01 = F
180     F01F=FE
181     LI = JTOP-1
182     LR = KR
183     GO TO 58
184 C
185 C ENTER MESH SQUARE FROM LEFT SIDE OR EXIT RECTANGLE AT RIGHT EDGE.
186 41 LR = LR+1
187     IF (LR .LE. JRT-1) GO TO 42
188     NR E3 = NR E3+1
189     K EDGE3(NR E3) = LI+1
190     IF(MPRINT.NE.0) WRITE(11,990)
191     GO TO 10
192     42 F01=F11/E11
193     F01E=F11E
194     F00=F10/E10
195     F00E=F10E
196     43 CALL FINDFX(LR+1,LI+1,F11,F11E,TLEFT,TRIGHT)
197     CALL FINDFX(LR+1,LI,F10,F10E,TLEFT,TRIGHT)
198     SCALE=AMAX1(F00E,F01E,F10E,F11E)
199     IF(SCALE.GT.34.0) THEN
200     E00=EXP(F00E-SCALE)
201     E01=EXP(F01E-SCALE)
202     E10=EXP(F10E-SCALE)
203     E11=EXP(F11E-SCALE)
204     F00=F00*E00
205     F01=F01*E01
206     F10=F10*E10
207     F11=F11*E11
208     END IF
209     LEDGE = 1
210     ENTER R = 0.0
211     ENTER I = -AIMAG(F00)/AIMAG(F01-F00)
212     GO TO 60
213 C
214 C ENTER MESH SQUARE FROM BOTTOM SIDE OR EXIT RECTANGLE AT TOP EDGE.
215     46 LI = LI+1
216     IF (LI .LE. JTOP-1) GO TO 47
217     NR E4 = NR E4+1
218     K EDGE4(NR E4) = LR
219     IF(MPRINT.NE.0) WRITE(11,990)
220     GO TO 10

```

```

221    47 F00=F01/E01
222    F00F=F01F
223    F10=F11/E11
224    F10F=F11F
225    48 CALL FINDFX(LR,LI+1,F01,F01E,TLEFT,TRIGHT)
226    CALL FINDFX(LR+1,LI+1,F11,F11E,TLEFT,TRIGHT)
227    SCALE=AMAX1(F00E,F01E,F10E,F11E)
228    IF(SCALE.GT.34.0) THEN
229    E00=EXP(F00E-SCALE)
230    F01=EXP(F01E-SCALE)
231    F10=EXP(F10E-SCALE)
232    E11=EXP(F11E-SCALE)
233    F00=F00*E00
234    F01=F01*E01
235    F10=F10*E10
236    F11=F11*E11
237    END IF
238    LEDGE = 2
239    ENTER R = -AIMAG(F00)/AIMAG(F10-F00)
240    ENTER I = 0.0
241    GO TO 60
242 C
243 C ENTER MESH SQUARE FROM RIGHT SIDE OR EXIT RECTANGLE AT LEFT EDGE.
244    51 LR = LR-1
245    IF (LR .GE. JLT) GO TO 52
246    NR E1 = NR E1+1
247    K EDGE1(NR E1) = LI
248    IF(MPRINT.NE.0) WRITE(11,990)
249    GO TO 10
250    52 F11=F01/E01
251    F11E=F01E
252    F10=F00/E00
253    F10E=F00E
254    53 CALL FINDFX(LR,LI+1,F01,F01E,TLEFT,TRIGHT)
255    CALL FINDFX(LR,LI,F00,F00E,TLEFT,TRIGHT)
256    SCALE=AMAX1(F00E,F01E,F10E,F11E)
257    IF(SCALE.GT.34.0) THEN
258    E00=EXP(F00E-SCALE)
259    E01=EXP(F01E-SCALE)
260    E10=EXP(F10E-SCALE)
261    E11=EXP(F11E-SCALE)
262    F00=F00*E00
263    F01=F01*E01
264    F10=F10*E10
265    F11=F11*E11
266    END IF
267    LEDGE = 3
268    ENTER R = 1.0
269    ENTER I = -AIMAG(F10)/AIMAG(F11-F10)
270    GO TO 60
271 C
272 C ENTER MESH SQUARE FROM TOP SIDE OR EXIT RECTANGLE AT BOTTOM EDGE.
273    56 LI = LI-1
274    IF (LI .GE. JROT) GO TO 57
275    NR F2 = NR E2+1

```

```

276      K FDGF2(NR,E2) = LR+1
277      IF(MPRINT.NE.0) WRITE(11,990)
278      GO TO 10
279 57  F01=F00/E00
280      F01F=F00F
281      F11=F10/E10
282      F11F=F10E
283 58  CALL FINDFX(LR,LI,F00,F00F,TLEFT,TRIGHT)
284      CALL FINDFX(LR+1,LI,F10,F10E,TLEFT,TRIGHT)
285      SCALE=AMAX1(F00E,F01F,F10E,F11E)
286      IF(SCALE.GT.34.0) THEN
287      E00=EYP(F00E-SCALE)
288      E01=EXP(F01E-SCALE)
289      E10=EXP(F10E-SCALE)
290      E11=EXP(F11E-SCALE)
291      F00=F00*E00
292      F01=F01*E01
293      F10=F10*E10
294      F11=F11*E11
295      END IF
296      LEDGE = 4
297      ENTER R = -AIMAG(F01)/AIMAG(F11-F01)
298      ENTER I = 1.0
299      GO TO 60
300 C
301 C FOR DEBUGGING ONLY, PRINT CO-ORDINATE OF LOWER LEFT CORNER
302 C OF CURRENT MESH SQUARE. RESULTING SET OF PRINTED
303 C CO-ORDINATES GIVES TRACE OF EACH LINE ALONG WHICH
304 C IMAG(F)=0.0 FROM ITS ENTRY ON THE EDGE OF THE
305 C RECTANGLE TO ITS EXIT AT ANOTHER POINT ON THE
306 C RECTANGLE.
307      60 IF(MPRINT.NE.0) WRITE(11,960) LR,LI
308      960 FORMAT (' ',20X,2I5)
309 C TEST FOR THERE BEING TWO (HYPERBOLIC) LINES ENTERING AND LEAVING
310 C THE MESH SQUARE ALONG EACH OF WHICH IMAG(F)=0.0
311 C IF SO, SET 'LTWO' NON-ZERO.
312      LTWO = 0
313      NRSCU=NRSCU+1
314      IF(NRSCU.GT. MAXNSQ) GO TO 95
315      IF(((AIMAG(F00).GE. 0.0).AND.(AIMAG(F11).GE. 0.0))
316      & .AND.(AIMAG(F10).LE. 0.0).AND.(AIMAG(F01).LE. 0.0))
317      & .OR.((AIMAG(F00).LE. 0.0).AND.(AIMAG(F11).LE. 0.0))
318      & .AND.(AIMAG(F10).GE. 0.0).AND.(AIMAG(F01).GE. 0.0))) LTWO=1
319 C TEST FOR THERE BEING AT LEAST ONE (HYPERBOLIC) LINE ENTERING AND
320 C LEAVING THE MESH SQUARE ALONG WHICH REAL(F)=0.0
321 C IF NOT, SET 'I90' TO ZERO.
322      I90 = 1
323      IF ((REAL(F00).GT. 0.0 .AND. REAL(F10).GT. 0.0
324      & .AND. REAL(F01).GT. 0.0 .AND. REAL(F11).GT. 0.0)
325      & .OR. (REAL(F00).LT. 0.0 .AND. REAL(F10).LT. 0.0
326      & .AND. REAL(F01).LT. 0.0 .AND. REAL(F11).LT. 0.0))
327      & I90 = 0
328      IF (LTWO.EQ. 0 .AND. I90.EQ. 0) GO TO 70
329 C COMPUTATION OF COEFFICIENTS TO BE USED IN DESCRIBING THE VARIATION
330 C

```

```

331 C OF THE FUNCTION WITHIN A MESH SQUARE GIVEN THE
332 C VALUES AT THE CORNERS OF THE SQUARE AND LINEAR
333 C VARIATION ALONG ITS EDGES. ALSO, THE POSITION OF
334 C CROSSING OF THE HYPERBOLIC ASYMPTOTES (WHICH ARE
335 C PARALLEL TO THE SIDES OF THE SQUARE) FOR THE LINES
336 C  $\text{IMAG}(F)=0.0$  ARE COMPUTED IF BOTH LINES (BRANCHES)
337 C ENTER AND LEAVE THE SQUARE.

338 PARTS = F00
339 AR = PART(1)
340 AI = PART(2)
341 PARTS = F01-F00
342 BR = PART(1)
343 BI = PART(2)
344 PARTS = F10-F00
345 CR = PART(1)
346 CI = PART(2)
347 PARTS = F00+F11-F01-F10
348 DR = PART(1)
349 DI = PART(2)

350 C
351 IF (LTWO .EQ. 0) GO TO 61
352 CENTR R = -AI/DI
353 CENTR I = -CI/DI
354 IF (I90 .EQ. 0) GO TO 70

355 C
356 61 AB = AR*BI-AI*BR
357 AC = AR*CI-AI*CR
358 AD = AR*DI-AI*DR
359 BC = BR*CI-BI*CR
360 BD = BR*DI-BI*DR
361 CD = CR*DI-CI*DR

362 C
363 IF (ABS(BD) .LT. ABS(CD)) GO TO 64
364 C SOLUTION FOR TWO POSSIBLE POINTS AT WHICH THERE MAY BE CROSSINGS
365 C OF THE (HYPERBOLIC) LINES  $\text{REAL}(F)=0.0$  AND  $\text{IMAG}(F)=0.0$ .
366 C A CROSSING POINT IS CHOSEN TO BE A ZERO OF THE
367 C FUNCTION IF IT LIES WITHIN THE CURRENT MESH SQUARE
368 C AND IF IT LIES ON THE BRANCH OF  $\text{IMAG}(F)=0.0$  CURRENTLY
369 C BEING FOLLOWED. MULTIPLE CROSSINGS ALONG THIS BRANCH
370 C (ACTUALLY A SERIES OF CONNECTING HYPERBOLIC BRANCHES)
371 C IN THE SAME OR IN DIFFERENT SQUARES ARE NOTED SINCE
372 C THESE MUST LATER BE RESOLVED.

373 A = CD
374 B = (AD-BC)*0.5
375 C = AB
376 CALL QUAD (A,B,C,SOL,NR SOL)
377 IF (NR SOL .EQ. 0) GO TO 70
378 DO 63 N=1,NR SOL
379 UREAL = SOL(N)
380 IF (UREAL .LT. 0.0 .OR. UREAL .GT. 1.0) GO TO 63
381 D1 = BR+DR*UREAL
382 D2 = BI+DI*UREAL
383 IF (ABS(D1) .GE. ABS(D2)) UIMAG = -(AR+CR*UREAL)/D1
384 IF (ABS(D2) .GE. ABS(D1)) UIMAG = -(AI+CI*UREAL)/D2
385 IF (UIMAG .LT. 0.0 .OR. UIMAG .GT. 1.0) GO TO 63

```

```

386      IF (LTWO .EQ. 0) GO TO 62
387      IF ((ENTER R-CENTR R)*(U REAL-CENTR R) .LT. 0.0
388      S           .OR. (ENTER I-CENTR I)*(U IMAG-CENTR I) .LT. 0.0)
389      S           GO TO 63
390      62 THETA(1) = (LR+U REAL)*TMESH
391      THETA(2) = (LI+U IMAG)*TMESH
392      IF(IMPRINT.NE.0) WRITE(11,962) LR,LI,THETA(1),THETA(2)
393      962 FORMAT (' ',2I4,3X,'THETA =',2F9.4)
394      NRZ = NRZ+1
395      ZEROS(1,NRZ) = THETA(1)
396      ZEROS(2,NRZ) = THETA(2)
397      NR ZL = NR ZL+1
398      63 CONTINUE
399      GO TO 67
400 C
401 C ALTERNATE SOLUTION FOR THE ABOVE. TWO FORMS ARE NEEDED SINCE,
402 C           IN ANY GIVEN CASE, EITHER FORM (BUT NOT BOTH FORMS)
403 C           MAY BE INDETERMINATE.
404      64 A = BD
405      B = (AD+BC)*0.5
406      C = AC
407      CALL QUAD (A,B,C,SOL,NR SOL)
408      IF (NR SOL .EQ. 0) GO TO 70
409      DO 66 N=1,NR SOL
410      UIMAG = SOL(N)
411      IF (UIMAG .LT. 0.0 .OR. UIMAG .GT. 1.0) GO TO 66
412      D1 = CR+DR*UIMAG
413      D2 = CI+DI*UIMAG
414      IF (ABS(D1) .GE. ABS(D2)) UREAL = -(AR+RR*UIMAG)/D1
415      IF (ABS(D2) .GE. ABS(D1)) UREAL = -(AI+RI*UIMAG)/D2
416      IF (UREAL .LT. 0.0 .OR. UREAL .GT. 1.0) GO TO 66
417      IF (LTWO .EQ. 0) GO TO 65
418      IF ((ENTER R-CENTR R)*(U REAL-CENTR R) .LT. 0.0
419      S           .OR. (ENTER I-CENTR I)*(U IMAG-CENTR I) .LT. 0.0)
420      S           GO TO 66
421      65 THETA(1) = (LR+U REAL)*TMESH
422      THETA(2) = (LI+U IMAG)*TMESH
423      IF(IMPRINT.NE.0) WRITE(11,965) LR,LI,THETA(1),THETA(2)
424      965 FORMAT (' ',2I4,3X,'THETA =',2F9.4)
425      NRZ = NRZ+1
426      ZEROS(1,NRZ) = THETA(1)
427      ZEROS(2,NRZ) = THETA(2)
428      NR ZL = NR ZL+1
429      66 CONTINUE
430      67 CONTINUE
431 C
432      70 CONTINUE
433 C TEST FOR EXIT FROM LEFT EDGE OF MESH SQUARE.
434      IF (LEDGE .EQ. 1) GO TO 72
435      IF ((AIMAG(F00) .GT. 0.0 .AND. AIMAG(F01) .GT. 0.0)
436      S           .OR. (AIMAG(F00) .LT. 0.0 .AND. AIMAG(F01) .LT. 0.0))
437      S           GO TO 72
438      IF (LTWO .EQ. 0) GO TO 51
439      EXIT R = 0.0
440      EXIT I = -AIMAG(F00)/AIMAG(F01-F00)

```

```

441      IF ((ENTER R-CENTR R)*(EXIT R-CENTR R) .LT. 0.0
442      &           .OR. (ENTER I-CENTR I)*(EXIT I-CENTR I) .LT. 0.0)
443      &           GO TO 72
444      GO TO 51
445 C
446 C TEST FOR EXIT FROM BOTTOM EDGE OF MESH SQUARE.
447 72 IF (LEDGE .EQ. 2) GO TO 73
448      IF ((AIMAG(F00) .GT. 0.0 .AND. AIMAG(F10) .GT. 0.0)
449      &           .OR. (AIMAG(F00) .LT. 0.0 .AND. AIMAG(F10) .LT. 0.0))
450      &           GO TO 73
451      IF (LTWO .EQ. 0) GO TO 56
452      EXIT R = -AIMAG(F00)/AIMAG(F10-F00)
453      EXIT I = 0.0
454      IF ((ENTER R-CENTR R)*(EXIT R-CENTR R) .LT. 0.0
455      &           .OR. (ENTER I-CENTR I)*(EXIT I-CENTR I) .LT. 0.0)
456      &           GO TO 73
457      GO TO 56
458 C
459 C TEST FOR EXIT FROM RIGHT EDGE OF MESH SQUARE.
460 73 IF (LEDGE .EQ. 3) GO TO 74
461      IF ((AIMAG(F10) .GT. 0.0 .AND. AIMAG(F11) .GT. 0.0)
462      &           .OR. (AIMAG(F10) .LT. 0.0 .AND. AIMAG(F11) .LT. 0.0))
463      &           GO TO 74
464      IF (LTWO .EQ. 0) GO TO 41
465      EXIT R = 1.0
466      EXIT I = -AIMAG(F10)/AIMAG(F11-F10)
467      IF ((ENTER R-CENTR R)*(EXIT R-CENTR R) .LT. 0.0
468      &           .OR. (ENTER I-CENTR I)*(EXIT I-CENTR I) .LT. 0.0)
469      &           GO TO 74
470      GO TO 41
471 C
472 C TEST FOR EXIT FROM TOP EDGE OF MESH SQUARE.
473 74 IF (LEDGE .EQ. 4) GO TO 90
474      IF ((AIMAG(F01) .GT. 0.0 .AND. AIMAG(F11) .GT. 0.0)
475      &           .OR. (AIMAG(F01) .LT. 0.0 .AND. AIMAG(F11) .LT. 0.0))
476      &           GO TO 90
477      IF (LTWO .EQ. 0) GO TO 46
478      EXIT R = -AIMAG(F01)/AIMAG(F11-F01)
479      EXIT I = 1.0
480      IF ((ENTER R-CENTR R)*(EXIT R-CENTR R) .LT. 0.0
481      &           .OR. (ENTER I-CENTR I)*(EXIT I-CENTR I) .LT. 0.0)
482      &           GO TO 90
483      GO TO 46
484 C
485 80 IF (NR7.NE.0) CALL NOMSHY(TMESH,TOL,MPRINT,ZEROS,NRZ)
486      IF (NEWMSH .NE. 0) GO TO 5
487      RETURN
488 C
489 90 WRITE(11,909) LR,LI
490 909 FORMAT ('0', 'NO EXIT FROM MESH SQUARE', 216)
491      GO TO 5
492 C
493 95 WRITE(11,9500)
494 9500 FORMAT ('0', 'TOO MANY SQUARES ON SAME PHASE LINE--MAKE', 216)
495      & ' TMESH SMALLER.')

```

```
496      GO TO 5
497  C
498  990 FORMAT('0')
499  C
500  97  WRITE(11,9700)
501  9700 FORMAT('0','TMESH HAS BEEN REDUCED BUT PROBLEMS REMAIN IN'
502  'S, EXECUTING FZEROS')
503  NEWMSH = 1
504  NR Z=0
505  RETURN
506  C
507  END
```

```

1      SUBROUTINE QUAD (A,B,C,SOL,NR SOL)
2 C  FOR ROOT-FINDER
3 C
4 C  SOLUTION FOR THE REAL ROOTS OF A QUADRATIC EQUATION OF THE
5 C  FORM A*X**2+2.0*B*X+C=0.0, WHERE X IS CALLED 'SOL'.
6 C  IN THIS ROUTINE, THE NUMBER OF REAL ROOTS FOUND IS
7 C  GIVEN BY 'NR SOL'. A VALUE OF 1 FOR 'NR SOL' RESULTS
8 C  FROM THE QUADRATIC EQUATION APPROACHING LINEARITY.
9 C  USED BY SUBROUTINES FZEROS AND NO MESH.
10 C
11      IMPLICIT DOUBLE PRECISION*6 (A-H,O-Z)
12      DIMENSION SOL(2)
13 C
14 C
15      ACORSG=(A/B)*(C/B)
16      IF(ABS(ACORSG).LT.(0.3)) GO TO 20
17      ARG=1.0-ACORSG
18      NRSOL=0
19      IF(ARG.LT.(0.0)) RETURN
20      NRSOL=2
21      ROOT=ABS(B)*SQRT(ARG)
22 C
23 C****
24 C
25      SOL(1) = (-B+ROOT)/A
26      SOL(2) = (-B-ROOT)/A
27      RETURN
28 C
29      20 TERM = 1.0
30      SUM = 1.0
31      DO 21 K=1,50
32      TERM = TERM*((K-0.5)/(K+1.0))*ACORSG
33      SUM = SUM+TERM
34      IF (ABS(TERM) .LT. 1.0E-10) GO TO 22
35      21 CONTINUE
36      22 SOL(1) = -C/(2.0*B)*SUM
37      NR SOL = 1
38      IF (ABS(A/(2.0*R)) .LT. 1.0E-30) RETURN
39      NR SOL = 2
40      SOL(2) = -2.0*B/A-SOL(1)
41      RETURN
42 C
43      END

```

```

1      SUBROUTINE NOMSHX(TMESH,TOL,MPRINT,ZEROS,NRZ)
2 C  FOR ROOT-FINDER
3 C  THIS VERSION UPDATED TO MODIFY GMAX AND TMESH. JAN 6 1982.
4 C  ROUTINE FOR FINDING EXACT (IN THE SENSE OF NO MESH APPROXIMATION)
5 C  LOCATIONS OF ZEROS OF THE FUNCTION, F, FOR WHICH
6 C  A COMPLETE, BUT APPROXIMATE, SET WAS FCLND IN
7 C  SUBROUTINE FZEROS.
8 C  TWO DEFICIENCIES REMAIN IN THIS ROUTINE. ONE IS
9 C  THAT ZEROS CLOSER THAN THE FINITE VALUE 'TOL' CANNOT
10 C  BE RESOLVED. THIS HAS CAUSED A PROBLEM A FEW TIMES
11 C  IN USAGE TO DATE, BUT HAS ALWAYS BEEN RESOLVED BY
12 C  USING A SMALLER VALUE OF 'TOL'. THE SECOND PROBLEM
13 C  IS THAT THE RESOLUTION OF 'MULTIPLE CROSSINGS',
14 C  WHICH OCCUR BECAUSE OF THE NON-ANALITICITY OF THE
15 C  MESH APPROXIMATION, IS SUCH THAT IN PRINCIPLE A
16 C  ZERO CAN BE MISSED. THERE IS NO EVIDENCE THIS HAS
17 C  EVER OCCURRED IN PRACTICE. IT MAY OR MAY NOT BE
18 C  COST EFFECTIVE TO DEVELOP THE PROGRAM FURTHER TO
19 C  CORRECT THESE TWO PROBLEMS.
20 C
21      IMPLICIT DOUBLE PRECISION*6 (A-H,O-Z)
22      COMMON/NEWMESH/NEWMESH
23      DIMENSION PART(2)
24      COMPLEX ZEROS(1),
25      *      THETA,
26      *      F,DFDT,DELT,
27      *      PARTS,
28      *      ZEROS0(100)
29      EQUIVALENCE (PART(1),PARTS)
30 C
31 C
32      IF (MPRINT.NE.0) WRITE(11,900)
33      900 FORMAT ('1','ITERATIONS TO REMOVE MESH')
34 C
35 C  NEWTON-RAPSON (FIRST-ORDER) ITERATION TO FIND EXACT LOCATIONS
36 C  OF THE ZEROS OF F.
37 C
38      DO 29 JZ=1,NRZ
39      ZEROS0(JZ) = ZEROS(JZ)
40      IF (MPRINT.NE.0) WRITE(11,901) JZ
41      901 FORMAT (' ',I8)
42      21 IF (MPRINT.NE.0) WRITE(11,902) ZEROS(JZ)
43      902 FORMAT (' ',10X,2(F9.4))
44      THETA = ZEROS(JZ)
45      CALL FDFDTX(THETA,F,FE,DFDT,DFDTE)
46      DELT=-(F/DFDT)*EXP(IFE-DFDTE)
47      ZEROS(JZ) = ZEROS(JZ)+DELT
48      IF (CABS(DELT) .GT. 0.3*TOL) GO TO 21
49      29 CONTINUE
50 C
51 C  NUMBER OF UNIQUE ZEROS COMPARED TO TOTAL NUMBER
52      30 IF(NRZ .LE. 1) RETURN
53      MATCH = 0
54      DO 33 J=2,NRZ
55      JM1 = J-1

```

```
56      DO 32 JJ=1,JM1
57      IF (CAES(ZEROS(J))-ZEROS(JJ)) .GT. TOL GO TO 32
58      IF (MPRINT.NE.0) WRITE(11,905) J,JJ
59 905 FORMAT ('0','ZEROS NR',I3,1X,'AND',I3,1X,
60      *          'ARE THE SAME')
61      MATCH = 1
62      32 CONTINUE
63      33 CONTINUE
64 C
65      IF (MATCH .EQ. 0) RETURN
66 40      NEWMESH = NEWMESH+1
67      IF (NEWMESH.LE.2) WRITE(11,400)
68 400  FORMAT ('0',' PROBLEMS IN THIS RANGER-RANGE1 BOX.  PROGRAM WILL US
69      RE TMESH/2 AND RE-EXECUTE THE PROGRAM')
70      IF (NEWMESH.GE.3) WRITE(11,405)
71 405  FORMAT ('0',' PROBLEMS IN THIS RANGER-RANGE1 BOX.  USER MUST DECRE
72      SASE GMAX AND RE-EXECUTE THE PROGRAM')
73      NR 7 = 0
74 C
75      RETURN
76      END
```

```

1      SUBROUTINE FINDFX(JR, JT, F, FE, TLEFT, TRIGHT)
2 C*****+
3 C      THIS SUBROUTINE INCORPORATES CHANGES NEEDED IN EVALUATING
4 C      THE MODAL FUNCTION ALONG THE IMAGINARY AXIS WHEN SURFACE
5 C      ROUGHNESS IS INCORPORATED INTO THE MODEL
6 C*****+
7      IMPLICIT DOUBLE PRECISION*6 (A-F,0-7)
8      COMPLEX F,7,PARTS
9      DIMENSION PART(2)
10     COMMON/TMCCOM/TMESH
11     EQUIVALENCE (PART,PARTS)
12 C
13 C      DEFINE SMALL OFFSET VALUE
14 C
15     DATA  OFFSET/1.0E-9/
16 C*****
17 C
18     PART(1)=DFLOAT(JR)*TMESH
19     PART(2)=DFLOAT(JI)*TMESH
20 C*****
21 C      IF EVALUATING MODAL FUNCTION ALONG IMAGINARY AXIS,
22 C      SHIFT ARGUMENT OF FUNCTION OFF OF AND SLIGHTLY TO THE
23 C      RIGHT OF THE IMAGINARY AXIS IF THE SEARCH RECTANGLE
24 C      LIES TO THE RIGHT OF THE IMAGINARY AXIS.
25 C      IF EVALUATING MODAL FUNCTION ALONG IMAGINARY AXIS,
26 C      SHIFT ARGUMENT OF FUNCTION OFF OF AND SLIGHTLY TO THE
27 C      LEFT OF THE IMAGINARY AXIS IF THE SEARCH RECTANGLE
28 C      LIES TO THE LEFT OF THE IMAGINARY AXIS.
29 C
30     IF(JR.EQ.0) THEN
31     IF(TLEFT.EQ.0.0) SHIFT=OFFSET
32     IF(TRIGHT.EQ.0.0) SHIFT=-OFFSET
33     PART(1)=SHIFT
34     END IF
35     Z=PARTS
36     CALL FCTVLX(Z,F,FE)
37     RETURN
38     END

```

```

1      SUBROUTINE EXCFAC(XFAC,XFACE,Q11)
2 C*****+
3 C      THIS SUBROUTINE EVALUATES THE EXCITATION FACTOR, XFAC*EXP(XFACE),
4 C      FOR THE MODE ASSOCIATED WITH THE EIGENVALUE Q11
5 C
6 C      INPUTS VIA COMMON BLOCK...
7 C          A1H - ALPHAH*H
8 C          WAVENO - WAVE NUMBER
9 C          C11 - CBRT(ALPHAH/WAVENO)
10 C
11 C      SUBROUTINES USED...
12 C          FDFDTX
13 C*****+
14 C      IMPLICIT DOUBLE PRECISION*6 (A-H,O-Z)
15 C      COMPLEX XFAC,Q11,RHO,F,DFDT,CSQRT,I,Q11T
16 C      COMPLEX SQNG
17 C      COMMON/COMTWO/ETAARS,ALPHAH,H,C11,SQNG
18 C      COMMON/COMTHR/Z2,Z3,A2MAG,ALPHA3,WAVENO,ALPHA2
19 C      DATA I/(0.0,1.0)/
20 C*****+
21 C      EVALUATE RHO
22 C
23 C      RHO=WAVENO*CSQRT(1.0+I*ETAARS-ALPHAH*C11*C11*G11)
24 C
25 C      THE NEXT STATEMENT COMPENSATES FOR THE SHIFT IN C11 INTRODUCED
26 C      IN SUBROUTINE 'FDFDTX'
27 C
28 C      Q11T=Q11+I*0.003
29 C
30 C      EVALUATE THE DERIVATIVE OF THE MODAL FUNCTION
31 C
32 C      CALL FDFDTX(Q11T,F,FE,DFDT,DFDTE)
33 C
34 C      EVALUATE THE EXCITATION FACTOR
35 C
36 C      XFAC=-WAVENO*WAVENO*C11*C11/(2.0*CSQRT(RHO)*DFDT)
37 C      XFACE=-DFDTE
38 C
39 C      NORMALIZE XFAC
40 C
41 C      XNORM=CARS(XFAC)
42 C      XFAC=XFAC/XNORM
43 C      XFACE=XFACE+DLOG(XNORM)
44 C      RETURN
45 C*****+
46 C      END

```

```

1      SUBROUTINE HTGAIN(ENZA,ENZE,Q11,ZRCVR,ZXMTR)
2 C*****C
3 C      THIS PROGRAM EVALUATES THE HEIGHT-GAIN FUNCTIONS FOR A
4 C      TRILINEAR MODEL OF THE MODIFIED REFRACTIVITY OF THE TROPOSPHERE.
5 C
6 C      INPUTS...
7 C          Q11 - MODAL EIGENVALUE
8 C          ZRCVR - HEIGHT (IN METERS) OF THE RECEIVER ABOVE GROUND
9 C          LEVEL
10 C         ZXMTR - HEIGHT (IN METERS) OF THE TRANSMITTER ABOVE GROUND
11 C          LEVEL
12 C
13 C      OUTPUTS...
14 C          EN7 - HEIGHT-GAIN FUNCTION FOR THE MODAL EIGENVALUE
15 C          Q11 EVALUATED FOR THE TRANSMITTER LOCATED AT ZXMTR
16 C          AND THE RECEIVER LOCATED AT ZRCVR
17 C          FN2=ENZA*EXP(ENZE)
18 C
19 C      SUBROUTINES USED...
20 C          HNKXLX,KHNKLX,CADE,KHATX
21 C*****C
22      IMPLICIT DOUBLE PRECISION*6 (A-H,O-Z)
23      COMPLEX Q11,Q12,Q22,Q23,Q33,
24      $ Q12A1,Q12A2,DQ12A1,DQ22A1,C22A2,DQ22A1,DQ22A2,
25      $ Q23A1,Q23A2,DQ23A1,DQ23A2,Q33A1,C33A2,DQ33A1,DQ33A2,
26      $ SONG,I,W,KHATA1,KHATA2,QR,CT,
27      $ QRA1,QRA2,DQRA1,DQRA2,QTA1,QTA2,DQTA1,DQTA2,
28      $ R1,R2,R3,XAA,XBA,YAA,YBA,7AA,YCA,YBA,7PA,FK11A,
29      $ YEA,FK12A,YFA,FK22A,ENZA,T33A1,T33A2,DT33A1,DT33A2,EPI,
30      $ TRA1,TRA2,DTRA1,DTRA2,TTA1,TTA2,DTTA1,DTTA2,DKHTA1,
31      $ DKHTA2
32      DOUBLE PRECISION*6 KHATE1,KHATE2
33      COMMON/ COMONE /C1,C3,C4,C5,C6,C7,C8,C9,SGNA2
34      COMMON/ COMTWO / ETAAPS,ALPHA1,H,C11,SONG
35      COMMON/ COMTHR / Z2,Z3,A2MAG,ALPHA3,AVENNO,ALPHA2
36      DATA I/(0.0,1.0)/
37      DATA W/(0.0,-1.45749544)/
38      DATA EPI/(-0.5,0.866025404)/
39 C*****
40 C      FUNCTION DEFINITION
41 C
42      CBRT(X)=X**(1.0/3.0)
43 C*****
44 C      EVALUATE Q12,Q22,Q23,Q33
45 C
46      Q12 = Q11+C4
47      Q22 = C5*Q11+C6
48      Q23 = C5*Q11+C7
49      Q33 = C8*Q11+C9
50 C*****
51 C      EVALUATE MODIFIED HANKEL FUNCTIONS NEEDED
52 C
53      CALL KHNKLX(Q12,Q12A1,Q12E1,Q12A2,Q12E2,DQ12A1,DQ12E1,
54      $ DQ12A2,DQ12E2)
55      CALL KHNKLX(Q22,Q22A1,Q22E1,Q22A2,Q22E2,DQ22A1,DQ22E1,

```

```

56      * DQ22A2,DQ22E2)
57      CALL KHNLX(Q23,Q23A1,Q23E1,Q23A2,Q23E2,DQ23A1,DQ23E1,
58      * DG23A2,DG23E2)
59      CALL HNLX(Q33,T33A1,T33E1,T33A2,T33E2,DT33A1,DT33E1,
60      * DT33A2,DT33E2)
61      CALL CADD(Q33A1,Q33E1,T33A1,T33E1,-EPI*T33A2,T33E2)
62      CALL CADD(DQ33A1,DQ33E1,DT33A1,DT33E1,-EPI*DT33A2,DT33E2)
63      Q33A2=T33A2
64      Q33E2=T33E2
65      DQ33A2=DT33A2
66      DQ33E2=DT33E2
67      CALL KHATX(Q11,KHATA1,KHATE1,KHATA2,KHATE2,DKHTA1,DKHTE1,
68      * DKHTA2,DKHTE2)
69 C*****
70 C      DETERMINE WHICH LAYERS TRANSMITTER AND RECEIVER ARE IN
71 C      AND EVALUATE QR AND QT AND MODIFIED HANKEL FUNCTIONS
72 C
73      IF(ZRCVR.LE.72)THEN
74 C
75 C      RECEIVER IN FIRST LAYER
76 C
77      LRCVR=1
78      QR=Q11+ALPHA1*ZRCVR/(C11*C11)
79      CALL KHNLX(QR,QRA1,QRE1,QRA2,CRE2,DGRA1,DGRE1,
80      * DQRA2,DQRE2)
81      ELSE IF((ZRCVR.LE.23).AND.(ZRCVR.GT.22)) THEN
82 C
83 C      RECEIVER IN SECOND LAYER
84 C
85      LRCVR=2
86      QR=C5*Q11+C6+CRRT(WAVENO*WAVENO/(A2MAG*A2MAG))+*
87      * ALPHA2*(ZRCVR-22)
88      CALL HNLX(QR,QRA1,QRE1,QRA2,CRE2,DGRA1,DGRE1,
89      * DQRA2,DQRE2)
90      ELSE
91 C
92 C      RECEIVER IN THIRD LAYER
93 C
94      LRCVR=3
95      QR=C8*Q11+C9+CRRT(WAVENO*WAVENO/(ALPHA3*ALPHA3))+*
96      * ALPHA3*(ZRCVR-23)
97      CALL HNLX(QR,TRA1,TRE1,TRA2,TRE2,DTRA1,DTRE1,
98      * DTRA2,DTRE2)
99      CALL CADD(QRA1,QRE1,TRA1,TRE1,-EPI*TRA2,TRE2)
100     CALL CADD(DQRA1,DQRE1,DTRA1,DTRE1,-EPI*DTRA2,DTRE2)
101     QRA2=TRA2
102     QRE2=TRE2
103     DQRA2=CTRA2
104     DQRE2=CTRE2
105     FND IF
106     IF(ZXMTR.LE.22) THEN
107 C
108 C      TRANSMITTER IN THE FIRST LAYER
109 C
110      LXMTR=1

```

```

111      QT=C11+ALPHA1*ZXMT/((C11+C11)
112      CALL KHNKLX(QT,OTA1,QTE1,QTA2,QTE2,DTA1,DTE1,
113      * DOTA2,DCTE2)
114      ELSE IF((ZXMT.LE.Z3).AND.(ZXMT.GT.Z2)) THEN
115 C
116 C      TRANSMITTER IN SECOND LAYER
117 C
118      LXMT=2
119      QT=C5+C6+CBRT(WAVENO*WAVENO/(A2MAG*A2MAG))*_
120      * ALPHA2*(ZXMT-Z2)
121      CALL KHNKLX(QT,OTA1,QTE1,QTA2,QTE2,DTA1,DTE1,
122      * DOTA2,DCTE2)
123      ELSE
124 C
125 C      TRANSMITTER IN THIRD LAYER
126 C
127      LXMT=3
128      QT=C8+C9+CBRT(WAVENO*WAVENO/(ALPHA3*ALPHA3))*_
129      * ALPHA3*(ZXMT-Z3)
130      CALL HNKLX(QT,TTA1,TTE1,TTA2,TTE2,DTA1,DTTE1,
131      * DTTA2,DTTE2)
132      CALL CADD(OTA1,OTE1,TTA1,TTE1,-EPI+TTA2,TTE2)
133      CALL CADD(DOTA1,DOTE1,TTA1,DTTE1,-EPI+DTTA2,DTTE2)
134      OTA2=TTA2
135      OTE2=TTE2
136      DOTA2=DTTA2
137      DOTE2=DTTE2
138      END IF
139 C*****
140 C      EVALUATE HEIGHT-GAIN FUNCTIONS
141 C**
142      IF((LRCVR.EQ.1).AND.(LXMT.EQ.1)) THEN
143 C
144 C      RECEIVER IN FIRST LAYER --- TRANSMITTER IN FIRST LAYER
145 C
146      R1=C11*C11/(W*ALPHA1)
147      XAA=SGNA2*DQ33A2*Q23A2/C3
148      XAE=DQ33E2*Q23E2
149      XBA=Q33A2*DQ23A2
150      XBE=Q33E2*DQ23E2
151      CALL CADD(YAA,YAE,XAA,XAE,XBA,XBE)
152      XAA=SGNA2*DQ22A1*Q12A2*C1
153      XAE=DQ22E1*Q12E2
154      XBA=Q22A1*DQ12A2
155      XBE=Q22E1*DQ12E2
156      CALL CADD(YBA,YRE,XAA,XAE,XBA,XBE)
157      ZAA=YAA*YBA*KHATA2
158      ZAE=YAE*YBE*KHATE2
159      XAA=SGNA2*DQ33A2*Q23A1/C3
160      XAE=DQ33E2*Q23E1
161      XBA=Q33A2*DQ23A1
162      XBE=Q33E2*DQ23E1
163      CALL CADD(YCA,YCE,XAA,XAE,XBA,XBE)
164      XAA=-SGNA2*DQ22A2*Q12A2*C1
165      XAE= DQ22E2*Q12E2

```

```

166      XBA=-C22A2*DQ12A2
167      XBE=D22E2+DQ12E2
168      CALL CADD(YDA,YDE,XAA,XAE,XRA,XRE)
169      ZBA=YCA*YDA*KHATA2
170      ZBE=YCE+YDE+KHATE2
171      CALL CADD(FK11A,FK11E,ZAA,ZAE,ZRA,ZBE)
172 C    ZAA=-YAA*YRA*KHATA1
173 C    ZAE=YAF+YBE+KHATE1
174 C    ZBA=-YCA*YDA*KHATA1
175 C    ZBE=YCE+YDE+KHATE1
176 C    CALL CADD(FK12A,FK12E,ZAA,ZAE,ZRA,ZBE)
177      XAA=SGNA2*DQ22A1*DQ12A1*C1
178      XAE=D22E1+DQ12E1
179      XBA=C22A1*DQ12A1
180      XBE=D22E1+DQ12E1
181      CALL CADD(YEA,YEE,XAA,XAE,XRA,XRE)
182      ZAA=YAA*YEA*KHATA1
183      ZAE=YAE+YEF+KHATE1
184      XAA=-SGNA2*DQ22A2*DQ12A1*C1
185      XAE=D22E2+DQ12E1
186      XBA=-C22A2*DQ12A1
187      XBE=D22E2+DQ12E1
188      CALL CADD(YFA,YFE,XAA,XAE,XRA,XRE)
189      ZBA=YCA*YFA*KHATA1
190      ZBE=YCE+YFE+KHATE1
191      CALL CADD(FK22A,FK22E,ZAA,ZAE,ZRA,ZBE)
192 C    ZAA=-YAA*YEA*KHATA2
193      ZAE=YAE+YEE+KHATE2
194      ZBA=-YCA*YFA*KHATA2
195      ZBE=YCE+YFE+KHATE2
196      CALL CADD(FK12A,FK12E,ZAA,ZAE,ZRA,ZBE)
197
198 C    XAA=FK11A*GTA1*DRA1
199      XAE=FK11E+GTE1+GRE1
200      XBA=FK22A*GTA2*DRA2
201      XBE=FK22E+GTE2+GRE2
202      CALL CADD(ZAA,ZAE,XAA,XAE,XRA,XBE)
203      XAA=FK12A*GTA2*DRA1
204      XAE=FK12E+GTE2+GRE1
205      XBA=FK12A*GTA1*DRA2
206      XBE=FK12E+GTE1+GRE2
207      CALL CADD(ZBA,ZRE,XAA,XAE,XRA,XRE)
208      CALL CADD(ENZA,ENZE,ZAA,ZAE,ZRA,ZRE)
209      ENZA=R1*EN7A
210      RETURN
211      END IF
212
213 C**
214      IF(((LRCVR.EQ.1).AND.(LXMTR.EQ.2)).OR.((LRCVP.EQ.2).
215      &     .AND.(LXMTR.EQ.1))) THEN
216 C
217 C    RECEIVER IN FIRST LAYER --- TRANSMITTER IN SECOND LAYER
218 C
219 C    OR
220 C    RECEIVER IN SECOND LAYER --- TRANSMITTER IN FIRST LAYER

```

```

221      RIW=C11*C11/ALPHA1
222      XAA=SGNA2*DQ33A2*Q23A2/C3
223      XAF=DQ33E2*Q23E2
224      XBA=Q33A2*DQ23A2
225      XBE=Q33E2*DQ23E2
226      CALL CADD(YAA,YAE,XAA,XAE,XRA,XRE)
227      XAA=SGNA2*DQ33A2*Q23A1/C3
228      XAE=DQ33E2*Q23E1
229      XBA=Q33A2*DQ23A1
230      XBE=Q33E2*DQ23E1
231      CALL CADD(YBA,YRE,XAA,XAE,XRA,XRE)
232      XAA=YAA*KHATA2*QTA1*QRA1
233      XAE=YAE*KHATE2*QTE1*QRE1
234      XBA=YBA*KHATA1*QTA2*QRA2
235      XBE=YBE*KHATE1*QTE2*QRE2
236      CALL CADD(ZAA,ZAE,XAA,XAE,XBA,XRE)
237      IF(LRCVR.EQ.1) THEN
238          XAA=-YBA*KHATA2*QTA2*QRA1
239          XAE=YBE*KHATE2*QTE2*QRE1
240          XBA=-YAA*KHATA1*QTA1*QRA2
241          XBE=YAE*KHATE1*QTE1*QRE2
242      ELSE
243          XAA=-YBA*KHATA2*QTA1*QRA2
244          XAE=YBE*KHATE2*QTE1*QRE2
245          XBA=-YAA*KHATA1*QTA2*QRA1
246          XBE=YAE*KHATE1*QTE2*QRE1
247      END IF
248      CALL CADD(ZBA,ZPE,XAA,XAE,XBA,XRE)
249      CALL CADD(ENZA,ENZE,ZAA,ZAE,ZBA,ZPE)
250      ENZA=RIW*ENZA
251      RETURN
252  END IF
253 C**
254  IF(((LRCVR.EQ.1).AND.(LXMTR.EQ.3)).OR.((LRCVR.EQ.3).
255 * AND.(LXMTR.EQ.1))) THEN
256 C
257 C      RECEIVER IN FIRST LAYER --- TRANSMITTER IN THIRD LAYER
258 C          OR
259 C      RECEIVER IN THIRD LAYER---TRANSMITTER IN FIRST LAYER
260 C
261      RIW=C11*C11/ALPHA1
262      XAA=KHATA1*QRA2*QTA2
263      XAE=KHATE1*QRF2*QTE2
264      IF(LRCVR.EQ.1) THEN
265          XBA=-KHATA2*QRA1*QTA2
266          XBE=KHATE2*QRE1*QTE2
267      ELSE
268          XBA=-KHATA2*QTA1*QRA2
269          XBE=KHATE2*QTE1*QRE2
270      END IF
271      CALL CADD(ENZA,ENZE,XAA,XAE,YAA,XRE)
272      FNZA=-RIW*W*ENZA
273      RETURN
274  END IF
275 C**

```

```

276      IF((LRCVR.EQ.2).AND.(LXMTR.EQ.2)) THEN
277 C
278 C      RECEIVFR IN SECOND LAYER --- TRANSMITTER IN SECND LAYER
279 C
280      R2=CBRT(ALPHA2*ALPHA2/(WAVENC*WAVENC))/(ALPHA2*k)
281      IF(ALPHA2.LT.0.0)THEN
282      XAA=DG33A2*Q23A2/C3
283      XAE=DG33E2*Q23E2
284      XBA=Q33A2*DQ23A2
285      XBE=Q33E2*DQ23E2
286      CALL CADD(YAA,YAE,XAA,XAE,XBA,XRE)
287      XAA=C1*DQ22A2*Q12A2
288      XAF=DQ22E2*Q12E2
289      XBA=Q22A2*DQ12A2
290      XBE=Q22E2*DQ12E2
291      CALL CADD(YBA,YRE,XAA,XAE,XBA,XRE)
292      XAA=C1*DQ22A2*Q12A1
293      XAF=DQ22E2*Q12E1
294      XBA=Q22A2*DQ12A1
295      XBE=Q22E2*DQ12E1
296      CALL CADD(YCA,YCE,XAA,XAE,XBA,XRE)
297      XAA=DG33A2*Q23A1/C3
298      XAE=DG33E2*Q23E1
299      XBA=Q33A2*DQ23A1
300      XBE=Q33E2*DQ23E1
301      CALL CADD(YDA,YDE,XAA,XAE,XBA,XRE)
302      XAA=C1*DQ22A1*Q12A2
303      XAF=DQ22E1*Q12E2
304      XBA=Q22A1*DQ12A2
305      XBE=Q22E1*DQ12E2
306      CALL CADD(YEA,YEE,XAA,XAE,XBA,XRE)
307      XAA=C1*DQ22A1*Q12A1
308      XAE=DQ22E1*Q12E1
309      XBA=Q22A1*DQ12A1
310      XBE=Q22E1*DQ12E1
311      CALL CADD(YFA,YFE,XAA,XAE,XBA,XRE)
312      XAA=YBA*KHATA1
313      XAF=YBF*KHATE1
314      XBA=-YCA*KHATA2
315      XBF=YCF*KHATE2
316      CALL CADD(ZAA,ZAE,XAA,XAE,XBA,XRE)
317      FK11A=ZAA*YAA
318      FK11E=ZAE*YAE
319      FK12A=-ZAA*YDA
320      FK12E=ZAE*YDE
321      YAA=YFA*KHATA1
322      XAF=YFE*KHATE1
323      XBA=-YFA*KHATA2
324      XBF=YFF*KHATE2
325      CALL CADD(ZAA,ZAE,XAA,XAE,XBA,XRE)
326      FK22A=YDA*ZAA
327      FK22E=YDE*ZAE
328      YAA=FK11A*GTA1*QRA1
329      XAF=FK11F*GTE1*QRE1
330      XBA=FK22A*GTA2*QRA2

```

```

331      YBF=FK22E+GTE2+QRE2
332      CALL CADD(ZAA,ZAE,XAA,XAE,XBA,YRE)
333      XAA=FK12A*QTA2*QRA1
334      XAE=FK12E+GTE2+QRE1
335      XBA=FK12A*QTA1*QRA2
336      XBE=FK12E+GTE1+QRE2
337      CALL CADD(ZBA,ZPE,XAA,XAE,XRA,XRE)
338      CALL CADD(ENZA,ENZE,ZAA,ZAE,ZBA,ZPE)
339      ENZA=R2*ENZA
340      RETURN
341      FLSF
342      XAA=-DG33A2*Q23A2/C3
343      XAE=DG33E2*Q23E2
344      XBA=Q33A2*D023A2
345      XBE=Q33E2*DQ23E2
346      CALL CADD(YAA,YAE,XAA,XAE,XBA,YRE)
347      XAA=-C1*DQ22A2*Q12A2
348      XAE=DG22E2*Q12E2
349      XBA=Q22A2*DQ12A2
350      XBE=Q22E2*DQ12E2
351      CALL CADD(YBA,YBE,XAA,XAE,XBA,XRE)
352      XAA=C1*DQ22A2*Q12A1
353      XAE=DG22E2*Q12E1
354      XBA=-Q22A2*DQ12A1
355      XBE=Q22E2*DQ12E1
356      CALL CADD(YCA,YCE,XAA,XAE,XBA,XRE)
357      XAA=C1*DQ22A1*Q12A2
358      XAE=DG22E1*Q12E2
359      XBA=-Q22A1*DQ12A2
360      XBE=Q22E1*DQ12E2
361      CALL CADD(YDA,YDE,XAA,XAE,XBA,XRE)
362      XAA=-C1*DQ22A1*Q12A1
363      XAE=DG22E1*Q12E1
364      XBA=Q22A1*DQ12A1
365      XBE=Q22E1*DQ12E1
366      CALL CADD(YEA,YEE,XAA,XAE,XBA,XRE)
367      XAA=-DG33A2*Q23A1/C3
368      XAE=DG33E2*Q23E1
369      XBA=Q33A2*DQ23A1
370      XBE=Q33E2*DQ23E1
371      CALL CADD(YFA,YFE,XAA,XAE,XBA,XRE)
372      YAA=YPA*KHATA1
373      XAE=YRE*KHATE1
374      XBA=YCA*KHATA2
375      XBE=YCE*KHATE2
376      CALL CADD(ZAA,ZAE,XAA,XAE,XBA,XRE)
377      FK11A=YAA*ZAA
378      FK11E=YAE*ZAE
379      XAA=YCA*KHATA1
380      XAE=YDE*KHATE1
381      YBA=YFA*KHATA2
382      XBE=YFE*KHATE2
383      CALL CADD(ZAA,ZAE,XAA,XAE,YPA,XRE)
384      FK12A=YAA*ZAA
385      FK12E=YAE*ZAE

```

```

386      FK22A=-YFA+ZAA
387      FK22E=YFE+ZAE
388      XAA=FK11A+GTA1+GRA1
389      XAE=FK11E+GTE1+GRE1
390      XBA=FK22A+GTA2+GRA2
391      XBE=FK22E+GTE2+GRE2
392      CALL CADD(7AA,ZAE,XAA,XAE,XBA,XRE)
393      XAA=FK12A+GTA2+GRA1
394      XAE=FK12E+GTE2+GRE1
395      XBA=FK12A+GTA1+GRA2
396      XBF=FK12E+GTE1+GRE2
397      CALL CADD(7BA,7PE,XAA,XAE,XBA,XRE)
398      CALL CADD(FN7A,ENZE,ZAA,ZAE,ZBA,7PE)
399      FN7A=R2*EN7A
400      RETURN
401      FND IF
402      END IF
403  C**
404  IF(((LRCVR.EQ.2).AND.(LXMTR.EQ.3)).OR.((LRCVR.EQ.3).
405  *      AND.(LXMTR.EQ.2))) THEN
406  C
407  C      RECEIVER IN SECOND LAYER---TRANSMITTER IN THIRD LAYER
408  C          OR
409  C      RECEIVER IN THIRD LAYER---TRANSMITTER IN SECOND LAYER
410  C
411      R2W=CBRT(A2MAG*A2MAG/(WAVENO*WAVENO1)/ALPHA2
412      XAA=SGNA2*C1*DQ22A2*Q12A2
413      XAE=DQ22E2+Q12E2
414      XBA=Q22A2*DQ12A2
415      XBE=Q22E2*DQ12E2
416      CALL CADD(YAA,YAE,XAA,XAE,XBA,XRE)
417      XAA=SGNA2*DQ22A2*Q12A1*C1
418      XAE=DQ22E2+Q12E1
419      YBA=Q22A2*DQ12A1
420      XBE=Q22E2+DQ12E1
421      CALL CADD(YBA,YRE,XAA,XAE,XBA,XRE)
422      XAA=SGNA2*C1*DQ22A1*Q12A2
423      XAE=DQ22E1+Q12E2
424      XBA=Q22A1*DQ12A2
425      XBE=Q22E1+DQ12E2
426      CALL CADD(YCA,YCE,XAA,XAE,XBA,XRE)
427      XAA=SGNA2*C1*DQ22A1*Q12A1
428      XAF=DQ22E1+Q12E1
429      XBA=Q22A1*DQ12A1
430      XRE=Q22F1+DQ12E1
431      CALL CADD(YDA,YDE,XAA,XAE,XBA,XRE)
432      XAA=YAA*KHATA1
433      XAF=YAE*KHATE1
434      XBA=-YEA*KHATA2
435      XBF=YEF*KHATE2
436      CALL CADD(FK12A,FK12E,XAA,XAE,XBA,XRE)
437      XAA=-YCA*KHATA1
438      XAF=YCF*KHATE1
439      XBA=YEA*KHATA2
440      YBF=YDE*KHATE2

```

```

441      CALL CADD(FK22A,FK22E,XAA,XAE,XRA,XRE)
442      IF(LPCVR.EQ.2) THEN
443          ZAA=FK12A*QTA2*GRA1
444          ZAE=FK12E+QTE2+GRE1
445          ZRA=FK22A*QTA2*GRA2
446          ZRE=FK22E+QTE2+GRE2
447          CALL CADD(EN7A,EN7E,ZAA,ZAE,ZRA,ZRE)
448      ELSE
449          ZAA=FK12A*QTA1*GRA2
450          ZAE=FK12E+QTE1+GRE2
451          ZRA=FK22A*QTA2*GRA2
452          ZRE=FK22E+QTE2+GRE2
453          CALL CADD(EN7A,EN7E,ZAA,ZAE,ZRA,ZRE)
454      END IF
455      FN7A=R2W*FNZA
456      RETURN
457      END IF
458  C**
459  IF((LRCVR.EQ.3).AND.(LXMTR.EQ.3)) THEN
460  C
461  C      RECFIVER IN THIRD LAYER--- TRANSMITTER IN THIRE LAYER
462  C
463      R3=CRRT(ALPHA3*ALPHA3/(WAVENC*WAVENC))/(ALPHA3*W)
464      XAA=SGNA2*C1*DQ22A1*Q12A2
465      XAE=DG22E1+Q12E2
466      XBA=G22A1*DQ12A2
467      XBE=Q22E1+DQ12E2
468      CALL CADD(YAA,YAE,XAA,XAE,XBA,XRE)
469      XAA=SGNA2*Q23A2*DQ33A1/C3
470      XAE=Q23E2+DQ33E1
471      XBA=DG23A2*Q33A1
472      XBE=DG23E2+Q33E1
473      CALL CADD(YRA,YRE,XAA,XAE,XBA,XRE)
474      XAA=SGNA2*C1*DQ22A2*Q12A2
475      XAE=DG22E2+Q12E2
476      XBA=G22A2*DQ12A2
477      XBE=Q22E2+DQ12E2
478      CALL CADD(YCA,YCE,XAA,XAE,XBA,XRE)
479      XAA=SGNA2*DQ33A1*Q23A1/C3
480      XAE=DQ33E1+Q23E1
481      XBA=Q33A1*DQ23A1
482      XBE=Q33E1+DQ23E1
483      CALL CADD(YDA,YDE,XAA,XAE,XBA,XRE)
484      XAA=SGNA2*C1*DQ22A1*Q12A1
485      XAE=DG22E1+Q12E1
486      XBA=G22A1*DQ12A1
487      XBE=Q22E1+DQ12E1
488      CALL CADD(YEA,YEE,XAA,XAE,XBA,XRE)
489      XAA=SGNA2*C1*DQ22A2*Q12A1
490      XAE=DG22E2+Q12E1
491      XBA=G22A2*DQ12A1
492      XBE=Q22E2+DQ12E1
493      CALL CADD(YFA,YFE,XAA,XAE,XBA,XRE)
494      XAA=-YAA*YPA*KHATA1
495      XAE=YAF+YBE*KHATE1

```

496 XBA=YCA*YDA*KHATA1
497 XBE=YCE+YDE+KHATE1
498 CALL CADD(ZAA,ZAE,XAA,XAE,XBA,XRE)
499 XAA=YEA*YBA*KHATA2
500 XAF=YEF+YBE+KHATE2
501 XBA=-YFA*YDA*KHATA2
502 XBE=YFE+YDE+KHATE2
503 CALL CADD(7RA,ZRE,XAA,XAE,XBA,XRE)
504 CALL CADD(FK22A,FK22E,7AA,7AE,7RA,ZBE)
505 FNZA=R3*QTA2*QRA2*FK22A
506 FNZE=CTE2+GRE2+FK22E
507 RETURN
508 END IF
509 C*****
510 END

```

1      SUBROUTINE MODSUM(ECMS,ETMS,RNG,ZRCVR,ZXMTR,ZEROS,NRZ,NRMODE)
2 C*****
3 C      THIS PROGRAM EVALUATES THE FIELD STRENGTH IN A TRILINEAR
4 C      MODEL OF THE MODIFIED REFRACTIVITY OF THE TROPOSPHERE RELATIVE TO
5 C      THE FREE SPACE VALUE. THE FIELD IS HORIZONTALLY POLARIZED.
6 C
7 C      INPUTS...
8 C          RNG - RANGE (IN KILOMETERS) AT WHICH THE FIELD STRENGTH
9 C          IS TO BE EVALUATED.
10 C         ZRCVR - HEIGHT (IN METERS) AT WHICH THE FIELD STRENGTH
11 C          IS TO BE EVALUATED.
12 C         ZXMTR - HEIGHT (IN METERS) OF THE TRANSMITTER
13 C         ZEROS - ARRAY CONTAINING THE MODAL EIGENVALUES Q11
14 C         NRZ - DIMENSION OF ARRAY 'ZEROS'
15 C         NRMODE - NUMBER OF MODAL EIGENVALUES CONTAINED IN ARRAY 'ZEROS'
16 C
17 C      OUTPUTS...
18 C          ECMS - COHERENT MODE SUM FIELD STRENGTH (IN DB) RELATIVE
19 C          TO FREE SPACE VALUE
20 C          ETMS - INCOHERENT MODE SUM FIELD STRENGTH (IN DB) RELATIVE
21 C          TO FREE SPACE VALUE
22 C
23 C      SUBROUTINES USED....
24 C          EXCFAC,HTGAIN,CADD,ANEX
25 C*****
26      IMPLICIT DOUBLE PRECISION*8 (A-H,O-Z)
27      COMPLEX ZEROS,XFAC,ENZA,CEXP,I,RHO,CSORT,HFACA,SUMCA,XAA,XEA
28      COMPLEX SONG
29      DIMENSION ZEROS(NRZ)
30      COMMON/COMTWO/ETAABS,ALPHA1,H,C11,SONG
31      COMMON/COMTHR/Z2,Z3,A2MAG,ALPHA3,WAENO,ALPHA2
32      DATA I/10.0,1.0/
33      DATA PI/3.14159265/
34      DATA ELOG10/0.434294482/
35 C*****
36 C      INITIALIZE
37 C
38      RNGM=RNG*1000.0
39      BETA=2.0*SQRT(2.0*PI*RNGM)
40      A1H=1.0-ALPHA1*H
41      C11SC=C11*C11
42      SUMCA=(0.0,0.0)
43      SUMCE=0.0
44      XBA=(0.0,0.0)
45      XBE=0.0
46      SUMIA=0.0
47      SUMTE=0.0
48      XDA=0.0
49      XDE=0.0
50 C
51 C      EVALUATE MODE SUMS
52 C
53      DO 100 JMODE=1,NRMODE
54      RHO=WAENO*CSORT(A1H+I*ETAABS-C11SC*ZEROS(JMODE))
55      HFACA=CEXP(-I*(REAL(RHO)-WAENO)*RNGM)

```

```

56      HFAC=AIMAG(RHO)*RNGM
57      CALL EXCFAC(XFAC,XFACE,ZEROS(JMORE))
58      CALL HTGAIN(ENZA,ENZE,ZEROS(JMORE),7RCVR,7XMTP)
59      XAA=XFAC*ENZA*HFAC
60      XAE=XFACE+ENZE+HFAC
61 C
62 C      COHERENT MODE SUM
63 C
64      CALL CADD(SUMCA,SUMCE,XAA,XAE,XPA,XPE)
65      XBA=SUMCA
66      XRE=SUMCE
67 C
68 C      INCOHERENT MODE SUM
69 C
70      XCA=CARS(XAA)*CARS(XAA)
71      XCE=2.0*XAE
72      CALL ADEY(SUMIA,SUMIE,XCA,XCE,XDA,XDE)
73      XDA=SUMIA
74      XDE=SUMIE
75      100 CONTINUE
76 C
77 C      CALCULATE COHERENT MODE SUM FIELD STRENGTH
78 C
79      ECMS=20.0*(DLOG10(BETA*CARS(SUMCA))+SUMCE*ELCG10)
80 C
81 C      CALCULATE INCOHERENT MODE SUM FIELD STRENGTH
82 C
83      EIMS=20.0*(DLOG10(BETA*SQRT(SUMIA))+0.5*SUMIE*ELCG10)
84      RETURN
85 C*****
86      END

```

```

1      SUBROUTINE SEAH20(SIGEFF,EPSEFF,T,S,FREQ)
2  C*****C
3  C      THIS PROGRAM EVALUATES THE REAL EFFECTIVE RELATIVE
4  C      DIELECTRIC CONSTANT AND THE REAL EFFECTIVE CONDUCTIVITY
5  C      OF SEAWATER AS A FUNCTION OF TEMPERATURE, SALINITY, AND
6  C      FREQUENCY. THIS PROGRAM IS BASED ON THE PAPER:
7  C      L.A. KLEIN AND C.T. SWIFT "AN IMPROVED MODEL FOR THE
8  C      DIELECTRIC CONSTANT OF SEA WATER AT MICROWAVE
9  C      FREQUENCIES" IEEE TRANS. ANT. AND PROP., VOL. 25 (1977)
10 C      104-111.
11 C
12 C      NOTE: THE VALUES THIS PROGRAM GIVES FOR EPSEFF AND
13 C      SIGEFF AS THE SALINITY APPROACHES ZERO ARE NOT
14 C      CONTINUOUS WITH THE VALUES GIVEN WHEN THE SALINITY
15 C      EQUALS ZERO. SEE THE PAPER BY KLEIN AND SWIFT.
16 C
17 C      INPUTS...
18 C          T - TEMPERATURE OF SEAWATER (IN DEGREES CELSIUS)
19 C          S - SALINITY OF SEAWATER (IN GRAMS SALT/KG SEAWATER)
20 C          FREQ - FREQUENCY (IN HERTZ)
21 C
22 C      OUTPUTS...
23 C          SIGEFF - THE REAL EFFECTIVE CONDUCTIVITY (IN SI/M)
24 C          EPSFFF - THE REAL EFFECTIVE RELATIVE DIELECTRIC CONSTANT
25 C
26 C      NOTE: THE COMPLEX DIELECTRIC CONSTANT, EPS, IS EQUAL TO
27 C          EPS=EPSEFF-I*SIGEFF/(2*PI*FREQ*EPS0)
28 C          WHERE EPS0 IS THE PERMITTIVITY OF FREE SPACE
29 C*****C
30      IMPLICIT DOUBLE PRECISION*6 (A-H,O-Z)
31      DATA PI/3.1415926536/
32      DATA EPS0/8.85434E-12/
33 C
34      OMEGA=2.0*PI*FREQ
35 C*****C
36 C      CALCULATE THE STATIC DIELECTRIC CONSTANT
37 C
38      IF(S.GT.0.0) THEN
39      ET=87.134+T*(-0.1949+T*(-1.276E-2+2.491E-4*T))
40      AST=1.0+1.613E-5*S*T+S*(-3.656E-3+S*(3.210E-5-4.232E-7*S))
41      ES=ET*AST
42      ELSE
43      ES=88.045+T*(-0.4147+T*(6.295E-4+1.075E-5*T))
44      END IF
45 C*****C
46 C      CALCULATE THE RELAXATION TIME
47 C
48      TT=1.768E-11+T*(-6.086E-13+T*(1.104E-14-8.111E-17*T))
49      BST=1.0+2.282E-5*S*T+S*(-7.638E-4+S*(-7.760E-6+1.105E-8*S))
50      TAU=TT*BST
51 C*****C
52 C      CALCULATE THE IONIC CONDUCTIVITY
53 C
54      DEL=25.0-T
55      BETA=2.033E-2+DEL*(1.266E-4+2.464E-6*DEL)-S*(1.849E-5

```

```
56      S +DEL*(-2.551E-7+2.551E-8*DEL))
57      SIG=S*(0.182521+S*(-1.46192E-3+S*(2.09324E-5-1.28205E-7*S)))
58      SIGMA=SIG*DEXP(-DEL*BETA)
59 C*****
60 C      CALCULATE THE REAL EFFECTIVE RELATIVE DIELECTRIC CONSTANT
61 C
62      EPSINF=4.9
63      FAC=(ES-EPSINF)/(1.0+(OMEGA*TAU)**2)
64      EPSEFF=EPSINF+FAC
65 C*****
66 C      CALCULATE THE REAL EFFECTIVE CONDUCTIVITY
67 C
68      SIGEFF=OMEGA*OMEGA*TAU*EPS0*FAC+SIGMA
69 C*****
70      RETURN
71      END
```

```
1      SUBROUTINE DHORIZ(DHZ,ZRCVR,ZXMTR)
2 C*****
3 C      THIS PROGRAM CALCULATES THE HORIZON DISTANCE FOR A RECEIVER
4 C      AT HEIGHT ZRCVR AND A TRANSMITTER AT HEIGHT ZXMTR
5 C
6 C      INPUTS...
7 C          ZRCVR - RECEIVER HEIGHT (IN METERS)
8 C          ZXMTR - TRANSMITTER HEIGHT (IN METERS)
9 C
10 C      OUTPUTS...
11 C          DHZ - HORIZON DISTANCE (IN KILOMETERS)
12 C*****
13      IMPLICIT DOUBLE PRECISION*6 (A-H,O-Z)
14 C
15 C      RADIUS OF EARTH (IN METERS)
16 C
17      DATA  R/6.378160E6/
18 C*****
19 C      CALCULATE EFFECTIVE EARTH RADILS
20 C
21      REFF=4.0*R/3.0
22 C*****
23 C      CALCULATE APPROXIMATE HORIZON DISTANCE FOR RECEIVER AND
24 C      TRANSMITTER
25 C
26      HRCVR=DSQRT(2.0*REFF*ZRCVR)
27      HXMTR=DSQRT(2.0*REFF*ZXMTR)
28 C*****
29 C      COMBINED HORIZON DISTANCE IN KILOMETERS
30 C
31      DHZ=(HRCVR+HXMTR)*1.0E-3
32      RETURN
33      END
```

```
1      FUNCTION CASIN(Z)
2 C*****  
3 C      THIS SUBPROGRAM COMPUTES THE COMPLEX ARCSINE OF THE COMPLEX
4 C      NUMBER Z
5 C*****  
6      COMPLEX  CASIN,Z,CLOG,CSORT,I
7      DATA I/(0.0,1.0)/
8      CASIN=I*CLOG(CSQR(1.0-Z*Z)+I*Z)
9      RETURN
10     END
```

10. SAMPLE OUTPUT FROM XWVG

FRFO = 520.0000 MHZ
ALPHAL = 0.2360E-06 /M
ALPHA2 = -0.6496E-06 /M
ALPHA3 = 0.5184E-06 /M
Z2 = 182.9000 M
Z3 = 304.8000 M
ALOSS = 1.0000 DB/KM

M(0.00) = 341.00

HORIZONTAL POLARIZATION

SEAWATER TEMPERATURE = 1.6000E+01 DEGREES CELSIUS
SEAWATER SALINITY = 3.5000E+01 GRAMS SALT/KG SEAWATER
DEFLTA = 0.0000E+00 M
EPSGND = 6.5257E-10 FARADS/M
SGMGND = 4.4544E+00 MHOS/M
ETA = 0.0000E+00

ZEROS FOUND IN EXPANDED SEARCH RECTANGLE DEFINED BY
TLLEFT = 0.00 TRIGHT = 2.00 TRCT = 0.00 TTOP = 2

FIGEN(1) = 1.0946E+00 1.5815E-04

ZEROS FOUND IN EXPANDED SEARCH RECTANGLE DEFINED BY
TLLEFT = -2.00 TRIGHT = 0.00 TRCT = 0.00 TTOP = 2

FIGEN(1) = -1.3124E+00 8.8007E-06
FIGEN(2) = -1.4630E-01 3.9252E-05

ZEROS FOUND IN EXPANDED SEARCH RECTANGLE DEFINED BY
TLLEFT = -4.00 TRIGHT = -2.00 TRCT = 0.00 TTOP = 2

FIGEN(1) = -2.5895E+00 4.6858E-07

ZEROS FOUND IN EXPANDED SEARCH RECTANGLE DEFINED BY
TLLEFT = -6.00 TRIGHT = -4.00 TRCT = 0.00 TTOP = 2

EIGEN(1) = -4.2052E+00 2.2410E-09

ZEROS FOUND IN EXPANDED SEARCH RECTANGLE DEFINED BY
TLLEFT = -8.00 TRIGHT = -6.00 TRCT = 0.00 TTOP = 2

ZEROS FOUND IN EXPANDED SEARCH RECTANGLE DEFINED BY
TLLEFT = -10.00 TRIGHT = -8.00 TRCT = 0.00 TTOP = 2

ZEROS FOUND IN EXPANDED SEARCH RECTANGLE DEFINED BY
TLLEFT = -12.00 TRIGHT = -10.00 TRCT = 0.00 TTOP = 2

ZEROS FOUND IN EXPANDED SEARCH RECTANGLE DEFINED BY
TLLEFT = -14.00 TRIGHT = -12.00 TRCT = 0.00 TTOP = 2

ZEROS FOUND IN EXPANDED SEARCH RECTANGLE DEFINED BY
TLLEFT = -16.00 TRIGHT = -14.00 TRCT = 0.00 TTOP = 2

ZEROS FOUND IN EXPANDED SEARCH RECTANGLE DEFINED BY
TLLEFT = 2.00 TRIGHT = 4.00 TRCT = 0.00 TTOP = 2

EIGEN(1) = 2.4514E+00 3.6817E-03
EIGEN(2) = 3.8044E+00 5.8611E-02

ZEROS FOUND IN EXPANDED SEARCH RECTANGLE DEFINED BY
TLEFT = 4.00 TRIGHT = 6.00 TRECT = 0.00 TTCP = 2

EIGEN(1) = 5.2977E+00 2.9019E-01

ZEROS FOUND IN EXPANDED SEARCH RECTANGLE DEFINED BY
TLEFT = 6.00 TRIGHT = 8.00 TRECT = 0.00 TTCP = 2

EIGEN(1) = 7.0447E+00 6.3569E-01

ZEROS FOUND IN EXPANDED SEARCH RECTANGLE DEFINED BY
TLEFT = 8.00 TRIGHT = 10.00 TRECT = 0.00 TTCP = 2

EIGEN(1) = 9.1272E+00 9.7805E-01

ZEROS FOUND IN EXPANDED SEARCH RECTANGLE DEFINED BY
TLEFT = 10.00 TRIGHT = 12.00 TRECT = 0.00 TTCP = 2

EIGEN(1) = 1.1421E+01 1.3358E+00

ZEROS FOUND IN EXPANDED SEARCH RECTANGLE DEFINED BY
TLEFT = 12.00 TRIGHT = 14.00 TRECT = 0.00 TTCP = 2

EIGEN(1) = 1.3989E+01 1.6259E+00

ZEROS FOUND IN EXPANDED SEARCH RECTANGLE DEFINED BY
TLEFT = 14.00 TRIGHT = 16.00 TRECT = 0.00 TTCP = 2

EIGEN(1) = 1.3989E+01 1.6259E+00

ZEROS FOUND IN EXPANDED SEARCH RECTANGLE DEFINED BY
TLEFT = 16.00 TRIGHT = 18.00 TRECT = 0.00 TTCP = 2

EIGEN(1) = 1.6795E+01 1.9917E+00

ZEROS FOUND IN EXPANDED SEARCH RECTANGLE DEFINED BY
TLEFT = 18.00 TRIGHT = 20.00 TRECT = 0.00 TTCP = 2

EIGEN(1) = 1.9789E+01 2.2808E+00

ZEROS FOUND IN EXPANDED SEARCH RECTANGLE DEFINED BY
TLEFT = 20.00 TRIGHT = 22.00 TRECT = 0.00 TTCP = 2

ZEROS FOUND IN EXPANDED SEARCH RECTANGLE DEFINED BY
TLEFT = 22.00 TRIGHT = 24.00 TRECT = 0.00 TTCP = 2

EIGEN(1) = 2.3103E+01 2.6178E+00

ZEROS FOUND IN EXPANDED SEARCH RECTANGLE DEFINED BY
TLEFT = 24.00 TRIGHT = 26.00 TRECT = 0.00 TTCP = 2

ZEROS FOUND IN EXPANDED SEARCH RECTANGLE DEFINED BY
TLEFT = 26.00 TRIGHT = 28.00 TRECT = 0.00 TTCP = 2

ZEROS FOUND IN EXPANDED SEARCH RECTANGLE DEFINED BY

AD-A133 667 XWVG: A WAVEGUIDE PROGRAM FOR TRILINEAR TROPOSPHERIC
DUCTS COMPUTER PROGR. (U) NAVAL OCEAN SYSTEMS CENTER
SAN DIEGO CA G B BAUMGARTNER 30 JUN 83 NOSC/TD-610

3/3

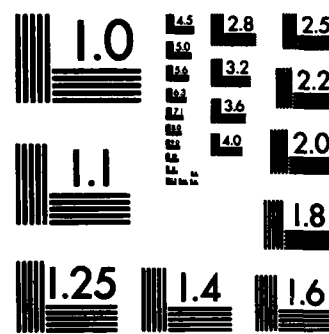
UNCLASSIFIED

F/G 20/14

NL

END

FILMED
FILED
1983



MICROCOPY RESOLUTION TEST CHART
NATIONAL BUREAU OF STANDARDS-1963-A

TLEFT = 28.00 TRIGHT = 30.00 TECT = 0.00 TTCP = 2

ZFROS FOUND IN EXPANDED SEARCH RECTANGLE DEFINED BY

TLEFT = 30.00 TRIGHT = 32.00 TECT = 0.00 TTCP = 2

ZFROS FOUND IN EXPANDED SEARCH RECTANGLE DEFINED BY

TLEFT = 32.00 TRIGHT = 34.00 TECT = 0.00 TTCP = 2

SOLUTIONS OF THE MODAL EQUATION

011(1) =	-4.2052E+00	2.2410E-09	THETA(1) =	3.2552E-13	2.67
011(2) =	-2.5895E+00	4.6858E-07	THETA(2) =	6.8669E-11	2.64
011(3) =	-1.3124E+00	8.8007E-06	THETA(3) =	1.2989E-09	2.63
011(4) =	-1.4630E-01	3.9252E-05	THETA(4) =	5.8317E-09	2.61
011(5) =	1.0946E+00	1.5815E-04	THETA(5) =	2.3665E-08	2.59
011(6) =	2.4514E+00	3.6817E-03	THETA(6) =	5.5526E-07	2.57
011(7) =	3.8044E+00	5.8611E-02	THETA(7) =	8.9105E-06	2.55
011(8) =	5.2977E+00	2.9019E-01	THETA(8) =	4.4515E-05	2.53
011(9) =	7.0447E+00	6.3569E-01	THETA(9) =	9.8564E-05	2.50
011(10) =	9.1272E+00	9.7805E-01	THETA(10) =	1.5364E-04	2.47
011(11) =	1.1421E+01	1.3358E+00	THETA(11) =	2.1297E-04	2.43
011(12) =	1.3989E+01	1.6259E+00	THETA(12) =	2.6368E-04	2.39
011(13) =	1.6795E+01	1.9917E+00	THETA(13) =	3.2932E-04	2.34
011(14) =	1.9789E+01	2.2808E+00	THETA(14) =	3.8532E-04	2.29
011(15) =	2.3103E+01	2.6178E+00	THETA(15) =	4.5343E-04	2.24

FIELD STRENGTH RELATIVE TO FREE SPACE VALUE

RANGE (KM)	ZXMTR (M)	ZRCVR (M)	COHERENT MODE SUM (DB)	INCOHERENT MODE SUM (DB)	HORIZON DISTANCE (KM)
185.32	30.480	0.000	-68.7303	-57.8077	22.77
185.32	30.480	2.000	-19.6559	-8.7228	28.60
185.32	30.480	4.000	-13.7076	-2.7435	31.02

185.32	30.480	6.000	-10.2968	0.7192	32.87
185.32	30.480	8.000	-7.9531	3.1361	34.43
185.32	30.480	10.000	-6.2162	4.9679	35.81
185.32	30.480	12.000	-4.8815	6.4194	37.06
185.32	30.480	14.000	-3.8410	7.5994	38.20
185.32	30.480	16.000	-3.0307	8.5726	39.27
185.32	30.480	18.000	-2.4098	9.3802	40.27
185.32	30.480	20.000	-1.9510	10.0503	41.21
185.32	30.480	22.000	-1.6348	10.6024	42.11
185.32	30.480	24.000	-1.4466	11.0509	42.97
185.32	30.480	26.000	-1.3746	11.4064	43.80
185.32	30.480	28.000	-1.4074	11.6771	44.59
185.32	30.480	30.000	-1.5330	11.8693	45.36
185.32	30.480	32.000	-1.7360	11.9882	46.10
185.32	30.480	34.000	-1.9951	12.0383	46.82
185.32	30.480	36.000	-2.2798	12.0234	47.51
185.32	30.480	38.000	-2.5512	11.9473	48.19
185.32	30.480	40.000	-2.7582	11.8141	48.85
185.32	30.480	42.000	-2.8472	11.6283	49.50
185.32	30.480	44.000	-2.7757	11.3957	50.13
185.32	30.480	46.000	-2.5264	11.1233	50.74
185.32	30.480	48.000	-2.1143	10.8204	51.34
185.32	30.480	50.000	-1.5787	10.4984	51.93
185.32	30.480	52.000	-0.9676	10.1715	52.51
185.32	30.480	54.000	-0.3248	9.8562	53.07
185.32	30.480	56.000	0.3167	9.5705	53.63
185.32	30.480	58.000	0.9352	9.3314	54.18
185.32	30.480	60.000	1.5163	9.1532	54.71
185.32	30.480	62.000	2.0600	9.0440	55.24
185.32	30.480	64.000	2.5587	9.0042	55.76
185.32	30.480	66.000	3.0153	9.0266	56.27
185.32	30.480	68.000	3.4318	9.0978	56.78
185.32	30.480	70.000	3.8103	9.2011	57.27
185.32	30.480	72.000	4.1528	9.3193	57.76
185.32	30.480	74.000	4.4602	9.4366	58.25
185.32	30.480	76.000	4.7322	9.5399	58.72
185.32	30.480	78.000	4.9672	9.6193	59.19
185.32	30.480	80.000	5.1623	9.6680	59.66
185.32	30.480	82.000	5.3132	9.6821	60.11
185.32	30.480	84.000	5.4143	9.6604	60.57
185.32	30.480	86.000	5.4590	9.6039	61.01
185.32	30.480	88.000	5.4396	9.5161	61.46
185.32	30.480	90.000	5.3476	9.4021	61.89
185.32	30.480	92.000	5.1737	9.2693	62.33
185.32	30.480	94.000	4.9079	9.1263	62.75
185.32	30.480	96.000	4.5401	8.9828	63.18
185.32	30.480	98.000	4.0608	8.8487	63.60
185.32	30.480	100.000	3.4633	8.7331	64.01
185.32	30.480	102.000	2.7492	8.6430	64.42
185.32	30.480	104.000	1.9395	8.5827	64.83
185.32	30.480	106.000	1.0961	8.5528	65.23
185.32	30.480	108.000	0.3532	8.5503	65.63
185.32	30.480	110.000	-0.0739	8.5693	66.02
185.32	30.480	112.000	0.0218	8.6020	66.41
185.32	30.480	114.000	0.6666	8.6398	66.80

185.32	30.480	116.000	1.6773	8.6745	67.19
185.32	30.480	118.000	2.8228	8.6991	67.57
185.32	30.480	120.000	3.9438	8.7081	67.95
185.32	30.480	122.000	4.9591	8.6984	68.32
185.32	30.480	124.000	5.8347	8.6686	68.69
185.32	30.480	126.000	6.5594	8.6196	69.06
185.32	30.480	128.000	7.1312	8.5544	69.43
185.32	30.480	130.000	7.5505	8.4774	69.79
185.32	30.480	132.000	7.8178	8.3946	70.15
185.32	30.480	134.000	7.9315	8.3123	70.51
185.32	30.480	136.000	7.8879	8.2372	70.86
185.32	30.480	138.000	7.6802	8.1751	71.22
185.32	30.480	140.000	7.2993	8.1301	71.57
185.32	30.480	142.000	6.7340	8.1044	71.91
185.32	30.480	144.000	5.9749	8.0976	72.26
185.32	30.480	146.000	5.0246	8.1071	72.60
185.32	30.480	148.000	3.9254	8.1283	72.94
185.32	30.480	150.000	2.8227	8.1557	73.28
185.32	30.480	152.000	2.0505	8.1834	73.61
185.32	30.480	154.000	2.0454	8.2059	73.95
185.32	30.480	156.000	2.9106	8.2186	74.28
185.32	30.480	158.000	4.2767	8.2184	74.61
185.32	30.480	160.000	5.7398	8.2040	74.94
185.32	30.480	162.000	7.0905	8.1751	75.26
185.32	30.480	164.000	8.2566	8.1337	75.58
185.32	30.480	166.000	9.2248	8.0824	75.90
185.32	30.480	168.000	10.0009	8.0253	76.22
185.32	30.480	170.000	10.5953	7.9667	76.54
185.32	30.480	172.000	11.0168	7.9109	76.86
185.32	30.480	174.000	11.2720	7.8616	77.17
185.32	30.480	176.000	11.3637	7.8213	77.48
185.32	30.480	178.000	11.2919	7.7909	77.79
185.32	30.480	180.000	11.0534	7.7699	78.10
185.32	30.480	182.000	10.6430	7.7561	78.41
185.32	30.480	184.000	10.0548	7.7467	78.71
185.32	30.480	186.000	9.2906	7.7416	79.01
185.32	30.480	188.000	8.3716	7.7441	79.32
185.32	30.480	190.000	7.3596	7.7568	79.62
185.32	30.480	192.000	6.4019	7.7822	79.91
185.32	30.480	194.000	5.7635	7.8220	80.21
185.32	30.480	196.000	5.7329	7.8775	80.51
185.32	30.480	198.000	6.3683	7.9494	80.80
185.32	30.480	200.000	7.4356	8.0383	81.09
185.32	30.480	202.000	8.6476	8.1439	81.38
185.32	30.480	204.000	9.8260	8.2659	81.67
185.32	30.480	206.000	10.8939	8.4032	81.96
185.32	30.480	208.000	11.8288	8.5548	82.25
185.32	30.480	210.000	12.6314	8.7193	82.53
185.32	30.480	212.000	13.3109	8.8949	82.82
185.32	30.480	214.000	13.8787	9.0796	83.10
185.32	30.480	216.000	14.3463	9.2713	83.38
185.32	30.480	218.000	14.7239	9.4675	83.66
185.32	30.480	220.000	15.0208	9.6658	83.94
185.32	30.480	222.000	15.2449	9.8635	84.22
185.32	30.480	224.000	15.4035	10.0577	84.49

185.32	30.480	226.000	15.5028	10.2458	84.77
185.32	30.480	228.000	15.5482	10.4250	85.04
185.32	30.480	230.000	15.5448	10.5928	85.31
185.32	30.480	232.000	15.4969	10.7468	85.59
185.32	30.480	234.000	15.4085	10.8846	85.86
185.32	30.480	236.000	15.2831	11.0044	86.12
185.32	30.480	238.000	15.1240	11.1042	86.39
185.32	30.480	240.000	14.9340	11.1825	86.66
185.32	30.480	242.000	14.7157	11.2380	86.93
185.32	30.480	244.000	14.4714	11.2695	87.19
185.32	30.480	246.000	14.2030	11.2762	87.45
185.32	30.480	248.000	13.9125	11.2573	87.72
185.32	30.480	250.000	13.6012	11.2123	87.98
185.32	30.480	252.000	13.2705	11.1408	88.24
185.32	30.480	254.000	12.9217	11.0426	88.50
185.32	30.480	256.000	12.5556	10.9175	88.75
185.32	30.480	258.000	12.1732	10.7657	89.01
185.32	30.480	260.000	11.7751	10.5872	89.27
185.32	30.480	262.000	11.3621	10.3823	89.52
185.32	30.480	264.000	10.9348	10.1512	89.78
185.32	30.480	266.000	10.4938	9.8944	90.03
185.32	30.480	268.000	10.0396	9.6123	90.28
185.32	30.480	270.000	9.5730	9.3056	90.54
185.32	30.480	272.000	9.0947	8.9748	90.79
185.32	30.480	274.000	8.6055	8.6207	91.04
185.32	30.480	276.000	8.1063	8.2441	91.28
185.32	30.480	278.000	7.5984	7.8460	91.53
185.32	30.480	280.000	7.0830	7.4275	91.78
185.32	30.480	282.000	6.5616	6.9898	92.02
185.32	30.480	284.000	6.0360	6.5343	92.27
185.32	30.480	286.000	5.5083	6.0627	92.51
185.32	30.480	288.000	4.9808	5.5769	92.76
185.32	30.480	290.000	4.4562	5.0791	93.00
185.32	30.480	292.000	3.9376	4.5719	93.24
185.32	30.480	294.000	3.4283	4.0583	93.48
185.32	30.480	296.000	2.9322	3.5418	93.72
185.32	30.480	298.000	2.4538	3.0268	93.96
185.32	30.480	300.000	1.9977	2.5180	94.20
185.32	30.480	302.000	1.5692	2.0214	94.44
185.32	30.480	304.000	1.1743	1.5434	94.68
185.32	30.480	306.000	0.8187	1.0913	94.91
185.32	30.480	308.000	0.5035	0.6678	95.15
185.32	30.480	310.000	0.2255	0.2716	95.38
185.32	30.480	312.000	-0.0186	-0.0987	95.62
185.32	30.480	314.000	-0.2324	-0.4445	95.85
185.32	30.480	316.000	-0.4191	-0.7674	96.08
185.32	30.480	318.000	-0.5820	-1.0689	96.31
185.32	30.480	320.000	-0.7240	-1.3504	96.54
185.32	30.480	322.000	-0.8478	-1.6134	96.77
185.32	30.480	324.000	-0.9559	-1.8591	97.00
185.32	30.480	326.000	-1.0504	-2.0890	97.23
185.32	30.480	328.000	-1.1333	-2.3042	97.46
185.32	30.480	330.000	-1.2063	-2.5088	97.69
185.32	30.480	332.000	-1.2708	-2.6980	97.91
185.32	30.480	334.000	-1.3282	-2.8728	98.14

185.32	30.480	336.000	-1.3794	-3.0399	98.37
185.32	30.480	338.000	-1.4254	-3.1974	98.59
185.32	30.480	340.000	-1.4671	-3.3459	98.81
185.32	30.480	342.000	-1.5051	-3.4862	99.04
185.32	30.480	344.000	-1.5401	-3.6190	99.26
185.32	30.480	346.000	-1.5724	-3.7447	99.48
185.32	30.480	348.000	-1.6026	-3.8640	99.70
185.32	30.480	350.000	-1.6309	-3.9773	99.92
185.32	30.480	352.000	-1.6578	-4.0851	100.14
185.32	30.480	354.000	-1.6835	-4.1878	100.36
185.32	30.480	356.000	-1.7081	-4.2858	100.58
185.32	30.480	358.000	-1.7319	-4.3793	100.80
185.32	30.480	360.000	-1.7551	-4.4688	101.02
185.32	30.480	362.000	-1.7778	-4.5545	101.24
185.32	30.480	364.000	-1.8000	-4.6366	101.45
185.32	30.480	366.000	-1.8220	-4.7155	101.67
185.32	30.480	368.000	-1.8438	-4.7912	101.88
185.32	30.480	370.000	-1.8654	-4.8640	102.10
185.32	30.480	372.000	-1.8869	-4.9341	102.31
185.32	30.480	374.000	-1.9084	-5.0017	102.53
185.32	30.480	376.000	-1.9299	-5.0669	102.74
185.32	30.480	378.000	-1.9514	-5.1298	102.95
185.32	30.480	380.000	-1.9731	-5.1906	103.16
185.32	30.480	382.000	-1.9948	-5.2494	103.37
185.32	30.480	384.000	-2.0166	-5.3063	103.58
185.32	30.480	386.000	-2.0387	-5.3614	103.80
185.32	30.480	388.000	-2.0608	-5.4148	104.00
185.32	30.480	390.000	-2.0832	-5.4666	104.21
185.32	30.480	392.000	-2.1057	-5.5169	104.42
185.32	30.480	394.000	-2.1284	-5.5658	104.63
185.32	30.480	396.000	-2.1513	-5.6133	104.84
185.32	30.480	398.000	-2.1744	-5.6594	105.04
185.32	30.480	400.000	-2.1977	-5.7043	105.25
185.32	30.480	402.000	-2.2212	-5.7481	105.46
185.32	30.480	404.000	-2.2449	-5.7907	105.66
185.32	30.480	406.000	-2.2686	-5.8320	105.87
185.32	30.480	408.000	-2.2928	-5.8725	106.07
185.32	30.480	410.000	-2.3171	-5.9120	106.28
185.32	30.480	412.000	-2.3417	-5.9505	106.48
185.32	30.480	414.000	-2.3664	-5.9881	106.68
185.32	30.480	416.000	-2.3914	-6.0249	106.88
185.32	30.480	418.000	-2.4166	-6.0608	107.09
185.32	30.480	420.000	-2.4419	-6.0959	107.29
185.32	30.480	422.000	-2.4675	-6.1302	107.49
185.32	30.480	424.000	-2.4933	-6.1638	107.69
185.32	30.480	426.000	-2.5192	-6.1967	107.89
185.32	30.480	428.000	-2.5454	-6.2288	108.09
185.32	30.480	430.000	-2.5717	-6.2603	108.29
185.32	30.480	432.000	-2.5983	-6.2912	108.49
185.32	30.480	434.000	-2.6250	-6.3214	108.69
185.32	30.480	436.000	-2.6520	-6.3510	108.88
185.32	30.480	438.000	-2.6791	-6.3801	109.08
185.32	30.480	440.000	-2.7065	-6.4086	109.28
185.32	30.480	442.000	-2.7340	-6.4365	109.47
185.32	30.480	444.000	-2.7617	-6.4640	109.67

185.32	30.480	446.000	-2.7896	-6.4909	109.87
185.32	30.480	448.000	-2.8176	-6.5173	110.06
185.32	30.480	450.000	-2.8459	-6.5433	110.25
185.32	30.480	452.000	-2.8743	-6.5688	110.45
185.32	30.480	454.000	-2.9030	-6.5938	110.64
185.32	30.480	456.000	-2.9318	-6.6184	110.84
185.32	30.480	458.000	-2.9607	-6.6426	111.03
185.32	30.480	460.000	-2.9899	-6.6664	111.22
185.32	30.480	462.000	-3.0192	-6.6908	111.41
185.32	30.480	464.000	-3.0488	-6.7128	111.61
185.32	30.480	466.000	-3.0784	-6.7354	111.80
185.32	30.480	468.000	-3.1083	-6.7576	111.99
185.32	30.480	470.000	-3.1384	-6.7795	112.18
185.32	30.480	472.000	-3.1686	-6.8011	112.37
185.32	30.480	474.000	-3.1990	-6.8223	112.56
185.32	30.480	476.000	-3.2295	-6.8432	112.75
185.32	30.480	478.000	-3.2603	-6.8638	112.94
185.32	30.480	480.000	-3.2912	-6.8840	113.12
185.32	30.480	482.000	-3.3222	-6.9040	113.31
185.32	30.480	484.000	-3.3535	-6.9236	113.50
185.32	30.480	486.000	-3.3849	-6.9430	113.69
185.32	30.480	488.000	-3.4165	-6.9621	113.87
185.32	30.480	490.000	-3.4482	-6.9809	114.06
185.32	30.480	492.000	-3.4801	-6.9994	114.25
185.32	30.480	494.000	-3.5122	-7.0177	114.43
185.32	30.480	496.000	-3.5445	-7.0357	114.62
185.32	30.480	498.000	-3.5769	-7.0535	114.80
185.32	30.480	500.000	-3.6094	-7.0710	114.99
185.32	30.480	502.000	-3.6422	-7.0883	115.17
185.32	30.480	504.000	-3.6750	-7.1053	115.36
185.32	30.480	506.000	-3.7081	-7.1222	115.54
185.32	30.480	508.000	-3.7413	-7.1388	115.72
185.32	30.480	510.000	-3.7747	-7.1551	115.90
185.32	30.480	512.000	-3.8082	-7.1713	116.09
185.32	30.480	514.000	-3.8419	-7.1873	116.27
185.32	30.480	516.000	-3.8757	-7.2030	116.45
185.32	30.480	518.000	-3.9097	-7.2186	116.63
185.32	30.480	520.000	-3.9438	-7.2339	116.81
185.32	30.480	522.000	-3.9781	-7.2491	116.99
185.32	30.480	524.000	-4.0125	-7.2640	117.17
185.32	30.480	526.000	-4.0471	-7.2788	117.35
185.32	30.480	528.000	-4.0818	-7.2934	117.53
185.32	30.480	530.000	-4.1167	-7.3078	117.71
185.32	30.480	532.000	-4.1517	-7.3221	117.89
185.32	30.480	534.000	-4.1869	-7.3362	118.07
185.32	30.480	536.000	-4.2222	-7.3501	118.25
185.32	30.480	538.000	-4.2576	-7.3638	118.43
185.32	30.480	540.000	-4.2932	-7.3774	118.60
185.32	30.480	542.000	-4.3289	-7.3908	118.78
185.32	30.480	544.000	-4.3648	-7.4041	118.96
185.32	30.480	546.000	-4.4008	-7.4172	119.14
185.32	30.480	548.000	-4.4369	-7.4301	119.31
185.32	30.480	550.000	-4.4731	-7.4429	119.49
185.32	30.480	552.000	-4.5095	-7.4556	119.66
185.32	30.480	554.000	-4.5460	-7.4681	119.84

185.32	30.480	556.000	-4.5826	-7.4805	120.01
185.32	30.480	558.000	-4.6194	-7.4927	120.19
185.32	30.480	560.000	-4.6563	-7.5049	120.36
185.32	30.480	562.000	-4.6933	-7.5168	120.54
185.32	30.480	564.000	-4.7304	-7.5287	120.71
185.32	30.480	566.000	-4.7676	-7.5404	120.88
185.32	30.480	568.000	-4.8050	-7.5520	121.06
185.32	30.480	570.000	-4.8424	-7.5634	121.23
185.32	30.480	572.000	-4.8800	-7.5748	121.40
185.32	30.480	574.000	-4.9177	-7.5860	121.58
185.32	30.480	576.000	-4.9555	-7.5971	121.75
185.32	30.480	578.000	-4.9934	-7.6081	121.92
185.32	30.480	580.000	-5.0314	-7.6189	122.09
185.32	30.480	582.000	-5.0695	-7.6297	122.26
185.32	30.480	584.000	-5.1077	-7.6403	122.43
185.32	30.480	586.000	-5.1461	-7.6508	122.60
185.32	30.480	588.000	-5.1845	-7.6613	122.77
185.32	30.480	590.000	-5.2230	-7.6716	122.94
185.32	30.480	592.000	-5.2616	-7.6818	123.11
185.32	30.480	594.000	-5.3003	-7.6919	123.28
185.32	30.480	596.000	-5.3391	-7.7019	123.45
185.32	30.480	598.000	-5.3780	-7.7118	123.62
185.32	30.480	600.000	-5.4169	-7.7216	123.79
185.32	30.480	602.000	-5.4560	-7.7313	123.96
185.32	30.480	604.000	-5.4951	-7.7409	124.13
185.32	30.480	606.000	-5.5343	-7.7504	124.29
185.32	30.480	608.000	-5.5736	-7.7599	124.46
185.32	30.480	610.000	-5.6130	-7.7692	124.63
185.32	30.480	612.000	-5.6525	-7.7784	124.79
185.32	30.480	614.000	-5.6920	-7.7876	124.96
185.32	30.480	616.000	-5.7316	-7.7966	125.13
185.32	30.480	618.000	-5.7713	-7.8056	125.29
185.32	30.480	620.000	-5.8110	-7.8145	125.46
185.32	30.480	622.000	-5.8509	-7.8233	125.62
185.32	30.480	624.000	-5.8907	-7.8320	125.79
185.32	30.480	626.000	-5.9307	-7.8407	125.95
185.32	30.480	628.000	-5.9707	-7.8492	126.12
185.32	30.480	630.000	-6.0107	-7.8577	126.28
185.32	30.480	632.000	-6.0509	-7.8661	126.45
185.32	30.480	634.000	-6.0911	-7.8744	126.61
185.32	30.480	636.000	-6.1313	-7.8826	126.78
185.32	30.480	638.000	-6.1716	-7.8908	126.94
185.32	30.480	640.000	-6.2119	-7.8989	127.10
185.32	30.480	642.000	-6.2523	-7.9069	127.26
185.32	30.480	644.000	-6.2928	-7.9148	127.43
185.32	30.480	646.000	-6.3333	-7.9227	127.59
185.32	30.480	648.000	-6.3738	-7.9305	127.75
185.32	30.480	650.000	-6.4144	-7.9382	127.91
185.32	30.480	652.000	-6.4550	-7.9459	128.08
185.32	30.480	654.000	-6.4957	-7.9535	128.24
185.32	30.480	656.000	-6.5364	-7.9610	128.40
185.32	30.480	658.000	-6.5772	-7.9684	128.56
185.32	30.480	660.000	-6.6180	-7.9758	128.72
185.32	30.480	662.000	-6.6588	-7.9831	128.88
185.32	30.480	664.000	-6.6996	-7.9904	129.04

185.32	30.480	666.000	-6.7405	-7.9976	129.20
185.32	30.480	668.000	-6.7814	-8.0047	129.36
185.32	30.480	670.000	-6.8224	-8.0118	129.52
185.32	30.480	672.000	-6.8634	-8.0188	129.68
185.32	30.480	674.000	-6.9044	-8.0257	129.84
185.32	30.480	676.000	-6.9454	-8.0326	130.00
185.32	30.480	678.000	-6.9864	-8.0394	130.15
185.32	30.480	680.000	-7.0275	-8.0461	130.31
185.32	30.480	682.000	-7.0686	-8.0528	130.47
185.32	30.480	684.000	-7.1097	-8.0595	130.63
185.32	30.480	686.000	-7.1508	-8.0661	130.79
185.32	30.480	688.000	-7.1920	-8.0726	130.94
185.32	30.480	690.000	-7.2332	-8.0791	131.10
185.32	30.480	692.000	-7.2743	-8.0855	131.26
185.32	30.480	694.000	-7.3155	-8.0918	131.41
185.32	30.480	696.000	-7.3567	-8.0981	131.57
185.32	30.480	698.000	-7.3979	-8.1044	131.73
185.32	30.480	700.000	-7.4392	-8.1106	131.88
185.32	30.480	702.000	-7.4804	-8.1167	132.04
185.32	30.480	704.000	-7.5216	-8.1228	132.19
185.32	30.480	706.000	-7.5629	-8.1289	132.35
185.32	30.480	708.000	-7.6041	-8.1349	132.50
185.32	30.480	710.000	-7.6454	-8.1408	132.66
185.32	30.480	712.000	-7.6867	-8.1467	132.81
185.32	30.480	714.000	-7.7279	-8.1525	132.97
185.32	30.480	716.000	-7.7692	-8.1583	133.12
185.32	30.480	718.000	-7.8104	-8.1641	133.28
185.32	30.480	720.000	-7.8517	-8.1698	133.43
185.32	30.480	722.000	-7.8930	-8.1754	133.58
185.32	30.480	724.000	-7.9342	-8.1810	133.74
185.32	30.480	726.000	-7.9755	-8.1866	133.89
185.32	30.480	728.000	-8.0167	-8.1921	134.04
185.32	30.480	730.000	-8.0580	-8.1975	134.20
185.32	30.480	732.000	-8.0992	-8.2030	134.35
185.32	30.480	734.000	-8.1404	-8.2083	134.50
185.32	30.480	736.000	-8.1816	-8.2137	134.65
185.32	30.480	738.000	-8.2228	-8.2190	134.81
185.32	30.480	740.000	-8.2640	-8.2242	134.96
185.32	30.480	742.000	-8.3052	-8.2294	135.11
185.32	30.480	744.000	-8.3464	-8.2345	135.26
185.32	30.480	746.000	-8.3876	-8.2397	135.41
185.32	30.480	748.000	-8.4287	-8.2447	135.56
185.32	30.480	750.000	-8.4698	-8.2498	135.71
185.32	30.480	752.000	-8.5109	-8.2548	135.86
185.32	30.480	754.000	-8.5520	-8.2597	136.01
185.32	30.480	756.000	-8.5931	-8.2646	136.16
185.32	30.480	758.000	-8.6342	-8.2695	136.31
185.32	30.480	760.000	-8.6752	-8.2743	136.46
185.32	30.480	762.000	-8.7163	-8.2791	136.61
185.32	30.480	764.000	-8.7573	-8.2838	136.76
185.32	30.480	766.000	-8.7982	-8.2886	136.91
185.32	30.480	768.000	-8.8392	-8.2932	137.06
185.32	30.480	770.000	-8.8801	-8.2979	137.21
185.32	30.480	772.000	-8.9211	-8.3025	137.36
185.32	30.480	774.000	-8.9619	-8.3070	137.51

185.32	30.480	776.000	-9.0028	-8.3116	137.65
185.32	30.480	778.000	-9.0437	-8.3160	137.80
185.32	30.480	780.000	-9.0845	-8.3205	137.95
185.32	30.480	782.000	-9.1253	-8.3249	138.10
185.32	30.480	784.000	-9.1660	-8.3293	138.24
185.32	30.480	786.000	-9.2068	-8.3336	138.39
185.32	30.480	788.000	-9.2475	-8.3379	138.54
185.32	30.480	790.000	-9.2882	-8.3422	138.69
185.32	30.480	792.000	-9.3289	-8.3465	138.83
185.32	30.480	794.000	-9.3695	-8.3507	138.98
185.32	30.480	796.000	-9.4101	-8.3548	139.12
185.32	30.480	798.000	-9.4506	-8.3590	139.27
185.32	30.480	800.000	-9.4912	-8.3631	139.42
185.32	30.480	802.000	-9.5317	-8.3672	139.56
185.32	30.480	804.000	-9.5722	-8.3712	139.71
185.32	30.480	806.000	-9.6126	-8.3752	139.85
185.32	30.480	808.000	-9.6530	-8.3792	140.00
185.32	30.480	810.000	-9.6934	-8.3831	140.14
185.32	30.480	812.000	-9.7338	-8.3871	140.29
185.32	30.480	814.000	-9.7741	-8.3909	140.43
185.32	30.480	816.000	-9.8144	-8.3948	140.58
185.32	30.480	818.000	-9.8547	-8.3986	140.72
185.32	30.480	820.000	-9.8949	-8.4024	140.87
185.32	30.480	822.000	-9.9351	-8.4061	141.01
185.32	30.480	824.000	-9.9753	-8.4099	141.15
185.32	30.480	826.000	-10.0154	-8.4136	141.30
185.32	30.480	828.000	-10.0555	-8.4172	141.44
185.32	30.480	830.000	-10.0956	-8.4209	141.58
185.32	30.480	832.000	-10.1356	-8.4245	141.73
185.32	30.480	834.000	-10.1756	-8.4281	141.87
185.32	30.480	836.000	-10.2156	-8.4316	142.01
185.32	30.480	838.000	-10.2556	-8.4351	142.15
185.32	30.480	840.000	-10.2955	-8.4386	142.30
185.32	30.480	842.000	-10.3354	-8.4421	142.44
185.32	30.480	844.000	-10.3752	-8.4455	142.58
185.32	30.480	846.000	-10.4151	-8.4490	142.72
185.32	30.480	848.000	-10.4549	-8.4523	142.87
185.32	30.480	850.000	-10.4946	-8.4557	143.01
185.32	30.480	852.000	-10.5344	-8.4590	143.15
185.32	30.480	854.000	-10.5741	-8.4623	143.29
185.32	30.480	856.000	-10.6138	-8.4656	143.43
185.32	30.480	858.000	-10.6534	-8.4689	143.57
185.32	30.480	860.000	-10.6931	-8.4721	143.71
185.32	30.480	862.000	-10.7327	-8.4753	143.85
185.32	30.480	864.000	-10.7723	-8.4784	143.99
185.32	30.480	866.000	-10.8118	-8.4816	144.13
185.32	30.480	868.000	-10.8514	-8.4847	144.27
185.32	30.480	870.000	-10.8909	-8.4878	144.41
185.32	30.480	872.000	-10.9304	-8.4909	144.55
185.32	30.480	874.000	-10.9699	-8.4939	144.69
185.32	30.480	876.000	-11.0094	-8.4969	144.83
185.32	30.480	878.000	-11.0488	-8.4999	144.97
185.32	30.480	880.000	-11.0882	-8.5029	145.11
185.32	30.480	882.000	-11.1276	-8.5059	145.25
185.32	30.480	884.000	-11.1670	-8.5088	145.39

185.32	30.480	886.000	-11.2064	-8.5117	145.53
185.32	30.480	888.000	-11.2458	-8.5145	145.66
185.32	30.480	890.000	-11.2852	-8.5174	145.80
185.32	30.480	892.000	-11.3245	-8.5202	145.94
185.32	30.480	894.000	-11.3639	-8.5230	146.08
185.32	30.480	896.000	-11.4032	-8.5258	146.22
185.32	30.480	898.000	-11.4426	-8.5286	146.36
185.32	30.480	900.000	-11.4819	-8.5313	146.49
185.32	30.480	902.000	-11.5212	-8.5340	146.63
185.32	30.480	904.000	-11.5606	-8.5367	146.77
185.32	30.480	906.000	-11.5999	-8.5394	146.90
185.32	30.480	908.000	-11.6393	-8.5420	147.04
185.32	30.480	910.000	-11.6786	-8.5446	147.18
185.32	30.480	912.000	-11.7180	-8.5472	147.31
185.32	30.480	914.000	-11.7573	-8.5498	147.45
185.32	30.480	916.000	-11.7967	-8.5524	147.59
185.32	30.480	918.000	-11.8361	-8.5549	147.72
185.32	30.480	920.000	-11.8755	-8.5574	147.86
185.32	30.480	922.000	-11.9150	-8.5599	148.00
185.32	30.480	924.000	-11.9544	-8.5624	148.13
185.32	30.480	926.000	-11.9939	-8.5648	148.27
185.32	30.480	928.000	-12.0334	-8.5673	148.40
185.32	30.480	930.000	-12.0729	-8.5697	148.54
185.32	30.480	932.000	-12.1125	-8.5721	148.67
185.32	30.480	934.000	-12.1521	-8.5744	148.81
185.32	30.480	936.000	-12.1917	-8.5768	148.94
185.32	30.480	938.000	-12.2313	-8.5791	149.08
185.32	30.480	940.000	-12.2710	-8.5814	149.21
185.32	30.480	942.000	-12.3108	-8.5837	149.35
185.32	30.480	944.000	-12.3506	-8.5860	149.48
185.32	30.480	946.000	-12.3904	-8.5882	149.62
185.32	30.480	948.000	-12.4303	-8.5904	149.75
185.32	30.480	950.000	-12.4703	-8.5926	149.88
185.32	30.480	952.000	-12.5103	-8.5948	150.02
185.32	30.480	954.000	-12.5503	-8.5970	150.15
185.32	30.480	956.000	-12.5905	-8.5992	150.28
185.32	30.480	958.000	-12.6307	-8.6013	150.42
185.32	30.480	960.000	-12.6709	-8.6034	150.55
185.32	30.480	962.000	-12.7113	-8.6055	150.68
185.32	30.480	964.000	-12.7517	-8.6076	150.82
185.32	30.480	966.000	-12.7922	-8.6096	150.95
185.32	30.480	968.000	-12.8328	-8.6117	151.08
185.32	30.480	970.000	-12.8735	-8.6137	151.21
185.32	30.480	972.000	-12.9142	-8.6157	151.35
185.32	30.480	974.000	-12.9551	-8.6177	151.48
185.32	30.480	976.000	-12.9960	-8.6196	151.61
185.32	30.480	978.000	-13.0371	-8.6216	151.74
185.32	30.480	980.000	-13.0782	-8.6235	151.87
185.32	30.480	982.000	-13.1195	-8.6254	152.01
185.32	30.480	984.000	-13.1609	-8.6273	152.14
185.32	30.480	986.000	-13.2024	-8.6292	152.27
185.32	30.480	988.000	-13.2440	-8.6311	152.40
185.32	30.480	990.000	-13.2858	-8.6329	152.53
185.32	30.480	992.000	-13.3277	-8.6347	152.66
185.32	30.480	994.000	-13.3697	-8.6365	152.79

185.32	30.480	996.000	-13.4118	-8.6383	152.92
185.32	30.480	998.000	-13.4541	-8.6401	153.05
185.32	30.480	1000.000	-13.4965	-8.6419	153.19
185.32	30.480	1002.000	-13.5391	-8.6436	153.32
185.32	30.480	1004.000	-13.5819	-8.6453	153.45
185.32	30.480	1006.000	-13.6248	-8.6470	153.58
185.32	30.480	1008.000	-13.6678	-8.6487	153.71
185.32	30.480	1010.000	-13.7111	-8.6504	153.84
185.32	30.480	1012.000	-13.7545	-8.6521	153.97
185.32	30.480	1014.000	-13.7981	-8.6537	154.09
185.32	30.480	1016.000	-13.8418	-8.6553	154.22
185.32	30.480	1018.000	-13.8858	-8.6570	154.35
185.32	30.480	1020.000	-13.9300	-8.6585	154.48
185.32	30.480	1022.000	-13.9743	-8.6601	154.61
185.32	30.480	1024.000	-14.0189	-8.6617	154.74
185.32	30.480	1026.000	-14.0636	-8.6632	154.87
185.32	30.480	1028.000	-14.1086	-8.6648	155.00
185.32	30.480	1030.000	-14.1538	-8.6663	155.13
185.32	30.480	1032.000	-14.1992	-8.6678	155.26
185.32	30.480	1034.000	-14.2448	-8.6693	155.38
185.32	30.480	1036.000	-14.2907	-8.6707	155.51
185.32	30.480	1038.000	-14.3368	-8.6722	155.64
185.32	30.480	1040.000	-14.3832	-8.6736	155.77
185.32	30.480	1042.000	-14.4298	-8.6751	155.90
185.32	30.480	1044.000	-14.4767	-8.6765	156.02
185.32	30.480	1046.000	-14.5238	-8.6779	156.15
185.32	30.480	1048.000	-14.5712	-8.6793	156.28
185.32	30.480	1050.000	-14.6189	-8.6806	156.41
185.32	30.480	1052.000	-14.6668	-8.6820	156.53
185.32	30.480	1054.000	-14.7150	-8.6833	156.66
185.32	30.480	1056.000	-14.7636	-8.6846	156.79
185.32	30.480	1058.000	-14.8124	-8.6859	156.91
185.32	30.480	1060.000	-14.8615	-8.6872	157.04
185.32	30.480	1062.000	-14.9109	-8.6885	157.17
185.32	30.480	1064.000	-14.9606	-8.6898	157.29
185.32	30.480	1066.000	-15.0107	-8.6910	157.42
185.32	30.480	1068.000	-15.0611	-8.6923	157.55
185.32	30.480	1070.000	-15.1118	-8.6935	157.67
185.32	30.480	1072.000	-15.1629	-8.6947	157.80
185.32	30.480	1074.000	-15.2143	-8.6959	157.92
185.32	30.480	1076.000	-15.2660	-8.6971	158.05
185.32	30.480	1078.000	-15.3181	-8.6983	158.18
185.32	30.480	1080.000	-15.3706	-8.6994	158.30
185.32	30.480	1082.000	-15.4235	-8.7006	158.43
185.32	30.480	1084.000	-15.4767	-8.7017	158.55
185.32	30.480	1086.000	-15.5303	-8.7028	158.68
185.32	30.480	1088.000	-15.5843	-8.7039	158.80
185.32	30.480	1090.000	-15.6387	-8.7050	158.93
185.32	30.480	1092.000	-15.6936	-8.7061	159.05
185.32	30.480	1094.000	-15.7488	-8.7071	159.18
185.32	30.480	1096.000	-15.8044	-8.7082	159.30
185.32	30.480	1098.000	-15.8605	-8.7092	159.43
185.32	30.480	1100.000	-15.9170	-8.7102	159.55
185.32	30.480	1102.000	-15.9740	-8.7112	159.67
185.32	30.480	1104.000	-16.0314	-8.7122	159.80

185.32	30.480	1106.000	-16.0893	-8.7132	159.92
185.32	30.480	1108.000	-16.1476	-8.7142	160.05
185.32	30.480	1110.000	-16.2064	-8.7151	160.17
185.32	30.480	1112.000	-16.2658	-8.7161	160.29
185.32	30.480	1114.000	-16.3255	-8.7170	160.42
185.32	30.480	1116.000	-16.3858	-8.7179	160.54
185.32	30.480	1118.000	-16.4466	-8.7189	160.67
185.32	30.480	1120.000	-16.5080	-8.7197	160.79
185.32	30.480	1122.000	-16.5698	-8.7206	160.91
185.32	30.480	1124.000	-16.6322	-8.7215	161.03
185.32	30.480	1126.000	-16.6951	-8.7224	161.16
185.32	30.480	1128.000	-16.7586	-8.7232	161.28
185.32	30.480	1130.000	-16.8227	-8.7240	161.40
185.32	30.480	1132.000	-16.8873	-8.7249	161.53
185.32	30.480	1134.000	-16.9525	-8.7257	161.65
185.32	30.480	1136.000	-17.0183	-8.7265	161.77
185.32	30.480	1138.000	-17.0847	-8.7273	161.89
185.32	30.480	1140.000	-17.1517	-8.7280	162.02
185.32	30.480	1142.000	-17.2193	-8.7288	162.14
185.32	30.480	1144.000	-17.2876	-8.7296	162.26
185.32	30.480	1146.000	-17.3565	-8.7303	162.38
185.32	30.480	1148.000	-17.4261	-8.7310	162.50
185.32	30.480	1150.000	-17.4963	-8.7317	162.62
185.32	30.480	1152.000	-17.5672	-8.7324	162.75
185.32	30.480	1154.000	-17.6388	-8.7331	162.87
185.32	30.480	1156.000	-17.7112	-8.7338	162.99
185.32	30.480	1158.000	-17.7842	-8.7345	163.11
185.32	30.480	1160.000	-17.8579	-8.7352	163.23
185.32	30.480	1162.000	-17.9325	-8.7358	163.35
185.32	30.480	1164.000	-18.0077	-8.7364	163.47
185.32	30.480	1166.000	-18.0837	-8.7371	163.59
185.32	30.480	1168.000	-18.1605	-8.7377	163.72
185.32	30.480	1170.000	-18.2382	-8.7383	163.84
185.32	30.480	1172.000	-18.3166	-8.7389	163.96
185.32	30.480	1174.000	-18.3958	-8.7395	164.08
185.32	30.480	1176.000	-18.4759	-8.7400	164.20
185.32	30.480	1178.000	-18.5569	-8.7406	164.32
185.32	30.480	1180.000	-18.6387	-8.7411	164.44
185.32	30.480	1182.000	-18.7214	-8.7417	164.56
185.32	30.480	1184.000	-18.8050	-8.7422	164.68
185.32	30.480	1186.000	-18.8896	-8.7427	164.80
185.32	30.480	1188.000	-18.9751	-8.7432	164.92
185.32	30.480	1190.000	-19.0615	-8.7437	165.04
185.32	30.480	1192.000	-19.1490	-8.7442	165.16
185.32	30.480	1194.000	-19.2374	-8.7447	165.28
185.32	30.480	1196.000	-19.3269	-8.7451	165.39
185.32	30.480	1198.000	-19.4174	-8.7456	165.51
185.32	30.480	1200.000	-19.5090	-8.7460	165.63
185.32	30.480	1202.000	-19.6017	-8.7465	165.75
185.32	30.480	1204.000	-19.6955	-8.7469	165.87
185.32	30.480	1206.000	-19.7904	-8.7473	165.99
185.32	30.480	1208.000	-19.8865	-8.7477	166.11
185.32	30.480	1210.000	-19.9838	-8.7481	166.23
185.32	30.480	1212.000	-20.0823	-8.7485	166.35
185.32	30.480	1214.000	-20.1821	-8.7489	166.46
185.32	30.480	1216.000	-20.2831	-8.7492	166.58
185.32	30.480	1218.000	-20.3854	-8.7496	166.70
185.32	30.480	1220.000	-20.4890	-8.7499	166.82

11. REMARKS

XWVG has been run for cases involving over 50 different trilinear modified refractivity profiles and for frequencies between 50 MHz and 94 GHz. In some of these cases modes with attenuation rates up to 3 dB/km were found. In every case XWVG ran without problems. XWVG works reliably in the diffraction region and well into the line-of-sight region. The results of XWVG were compared to results from other waveguide programs in the diffraction region and to results from a ray trace program in the line-of-sight region. The comparison was very good in the diffraction region and well into the line-of-sight region.

For elevated layers XWVG's strength is in the frequency range of 50 to several hundred MHz. Here the diffraction type modes have attenuation rates as low as a few tenths of a dB per kilometer and could therefore affect the signal level value. XWVG easily finds these diffraction type modes while "G trace" type waveguide programs [6] may miss them. Also, for these frequencies the number of modes with attenuation rates below, for example, 1 dB/km is small. The region of the complex q_{11} -plane that has to be searched for these modes is also small. Therefore, the computer time required by XWVG is not excessively long. At higher frequencies the number of modes below a given attenuation rate increases. This increase in the number of modes comes with an increase in the region of the complex q_{11} -plane that has to be searched for modes. Therefore, the computer run time of XWVG increases, sometimes dramatically. At these higher frequencies the attenuation rate of the diffraction type modes increases, so the fact that G-trace type waveguide programs may fail to find them is no longer significant. In a sense XWVG is complementary to the G-trace type program of Pappert and Goodhart [6].

A major improvement to XWVG that is contemplated is the capability to handle modified refractivity profiles that have N linear segments, where N is a moderate sized number, e.g., 20. In order to do this, use will be made of an improved method for evaluating the derivative of a determinant [37, 38]. This extension of the capabilities of XWVG will be especially useful for multisegment evaporation duct models. It will also allow modeling of evaporation ducts in combination with elevated ducts. Since XWVG uses the

Shellman-Morfitt root-finding routine, all the modes with an attenuation rate less than some specified value are guaranteed to be found. This guarantee is something that multilayer extensions of the G-trace type program cannot give.

12. REFERENCES

1. SW Marcus, A Model to Calculate EM Fields in Tropospheric Duct Environments at Frequencies through SHF, *Radio Sci*, vol 17, p 895-901, 1982.
2. S Marcus and WD Stuart, A Model to Calculate EM Fields in Tropospheric Duct Environments at Frequencies through SHF, *Electromagnetic Compatibility Analysis Center Report ESD-TR-81-102*, Annapolis MD, September 1981.
3. S Marcus, WD Stuart, and FW Ellis, Instructions for Users of DUCT-- A Computer Program for Calculating Fields in Tropospheric Duct Environments, *Electromagnetic Compatibility Analysis Center Technical Note ECAC-TN-81-043*, Annapolis MD, September 1981.
4. DG Morfitt and CH Shellman, MODESRCH, an Improved Computer Program for Obtaining ELF/VLF/LF Mode Constants in the Earth Ionosphere Waveguide, *NOSC Code 532 letter report numbered Interim Report 77T*, San Diego CA, October 1976.
5. GB Baumgartner Jr, HV Hitney, and RA Pappert, Duct Propagation Modeling for the Integrated Refractive Effects Prediction System (IREPS), submitted to IEE for publication, 1982.
6. RA Pappert and CL Goodhart, Case Studies of Beyond-the-Horizon Propagation in Tropospheric Ducting Environments, *Radio Sci*, vol 12, p 75-87, 1977.
7. JC Schelleng, CR Burrows, and EB Ferrell, Ultra-short-wave propagation, *Proc IRE* vol 21, p 427-463, 1933.
8. JE Freehafer, Geometrical Optics, in *Propagation of Short Radio Waves*, edited by DE Kerr, McGraw-Hill, NY, 1951, p 41-58.

9. CL Pekeris, Accuracy of the Earth-Flattening Approximation in the Theory of Microwave Propagation, Phys Rev, vol 70, p 518-522, 1946.
10. KG Budden, The Wave-Guide Mode Theory of Wave Propagation, Prentice-Hall, Englewood Cliffs NJ, 1961.
11. JE Freehafer, Physical Optics, In Propagation of Short Radio Waves, edited by DE Kerr, McGraw-Hill, NY, 1951, p 58-87.
12. G Tyras, Radiation and Propagation of Electromagnetic Waves, Academic Press, NY, 1969.
13. Harvard Computation Laboratory, Tables of the Modified Hankel Functions of Order One-Third and Their Derivatives, Harvard University Press, Cambridge MA, 1945.
14. FE Hohn, Elementary Matrix Algebra, Macmillan, NY, 1964.
15. FWJ Olver, Bessel Functions of Integer Order, in Handbook of Mathematical Functions, edited by M Abramowitz and IA Stegun, US Government Printing Office, Washington DC, 1964, p 355-433.
16. H Bucker, Sound Propagation in a Channel with Lossy Boundaries, J Acous Soc Amer, vol 48, p 1187-1194, 1970.
17. P Beckmann and A Spizzichino, The Scattering of Electromagnetic Waves from Rough Surfaces, Macmillan, NY, 1963.
18. AC Vine, Oceanographic Data, in American Institute of Physics Handbook, edited by DE Gray, McGraw-Hill, NY, 1972, section 2, p 119-132.
19. P Debye, Polar Molecules, Chemical Catalogue Co, NY, 1929.
20. VV Daniel, Dielectric Relaxation, Academic Press, NY, 1967.

21. JB Hasted, Liquid Water: Dielectric Properties, in Water, A Comprehensive Treatise, vol 1: The Physics and Physical Chemistry of Water, edited by F Franks, Plenum Press, NY, 1972, p 225-309.
22. CH Collie, JB Hasted, and DM Ritson, The Dielectric Properties of Water and Heavy Water, Proc Phys Soc London, vol 60, p 145-160, 1948.
23. JB Hasted, DM Ritson, and CH Collie, Dielectric Properties of Aqueous Ionic Solutions, parts I and II, J Chem Phys, vol 16, p 1-21, 1948.
24. LA Klein and CT Swift, An Improved Model for the Dielectric Constant of Seawater at Microwave Frequencies, IEEE Trans Ant Prop, vol AP-25, p 104-111, 1977.
25. LM Delves and JN Lyness, A Numerical Method for Locating the Zeros of an Analytic Function, Math Comp, vol 21, p 543-560, 1967.
26. RP Rich and H Shaw, A Method for Finding all the Zeros of $f(z)$, J ACM, vol 10, p 545-549, 1963.
27. H Bach, Algorithm 365: Complex Root Finding, Comm ACM, vol 12, p 686-687, 1969.
28. CL Goodhart and RA Pappert, Application of a Root Finding Method for Tropospheric Ducting Produced by Trilinear Refractivity Profiles, NOSC TR 153, San Diego CA, September 1977.
29. RV Churchill, Complex Variables and Applications, McGraw-Hill, NY, 1960.
30. HA Antosiewicz, Bessel Functions of Fractional Order, in Handbook of Mathematical Functions, edited by M Abramowitz and IA Stegun, US Government Printing Office, Washington DC, 1964, p 435-478.
31. FWJ Olver, The Asymptotic Expansion of Bessel Functions of Large Order, Philos Trans Roy Soc London, vol A247, p 328-368, 1954.

32. ET Copson, On the Asymptotic Expansion of Airy's Integral, Proc Glasgow Math Assoc, vol 6, p 113-115, 1963.
33. FWJ Olver, Asymptotics and Special Functions, Academic Press, NY, 1974.
34. FWJ Olver, Error Bounds for Asymptotic Expansions, with an Application to Cylinder Functions of Large Argument, in Asymptotic Solutions of Differential Equations, edited by CH Wilcox, Wiley, NY, 1964, p 163-183.
35. FWJ Olver, Asymptotic Approximations and Error Bounds, SIAM Rev, vol 22, p 188-203, 1980.
36. PJ Davis, Gamma Function and Related Functions, in Handbook of Mathematical Functions, edited by M Abramowitz and IA Stegun, US Government Printing Office, Washington DC, 1964, p 253-293.
37. H Otsubo, K Ohta, and S Ozaki, Normal-Mode Solution in the Ocean with Absorbing Bottom Sediments Which Have a Sound-Speed Gradient, J Acous Soc Jpn, vol 1, p 47-57, 1980.
38. M Hall, DF Gordon, D White, Improved Methods for Determining Eigenfunctions in Multi-Layered Normal-Mode Problems, J Acous Soc Am, vol 73, p 153-162, 1983.

END

FILMED

11-83

DTIC